Heterogeneously catalysed hydrogenolysis of glycerol to 1,3-propanediol

TECHNISCHE UNIVERSITÄT DARMSTADT

Vom Fachbereich Chemie
der Technischen Universität Darmstadt
zur Erlangung des akademischen Grades eines
Doktor-Ingenieurs (Dr.-Ing.)
genehmigte

Dissertation

vorgelegt von

Dipl.-Ing. Johannes Kraft

aus Frankfurt/Main

Referent:	Prof. Dr. rer. nat. habil. Peter Claus
Korreferent:	Prof. Dr.-Ing. G. Herbert Vogel
Tag der Einreichung:	19. Juni 2017
Tag der mündlichen Prüfung:	16. Oktober 2017

Darmstadt 2017

D17

The present work has been carried out under the supervision of Prof. Dr. rer. nat. habil. Peter Claus. The first part of the experiments were performed at the Campinas State University (UNICAMP) from February 1st 2011 until September 30th 2012 in the laboratories of Prof. Dr. Gustavo Paim Valença whereas the second part of the project was done at the chemistry department of the Technical University of Darmstadt, at the Ernst Berl Institute for Technical and Macromolecular Chemistry from October 1st 2012 until December 23rd 2014.

Parts of the work have already been presented on congresses:

Posters

J. Kraft, G. Paim Valença, P. Claus, *Heterogeneously catalysed hydrogenolysis of glycerol to 1,3-propanediol.* 46. Jahrestreffen Deutscher Katalytiker 2013, Weimar, March 13th – 15th **2013**.

J. Kraft, G. Paim Valença, P. Claus, *Heterogeneously catalyzed hydrogenolysis of glycerol to 1,3-propanediol*. 23rd North American Catalysis Society Meeting (NAM), Louisville (KY, USA), June 2nd – 7th **2013**.

J. Kraft, G. Paim Valença, P. Claus, *Influence of support and other parameters on the hydrogenolysis of glycerol to 1,3-propanediol on Re-modified catalysts.* 47. Jahrestreffen Deutscher Katalytiker 2014, Weimar, March 12th – 14th **2014**.

J. Kraft, G. Paim Valença, P. Claus, *Influence of support and other parameters on the hydrogenolysis of glycerol to 1,3-propanediol on Re-modified catalysts.* Seventh Tokyo Conference on Advanced Catalytic Science and Technology (TOCAT7), Kyoto (Japan), June 1st – 6th **2014**.

Acknowledgement

First of all, I would like to thank Prof. Dr. Peter Claus for accepting me as his student and for the supervision and support of my work. I am especially grateful for the possibility to do a part of the practical work abroad, which was very helpful for my personal and professional development. I also thank Prof. Dr. Gustavo Paim Valença for giving me the chance to work in his lab at Unicamp and for the support given throughout the whole time.

I appreciated very much the good working environment as well in Darmstadt as in Campinas with very nice colleagues and hence thank the group members of the two groups for the great company and also the help in some situations. Very special thanks go to Martin Lucas who takes very good care of the Claus lab in Darmstadt and has a solution to any upcoming problem.

I am very grateful for the support of the students working with me on this subject, Axel Schüßler, Jennifer Doerfer, Sebastian Dewald and Hauke Christians, thanks for choosing me to be your supervisor!

I also appreciated the help from Dr. Kathrin Hofmann (XRD), Mathis M. Müller (TEM), Dr. Sergio Andres Villalba Morales (NH_3-TPD) and Dr. Volker Schmidts (NMR) who performed the respective analysis for me and helped me to understand the results.

All of this would not have been possible without the great support I received from my parents throughout my whole life. I am very grateful for the help I obtained from my family, the German as well as the Brazilian one, and my friends during all these years. Most importantly, I thank my big love Karen for all the good things she brought to my life and for the support I received from her.

For financial support, I thank the German Academic Exchange Service (DAAD) and the Darmstadt Graduate School of Excellence „Energy Science and Engineering“, as well as Umicore Brazil for supplying a free sample of platinum precursor.

“Nothing in life is to be feared, it is only to be understood. Now is the time to understand more, so that we may fear less.”

Marie Skłodowska Curie (1867 – 1934)

Table of content

1. Zusammenfassung und Einordnung der Ergebnisse in die Literatur

Der starke Anstieg der Biodieselproduktion in den letzten Jahren hat die Verfügbarkeit von Glycerol als Plattformchemikalie für die chemische Industrie stark verbessert. Die selektive Umsetzung von Glycerol zu hochwertigen Produkten wie 1,3-Propandiol ist jedoch weiterhin schwierig und leidet unter fehlender Effizienz, wodurch sich dieser Prozess als Flaschenhals für die Verfügbarkeit von wertvollen High-Tech-Produkten wie Polytrimethylenterephthalat (PTT), einem wichtigen Polymer für die Textilindustrie, erweist. Mit derartigen Folgeprodukten könnte der Anteil nachwachsender Rohstoffe signifikant erhöht werden, was zu einer Verringerung der Abhängigkeit von fossilen Rohstoffen und einer Eindämmung des Klimawandels beitragen würde.

Die Umsetzung von Glycerol biologischen Ursprungs wird bereits im industriellen Maßstab als biotechnologischer Prozess betrieben, belastet mit den typischen Nachteilen derartiger Prozesse wie schwacher Raum-Zeit-Ausbeute, dem Bedarf an Ko-Reaktanten etc. Außerdem leiden sowohl dieser als auch aktuelle heterogen katalysierte industrielle Prozesse unter nicht idealen Ausbeuten. Im Prinzip sollten heterogene Katalysatoren diese Probleme lösen können, die selektive Entfernung der sekundären Hydroxylgruppe hat sich jedoch als sehr viel schwieriger erwiesen als die Bildung von 1,2-Propandiol, weshalb auch die Leistung der Literaturkatalysatoren noch viel zu wünschen übrig lässt. Das Verständnis der Funktionsweise des Katalysators sowie des Reaktionsmechanismus ist entscheidend, um bessere Katalysatoren entwickeln zu können.

Es wurden bereits mehrere Reaktionsmechanismen für die für diese Reaktion verwendeten Katalysatoren vorgeschlagen. In den meisten Fällen wurde ein sauer katalysierter Mechanismus, entweder mit oder ohne Spillover von Wasserstoff, angenommen, wohingegen für bimetallische „State-of-the-art“ Iridium-Rhenium-Katalysatoren ein direkter Hydrogenolysemechanismus vorgeschlagen wurde. Basierend auf Publikationen direkt vor dem Beginn dieser Studie wurde dieser Katalysatortyp als Startpunkt für die Untersuchung des Reaktionsmechanismus und der Funktionsweise des Katalysators gewählt. Daneben wurde in der ersten Phase der Arbeit auch eine Reihe von Versuchen zu innovativen Katalysatorsystemen, z.B. mit Wolframcarbid, weiteren Wolframverbindungen oder anderen Hydriermetallen, durchgeführt, leider ohne vielversprechende Ergebnisse. Daher wurde der Fokus der Arbeit auf die Untersuchung des Reaktionsmechanismus gelegt.

Da die von der Tomishige-Gruppe für Ir-Re-Katalysatoren veröffentlichten Ergebnisse nicht reproduziert werden konnten und die Reaktionsbedingungen, insbesondere die sehr niedrige Menge an Reaktionslösung (6 g Glycerollösung in einem 190 ml Reaktor), sehr unpraktisch erschienen, wurden

in einer Reihe von Vorversuchen neue Standardbedingungen definiert. Die meisten Versuche dieser Studie liefen demzufolge 8 h bei 433 K und 5 MPa konstantem Wasserstoffdruck, ermöglicht durch einen externen Wasserstofftank, der das notwendige Gasvolumen im Reaktor verringerte. Als wichtigste zu untersuchende Parameter wurden die Aktivmetalle, das Trägermaterial und die Vorbehandlung ausgewählt. Im Laufe der Vorversuche wurde zudem die Wichtigkeit eines Glas- oder Teflon-einsatzes im Reaktor, vermutlich als Schutz gegen Eisenionen aus der Stahlwand des Reaktors, festgestellt und dieser bei allen folgenden Versuchen eingesetzt.

Das Trägermaterial hatte einen starken Einfluss auf den Glycerolumsatz, während die Selektivität relativ unberührt blieb. Die besten Ergebnisse konnten mit Ir-Re-Katalysatoren auf SiO_2 enthaltenen Trägermaterialien wie Zeolithen (H-ZSM-5, H-BEA und MCM-41) oder reinem Silica (G-6 und Q-6) erzielt werden, wobei die Verfügbarkeit von freien Si-OH-Gruppen auf der Oberfläche eine sehr wichtige Rolle spielte, vermutlich als Adsorptionsplätze für Glycerol. Andere Trägermaterialien wie Aluminiumoxid oder Kohlenstoffträger erwiesen sich als weniger aktiv in der Hydrogenolyse. Ein direkter Zusammenhang der Katalysatorleistung mit sauren Zentren, BET-Oberfläche oder Aufnahme von CO konnte nicht gefunden werden. Aufgrund dieser Ergebnisse wurden SiO_2 (G-6) und H-ZSM-5 (80) als wichtigste Träger für diese Studie ausgewählt.

Bezüglich der Aktivmetalle konnten die guten Ergebnisse der bimetallischen Iridium-Rhenium-Katalysatoren bestätigt werden. Die Anwesenheit von Rhenium, das direkten Kontakt zum Edelmetall haben musste, führte zu einer massiven Steigerung der Reaktionsgeschwindigkeit bei nahezu gleichbleibender Selektivität. Die Reihenfolge der Imprägnierung erwies sich ebenfalls als entscheidend, Iridium musste zuerst imprägniert werden, gefolgt von der Imprägnierung von Rhenium ohne zwischenzeitliche Reduktion. Dies galt jedoch nur für Iridium und Rhenium, eine Änderung der Imprägnierungsreihenfolge von Iridium und einem eventuellen Drittmetall zeigte keinen derartigen Effekt. Rhenium alleine war praktisch inaktiv und bildete kein 1,3-Propandiol, wohingegen Iridium alleine zu einer ähnlichen Produktverteilung führte wie der bimetallische Katalysator, dabei aber deutlich langsamer war. Ein Austausch von Iridium durch Platin im bimetallischen Katalysator mit Rhenium brachte keine großen Änderungen mit sich, hauptsächlich nur einen leichten Umsatzrückgang. Im Gegensatz dazu führten Ruthenium und Rhodium zu deutlich höheren Umsätzen, es wurde aber deutlich weniger 1,3-Propandiol gebildet, was zu deutlich geringeren Ausbeuten als bei Ir-Re-Katalysatoren führte.

Die Vorbehandlung wurde gründlich untersucht, wobei gezeigt werden konnte, dass die in der Literatur übliche Kalzinierung bei hohen Temperaturen von 773 K und mehr in Wirklichkeit die

Leistung des Katalysators hemmt, vermutlich aufgrund der Agglomeration der Metallpartikel und möglicherweise aufgrund verbleibender oxidierter Spezies. Eine einfache Reduktion im Wasserstoffstrom bei 503 K nach der Imprägnierung und dem Trocknen beschleunigte dagegen die Reaktion. Im späteren Verlauf der Arbeit wurde eine zusätzliche *in-situ* Reduktion in Wasser bei 473 K und 7 MPa Wasserstoffdruck eingeführt, die sowohl den Umsatz als auch die Selektivität zu 1,3-Propandiol erhöhte und eine Verringerung der Reaktionstemperatur auf 393 K bei einer Reaktionszeit von 20 Stunden ermöglichte. Hiermit wurde eine Ausbeute von 21% bei 43% Umsatz erreicht, ähnlich den Ergebnissen einer Gruppe, die – unabhängig von der Tomishige-Gruppe – mit ähnlichen Katalysatorsystemen arbeitete. Es konnte gezeigt werden, dass die Verbesserung der Leistung weder an der Re-Reduktion einer möglichen Oxidation während des Umfüllens unter Luft noch an der Anwesenheit von gelöstem Rhenium aus dem nicht vollständig reduzierten Precursor lag. Die Präsenz von Wasser und Wasserstoff erwies sich dabei als entscheidend für den Erfolg der *in-situ* Reduktion. Die Änderung der Selektivität deutete auf eine Modifikation der Katalysatorstruktur hin, die von dem, im Vergleich zur Reduktion *ex-situ*, hohen Wasserstoffdruck verursacht werden könnte.

In einer kleinen Versuchsserie mit verschiedenen organischen Lösungsmitteln mit Hydroxylgruppen wie Ethanol und 1,2-Butandiol wurde festgestellt, dass diese Lösungsmittel den Umsatz an Glycerol herabsetzen, vermutlich durch Adsorption an den aktiven Zentren. 1,2-Butandiol wurde langsam umgesetzt, während Ethanol mit nur einer Hydroxylgruppe kaum umgesetzt wurde, ähnlich wie 1- und 2-Propanol. Eine Reaktion in reinem Glycerol führte zu ähnlichen Mengen an Produkten wie im Falle einer 20%igen Glycerollösung, was darauf hindeutet, dass der Katalysator gesättigt und die Verfügbarkeit von Glycerol kein limitierender Faktor war. Die Rolle von Wasser konnte nicht untersucht werden, da alle verwendeten Lösungsmittel einen Restgehalt Wasser enthielten und keine Möglichkeit boten, zumindest zu Beginn der Reaktion unter wasserfreien Bedingungen zu arbeiten.

Im Einklang mit der Literatur war der Umsatz von 1,2-Propandiol als Edukt ähnlich dem von Glycerol, wohingegen 1,3-Propandiol deutlich langsamer reagierte. 1,2-Propandiol bildete etwa dreimal so viel 1-Propanol wie 2-Propanol, ein Hinweis darauf, dass die primäre Hydroxylgruppe eher auf dem Katalysator adsorbierte und die benachbarte Hydroxylgruppe eher die Hydrogenolyse durchlief.

Experimente mit Deuterium anstelle von Wasserstoff gaben einen Einblick in den Reaktionsmechanismus über einem Ir-Re/SiO_2 (G-6) Katalysator. Es zeigte sich, dass der Katalysator einen Austausch von Wasserstoff- (bzw. Deuterium-)atomen zwischen der Wasserstoff/Deuterium enthaltenen Gasphase und Wasser ermöglichte. Eine weitere Erkenntnis war, dass sowohl Glycerol als auch die Reaktionsprodukte einer schnellen Dehydratisierung und Re-Hydratisierung unterlagen, die

im Versuch zur Bildung hoch deuterierter Spezies von Edukten und Produkten führte. Die Neigung zur Dehydratisierung wurde bereits vorher in anderen Experimenten, sowohl bei der Reaktion ohne Wasserstoff als auch bei der Messung der Glyceroladsorption in der DRIFTS-Zelle, festgestellt, erst das Deuteriumexperiment zeigte aber das Ausmaß der Reaktion, die praktisch kein Molekül unberührt ließ. Aus diesen Ergebnissen ließ sich also schließen, dass die Hydrogenolyse einem sauer katalysierten Mechanismus folgt. Eine kürzlich von Falcone et al. veröffentlichte Studie, die, parallel zur hier vorliegenden Arbeit, mit stark beladenen Pt-Re/SiO_2-Katalysatoren durchgeführt wurde, kam zum selben Schluss bezüglich des Mechanismus, wenn auch mit anderen Versuchen und Argumenten, und ergänzt diese daher.[91] Die Forscher der erwähnten Studie waren ebenfalls nicht in der Lage, die Ergebnisse der Tomishige-Gruppe zu reproduzieren.

Letztendlich ist die wichtigste Errungenschaft dieser Arbeit der Nachweis, dass Ir-Re-Katalysatoren, anders als bisher angenommen, als bifunktionelle Dehydratisierungs-Hydrierungs-Katalysatoren fungieren. Die Ergebnisse korrelieren dabei mit den Veröffentlichungen zu Rh-Re- und Pt-Re-Katalysatoren der Gruppen um Prof. Dumesic und Prof. Davis, basierend auf DFT-Berechnungen und der o.g. Studie, widersprechen aber den Vorschlägen der Gruppe um Prof. Tomishige, die bisher die meisten Artikel zu Ir-Re-Katalysatoren bei dieser Reaktion veröffentlicht hat. Ein detaillierter Reaktionsmechanismus wurde entsprechend den Ergebnissen dieser Studie formuliert. Der Einfluss und die Wichtigkeit mehrerer Parameter, vor allem bezüglich der Vorbehandlung, wurden untersucht und beschrieben. Hiermit wird die zukünftige Arbeit der kommenden Wissenschaftler vereinfacht, indem mehrere wichtige Details aufgezeigt werden, die einen großen Einfluss auf die Leistung des Katalysators haben, wie beispielsweise der Glas-/Tefloneinsatz, die *in-situ* Reduktion und der Verzicht auf die Kalzinierung.

In Bezug auf das Ergebnis der Reaktion waren die Resultate sehr ähnlich zu denen, die von Deng und Scott[70] veröffentlicht wurden, während sich der von Tomishige et al. beschriebene Umsatz und die Selektivität nicht reproduzieren ließen, zumindest nicht mit literaturgemäß kalzinierten Katalysatoren. Nicht kalzinierte Katalysatoren erreichten die beschriebenen Selektivitäten, aber nicht den erwarteten Umsatz. Die beste erreichte Ausbeute an 1,3-Propandiol betrug 21% bei 43% Umsatz nach 20 Stunden bei 393 K und 5 MPa H_2. Typische Raum-Zeit-Ausbeuten betrugen 2,5 $mmol_{1,3\text{-}PDO}/g_{cat}\cdot h$ bei 393 K und 4,5 $mmol_{1,3\text{-}PDO}/g_{cat}\cdot h$ bei 433 K, das entspricht etwa 31 bzw. 56 mmol 1,3-PDO pro Stunde und Gramm Metall, wobei sowohl Iridium als auch Rhenium berücksichtigt wurden. Diese Raum-Zeit-Ausbeuten liegen im Bereich dessen, was als höchste Raum-Zeit-Ausbeute für Platin-Wolfram-Katalysatoren deklariert wurde,[78] und ähneln auch denen, die aus Publikationen anderer Arbeiten mit Ir-Re-Katalysatoren berechnet wurden.

Im Vergleich mit der Literatur der biotechnologischen Prozesse, wo die Raum-Zeit-Ausbeuten in g h^{-1} l^{-1} angegeben werden, entsprechen die Ergebnisse der vorliegenden Arbeit etwa 2 g h^{-1} l^{-1} bei 393 K und 3,5 g h^{-1} l^{-1} bei 433 K bei den verwendeten Reaktions-bedingungen und liegen damit im typischen Bereich der Literaturergebnisse für Bio-tech-Prozesse, die in der Regel unter 5 g h^{-1} l^{-1} bleiben. Im Fall der heterogen katalysierten Reaktion kann die Raum-Zeit-Ausbeute in Bezug auf das Reaktionsvolumen jedoch einfach durch Zugabe von mehr Katalysator erhöht werden, im Gegensatz zum biotechnologischen Prozess, der durch relativ geringe Substratkonzentrationen limitiert ist und maximal auf Endkonzentrationen von 1,3-PDO unter 100 g/l kommt. Weitere Nachteile sind sehr lange Reaktionszeiten und die komplexe Trennung des Wunschprodukts von der Reaktions-lösung.[100] Hohe Raum-Zeit-Ausbeuten implizieren bei den biologischen Prozessen in der Regel auch eine geringe Ausbeute an 1,3-PDO, wie etwa 0,30 mol/mol im Beispiel mit der höchsten berichteten Raum-Zeit-Ausbeute von 16,4 g h^{-1} l^{-1}.[101]

Im Vergleich zur Bildung von 1,2-Propandiol ist die für 1,3-Propandiol erreichte Raum-Zeit-Ausbeute deutlich geringer. Die höchste in unserer Gruppe erreichte Ausbeute an 1,2-PDO, die als Maßstab für folgende Arbeiten dient, betrug 22,1 $g_{1,2\text{-PDO}}$ / (g_{Cu}·h) bei 493 K, was 290 $mmol_{1,2\text{-PDO}}$ / (g_{Cu}·h) oder 70 $mmol_{1,2\text{-PDO}}$ / (g_{Cat}·h) entspricht. Zwar sind die höheren Ausbeuten teilweise durch die höhere Temperatur des Prozesses zu 1,2-PDO bedingt, es erscheint jedoch unwahrscheinlich, dass vergleichbare Ausbeuten an 1,3-PDO bei höheren Temperaturen mit den bekannten Katalysatorsystemen erreicht werden können. Es ist auch fraglich, ob Katalysatoren, die auf 1,3-Propandiol abzielen und auf einem Dehydratisierungs-Hydrierungs-Mechanismus beruhen, jemals die für die Bildung von 1,2-Propandiol konzipierten Katalysatoren übertreffen werden, aufgrund der ungünstigen Stabilität des Zwischenprodukts 3-Hydroxypropanal, verglichen mit dem deutlich stabileren Acetol.

Zusammenfassend lässt sich sagen, dass diese Arbeit mit der Aufklärung des Mechanismus und mehreren wichtigen Parametern ein weiteres Stück im Puzzle des perfekten Katalysators für die Hydrogenolyse von Glycerol darstellt, als Teil des Umbaus der Rohstoffbasis der modernen chemischen Industrie, weg von fossilen und hin zu nachwachsenden Rohstoffen.

2. Introduction

The world is currently undergoing rapid climate changes and humanity is facing the big challenge of a necessary radical reduction of the emission of the so-called greenhouse gases, like CO_2, methane or N_2O.[1] This goal means that the consumption of mineral oil has to be practically stopped, most likely employing a series of measures like efforts in energy efficiency and the substitution of fossil resources by renewable ones, not only in transport, but also in the chemical industry.

Beside the task of reducing the greenhouse gas emissions, the chemical industry is changing the base of resources from oil-based chemicals to renewable resources. In spite of a recent relaxation in the oil price, oil shortage is just a matter of time, which is why big attention is paid to the substitution of oil-derived basic chemicals by plant-based building blocks. One widely recognised publication on this field is the list of twelve building blocks, which are basic renewable compounds, named by the US department of energy.[2] These chemicals are supposed to substitute the actual ground chemicals like benzene, toluene and ethylene which are derived from fossil sources. One of the components listed is glycerol, beside levulinic acid, sorbitol, 2,5-furan dicarboxylic acid among others. These chemicals are supposed to be produced from biomass via fermentation or chemical conversion, possibly within a bio-refinery, analogous to the oil refinery concept. Just as mineral oil, the raw material for a bio-refinery would consist of a complex mixture of substances, with an even higher content of polymeric compounds, e.g. cellulose and lignin, than in the case of mineral oil. As the awareness of the necessary change has risen not so long ago, compared to the over 100 years of research and development on petrol derived chemistry, a lot of research still needs to be done in order to reach the level of technology and commercial competitiveness necessary to completely switch to renewable resources. This is why the list of the most promising building block chemicals needs to be revisited periodically, looking for the ones with the highest chances of commercial success, as has been done by Bozell and Petersen in 2010, for example.[3]

3. Background and motivation

3.1. Glycerol

Glycerol, traditionally called glycerine, is a simple polyol with three hydroxyl groups. At room temperature it is a highly viscous liquid without colour or odour. Due to its three hydroxyl groups it is easily soluble in water and ethanol and can undergo a wide range of reactions, such as esterification, dehydration, dehydrogenation, etherification and more. It was first discovered by K.W. Scheele in 1779 when obtaining sweet tasting substances by heating olive oil with lead oxide.[4]

The traditional production route for glycerol is either based on propylene gained from fossil sources with allyl chloride and epichlorohydrin as intermediates or on the occurrence as a by-product of soap production. Due to the immense increase of crude glycerol production as a by-product of the bio-diesel formation, the traditional propylene based route is only used in special cases for the synthesis of highly pure glycerol nowadays. Now, with glycerol being a cheap reagent, the reaction has been reversed and epichlorohydrin is being produced from glycerol, e.g. by Dow and Solvay (Epicerol® process, implemented in a recently opened plant in Map Ta Phut (Thailand) with a capacity of 100 kt/year) beside the traditional route based on propylene.[5-7]

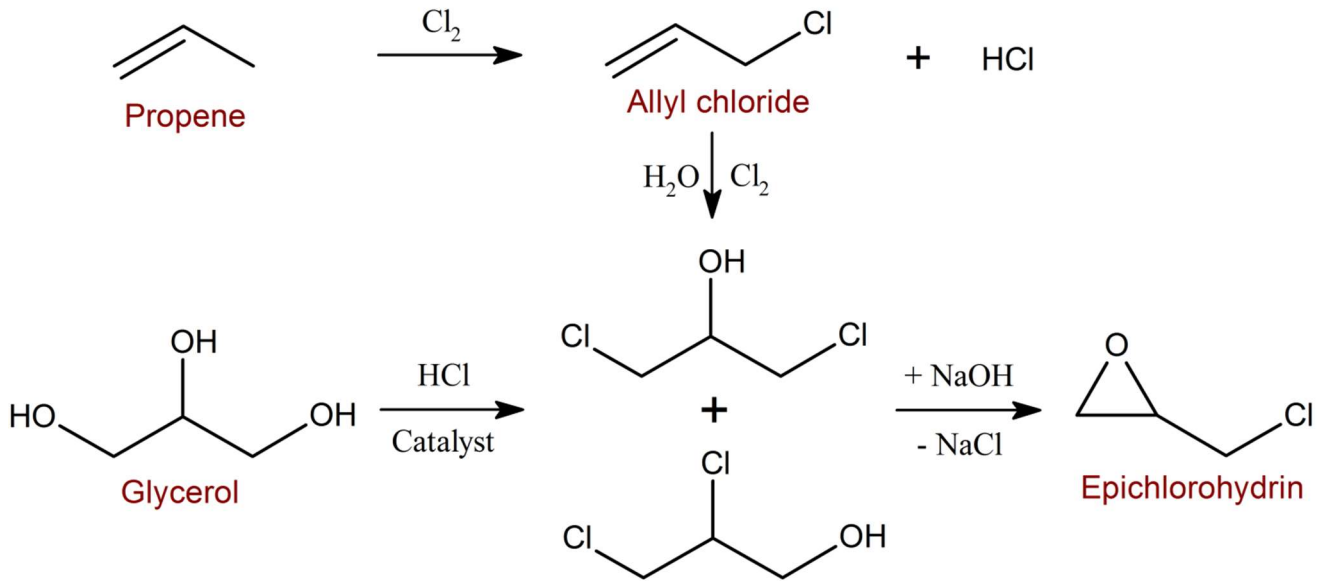

Figure 1 Industrial synthesis of epichlorohydrin, traditionally starting from propene and recently also from glycerol with one reaction step less and less energy, water and chlorine consumption (Epicerol® process by Solvay).[5]

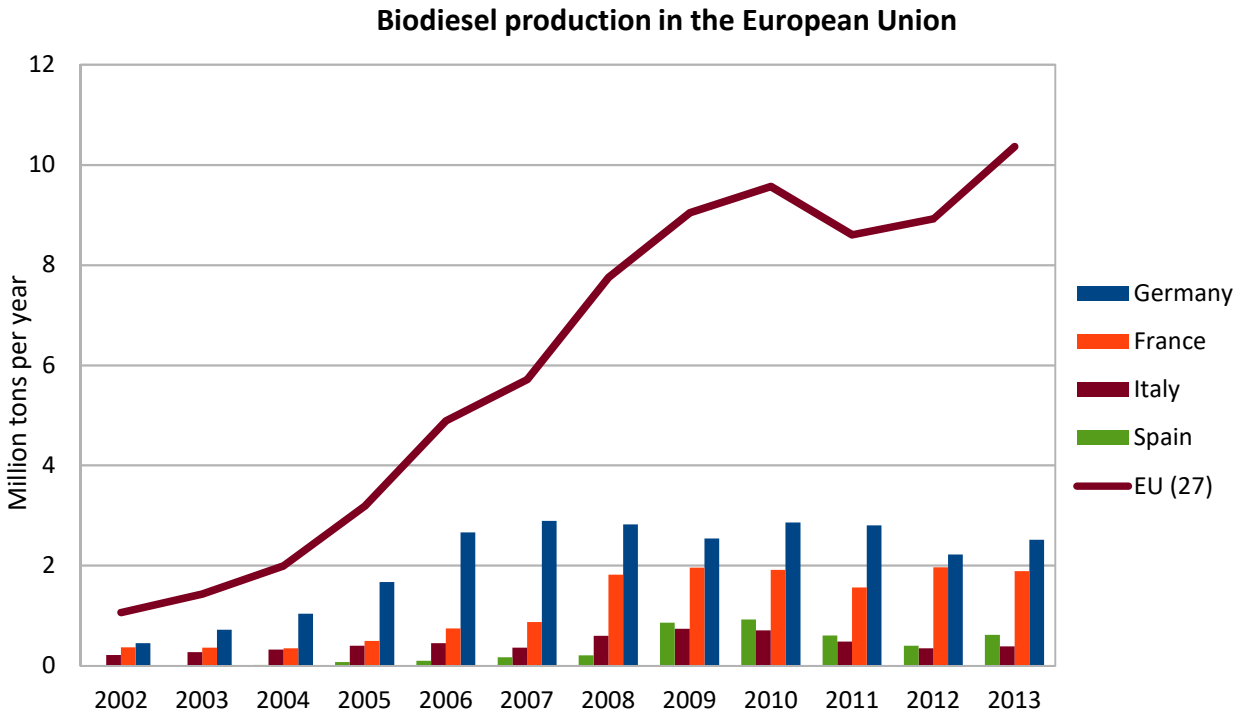

Figure 2 Biodiesel production in the European Union 2002 to 2013. Data: European Biodiesel Board.

The rapid increase of glycerol production is due to the rise in the production of biodiesel, reaching 10.4 million tons in the European Union in 2013, where glycerol surges as a by-product of the transesterification. In this process the triglycerides of vegetable oils or animal fat react with an alcohol, usually methanol or ethanol, to form the corresponding ester of the fatty acids and glycerol. Depending on the reagent (methanol or ethanol), the reaction product will either be a fatty acid methyl esters mixture (FAME) or a fatty acid ethyl esters mixture (FAEE). Due to its low cost and industrial availability, methanol is most commonly used for the biodiesel production.[8] Typical catalysts in the industrial transesterification are sodium hydroxide, potassium hydroxide and sodium methoxide which act homogeneously and ensure a very good yield with high reaction rates even under mild conditions with temperatures around 60°C.[9-10] The main drawback of these homogeneous catalysts, beside the more difficult and energy consuming product separation, is their need for a very clean feedstock with especially water and free fatty acids being a problem as they lead to soap formation with the alkaline catalyst, reducing the ester yield and also inhibiting the separation of glycerol.[11-12]

Possible alternatives are solid heterogeneous catalysts, usually containing either acid or basic functions or both, like CaO,[13-14] $Sr(NO_3)_2/ZnO$[15], WO_3/ZrO_2,[16] ionic exchange resins[17], CaO/SiO_2[18] or Sr/ZrO_2.[19] While basic catalysts are usually more active but very sensitive to impurities of water or free fatty acids, solid acidic catalysts have the great advantage of not suffering from leaching in the

presence of water and of being able to also catalyse the esterification of free fatty acids.[10] In order to combine the high activity of the basic with the acidic catalyst's ability to handle higher contents of free fatty acids, bifunctional catalysts containing basic and acidic sites are being developed with promising results, even with waste oils.[19-20]

The amount of glycerol that is formed as a by-product in the biodiesel synthesis is about 10% of the total weight of the products[12] and the enormous increase in the supply of glycerol has led to a strong decrease of the crude glycerol price during the last decade.[21] In spite of several concerns about the ecological impact of bio-diesel production, especially regarding changes in land use which often inhibit great savings of greenhouse gases, beside other possible ecological drawbacks, glycerol as a by-product is generally considered a fundamental platform molecule for the "green chemistry", aiming to use renewable resources only.

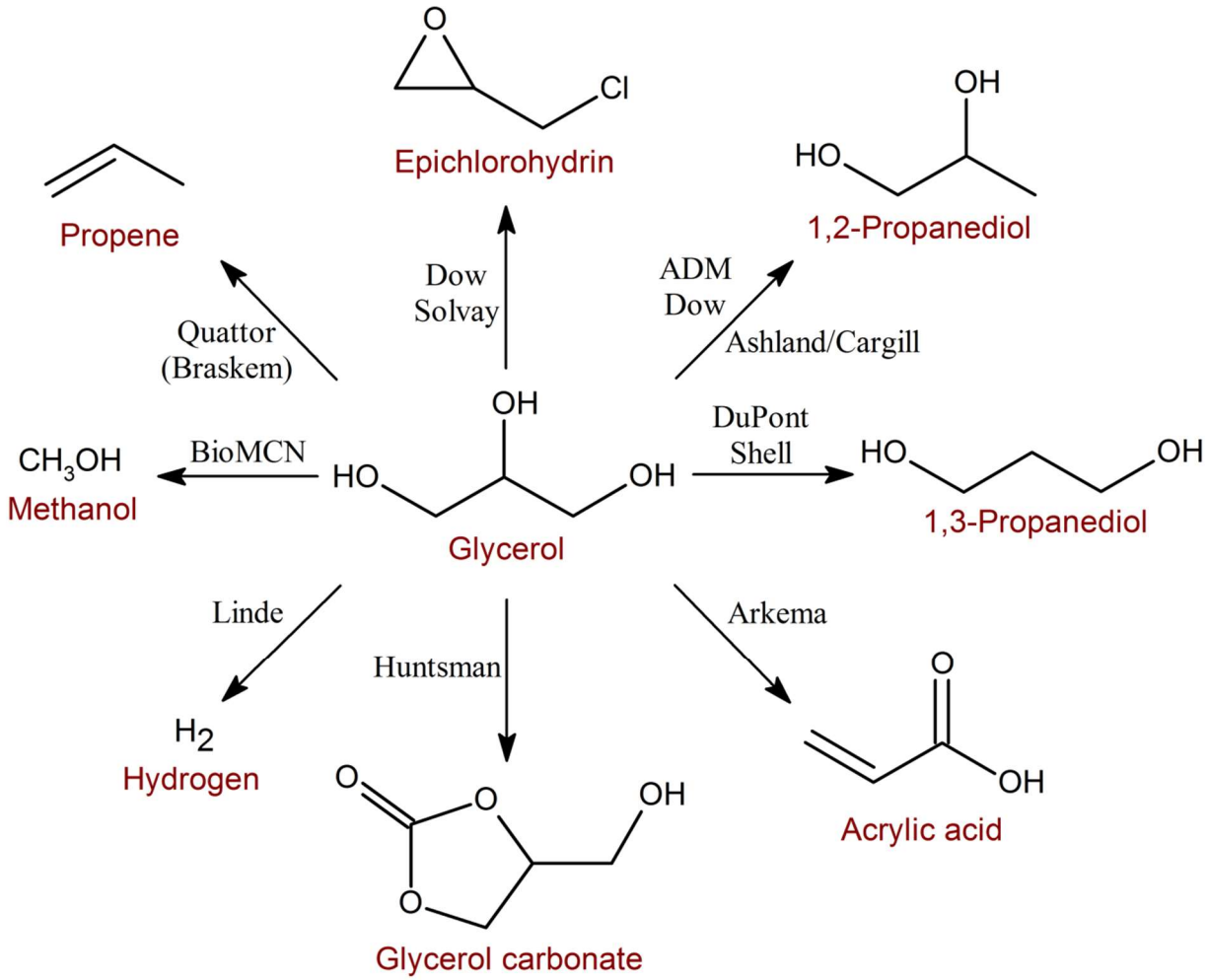

Figure 3 Selection of industrial applications of glycerol as a building block for other important chemicals. Due to economic reasons, not all of the shown processes are currently performed on industrial scale.[22]

Examples for higher valued glycerol derivatives could be fuel additives[4] or 1,3-propanediol as well as dihydroxyacetone,[23] hydrogen production by steam reforming, methanol via synthesis gas, ethanol via bioconversion or acrolein with the respective consecutive products.[21] An overview of industrial applications of glycerol and the owning company of each technology is presented in Figure 3. An effective use of the crude glycerol to substitute fossil based reagents in large scale reactions would also improve the life cycle assessment of bio-diesel significantly.

Crude glycerol originating from processes with homogeneous catalysts usually contains about 5-7% of salt and other impurities which tend to accumulate in the glycerol phase.[24] However, new developed processes like Ambersep BD50, an industrial simulated moving bed chromatography process by Dow with the flexibility to produce glycerol with a broad range of purities, are likely to reduce the purification costs of crude glycerol and hence raise the availability of purified glycerol. New heterogeneous metal-oxide catalysed processes are in development, but the resulting glycerol will still carry impurities from the feedstock which tend to accumulate in the glycerol phase.[25] An interesting alternative to the purification would be the direct utilisation of crude glycerol, which is a big challenge due to the changing composition with large amount of impurities, mainly methanol, soap, water and catalyst residues.[26-27]

3.2. 1,3-propanediol

3.2.1. Use of 1,3-propanediol

Due to the two terminal hydroxyl groups, 1,3-propanediol is very well suited for polymerisation reactions and therefore more valuable than the isomer 1,2-propanediol which is principally used as an ecological friendly anti-freezing agent. The main application for 1,3-PDO is the production of polytrimethylene terephthalate (PTT), an important material in textile industry which is advertised by DuPont as the biggest revolution in carpet industry in two decades. According to Shell, it combines the chemical resistance characteristics of polyester and the shape recovery properties of nylon, with PTT fibres being softer, easier to be dyed and cleaned and maintaining colours longer. DuPont's brand names are Susterra® for 1,3-PDO and Sorona® for PTT. Price and availability of 1,3-PDO have always been the most important limiting factors for the production of PTT, allowing a production on a larger scale only with the development of more cost effective processes for the formation of 1,3-PDO in the 1990s. Beside the use in carpets, 1,3-PDO is an important basis chemical for brilliant and durable plastic components and can also substitute oxetane in the production of polyols (brand name Cerenol®), saving 30% of energy and 40% of greenhouse gas emissions in an one-step, acid-catalysed condensation polymerisation process.[28] Further applications include polyurethane, cosmetic, personal care, home cleaning, coolant fluids and unsaturated polyester resins.[29]

3.2.2. Industrial production

The annual world production of 1,3-PDO is in the order of 120.000 tons (Ullmann's) with DuPont Tate & Lyle and Shell being the main producers.[30] In spite of the actual domination of the market by the two companies, many new players are expected to enter the market in the next few years. The volume of the global 1,3-propanediol market in 2012 is estimated to be $157 million and predicted to exceed $500 million by 2019.[29]

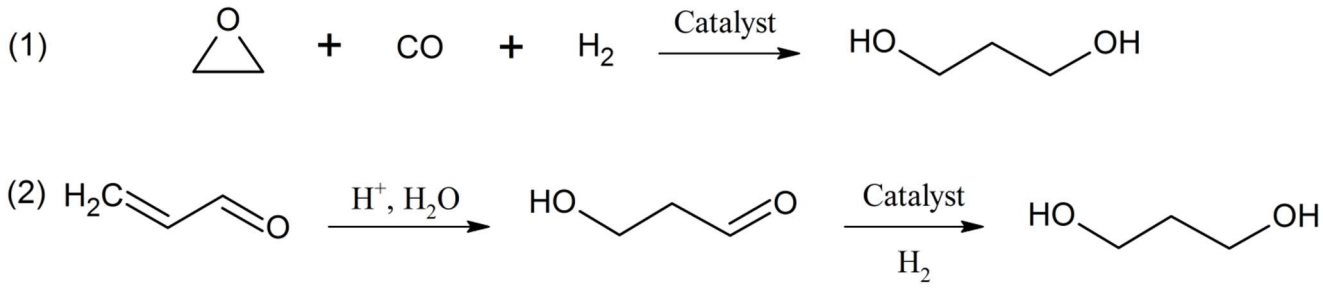

Figure 4 Industrial catalytic synthesis of 1,3-propanediol by Shell (1) and Degussa/DuPont (2).

Catalytic industrial production methods of 1,3-PDO, shown in Figure 4, are hydroformylation of ethylene oxide followed by hydrogenation (Shell),[31-32] and hydration of acrolein, from the oxidation of propylene, followed by hydrogenation (Degussa Process, now owned by DuPont).[31] Both processes are facing selectivity problems with a maximum yield of 80% and 40%, respectively. The main reason for the low yield of the process based on acrolein is the strong tendency to the formation of polymers due to the self-condensation of acrolein so that the hydration always has to compete with this side reaction.

The industrial bio-technologic process at DuPont, developed in cooperation with Genencor, involves genetically modified bacteria based on an *E. coli* K12 strain that enable a process in the presence of oxygen and with a single organism catalyst. In spite of the higher oxidation state and the need for more co-reactants, D-glucose is often used instead of glycerol as a feedstock due to the lower price of glucose. The process involves the conversion of glucose dihydroxyacetone phosphate (DHAP) followed by the transformation to glycerol and then 1,3-propanediol (Figure 5), catalysed by the artificially introduced genes. In 2003, DuPont and Genencor reported the metabolically modified organisms to produce 1,3-PDO at a weight yield of 51%, a rate of 3.5 g/L/h and a titer of 135 g/L in 10 L fed-batch fermentations of D-glucose.[33] Unfortunately, the actual performance of their industrial process is not revealed.

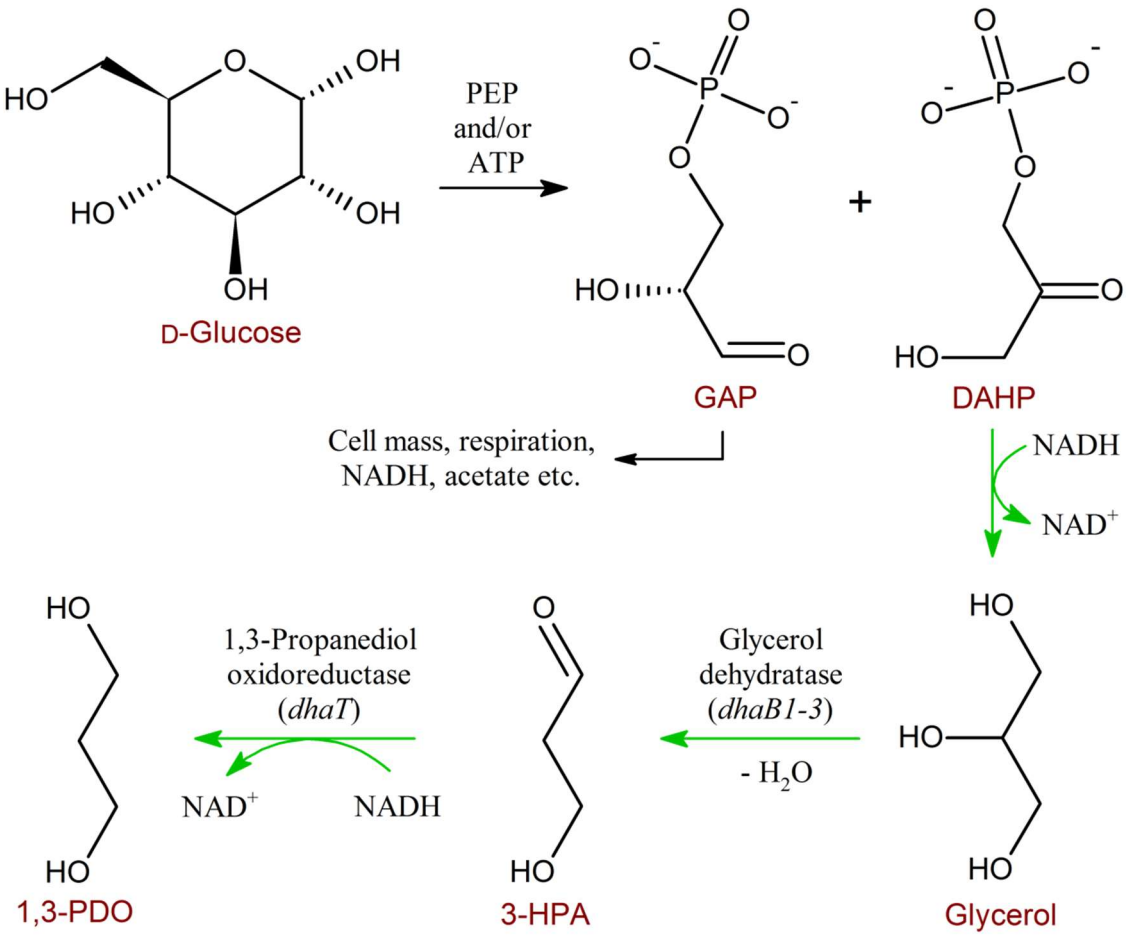

Figure 5 Reaction pathway for the production of 1,3-propanediol from glucose. Black arrows (in the first line) show the reaction encoded by genes that are native to the host organism, green arrows indicate reactions catalysed by genes from donor organisms that were inserted into the host organism. Genes that were deleted from the host organism in order to prevent undesired side reactions are not indicated in this figure. ATP: Adenosine triphosphate; PEP: Phosphoenolpyruvic acid; NADH: Nicotinamide adenine dinucleotide (reduced form); NADPH: Nicotinamide adenine dinucleotide phosphate (reduced form); DHAP: Dihydroxyacetone phosphate; GAP: D-Glyceraldehyde 3-phsophate; 3-HPA: 3-hydroxypropanal; 1,3-PDO: 1,3-propanediol.[33]

Another approach to transform glycerol into more valuable products is a heterogeneously catalysed reaction, resulting in the same products mentioned before for the biological route, but with other focuses. One promising development beside the production of possible monomers like 1,3-propanediol is the formation of oxygenated fuel additives for the automotive industry, e.g. as a part of a bio refinery concept.[4, 25]

4.1. The reaction network

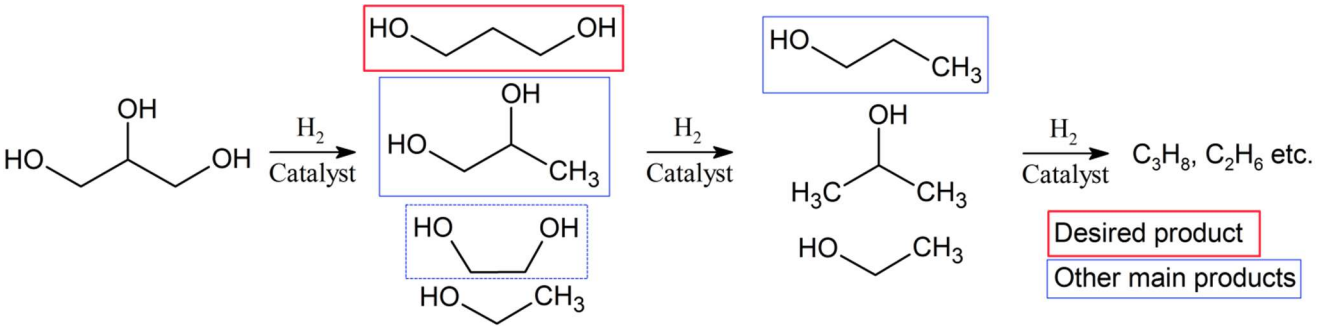

Figure 6 Reaction scheme showing the main products of the hydrogenolysis of glycerol. The desired product 1,3-propanediol is marked in red while the other main products that were formed in this work are marked in blue with ethylene glycol marked with dotted lines as it only appeared as a main product in some special cases.

Glycerol with its three hydroxyl groups can undergo a large series of reactions like oxidation, dehydration or reduction. Under hydrogenolysis conditions either C-O- or C-C-bonds can be broken. At first, 1,2-propanediol and – depending on the catalyst – 1,3-propanediol are formed, usually already together with 1- and 2-propanol. With a catalyst favouring the C-C-scission, e.g. a ruthenium containing catalyst, reasonable quantities of ethylene glycol and ethanol will be formed. In case of high reaction temperatures and acidic sites being present, an especially wide variety of products can be expected due to dehydration, dehydrogenation and condensation reactions, leading to more than 60 detected substances.[34-35]

4.2. Metal containing catalytic systems

4.2.1. The beginning: Homogeneous catalysis

The main work on this topic started with a relatively broad range of catalytic systems, including homogeneous catalysts. Most early works also used organic solvents as water was expected (and with the used catalyst systems also found) to obstruct the reaction. A patent from 1987 claimed a yield of 1,3-propanediol of 21% after 24 hours at high temperature (473 K) and very high pressure (32 MPa) of synthesis gas ($CO:H_2 = 1:2$) using H_2WO_4 and $Rh(CO)_2(acac)$ as a homogeneous catalyst in 1-Methyl-pyrrolidinone.[36] In spite of the relatively high yield, no further repercussion of this patent could be found. In 2000, Shell researchers claimed a selectivity of 30.8% towards 1,3-propanediol at a turnover

rate of 12.8 $mol_{Glycerol}/mol_{Pd}\cdot h$, which can be calculated to equal a conversion of around 20 to 25%. In this case, synthesis gas ($CO:H_2$ = 1:2) was used as well, but this time under less harsh conditions (313 K, 6 MPa), the catalytic system consisted of a homogeneous palladium complex in sulfolane and water, using methanesulphonic acid as an additive.[37]

A broader work focussing not only on glycerol, but on the removal of the secondary hydroxyl group in general, with a homogeneous ruthenium complex in sulfolane under mild conditions (383 K, 5.2 MPa H_2) reported the hydrogenolysis taking place, but reaching very low yields only.[38] Three years later, Wang et al described a three-step technical process, consisting of acetalisation, tosylation, and detosyloxylation, with a yield of 72%, even without optimised conditions.[39] In spite of the very good yield and the possibility of a continuous process for large scale production, this idea mainly suffers from the consumption of tosyl chloride which increases the process costs and also leads to p-toluenesulfonic acid as an undesired by-product.

4.3. Recent Developments in heterogeneous catalysis

4.3.1. Continuous flow reactions

The heterogeneously catalysed conversion of glycerol to 1,3-propanediol, which is the focus of this present work, is generally performed in a batch reactor in liquid (usually aqueous) phase - although some examples of successful experiments of continuous mode reactors as well in gas as in liquid phase can be found in the literature, especially in very recent years. Continuous reactions have principally been reported by a group of Chinese researchers around Yongwang Li who used silica-based catalysts employing heteropolic acids and noble metals in continuous gas[34] and liquid[40-45] phase reactions. In the gas phase, they achieved a selectivity to 1,3-PDO of 32% at a glycerol conversion of 83% using a $Cu\text{-}H_4SiW_{12}O_{40}/SiO_2$ catalyst at 0.54 MPa, 483 K and a weight hourly space velocity (WHSV) of 0.1 h^{-1}. Their bifunctional catalyst combined the acidic support, determined to dehydrate glycerol in gas phase,[46] with a metal component, in this case copper, to hydrogenate the emerging 3-hydroxypropanal to 1,3-propanediol (see Figure 7).

A similar catalyst ($Pt\text{-}H_4SiW_{12}O_{40}/SiO_2$) was used by the same group in a liquid phase flow reactor with 10 mass% glycerol aqueous solution and a selectivity of 38% to 1,3-propanediol at a glycerol conversion of 81.2% at 473 K and 6 MPa was reported. However, the WHSV of 0.045 h^{-1} was very low and in spite of great advances concerning the selectivity (66% Selectivity at 64% conversion),[43] the space time yield remained the main drawback. Still at a low WHSV, but at far lower temperatures of 110°C to 140°C, $Pt/WO_3/ZrO_2$ led to a 1,3-PDO yield of 32% and Qin and co-workers proposed a mechanism involving acid sites and a hydrogen spill over from platinum to surface tungsten oxide.[47] Feng and Jiang used Cu/MO_x and $Cu/ZnO/MO_x$ (MO_x = TiO_2, Al_2O_3 or ZrO_2) at very high

temperatures (180°C – 300°C) to convert gas phase glycerol-water mixtures, reaching a 10% yield at full conversion with hydroxyacetone (also known as acetol) being the main product.[48-49] An Indian group published several reports on the gas phase hydrogenolysis of glycerol reaching 35% yield of 1,3-propanediol at full conversion over catalysts using $Pt/AlPO_4$, also at relatively high temperatures with partly unexpected results, like the domination of 2-propanol in the product stream under certain conditions.[50-51] In two following studies with Pt/WO_3/SBA-15 and Pt/H−mordenite, respectively, the same group reached up to 46% yield, still at relatively high temperature and also with an uncommon, strongly temperature dependent, selectivity. The WHSV of 1.02 continued relatively low, regarding the temperature of over 200°C, high levels of acetol (hydroxyacetone) were detected and a clearly bifunctional mechanism was assumed in which Brønsted acid sites play a central role in the formation of 1,3-propanediol. Similar to the results of several other groups working with tungsten, the best tungsten loading was found to be 10% by weight.[52-53] Another Indian group found Ru/MCM-41 to be an active, but not very selective catalyst for the desired 1,3-PDO.[54]

Very recently, a Chinese group came up with an egg-shell catalyst using highly disperse rhenium and iridium on silica spheres treated with trimethylchlorosilane and impregnated employing ethanol containing solutions. The ethanol turned out to help concentrate the active metals on the outer parts of the egg-shell catalyst, leaving them easier to reach by the 80%wt. glycerol solution. The reactions were performed at relatively low temperatures of 403 K in a trickle bed reactor under 8 MPa hydrogen pressure reaching 19% yield.[55] Other recent examples for glycerol conversion in gas phase were reported, leading mainly to 1,2-propanediol[56-57] at temperatures usually above 220°C, each time using catalysts containing zinc and copper.

4.3.2. Batch reactions

Until a few years ago, there were no reports about an effective heterogeneously catalysed hydrogenolysis of glycerol to 1,3-PDO with yields of more than 10%. The reactions were also conducted in organic solvents in order to maximise the potential yield but thereby also raising ecological concerns thinking about industrial application. The first reasonable selectivity towards 1,3-propanediol of 19% was reported in 2004 by Chaminand et al. using Rh/Nafion in water with the addition of tungstic acid.[58] However, the activity was low, taking 168 hours to reach 8% conversion.

Afterwards, the research on this reaction focussed on two different catalytic systems. While the Japanese group of Tomishige found rhenium, in combination with noble metals, to be a strongly beneficial component, several other groups focussed on supposedly bifunctional catalyst containing tungsten oxide species with noble metals.

The majority of the catalysts employed is based on SiO_2 which was reported to show a better adsorption of glycerol than e.g. activated carbon, Al_2O_3 or HZSM-5 and has a higher surface area than TiO_2.[59-60] However, silica with small mesopores of about 2 nm proved to be less effective for the dehydration of glycerol,[46] probably due to steric hindrance.

Firstly, WO_3 was introduced as an additional material in between the active metal and the catalyst support, for example in $Pt/WO_3/ZrO_2$[61] and $Pt/WO_3/TiO_2/SiO_2$.[60] The beneficial effect of WO_3 was explained with the higher amount of weak acid sites which needed to be in a certain relation to the number of active metal sites in order to increase the selectivity to 1,3-propanediol which reached 50% at low conversions of 15%.[60] Also, the high dispersion of the metal particles is crucial for a high catalytic activity.[61] In both cases, reaction temperature was about 443 – 453 K and hydrogen pressure around 5.5 to 8 MPa. Platinum on sulfated zirconia proved to be highly selective, forming 1,3-propanediol with 55.6% yield, but unfortunately only in 1,3-dimethyl-2-imidazolidinone (DMI) representing a big drawback regarding industrial application.[62] In water, the selectivity was much lower at similar conversions.

Soon after these results, the first ones with a reasonable selectivity towards the desired 1,3-propanediol, Rhenium was discovered to increase the selectivity even more when employed as a second metal. Bimetallic Pt-Re/C[63] at 443 K and 4 MPa as well as $Rh\text{-}ReO_x/SiO_2$,[64-65] and $Ir\text{-}ReO_x/SiO_2$[66-67] at lower temperatures (393 K) and 8 MPa led to selectivities of more than 60% at conversions of about 25% with a maximum yield of 1,3-propanediol of 38%. However, in later studies several influences on the reaction were examined, but no further improvement in yield was achieved by the Tomishige group. In their studies, the positive influence of rhenium as a second metal turned out to be stronger than the one of tungsten, leading to a better conversion and selectivity. A small addition of acid, either sulphuric acid or acidic solids like zeolites,[68] until pH = 3 (equimolarity of Re and H^+)[66] was found to have several advantageous effects like a higher activity and better stability of the catalyst, parts of what will be discussed together with the mechanism in chapter 4.4. Characterisation of the calcined (773 K) and reduced (473 K) catalysts indicated clusters of partially oxidised rhenium on fully reduced rhodium or iridium particles of about 2 – 3 nm. A curious fact was the very small amount of glycerol solution (4 g glycerol and 2 g water) and catalyst (150 mg), compared to the reactor capacity of 190 mL. An important detail was the glass insert vessel, to avoid a poisoning effect of the reactors stainless steel wall.

Recently two other works (both from the same author) employing bimetallic catalysts containing rhenium were published, one with Pt-Re/CNT[69] (carbon nanotubes) and the other one with Ir-Re/KIT-6[70] (mesoporous silica) together with amberlyst. While the first work focussed on the effect of

particle size on activity and selectivity, where bigger particles were beneficial for the formation of 1,3-PDO but on the other hand less active, the second study used a catalytic system very similar to the one of Tomishige and the ones used in the present work and came to very interesting results. Catalysts that did not pass a calcination step before the reduction showed a superior performance in the formation of 1,3-propanediol, compared to catalysts that were calcined after the impregnation. In XPS measurements, the calcined and reduced catalysts gave similar results to the Tomishige catalysts (which were pre-treated in a very similar way), indicating that rhenium maintains an oxidation state of around 2,5 even at high reduction temperatures, probably due to strong Re-O-bonding to the surface of either iridium or the support material. On the other hand, catalysts that were not calcined but directly reduced after impregnation seemed to form an alloy of the two completely reduced metals with strong hints for an interruption of iridium surface with rhenium atoms. These catalysts reached a yield of 1,3-propanediol of 22% (35% selectivity at 63% conversion),[70] very similar to the results obtained in the present study (see chapter 7).

In spite of the good results with rhenium containing catalysts, research with tungsten containing catalysts went on. In experiments with platinum on mesoporous and commercially available WO_3, the mesoporous catalyst led – on a lower level than the rhenium containing catalysts mentioned before – to better results than the commercial ones, assumed to be caused by the easier reducibility.[71] A study with different acidic additives that were combined with commercially available platinum on alumina catalysts showed their best results (14% yield at 49% conversion) when employing tungsten components like silicotungstic acids ($H_4SiW_{12}O_{40}$, STA).[72]

Incorporating the aluminium and tungsten into the solid catalyst led to the catalytic system with the highest yield of 1,3-propanediol so far, reaching 40% yield with Pt-AlO_x/WO_3[73] and as high as 66% with Pt/WO_x/AlOOH.[74] Aluminium was postulated to serve as an “anchor” for glycerol (see discussion of reaction mechanism in section 4.4) as the presence of hydroxyl groups on the alumina surface proved to be crucial for the activity. However, the overall performance was not as good as the yield suggests, the reaction temperature was relatively high (180°C) and a big mass of catalyst, almost equalling the amount of glycerol in the reactor, was used to reach these high conversions within 10 hours reaction time.[74] Similar problems were encountered in a study with platinum on mesoporous $TiWO_x$, in which 2 g of catalysts were necessary to convert 55% of 4 g of glycerol with a 15% yield at 180°C.[75]

A study focussing on the influences of tungsten surface concentration on Pt/WO_x/Al_2O_3 achieved good selectivity at high temperatures and also came to interesting insights into the mechanism. The authors found that the conversion decreased with increasing tungsten concentration while 1,3-PDO yield had

its maximum at around 2.4 tungsten atoms per surface nm² and concluded that hydroxyl groups on the aluminium surface served as "anchor" for glycerol and that the formation of WO_3 nanoparticles, which are formed as soon as the surface concentration of tungsten passes a certain threshold, negatively affected the reaction rate.[76]

Recently, a completely different catalytic system was presented: Cobalt nanorods with iridium as the nucleation agent and sodium stearate as the surfactant were formed in polyol and showed a decent conversion and 1,3-PDO selectivity of 82% and 23%, respectively.[77] The performance appeared to be strongly shape-dependent with [10-10] surfaces, present in hcp rods, being the most active ones while spheres were rather inactive and far less selective towards the desired product.

Another very recent study focussed more on the structure of the catalyst, using a Pt/WO_x catalyst in which platinum was highly disperse with particle sizes below 2.3 nm and possibly reaching single-atom state. A strong metal support interaction (SMSI) was detected between platinum and the rod-shaped mesoporous WO_x, rich in oxygen vacancies and hydroxyl functionalities, and found to be crucial for the performance, leading to a very high space-time-yield of 3.78 $g/g_{Pt}h$ at 433 K at relatively low hydrogen pressures of 1 MPa.[78]

4.4. Proposed reaction mechanisms

Several mechanisms have been proposed for the hydrogenolysis of glycerol, with acid-catalysed and transition metal catalysed mechanisms being the most common ones. The latter one was postulated initially by the Tomishige group and usually assumed for catalysts involving Re in combination with a noble metal like Rh or Ir, without the need for strong acidic components.[67] However, DFT calculations of similar catalysts indicate that bimetallic rhenium catalysts might actually show strong acidic properties as well.[79]

Most other groups designed their catalysts as bifunctional catalysts consisting of an acidic component and one for hydrogenation, at which two different acid-catalysed mechanisms can be distinguished. In one case, the catalyst is assumed to act in a real bifunctional way by first providing an acid site leading to dehydration to 3-hydroxypropanal or acetol, followed by a hydrogenation to 1,3- or 1,2-propanediol (see Figure 7). In other cases, especially in the studies involving platinum and tungsten oxides, hydrogen spillover from platinum to the tungsten oxide seems likely, leading to a more complex mechanism with a rather concerted action of proton and hydride species, with similarities as well to the acidic mechanism as to direct hydrogenolysis.

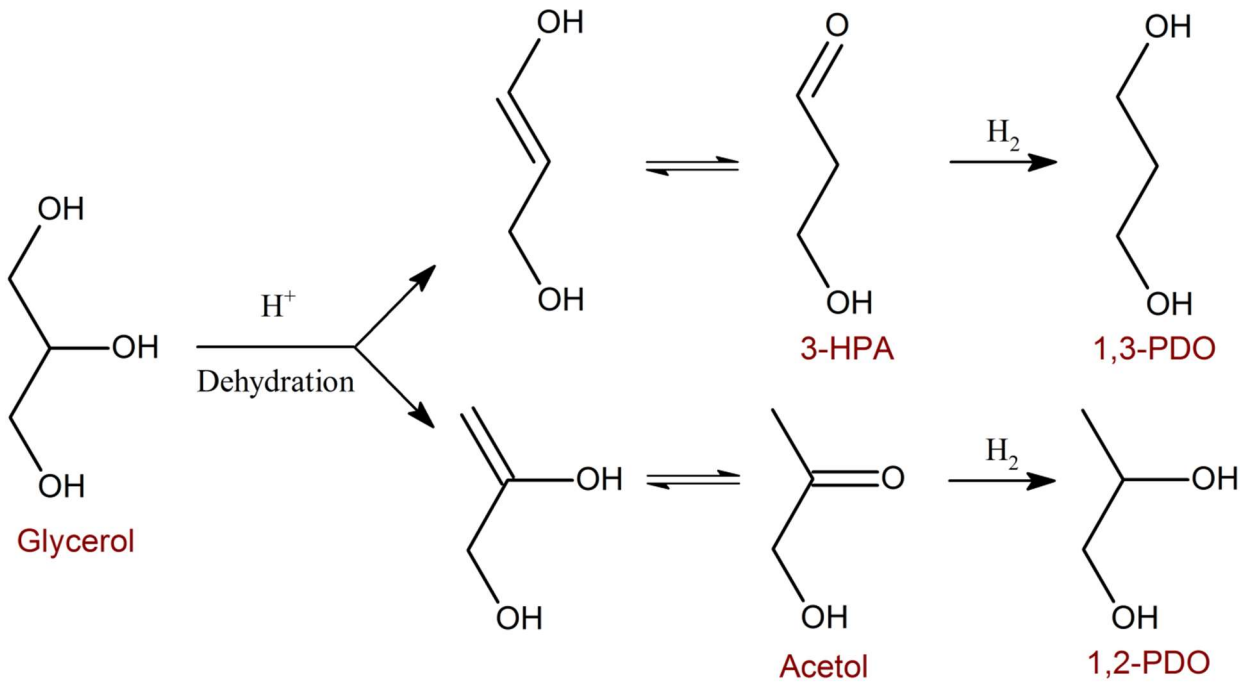

Figure 7 Reaction mechanism of the glycerol hydrogenolysis over a bifunctional catalyst containing an acid and a hydrogenation function. 3-HPA: 3-hydroxypropanal, PDO: propanediol

4.4.1. Direct hydrogenolysis over rhenium containing catalysts

This mechanism was first proposed in 2010 for Rh-ReO_x/SiO_2[65] and Ir-ReO_x/SiO_2[67] by the Tomishige group. It is based on the oxophilicity of rhenium which makes surface rhenium act as an "anchor" for the glycerol hydroxyl groups (see Figure 8), which was also assumed for Pt-Re/C,[63] and showed clearly better results than comparable catalysts without rhenium.[80] Non-local density functional theory (DFT) calculations of the hydrogenolysis of acetic acid on palladium and rhenium arrived at the conclusion that rhenium favoured the C-OH bond activation while palladium worked better for the hydrogenation.[81] In order to maintain this capability, it is necessary to work in an acidic medium, to avoid the formation of inactive Re-O^- oxorhenium species that were made responsible for the poor performance in the presence of basic additives like MgO and CeO_2.[68] The optimum conditions were found to be at a pH value around 3, with a molar ratio of Re to H^+ of 1:1, achieved with the addition of H_2SO_4 or solid acids.[66] The good selectivity towards 1,3-PDO is attributed to the bonding of the terminal OH-group of glycerol to rhenium and the more favourable 6-membered ring transition state (shown on the right hand side in Figure 8), compared to the suggested 7-membered ring transition state that leads to the formation of 1,2-PDO.

Extensive studies of the catalyst showed that rhenium is very likely to form partially oxidised small clusters on the surface of iridium (or other noble metal) particles with the iridium particles being about 2 – 3 nm in size. TPR (Temperature Programmed Reduction) data recorded at low hydrogen pressure

indicated a rhenium oxidation state of about +4, while X-Ray Adsorption Near Edge Spectra (XANES) and XPS (X-ray photoelectron spectra) rather showed an oxidation state of around +3 for rhenium (reduced at higher hydrogen pressure). An important point for the catalyst performance is the complete reduction of iridium, taking place around 200°C, catalysts pre-treated at this temperature clearly outpace the catalysts pre-reduced at 120°C. Only one reduction peak appeared in the TPR measurement, proving a direct connection between rhenium and iridium, underlined by X-Ray absorption showing the simultaneous reduction of iridium and rhenium, in contrast to rhodium and rhenium which also form a common reduction peak, but actually seem to be reduced one after the other.[65, 82]

The presumption of the ReO_x clusters on the iridium surface was backed up by the results of CO-Chemisorption, XANES and EXAFS (extended X-ray absorption fine structure). The amount of adsorbed CO decreased when rhenium was introduced into the catalyst, as rhenium oxide species do not adsorb CO – differently from iridium or rhenium in metallic state. XANES and EXAFS analyses indicated Re-Ir bonds of three-dimensional ReO_x clusters on cuboctahedron iridium metal particles, without the bridging oxygen atoms that are present in the precursor form.[82] However, there was no clear proof of these direct Ir-Re-bonds due to the big difficulty to distinguish rhenium and iridium, both with a very similar atomic mass, as a backscattering neighbour atom.

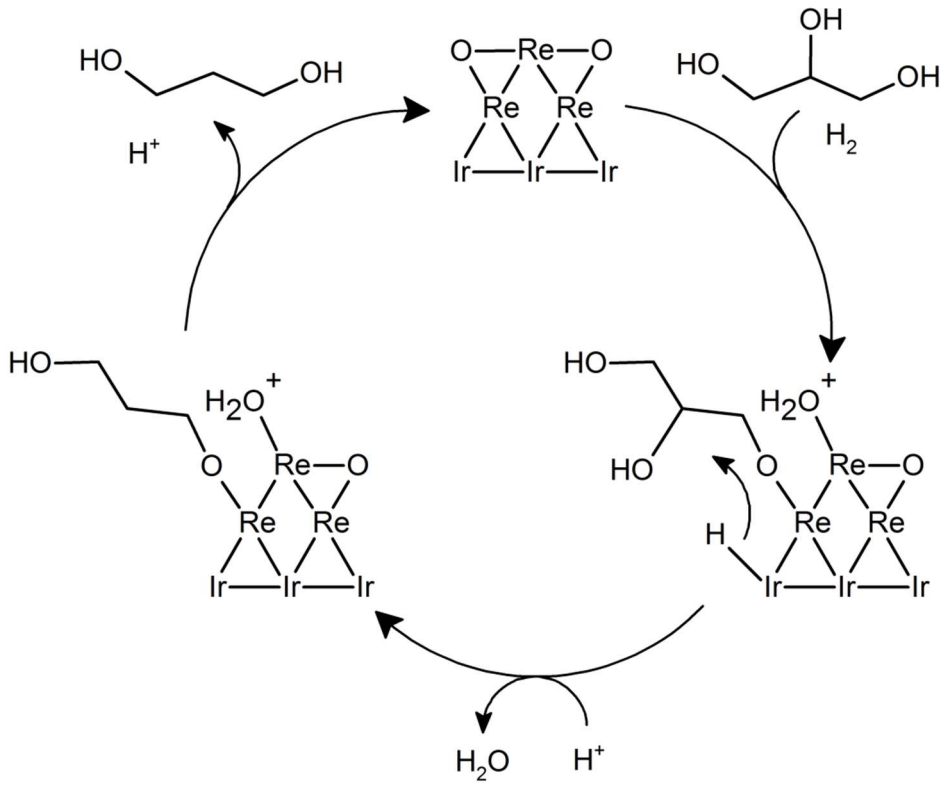

Figure 8 Possible mechanism for the hydrogenolysis of glycerol over Ir-ReO_x/SiO_2, suggested by the Tomishige group.[67]

It also should be noticed that basically all these assumptions are based on the characterisation data that was gained *ex-situ* and that might not be accurate under reaction conditions, especially under the presence of water. The catalysts were prepared by incipient-wetness impregnation followed by 3 h calcination at 773 K in static air and *in-situ* reduction in water at 473 K before the addition of glycerol. In contrast to this, the reduction preceding the characterisations mentioned above was carried out with/after dry reductions.

The proceeding of the reaction via an acid-catalysed mechanism as presented in section 4.4.2 was discarded because the addition of acid beyond the point of Re to H^+ of 1:1 did not show any positive effect and because the acidity of the support seemed to play only an inferior role. Moreover, no dehydration products like acetol (hydroxyacetone) or 3-hydroxypropanal were detected at any point. The addition of acid was believed to change the selectivity of the reaction, however – with a close look onto the data – the obvious change in the product distribution might also originate from the acceleration of all reactions, including the hydrogenolysis of 1,2-PDO, leading to the formation of more 1-propanol.

Reaction order towards glycerol was guessed to be zero, while the order towards hydrogen was proposed to be one, as the increase in hydrogen pressure led to a clear increase in activity while the change in glycerol concentration did not influence the conversion.[65] The reactions were always carried out using an inserted glass vessel to avoid the poisoning of the catalyst, presumably caused by iron leaving the wall of the steel reactor.[68] Looking for possible rate determining steps, transfer of the active hydrogen species to the adsorbate and the formation of the 3-hydroxy-propoxy-rhenium species were mentioned as possible candidates. The latter one would then have to depend basically on the availability of catalytic sites as the glycerol concentration was found to have no influence on the reaction rate after passing a relatively low concentration level.

Direct reaction routes to 1- and 2-propanol play an important role and decrease the yield of propanediol significantly.

4.4.2. Bifunctional acid-catalysed mechanism

A different approach is the explanation of the reaction as a two-step mechanism, involving an acid-catalysed dehydration, followed by a hydrogenation (see Figure 9). At first, a proton adds to one of the glycerol hydroxyl groups, preparing thereby the cleavage of the C-O-bond and the leaving of a water molecule. For this step, the glycerol molecule does not necessarily have to be adsorbed on the catalyst surface. In the second step, the formed acetol (hydroxyacetone) or the less stable[83-85] 3-hydroxypropanal (3-HPA), both detected in several studies, is hydrogenated by the noble metal on the

catalyst surface, leading to either 1,2- or 1,3-propanediol. Possible side or secondary products are 1- and 2-propanol (consecutive reaction of propanediol or of the intermediates), acrolein (from the dehydration of 3-HPA, detected for example over $H_4SiW_{12}O_{40}/SiO_2$[34] or even simple Al_2O_3[86] in vapour phase), allyl alcohol and propionaldehyde (propanal), among others. Degradation products of C-C-fission like ethylene glycol (only deriving from glycerol and not from 1,2-propanediol),[87] methanol and ethanol were detected in significant quantities over this type of catalyst, especially at elevated temperatures[48] or strongly acidic catalysts.[87] The distinction between the two steps of the reaction was shown for example in a study aiming for 1,2-propanediol where a temperature gradient inside the reactor, providing high temperatures at the beginning for the dehydration and lower temperatures towards the reactor exit to promote the hydrogenation, improved selectivity and yield.[56]

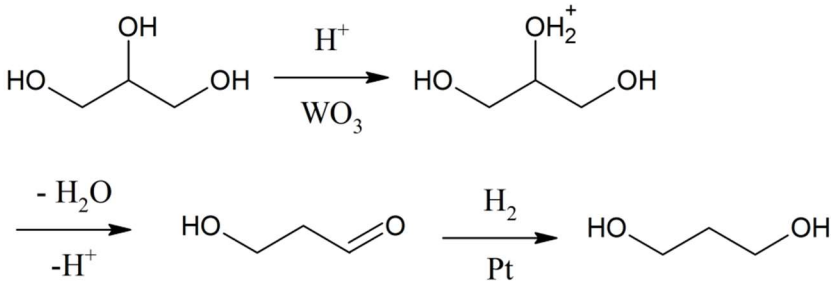

Figure 9 A possible mechanism for the acid catalysed hydrogenolysis of glycerol to 1,3-propanediol on an exemplar catalyst containing tungsten and platinum.

Typical examples for bifunctional catalysts working well to produce 1,3-propanediol are $Pt/WO_3/ZrO_2$,[61] $Cu\text{-}H_4SiW_{12}O_{40}/SiO_2$,[34] $Pt/WO_3/TiO_2/SiO_2$,[60] $Pt\text{-}H_4SiW_{12}O_{40}/SiO_2$,[41] mesoporous $Pt/TiWO_x$,[75] $Pt\text{-}AlO_x/WO_3$[73] and $Pt/WO_x/AlOOH$.[74] Interestingly, tungsten seems to play an important role in these catalysts, and not only because of its acidic properties, as it is – usually together with platinum – present in basically all successful bi-functional catalysts employed in this reaction. Studies showed that a physical mixture of Pt/ZrO_2 and WO_3/ZrO_2 was much less active than the $Pt/WO_3/ZrO_2$ catalyst, indicating the importance of tungsten and platinum having a direct contact.[61] Therefore, the denomination “bi-functional catalyst” has to be used with care.

In a study with $Pt/WO_3/TiO_2/SiO_2$ the influence of each component was examined. SiO_2, which was compared with active carbon, Al_2O_3, TiO_2 and HZSM-5, was supposed to provide a good glycerol adsorption and an easy product desorption, due to hydrophilic surface properties, besides the high surface area. TiO_2 (deposited on the SiO_2 surface) clearly improved conversion due to a better dispersion of the hydrogenating platinum particles while WO_3 led to a higher selectivity towards 1,3-PDO by providing more weak Brønsted acid sites. The presence of all these ingredients as well as the amount of each one was found to be crucial for the catalyst performance. The right concentration of

tungsten, for example, was found to be 5% (at 2% platinum and 10% TiO_2), however, the connection with the concept of the importance of a WO_x-monolayer mentioned in several works presented in section 4.4.3 was not yet made.[60]

The correlation between the concentration of (weak) Brønsted acid sites and the selectivity to 1,3-propanediol was mentioned by several groups,[41, 60, 62] once even distinguishing between the formation of 3-hydroxypropanal (leading to 1,3-PDO) on weak and acetol/hydroxyacetone (leading to 1,2-PDO) on strong acid sites.[48] For Pt-$H_4SiW_{12}O_{40}/SiO_2$ the best results in terms of conversion and 1,3-PDO selectivity were achieved with 15% of the highly disperse Keggin-structure heteropoly acid, explained by the high platinum dispersion and the high concentration of medium Brønsted acid sites at this point.[45]

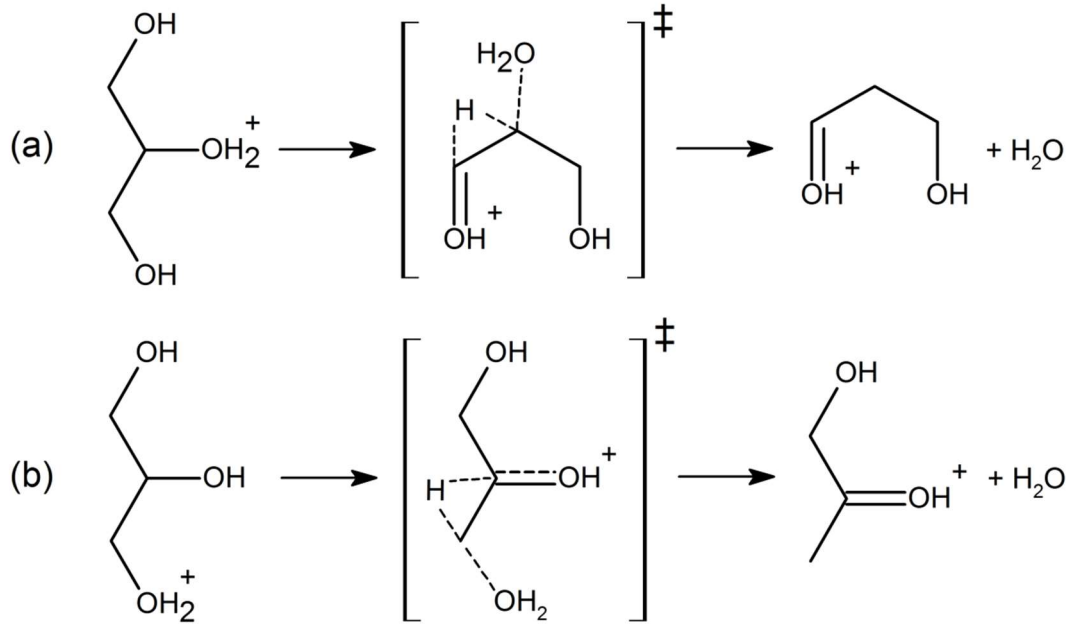

Figure 10 Mechanism of the formation of the precursors for (a) 1,3- and (b) 1,2-propanediol via hydride transfer in a protonated glycerol molecule in an acidic medium, as one of several possible pathways resulting from DFT calculations. While the transition state in reaction (a), leading to 1,3-PDO, is lower in energy, the cation resulting from reaction (b) is far more stable than in the case of (a).[85]

In a study with similar catalysts (also containing platinum and heteropoly acids, but this time based on ZrO_2), a linear correlation was found between the number of Brønsted acid sites and 1,3-PDO yield on the one hand and Lewis acid sites and 1,2-PDO yield on the other hand. The accuracy in the case of 1,3-PDO was better than in the case of 1,2-PDO, due to the relatively fast consecutive reaction of the latter one. The formation of small amounts of 1,3-PDO over Pt/ZrO_2 in spite of the absence of Brønsted acid sites was explained by the formation of these acid sites by the reaction of water with Lewis acid sites.[45] In the following work by the same group, $Pt/WO_x/ZrO_2$ was modified with SiO_2 in

order to adjust acid strength and surface properties. It turned out that an addition of 5% of silica had a promoting effect on the formation of 1,3-PDO, but it was not clear whether this was mainly due to the increase in the number of acid sites or to platinum and tungsten oxide occurring more disperse, leading also to a higher number of defects with W^{5+} species. With respect to the mechanism, it was speculated that the acidic sites actually might serve the adsorption of glycerol and the protonation of the secondary OH group.[42]

The question whether the effect of the acid sites or rather the platinum content and dispersion is the determining factor for the 1,3-PDO formation also appeared in studies comparing the influences of different supports for platinum. The best results were obtained using platinum on $AlPO_4$, compared to ZrO_2, sulfated ZrO_2, γ-Al_2O_3, active carbon and Y-Zeolite, which showed the highest number of (weak) acid sites, Brønsted and Lewis type, as well as the highest dispersion of platinum, due to the strong interaction between metal and support. However, even with a distinct conclusion in this case, including the results to the discussion would be risky because of the unusual reaction conditions (gas phase at up to 300°C) and the odd results like 100% yield of 2-propanol at 280°C while best results in terms of 1,3-PDO were achieved at 260°C.[50-51] The same group postulated, supported by the formation of considerable amounts of acetol, the two-step mechanism also for the hydrogenolysis over Pt-WO_3/SBA-15 and Pt/H-mordenite, naming the Brønsted acid sites as the responsible ones for the formation of 1,3-PDO.[52-53]

In the case of Pt/H-mordenite, a detailed reaction scheme was constructed (see Figure 11) starting with the adsorption of glycerol, in which one of the OH-groups binds via the oxygen atom to an acidic proton and via the hydrogen atom to an oxygen atom on the surface of the H-mordenite. The dehydration leads then to an intermediate in which the secondary carbon atom binds to an oxygen atom of a Si-O-Al bridge on the surface, followed by reallocation and formation of 3- hydroxypropanal and finally 1,3-propanediol.[52]

On the other hand, supposed Brønsted acid sites also have been postulated to improve the selectivity towards 1,2-propanediol, in case of ruthenium on different acidic supports. These acid sites were "supposed" because no experimental characterization was carried out to determine number, strength or type of acid sites.[88] On Ru/SiO_2 with H-ZSM-5, the Brønsted acid sites also did not lead to 1,3-PDO but rather to C-C scission and methane formation. In contrast to some other studies, aluminium addition had no promoting effect as acid sites were blocked.[89] The same group published a study in which several metals were combined with Pd/SBA-15 and the best results were achieved with rhenium as the second metal. In contrast to almost any other report employing rhenium, a bifunctional

mechanism was proposed, postulating a dehydration on acidic ReO_x-sites followed by hydrogenation on metallic Pd-Re sites.[90] Another recent report claimed to have proven a bifunctional mechanism over a Pt-Re/SiO_2 catalyst, contradicting the Tomishige group.[91]

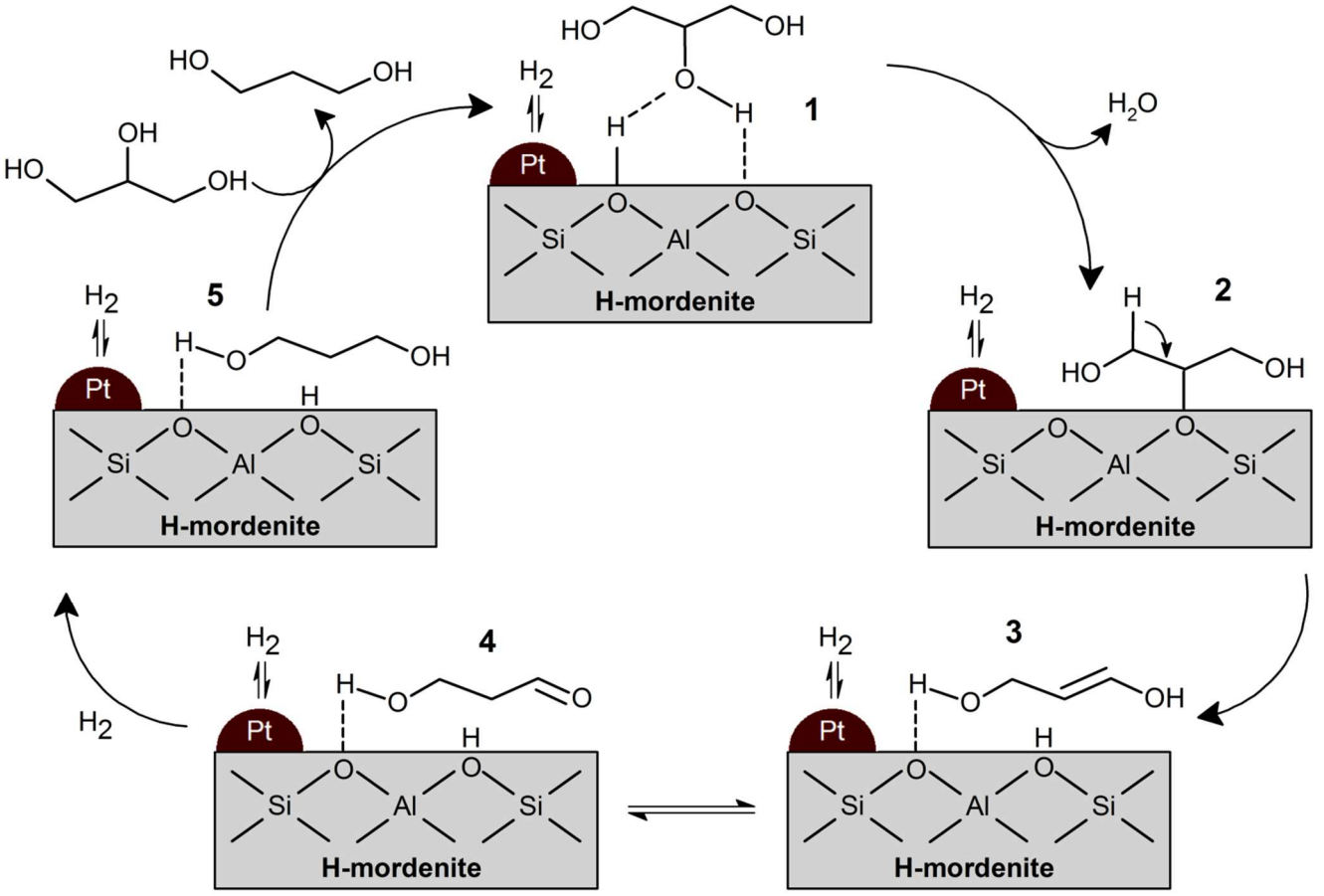

Figure 11 Proposed reaction mechanism for dehydration and hydrogenation on Pt/H-mordenite. The step from (1) to (2) might involve a 6-membered ring intermediate if one of the surface O-H bonds is broken.[52]

However, in context with the other studies mentioned before, it seems that the question of selectivity cannot be limited to the type of acid sites as many catalysts with Brønsted acid sites, but without components like tungsten, aluminium or rhenium, do not produce any 1,3-PDO. In the case of Ir-Co-nanorods, a bifunctional mechanism was assumed, due to the presence of acetol (precursor to 1,2-PDO), but unfortunately no examination of the acid sites was performed so that no further explanation for the unexpected performance in the formation of 1,3-propanediol was possible.[77]

DFT calculations predicted a beneficial effect of lithium[92] which was later confirmed in experiments for 1,3-PDO[44] and acrolein[93] synthesis. However, the authors of the experimental studies attributed the beneficial effect of lithium and other alkali elements to enhanced Brønsted acid sites.

An interesting fact shown in several studies was that the formation of ethylene glycol always originated from glycerol and never from 1,2-propanediol, indicating that C-C scission only takes place between two carbons with hydroxyl groups.

4.4.3. Direct hydrogenolysis over tungsten containing catalysts

With the selectivity obviously being influenced not only by the type and kind of acid sites, the direct hydrogenolysis of glycerol over tungsten containing catalysts tries to explain the experimental findings with a more sophisticated mechanism than in the case of the pure bifunctional catalyst. In this mechanism, which was first proposed in 2010,[47] a hydrogen spillover from platinum to tungsten, leading to proton ("H^+") and hydride ("H^-") species on the catalyst surface is the key element.

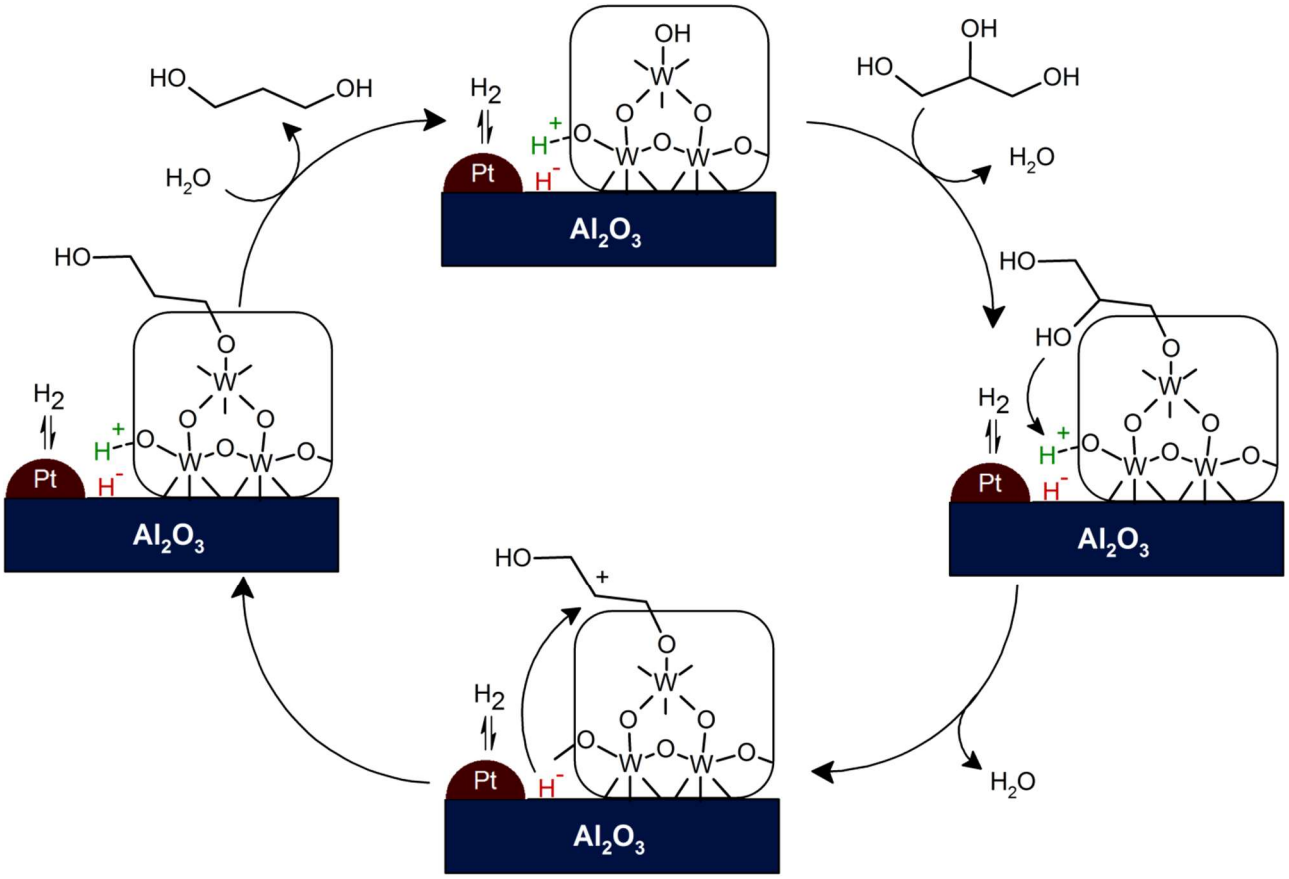

Figure 12 Mechanism for the direct hydrogenolysis of glycerol to 1,3-PDO over $Pt/WO_x/Al_2O_3$.[76]

Hydrogen adsorbs on platinum, a heterolytic bond scission then leads to a proton, attached to WO_x, and a hydride on another (not further specified) place on the catalyst surface. The glycerol adsorption was assumed – just like in section 4.4.1 – to take place by the substitution of a surface OH-group, either on aluminium oxide[73] or tungsten oxide.[71, 76] One of the free hydroxyl groups then adopts the proton in order to form water as a leaving group, resulting in a carbo cation which then reacts with the hydride, leading to the formation of an adsorbed propanediol.

Several groups proposed that the structure of the tungsten oxide is crucial for the reaction and that WO_x species, either in mesoporous tungsten oxide or – when positioned on a support – close to a monolayer concentration of polytungstate, are far more active than WO_3 particles that form at higher tungsten contents.[43, 47, 71, 75-76] One important point is that the reducibility of tungsten oxide and the resulting formation of oxygen defects – both more likely in WO_x than in WO_3 – play a significant role in the selectivity to 1,3-propanediol. With an unsaturated d-orbital, these tungsten species become very oxophilic, form acidic sites and readily react with glycerol OH-group, in a similar way as has been proposed for ReO_x species before. The better ability of polytungstate species for the delocalisation of the negative charge might help to stabilise the intermediate carbocations, preventing a second dehydration with the formation of acrolein. For Pt-WO_x/γ-Al_2O_3, signs of WO_x species on top of platinum particles, just like in the case of rhenium, were found and XPS indicated an electron donor effect from platinum to tungsten.[43] Another factor might be the better availability of the hydride species on spillover-enabling catalysts which helps to hydrogenate the unstable 3-hydroxypropanal more quickly. There was no agreement on the mechanism of the hydrogen spillover, which once was claimed to be connected to Lewis[47] and once to Brønsted acid sites at which has to be noted that DMI (1,3-dimethyl-2-imidazolidinone) was used as solvent in the latter case.[62] The mentioned work in DMI did actually not use a tungsten catalyst, but assumed a very similar reaction mechanism, incorporating the hydrogen spillover from platinum to sulphated ZrO_2 as a key step. These assumptions were also based on reports about the increase in the number of Brønsted acid sites through hydrogen spillover on the same type of catalyst.[94] Just like in many other studies, the right balance between the components (in this case hydrogen spillover and surface sulphate groups) was crucial for the overall catalyst performance.

In the case of Pt-AlO_x/WO_3, for example, the combination of the preference for the formation of primary alkoxide species on γ-alumina[95], combined with the high adsorption of hydrogen (144 H per Pt atom) on the catalyst was pointed out as the main reason for good 1,3-PDO yield.[73] When the WO_3 was substituted by WO_x and used in smaller quantities (8%, with AlOOH being the support), the yield could be increased even more.[74] The higher activity was explained with the bigger number of surface OH-groups on the AlOOH support and their preference for the formation of primary alkoxides, a conclusion taken from the fact that 1,2-PDO formed almost exclusively 1-PrOH and very little 2-PrOH. However, the existence of this high number of surface hydroxyl groups was doubted by other authors due to the high calcination temperature of 800°C.[76] Nevertheless, the basic connection between surface OH groups and glycerol adsorption (and hence activity of glycerol hydrogenolysis) was not questioned, as a variation of tungsten content in Pt/WO_x/Al_2O_3 showed a decreasing glycerol

conversion with increasing tungsten content, attributed to the obstruction of surface hydroxyl groups (not taking into account the discussion about the different activities of WO_3 vs. WO_x mentioned above). Acidic properties of the successful catalysts were analysed only in their calcined form and not after the pre-reduction (besides the problem that especially the presence of water under reaction conditions might change the catalyst structure even more), so that the results showing almost exclusively Lewis acid sites on the catalyst should be considered with care.

These studies had in common that all mentioned components (platinum as well as oxides of aluminium and tungsten) had to be present and closely together for a satisfactory performance of 1,3-PDO formation. The positive effects of hydrogen pressure as well as of platinum concentration on selectivity to 1,3-PDO could be attributed to the increasing presence of H^+/H^--pairs on the surface and thereby the rapid hydrogenation of the rather unstable 3-HPA intermediate.

4.4.4. Other mechanisms

A very different mechanism was proposed for glycerol hydrogenolysis over $Ru/Cs_{2.5}H_{0.5}[PW_{12}O_{40}]$ and $Rh/Cs_{2.5}H_{0.5}[PW_{12}O_{40}]$, assuming a dehydrogenation followed by a dehydration and a hydrogenation, usually to 1,2-PDO and in case of Rh also in some extend to 1,3-PDO. In contrast to most other catalysts presented so far, increasing hydrogen pressure actually led to a lower conversion in this case.[96]

4.5. Biocatalysis

The fermentation of glycerol to 1,3-propanediol is the oldest fermentation process involving glycerol and, discovered in 1881 by August Freund, one of the oldest known fermentation processes at all.[97]

As mentioned before, most of the actual production of 1,3-PDO occurs biotechnologically, either departing from glycerol or glucose. At the moment, DuPont is using glucose from corn starch as the basis for their process, advertising it as a breakthrough in biopolymer technology.[98] As DuPont is not revealing any details about their process, the heterogeneous process will be compared to the literature about the biotechnological conversion.

Several strains of microorganisms are available for the production of 1,3-PDO, some of them using solely glycerol as their feedstock, others needing additional material like starch or glucose. The most prominent strains are *Klebsiella* and *Clostridium* species as well as *Escherichia coli* by metabolic engineering.[99] Important parameters besides the organism itself are temperature, medium

composition, pH, end products and substrate concentrations. The main drawback of the biotechnological process is the relatively low maximum substrate concentration resulting in maximum end concentrations of 1,3-PDO of less than 100 g/L, beside very long reaction times.[100] Space-time-yields are also relatively low with usually below 5 g h^{-1} L^{-1} and a maximum value of 16.4 g h^{-1} L^{-1} in the literature.[101] However, a high space-time-yield usually implicates a low yield of 1,3-PDO like 0.30 mol/mol in the example mentioned before. Another disadvantage of the biological processes is the more complex separation of the desired product from the reaction solution.

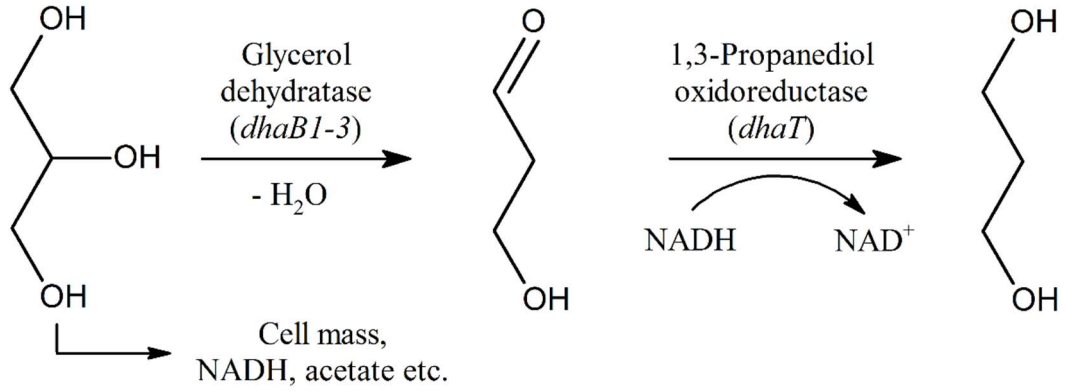

Figure 13 Formation of 1,3-propanediol in natural organisms under anaerobic conditions with the formation of by-products like cell mass, reduced nicotinamide adenine dinucleotide NADH (from its oxidised counterpart NAD^+) and acetate. The NADH formed in the first step reacts with the 3-hydroxypropionaldehyde to form 1,3-propanediol and NAD^+. The two steps are catalysed by glycerol dehydratase (encoded by the genes dhaB1-3) and 1,3-propanediol oxidoreductase (encoded by the gene dhaT).[33]

Of high interest are microorganisms that cope with crude glycerol as the price of crude glycerol is much lower than the one of purified glycerol.[102-103] These organisms might therefore compensate the low reaction rate yield by leaving the purification obsolete as the reaction rate for crude and purified glycerol was almost the same[104] and the possibility of an integrated process to yield PTT was shown.[99]

4.6. Industrial application of similar catalysts

Combinations of rhenium with noble metals like platinum or iridium are not very frequent in the chemical industry due to the costs of the noble metals and also the rareness of rhenium; however, there are some important applications, with the steam reforming of naphtha being the most significant one.

Alloys of rhenium and platinum group metals are known for their high temperature stability and extraordinary hardness and as components of superalloys.[105] Rhenium nanoparticles have also been found to catalyse, for example, the isomerisation of 10-undecen-1-ol to internal alkenols via long chain migration of the C=C double bond at about 470 K.[106] Besides, Re_2O_7/Al_2O_3 is used in industrial scale to catalyse olefin metathesis reactions.[107]

Zeolite, silica and mostly alumina based platinum-rhenium catalysts are used in steam reforming processes to produce aromatic components out of naphtha. In processes designed by Exxon and Amoco, iridium is added as a promoter in order to increase the periods between regeneration by facilitating hydrogenation and removal of coke precursors, similar to the effects of rhenium. Interestingly, the implementation of iridium into the steam reforming catalyst in the early 1970s[108] was noted due to a sudden increase in the sales of iridium. The active metals are supposed to be well distributed forming bimetallic (in case of platinum and iridium) clusters, but are also temperature-sensitive against sintering.[109] Typical amounts of active metals, according to several US patents, are 0.2 to 0.7% for platinum, 0 to 0.7% for rhenium and 0 to 0.3% for iridium, mentioning bimetallic (Pt-Re or Pt-Ir) as well as polymetallic catalysts. Similar to the cases presented in section 4.4.2, a good balance between the acidic function (for isomerisation and hydrocracking) and the metal centres for dehydrogenation reactions needs to be found.[110]

The reason for the implementation of rhenium into the platinum group metal catalysts is that the resulting catalysts are often exceptionally resistant to poisoning by nitrogen, sulphur and phosphorus and find their applications in hydrogenation of fine chemicals.[111]

4.7. 1,2-propanediol

As mentioned before, the two main products of the hydrogenolysis of glycerol are 1,2-propanediol and 1,3-propanediol. Even though 1,3-propanediol is usually considered the commercially more valuable isomer, the amount of 1,2-propanediol produced (> 10^6 t/year)[112-113] is one magnitude higher than the one of 1,3-propanediol. Similar to the latter, the commercial interest in the production of 1,2-propanediol from glycerol has increased significantly in the past decade, due to high yields obtained in new catalytic processes, the good availability of low-cost glycerol and the use of relatively inexpensive catalysts, with copper being the main metal.[112] The traditional industrial synthesis route for 1,2-propanediol is based on petrochemical resources, namely propylene and its derivatives like propylene oxide which is hydrated to give 1,2-PDO.[114]

1,2-propanediol is mainly used in the synthesis of polyesters (about 45%), other significant applications are the use as de-icing agent for planes and vehicles (substituting ethylene glycol for environmental reasons) as well as for food conservation and as a wetting agent.[114]

In the literature, a large variety of metals has been studied for the heterogeneously catalysed hydrogenolysis of glycerol to 1,2-propanediol, among noble metals like platinum, rhodium, palladium and ruthenium and other metals like copper, nickel, zinc, aluminium, iron, cobalt and magnesium.[115]

The best results have been obtained with copper catalysts, due to the tendency of the classic noble metals to catalyse C-C-scission, which limits especially the selectivity, like in the case of the extensively studied ruthenium catalysts.[116-118] Platinum, on the other hand, lacks activity and hence nullifies the good selectivity.[83] However, running the reaction in a basic medium or using basic co-catalysts clearly enhanced the performance of ruthenium as well as platinum catalysts, decreasing the gap to the copper catalysts.[119-120]

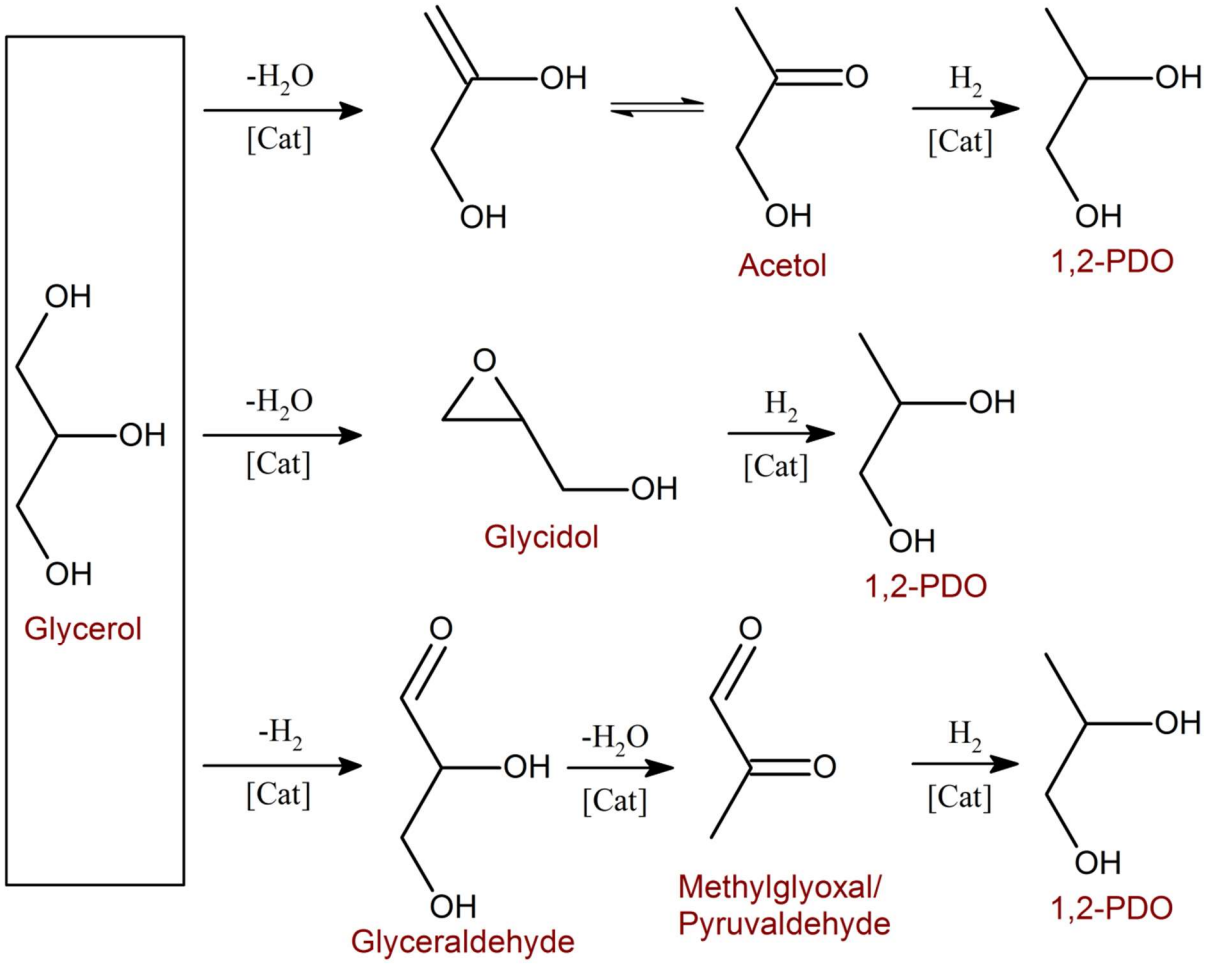

Figure 14 Selection of three reaction routes proposed in the literature. At the very top, the same reaction that has been shown in Figure 7, glycerol is dehydrated to acetol and then hydrogenated to 1,2-PDO.[121] Another suggestion is the formation of glycidol from the dehydrated glycerol, followed by the hydrogenation.[122] At the very bottom, the suggestion of a dehydrogenation to glyceraldehyde, followed by dehydration to methylglyoxal and hydrogenation to 1,2-PDO.[83]

With heterogeneous catalysts, the hydrogenolysis to 1,2-PDO has been successfully carried out in liquid and in gas phase, in both cases Cu/ZnO catalysts, often combined with other components, like Al_2O_3, gave very good results. Works in our group achieved very high selectivity and yields in liquid and in gas phase with Cu/ZnO catalysts with a clear correlation between copper surface area and catalyst activity[57] and also the highest space-time-yields for copper catalysts so far.[123] Besides, a

solution for the immense problem of catalyst deactivation could be found by incorporation Ga_2O_3 into the catalyst, leading to a stable (and reusable) catalyst resisting to even harsh conditions of 493 K in the presence of water and reaching space-time-yields of 22.1 $g_{1,2\text{-PDO}}$ / (g_{Cu}·h), setting a new benchmark for upcoming catalytic systems.[124]

Some of the mechanisms proposed for the hydrogenolysis of glycerol to 1,2-propanediol are similar to the ones presented before, for 1,3-propanediol (see Figure 14).

While the reaction routes pictured in Figure 14 assume an acidic site to catalyse the dehydration and the metal site to be responsible for the hydrogenation, Sato et al. proposed a different dehydration mechanism on copper sites, postulating a homolytic dissociation of the O-H bonding on a copper surface (see Figure 15) as the first step that leads to the breaking of the terminal C-O bond with the arising hydroxyl radical being stabilised on the copper surface. The resulting acetol is then hydrogenated to 1,2-propanediol, analogue to what has been shown before.

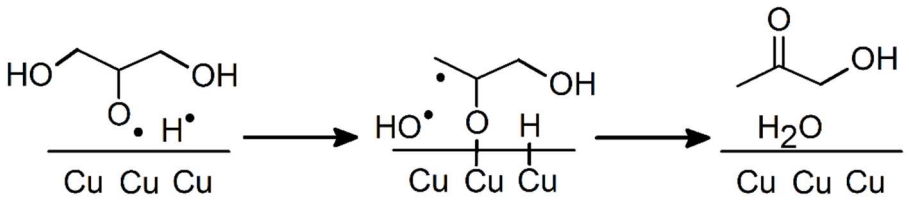

Figure 15 Key step of the radical mechanism of glycerol dehydration on a copper surface, proposed by Sato et al.[86]

In comparison to the results of the works aiming for 1,3-propanediol, the yields of the works looking for 1,2-propanediol have been a lot higher than the ones of the former studies. 1,2-PDO yields of more than 90% are possible whereas no good solution has been found for 1,3-PDO, yet, and any promising result, like yields of more than 60%, have important drawbacks such as very high amounts of catalysts and low space-time-yields. One of the main causes for this inequality might be the higher stability of acetol as the main intermediate on the way to 1,2-PDO, compared to 3-hydroxypropanal as the respective intermediate for the formation of 1,3-PDO.

The hydrogenolysis of glycerol to 1,2-propanediol has also been investigated using homogeneous[125-126] or biochemical[127-128] catalysts, however, as this work is focussed on heterogeneous catalysis, those publications will not be explained in more detail here.

5. Assignment of tasks

The aim of this work is to examine catalysts for the heterogeneously catalysed selective hydrogenolysis of glycerol to 1,3-propanediol and to gain a better understanding of the catalytic cycle for a future improvement of the catalyst. The selective formation of 1,3-propanediol is a difficult task and much harder to achieve than a selective formation of 1,2-propanediol, as has been explained before. However, the commercial value of 1,3-propanediol is much higher due to better properties of derivative products, especially in case of polymers like polytrimethylene terephthalate (PTT). The ready availability of bigger and cheaper amounts of 1,3-propanedol is the limiting factor for the implementation in larger scale of these derivative products which would lead to a higher degree of substitution of fossil resources by renewable ones.

For this long term target, several goals have been defined for this work:

- Investigate the influence of the support material, using commercially available materials which are used as received or after a simple treatment. The preparation of the catalyst has to be done in a way that is easy to reproduce and suitable for scale-up.
- Investigate the role of the active metals, focussing on established bimetallic iridium-rhenium catalysts, but also evaluating other noble metals.
- Find the appropriate pre-treatment in order to achieve a good performance of the catalyst.
- Evaluate other parameters that might influence the performance of the catalyst, like air contact before the reaction, acid addition or the direct contact with the reactor wall. Some of these parameters have been mentioned by other authors before, but were not always well explained or thoroughly investigated.
- Postulate a mechanism for the catalysed hydrogenolysis with as many details as possible, merging the results of the investigations mentioned before, influences of other reaction parameters and results from the numerous characterisation techniques to examine the catalyst (e.g. BET, Chemisorption, DRIFTS, TPDRO, TEM) and the reaction (NMR of reactions with deuterated species).
- If everything runs perfect, a more efficient catalytic system will be developed still within the time of this work, in any other case, the results of this work should be a basis for other researchers to enable the development of a more efficient catalyst for the hydrogenolysis of glycerol.

6. Experimental

6.1. Catalyst preparation

The catalysts were prepared by impregnation of the support material with the respective metal precursor(s). The following precursors were used: NH_4ReO_4 for rhenium, $H_2IrCl_6 \cdot x\ H_2O$ (standard) or $IrCl_3$ for iridium, $H_2PtCl_6 \cdot 6\ H_2O$ for platinum, $RhCl_3 \cdot x\ H_2O$ for rhodium and $RuCl_3 \cdot x\ H_2O$ for Ruthenium.

Table 1 Overview over the different metal precursors employed in the catalyst preparation. In case of an unclear amount of crystal water, the metal mass ratio was estimated.

Metal	Precursor	Metal mass ratio
Iridium	H_2IrCl_6 or $IrCl_3$	40% / 50%
Platinum	$H_2PtCl_6 \cdot 6\ H_2O$	38%
Rhenium	NH_4ReO_4	69%
Rhodium	$RhCl_3 \cdot x\ H_2O$	40%
Ruthenium	$RuCl_3 \cdot x\ H_2O$	49%

The precursor was dissolved in an appropriate amount of water and then impregnated onto the dry catalyst support by adding the solution and mixing with a Teflon-protected spatula, thus avoiding iron contamination of the catalyst. The catalyst was then dried at 383 K overnight and in case of a bimetallic catalyst, the impregnation procedure was repeated with the respective other precursor. In most cases, a noble metal was deposited in the first impregnation, followed by rhenium in the second step.

After drying, the impregnated support was either calcined or reduced before being brought into the reactor. Standard reduction conditions were 503 K (heating rate 10 K/min) for 1 hour at a hydrogen flow of 100 mL/min for 1 g of catalyst. The catalyst was then weighed (with air contact) and placed into the reactor. In case of a calcination, the impregnated support was either calcined in flowing air (30 mL/min) or in a muffle furnace at 773 K (heating rate 10 K/min) for 3 hours, followed by a reduction *ex-situ* (see description above) or *in-situ*. In case of the reduction *in-situ*, the catalyst (either calcined or pre-reduced, in order to avoid the dissolving of the precursors) was placed together with a certain amount – usually 50 g – of water in the reactor and heated up to 473 K at a hydrogen pressure of 7 MPa for 1 h. After cooling to room temperature, glycerol and water was added, resulting in a 20% wt. solution of glycerol and the reaction was started as described in section 6.3.

H-ZSM-5 was formed by calcination of NH_4-ZSM-5 at 873 K for 2 h in a muffle furnace. ZSM-5 is a medium pore (5.1-5.6 Å) silica-alumina zeolite with three-dimensional channels defined by 10-membered rings, firstly synthesised in 1972 by Argauer and Landolt of Mobil Oil Corporation.[129] This zeolite is usually supplied as NH_4-ZSM-5 because ammonium ions lead to a higher concentration of aluminium (and therefore acidic sites) close to the surface of the ZSM-5 zeolite, due to the preferential interaction with aluminate rather than with silicate anions, during the nucleation stage.[130]

6.2. Catalyst characterisation

Some catalysts were characterised by X-Ray Diffraction (XRD) in a powder diffractometer StadiP (Fa. Stoe & Cie. GmbH, Darmstadt) in transmission geometry on flat sample carriers using $Cu_{K\alpha1}$-radiation (wavelength: 1.5406 Å, Ge[111]-monochromator).

For the DRIFTS-studies (Diffuse reflectance infrared Fourier transform spectroscopy), an auxiliary equipment for measurements in diffuse reflection (Diffuse Reflection Accessory DRP-XXX by Harrick) was integrated into a conventional IR spectrometer (BRUKER IFS 55). Within the auxiliary equipment, a patented reaction cell[131] was fitted, in which the sample and the reference can be swapped by a step motor. In order to keep the sample dry, measurements were usually conducted at 393 K under a small N_2 flow of either 5 or 10 mL per minute, unless in case of pyridine adsorption which was performed at 313 K, followed by heating to higher temperatures.

Transmission electron microscopy (TEM) measurements were performed using a Model JEM2100F (JEOL, Tokyo, Japan) operating at 200 kV. The samples were dispersed in ethanol and dropped on a carbon coated copper grid, followed by a light carbon coating to minimize charging under the incident electron beam.

Several catalysts and support materials were analysed by temperature programmed desorption of ammonia (NH_3-TPD) on a Micromeritics Autochem II equipment. Samples of around 50 mg of catalyst were pre-treated *in-situ* for 1 h at 503 K in 10%vol. H_2/He and then cooled under helium to 323 K, followed by saturation with ammonia at this temperature for 15 minutes. After another 30 minutes of helium flow, desorption started with a heating rate of 10 K/min until 973 K.

The temperature programmed reduction (TPR) was performed on a TPDRO Porotec 1100. Samples of approx. 100 mg were dried *in-situ* under an argon flow of 15 mL/min at 433 K for 30 minutes before the TPR measurement. Alternatively, in some cases the sample was pre-treated in 4.91% oxygen in

helium at 473 K (10 K/min, 10 minutes hold; 10 mL/min flow rate). For the reduction, 50 mL/min 5.1% hydrogen in argon was passed at a heating rate of 5 K/min, the hydrogen consumption was measured by a thermal conductivity detector (TCD), comparing incoming and outgoing gas flow. In case of the precursors and the calcined Ir-Re bimetallic catalyst, with the original oxidation states of the deposited metals known, the final oxidation state of iridium OS_{Ir} and rhenium OS_{Re} (assuming a complete reduction of iridium) could be calculated:

$$\boldsymbol{OS_{Ir} = 4 - 2\frac{n_{H_2}}{n_{Ir}}} \tag{6.1}$$

$$\boldsymbol{OS_{Re} = 7 - 2\frac{n_{H_2} - 2n_{Ir}}{n_{Re}}} \tag{6.2}$$

The same equipment (TPDRO Porotec 1100 with TCD) was used for CO pulse chemisorption measurements. After an *in-situ* reduction treatment at 473 K for 1 h (50 mL/min pure hydrogen), the sample of approx. 200 mg was cooled to 273 K and pulses of 0.473 mL CO were passed over the sample every 10 minutes. The carrier gas was hydrogen (30 mL/min).

6.3. Catalyst evaluation

The reactions were carried out in two stainless steel autoclaves, one in Campinas, Brazil, and one in Darmstadt, Germany. Both reactors were Parr pressure autoclaves equipped with a thermo couple, a stirrer and a tube to take samples. However, the sampling part was demounted during the project due to rising awareness of possible poisoning by iron contact of the solution. Therefore, an inserted Teflon vessel was used for most reactions in the second part of the project and almost all results presented in this work originate from these experiments (with the Teflon vessel, in Darmstadt).

Figure 16 The stirrer (Darmstadt) after being enamel coated.

The reaction volume in Campinas was 500 mL, whereas the reactor in Darmstadt contained 300 mL. The latter one also possessed an additional tank for hydrogen storage, connected via a pressure regulator, which allowed to maintain a constant pressure throughout the reaction. To avoid iron contamination, the stirrer had been covered with an enamel coating by Muldenthaler Emaillierwerk GmbH, Penig, Germany (see Figure 16).

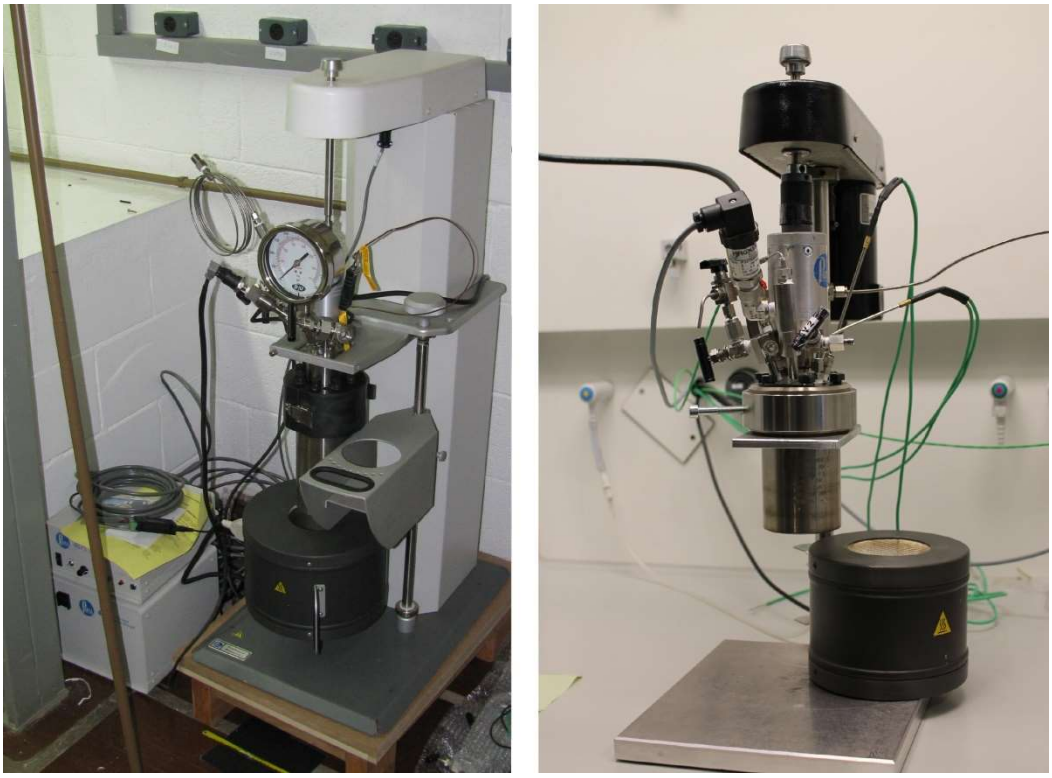

Figure 17 The pressure reactors in Campinas (left) and Darmstadt (right).

The reactions were carried out at temperatures between 393 and 473 K, taking about 30 minutes to heat up (see Figure 18). The reaction time was considered from the moment that the programmed temperature ramp reached the reaction temperature, the reaction was usually stopped after either 8 or 20 hours with some exceptions. Before heating up, the reactor was sealed and flushed at least three times with 1 MPa of hydrogen. The standard reaction pressure was 5 MPa of pure hydrogen and, unless stated differently, 880 mg of catalyst were used in 100 g of 20% wt. glycerol solution.

The samples were analysed by GC and GC-MS. In Campinas, an Agilent 6890 N gas chromatograph, equipped with a DB-WAX column and a flame ionisation detector (FID) was used, while in Darmstadt the analysis was carried out with a Shimadzu GC2010-plus, equipped with a split, a DB-WAX or Optima® Wax-plus column, an AOC-20i autosampler and a FID. 1,5-pentanediol (1,5-PDO) was used as an external standard in order to compensate fluctuations of the injected amount of sample. All major substances (glycerol, 1,2-PDO, 1,3-PDO, 1-propanol, 2-propanol, ethanol and ethylene glycol) were

calibrated individually and in mixtures similar to typical reaction solutions after the hydrogenolysis reaction, this calibration was verified from time to time. The peaks of other substances, like methanol, isopropyl-propyl-ether, dipropyl-ether, 3-ethoxy-1-propanol and 2-isopropoxy-1-propanol, which appeared in very small quantities (< 1%), were converted into concentrations by employing an estimated response factor for each substance, estimated by comparing to known substances with similar retention times. Each sample was measured three times, A_{Peak} therefore refers to the mean peak area determined from the three measurements.

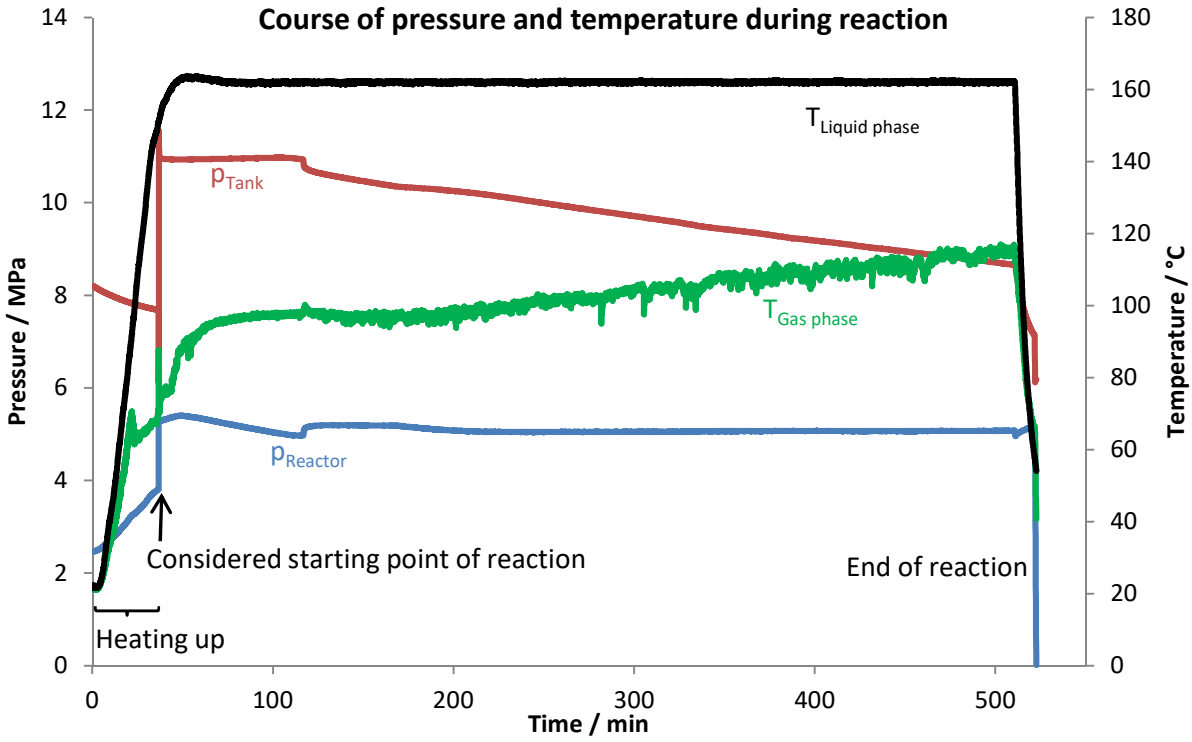

Figure 18 Typical course of pressure and temperature during a hydrogenolysis reaction at 160°C for 8 hours. After a heating ramp of 30 minutes, the pressure inside the reactor was adjusted to 5 MPa, the hydrogen tank was filled up and the reaction was considered to start at this moment, in spite of the temperature reaching its final value only a few minutes afterwards. The fluctuation of the gas phase temperature is due to condensation and evaporation of liquid on the temperature sensor. The refilling of the consumed hydrogen from the tank to the reactor, regulated by a valve, only started to work after a certain pressure drop in the reactor (in this case around 85 minutes after the reaction start). As can be seen in this graph, the hydrogen consumption stayed relatively stable throughout the reaction.

In some cases, the gas phase was analysed qualitatively by filling a 20 mL syringe with gas from the reactor and injecting it into a HP 5980 Series II gas chromatograph with an Rt-ShinCarbon ST packed column.

In case of ambiguous GC peaks, the sample was analysed in a Shimadzu GC2010plus (column: DB-WAX), connected to a QP2010-SE mass spectrometer. This system was also used to measure the mass spectrum of deuterated species (as in Figure 52, page 79).

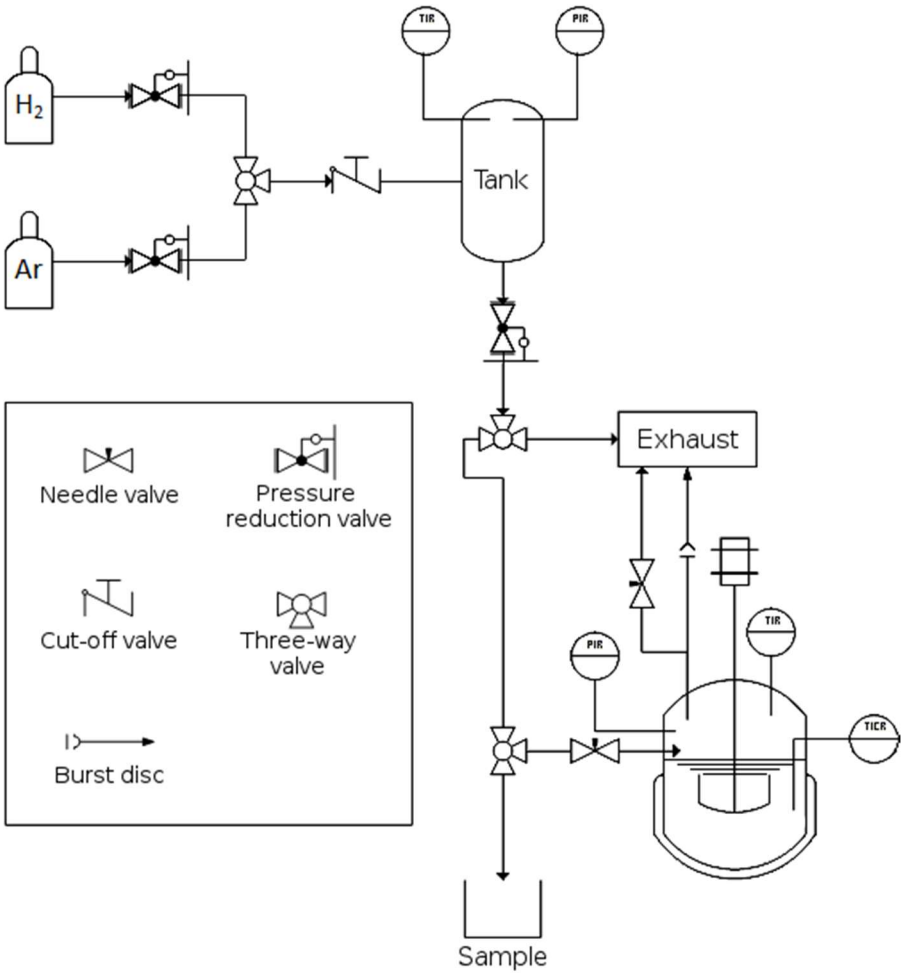

Figure 19 Design of the reaction system for the hydrogenolysis of glycerol. The system was designed to maintain a constant pressure within the reactor by refilling the consumed hydrogen. The controlled parameters were reactor and tank pressure as well as the temperature of the tank and the liquid and gas phase inside the reactor. Drawing by Hauke Christians.

The calculation of selectivity and conversion was performed as follows:

First of all, the response factor f of the standard 1,5-pentanediol was determined from the GC peak area A_{Peak} and the known concentration c of the standard (usually between 15 and 20 mmol/L).

$$f_{1,5\text{-PDO}} = \frac{c_{1,5-PDO}}{A_{Peak,1,5-PDO}} \tag{6.3}$$

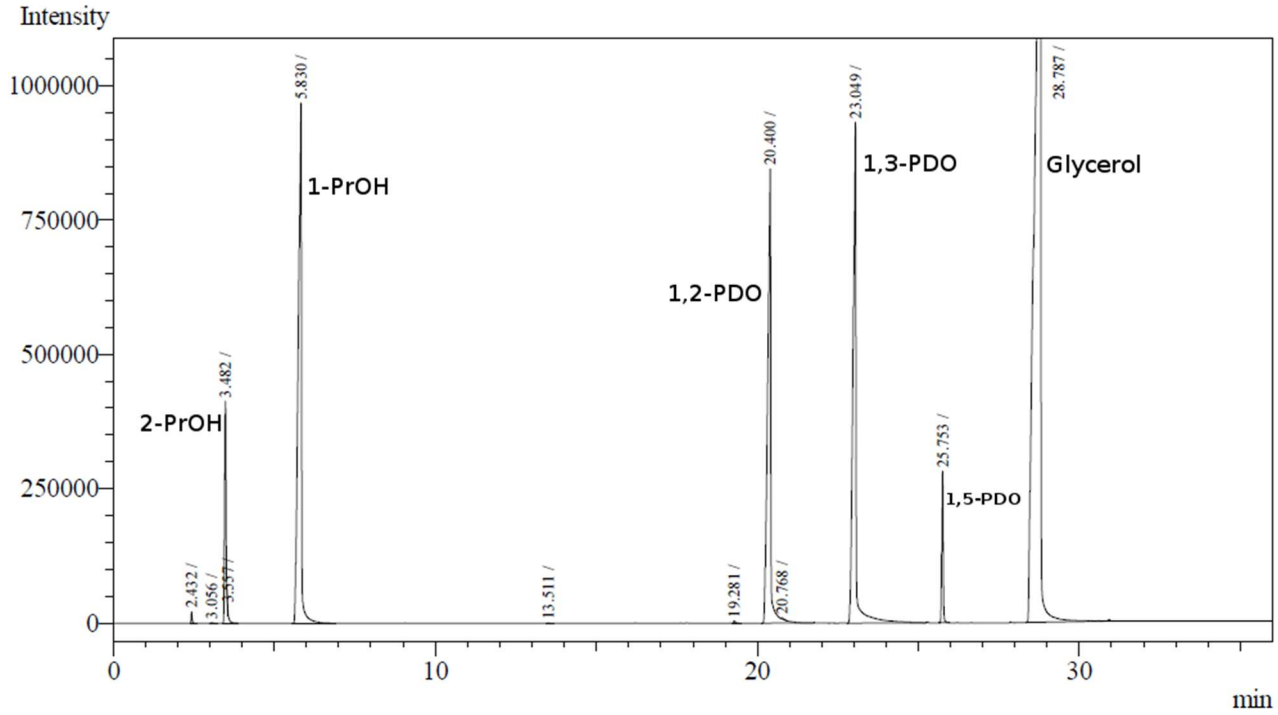

Figure 20 Typical gas chromatogram of the final reaction solution, showing the peaks of the main products 2-propanol (2-PrOH), 1-propanol (1-PrOH), 1,2-propanediol (1,2-PDO) and 1,3-propanediol (1,3-PDO) as well as the standard 1,5-pentanediol (1,5-PDO) and the remaining glycerol (peak not shown entirely due to height).

With the response factor of the standard, the response factor for each component can be calculated by multiplying the response factor of 1,5-PDO with a factor *a* determined by the calibration for each component, due to the fact that some substances cause a larger peak area than others at the same concentration. A very strong example was 2-propanol with a factor of $a_{2\text{-}propanol} = 3.5$ while the factor for 1,3-propanediol was only 1.9 within the typical (and calibrated) concentration range. This means that if the peak area of 2-propanol and 1,3-propanediol was equal, the concentration of 2-propanol would be almost twice the concentration of 1,3-PDO.

$$\boldsymbol{f_i = a_i \times f_{1,5\text{-PDO}}} \tag{6.4}$$

With the response factor for each component, the respective concentration can be calculated from the GC peak area.

$$\boldsymbol{c_i = f_i \times A_{Peak,i}} \tag{6.5}$$

With all concentration known, the selectivity *S* of each component in the liquid phase can be determined by dividing the respective concentration by the sum of all product concentrations Σc_i. This only counts for the liquid phase, because the gas phase was analysed sporadically only, as the vast majority of the products remained in liquid phase. Also the number of carbon atoms was not included

in the calculation due to the fact that all major products contained three carbon atoms, just like glycerol.

$$S_{i,liquid} = \frac{c_i}{\sum c_i} \tag{6.6}$$

The conversion X was determined in two ways, once (labelled X_1) by adding up all found products and once (labelled X_2) with the quantity of glycerol left after the reaction $c_{Glycerol,end}$. The initial glycerol concentration $c_{Glyerol,0}$ was assumed to be 2170 mmol/L.

$$X_1 = \frac{\sum c_i}{c_{Glycerol,0}} \tag{6.7}$$

$$X_2 = 1 - \frac{c_{Glycerol,end}}{c_{Glycerol,0}} \tag{6.8}$$

The two ways of calculating the conversion usually led to very similar results with a difference of less than 3%. Only in some cases, especially at higher temperatures and with catalysts containing ruthenium or rhodium, X_2 tended to be larger than X_1, due to the considerable formation of gaseous products under these conditions. For small conversions below 10%, only X_1 was considered because the absolute error margin of the big glycerol peak was much higher than of the small product peaks. The conversions depicted in chapter 7 usually show a mean conversion, except in special cases as the ones mentioned above.

The yield Y for 1,3-propanediol was calculated from the concentration of 1,3-PDO found, divided by the theoretical maximum concentration that could be reached (equal to the initial glycerol concentration). This method was considered more accurate than the multiplication of conversion and selectivity due to the lower error margin in case of the smaller peak of 1,3-propanediol, compared to the much bigger one of the remaining glycerol, beside the tendency of glycerol to form an irregular peak. Moreover, the formation of gaseous products will not have any influence in this case.

$$Y_{1,3-PDO} = \frac{c_{1,3-PDO}}{c_{Glycerol,0}} \tag{6.9}$$

The space time yield STY is calculated by dividing the concentration of 1,3-propandiol by the volume of the reaction solution V_R, the catalyst mass m_{Cat} and the time of reaction t_R.

$$STY_{1,3-PDO} = \frac{c_{1,3-PDO}}{V_R \times m_{Cat} \times t_R} \tag{6.10}$$

7. Results and discussion

At the beginning of this study, several catalytic tests were performed with the aim of finding new catalysts that had not been used for this reaction so far. The idea was to find an innovative solution to improve the reaction outcome and possibly also lower the cost of the catalyst material. However, the tested materials were not able to outperform the silica-based iridium-rhenium catalysts described in the literature which was the reason to shift the focus of this work towards the understanding of the (still controversial) reaction mechanism.

During the experiments, several different parameters have been changed in order to investigate the influence of every single one onto performance and selectivity, aiming to gain a better understanding of the catalyst and the mechanism of the reaction. First, the results will be presented separately for each parameter (section 7.3 to 7.8), followed by a summary in which the results are combined in order to draw the conclusions. Parameters examined in smaller scale with few experiments, e.g. acidity, are allocated in the bigger sections, wherever mentioning them makes most sense.

7.1. Initial tests of new catalytic systems

7.1.1. Tungsten carbide systems

Based on the findings by Iglesia, Ribeiro, Baumgartner, Levy and Boudart about the similarity of the catalytic behaviour of tungsten carbide and platinum[132] and its ability to also work in hydrogenations, beside isomerisation reactions,[133-135] the synthesis was reproduced and the tungsten carbide was used alone, supported by carbon, doped with nickel (prepared by Cristiane Rodella)[136] as well as in combination with rhenium and later also iridium-rhenium for the hydrogenolysis of glycerol. Yet, despite of several attempts, the catalyst activity was very disappointing, moreover without any 1,3-propanediol produced, and the further investigation of tungsten carbide catalysts was discarded. For reaction details, see Table 8 in the annex.

7.1.2. Nickel containing catalysts

In order to reduce the catalyst cost and also to avoid the dehydration catalysed by copper (leading to 1,2-propanediol), a series of tests with nickel containing catalysts was carried out. Besides, copper was combined with rhenium in order to check if the selectivity towards the undesired 1,2-propanediol could be reversed. However, the selectivity to 1,3-propanediol was very low with an also low overall conversion. The results are shown in Figure 21 with a selection of reactions under comparable reaction and pre-treatment conditions. Besides, some commercial nickel catalysts without rhenium were tested, namely Leuna 6503T (Ni/SiO_2) and Leuna Y43374 (Ni/ZrO_2), but produced almost exclusively 1,2-

propanediol at low conversions (< 5% after 22 h at 463 K) without forming any 1,3-propanediol. For more details, see reactions 4 to 9, 16, 58 and 60 in Table 8 in the annex.

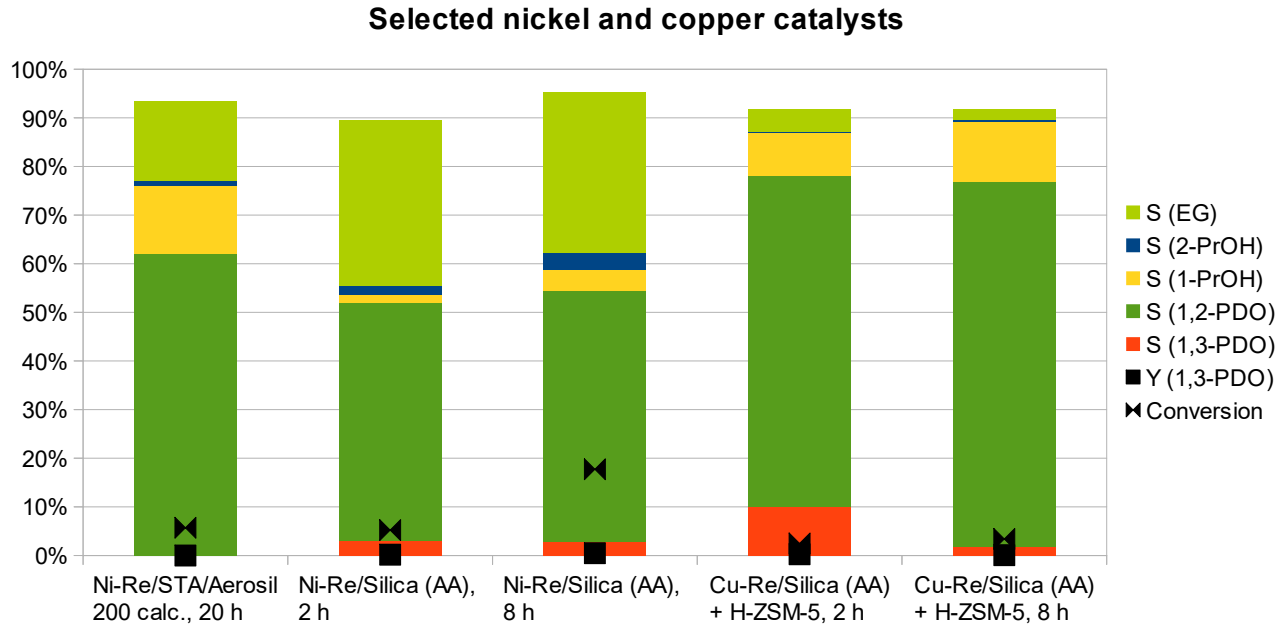

Figure 21 Selected reactions with catalysts containing copper and nickel, in combination with rhenium, at different reaction times under similar conditions, at 200°C and 5 to 5.4 MPa H_2. For detailed reaction and pre-treatment conditions, please see # 16, 58 and 60 in Table 8 in the annex. STA: Silicotungstic acid; Silica (AA): Silica provided by Alfa Aesar; calc.: calcined in air at 400°C for 3 h before reduction *ex-situ* at 300°C for 1.5 h.

Hence, experiments with nickel were not continued.

7.1.3. Catalysts with silicotungstic acid (STA)

With the intuition to exploit the promotional influence of tungsten reported in the literature, a series of catalysts containing silicotungstic acid was prepared and used in the hydrogenolysis reaction. Figure 22 shows a selection of the results with comparable catalysts. The silicotungstic acid was deposited on silica, in this case Aerosil 200, and calcined in static air at 623 K for 4 hours. Platinum, iridium, nickel (see section 7.1.2) and rhenium have been used as active metals with different preparation methods like calcination, reduction or a combination of both, in some cases after each impregnation step. With the findings of the influence of pre-treatment being the same as the ones presented in section 7.6 in more detail for other catalysts, these results will not be presented here. The best results in terms of selectivity and conversion, achieved with catalysts that were only reduced after the impregnation of the metals, are presented in Figure 22. Despite certain improvements in the catalytic activity compared to previous experiments, the implementation of zeolite as the support for bimetallic rhenium-containing catalysts in consecutive experiments led to a further increase in the formation of the desired 1,3-propanediol, clearly outpacing the tested tungsten containing catalysts. Due to these results, tungsten

was not furtherly investigated, except of one case in which tungstic acid was used as an additive, but resulted in an undesired effect with a strong catalyst deactivation (see #193 in Table 8 in the annex).

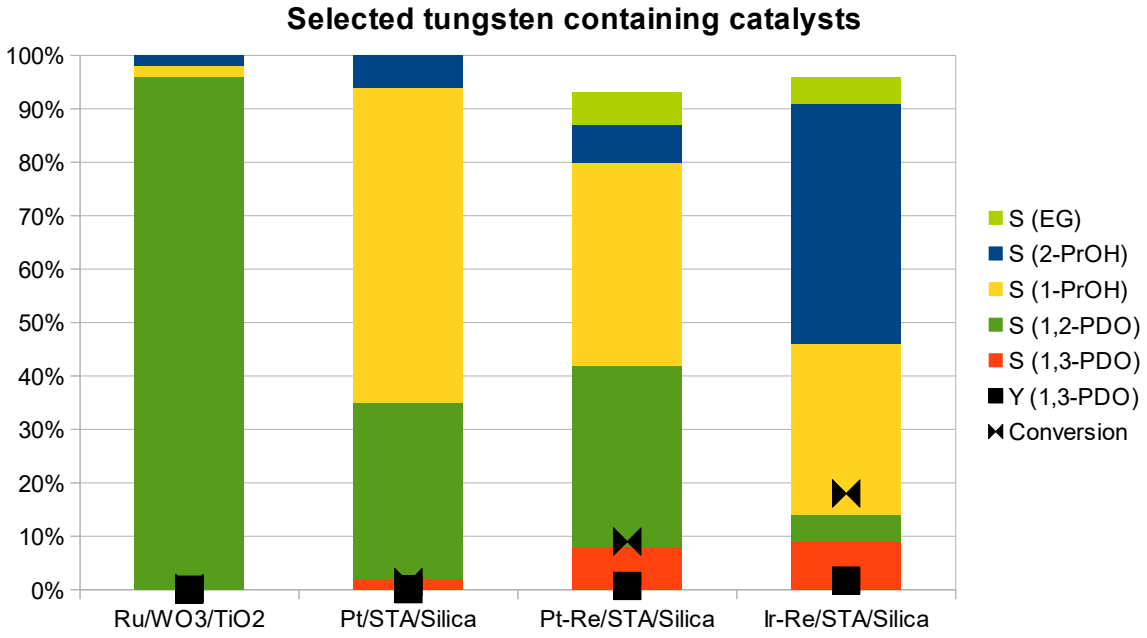

Figure 22 Selection of the results of experiments with tungsten containing catalysts with somewhat comparable reaction conditions, at 170°C ($Ru/WO_3/TiO_2$) or 200°C (Silica based catalysts). For detailed reaction and pre-treatment conditions, please see # 7, 15, 17 and 23 in Table 8 in the annex. STA: Silicotungstic acid; Silica: Aerosil 200.

7.2. Time dependent measurements

Due to the poisoning of the catalyst by iron, explained in section 7.4, the steel tube for sample collection was not used in most of the experiments. However, before the observation of the influence of iron and also in some later experiments, samples have been taken during the reaction in order to observe the reaction over time for a better understanding of the general processes and to reduce the risk of having any unnoticed anomalies.

Figure 23 depicts two examples of the evolution of reactions during the experiments in Campinas. The conversion increased almost linearly throughout the reaction whereas the selectivity behaved as expected, with an increase of propanols and a decrease of propanediols. The variation of the selectivity to 1,2-propanediol with reaction time is stronger than in the case of 1,3-propanediol, due to the higher reaction rate of the consecutive reaction of 1,2-propanediol that was mentioned in the literature and also found in this study, as will be shown in Table 3 on page 64. Aside from a small deviation of the data points at 20 h reaction time in the graph on the left-hand side of Figure 23, probably caused by experimental inaccuracies, the obtained results correlate well.

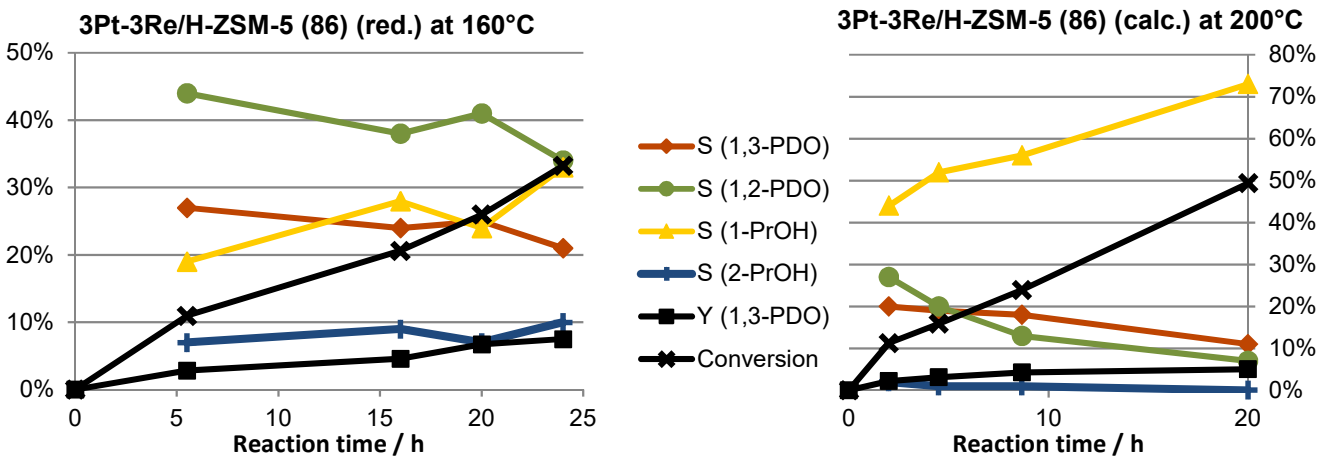

Figure 23 Evolution of the reaction over time shown for 3Pt-3Re/H-ZSM-5 (86) (reduced at 230°C) at 160°C and 3Pt-3Re/H-ZSM-5 (86) (calcined at 500°C) at 200°C, in both cases in a 500 mL reactor at 5 MPa H_2, 1.2 g_{Cat} and 125 – 130 g of 20%wt. aqueous glycerol solution.

Two of the experiments in Darmstadt, of which more than one sample was taken, are shown in Figure 24, confirming the trends mentioned before. No strong deactivation can be observed in the course of the reaction, even though there seems to be an elevated initial activity in some cases. Besides, the decrease of propanediol selectivity and the increase in propanol can be observed as well.

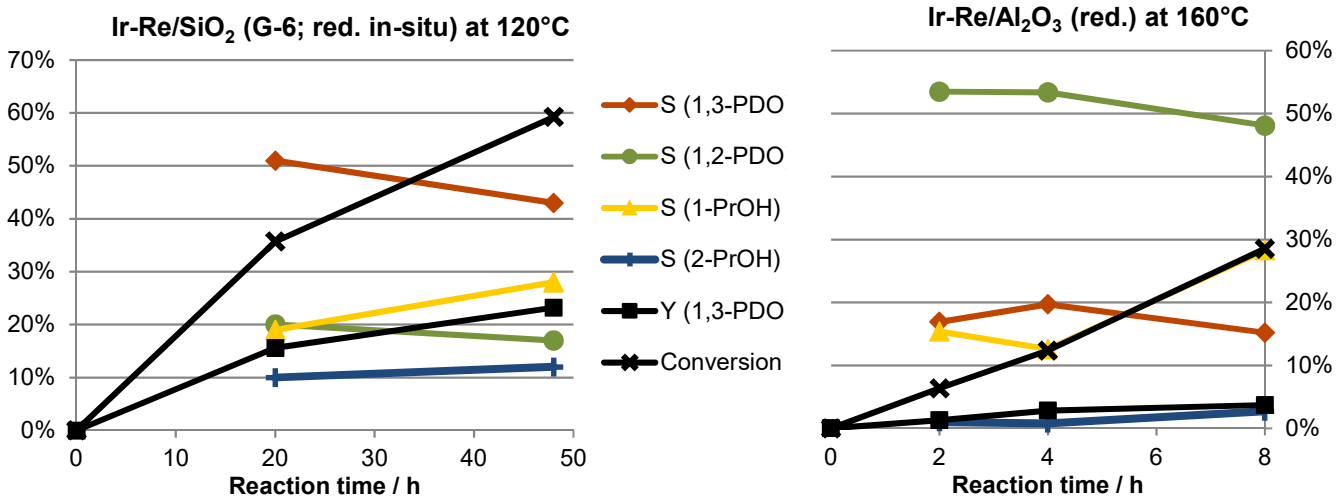

Figure 24 Evolution of the reaction over time shown for Ir-Re/SiO_2 (G-6) (reduced at 230°C and reduced in-situ at 200°C) at 120°C and Ir-Re/Al_2O_3 (reduced at 230°C) at 160°C, in both cases in a 300 mL reactor at 5 MPa H_2, 880 mg_{Cat} and 100 g of 20%wt. aqueous glycerol solution. The last sample was taken from the open reactor after cooling down.

Unless specifically mentioned, all results presented in this work are based on samples that were taken after opening the reactor. The reason for this measure is that the quantity of sample taken during reaction had to be limited to avoid taking out significant amounts of solution and thereby changing the ratios of solution, catalyst, reaction volume etc. On the other hand, the limited sample quantity bears the risk of not representing the actual composition of the reaction solution; hence, a compromise

needed to be found in between the two extremes. The difference between the last sample, at the end of the reaction, and the sample after opening the reactor was small in all cases, but some repeated discrepancies could be noticed. In most cases, the concentration of propanediols in the reactor was a bit lower than in the last sample taken through the tube whereas the concentration of the propanols was a bit higher, usually increasing the selectivity by 1% to 2%.

7.3. Influence of support

Several different supports have been tested in order to evaluate the influence of the support material upon the hydrogenolysis of glycerol. While no drastic change in selectivity was observed, the activity of the catalyst depended strongly on the support. In general, zeolites and silica supports gave the best results whereas carbon and alumina supports led to much lower conversions. But also within zeolites of the same type, strong differences were detected.

First of all, zeolites were tested, starting with ZSM-5: Comparing NH_4-ZSM-5 to H-ZSM-5, which was formed by calcination of NH_4-ZSM-5, the catalyst containing iridium and rhenium based on H-ZSM-5 was far more active than the one based on NH_4-ZSM-5, reaching 34% conversion versus 22% with very similar selectivities, after 8 hours of reaction at 433 K (see Figure 26). As will be discussed later, the acidic proton might play a role in the deposition of the metals which might be hindered with the presence of the ammonia cation. Due to the low performance of NH_4-ZSM-5, only H-ZSM-5 was furtherly investigated.

Several variations of the H-ZSM-5 zeolite were tested, with different Si/Al ratios and therefore also different acidic properties. A lower Si/Al ratio means that more aluminium is present and hence also more acidic sites. With the presumption of an acid-catalysed mechanism as proposed by several authors and discussed in section 4.4.2, a higher activity would be expected for aluminium-rich zeolites.

Interestingly, very low as well as very high Si/Al ratios showed – at similar selectivity – lower conversion than zeolites with a medium Si/Al ratio like 80 to 90 in the case of H-ZSM-5 and 150 in the case of H-BEA. Figure 25 also shows that a higher conversion usually leads to an increased formation of 1-PrOH, which seems to mainly be formed from 1,2-propanediol which is present in lower quantities in these cases. 2-propanol is formed in minor quantities only, similar to most literature results.

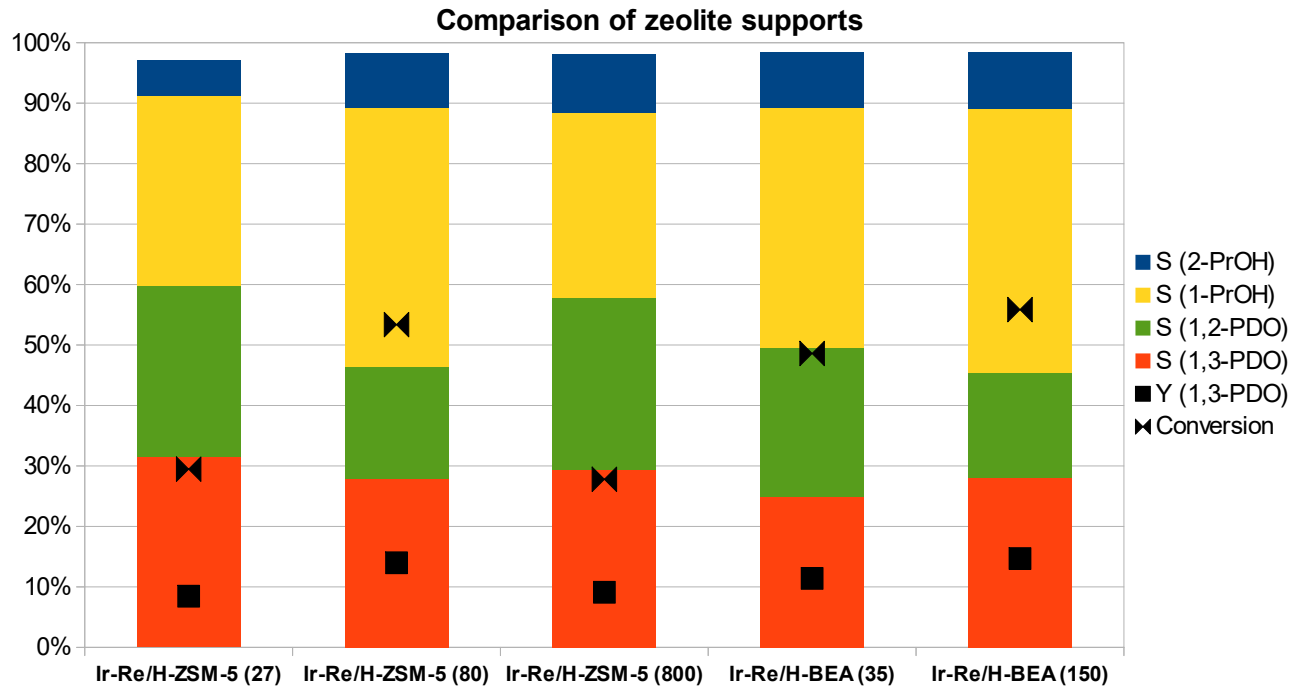

Figure 25 Conversion of glycerol and selectivity for several zeolite supported catalysts. Reaction conditions: 20%wt. aqueous glycerol solution, 160°C, 5 MPa H_2, 8 h.

In publications by the Tomishige group, generally a small amount of sulfuric acid was added to the reaction solution, which was reported to have an enhancing effect until reaching a ratio of H^+/Re of 1. As mentioned above, the explanation for this result was the assumption of the formation of inactive Re-O^- species in neutral or basic medium. However, this effect could not be found in any experiment in this study, acid addition of any type had either no or even an inhibiting effect on the reaction. One explanation might be that the reaction solution with the catalyst already was an acidic medium: The pH value of the product solution after the hydrogenolysis was measured in several occasions and always showed a pH of around 3 to 4, more or less the same as the initial solution of 20%wt. glycerol in water in the presence of a reduced Ir-Re/SiO_2 (G-6) catalyst. In contrast to that, the employed water, a 20%wt. glycerol solution in water and the glycerol solution in the presence of only the silica support (without the metals) showed neutral pH values close to 7. This means that either the metals introduce acidic sites, as proposed in the literature for Rh-Re,[79] or these sites are formed from a reaction of water with the metals on the catalyst, most likely with rhenium, forming a proton and some kind of species involving rhenium and the hydroxyl group, possibly as follows:

$$Re + H_2O \rightarrow [Re\text{–}OH]^- + H^+ \textit{ (simplified)}$$

In the literature, it was shown that rhenium in Ir-Re/SiO_2 (KIT-6, mesoporous silica) could be fully reduced to the metallic state to form an alloy with iridium when it was directly reduced from the precursor state.[70]

In the present study, the experiments comparing the reactions with and without acid addition were carried out with non-calcined catalysts that were reduced – usually *ex-situ* – before the reaction, whereas Tomishige and co-workers used calcined catalysts that were reduced *in-situ*. With the surface of the non-calcined catalysts containing completely reduced species of rhenium in an Ir-Re alloy, rhenium could react with water to form the acidic medium as mentioned above. The resulting structure might be, however, more complex than illustrated, due to the "spare" negative charge after the release of the proton, which needs to be allocated. In order to reach a pH value of 4, each rhenium atom would have to react with at least two water molecules, calculating with 0.19 mmol of Re and 4.44 mol of water and assuming that iridium does not react with water. Regarding the detection of around 1 to 2 Re-O bonds in the calcined and reduced catalyst with a total coordination number of around 7 to 8 for rhenium by the Tomishige group,[66, 82] these results sound reasonable and would also indicate a very high dispersity of rhenium on the catalyst surface of the present study. However, it is interesting that water seems to react more easily with the metals than air oxygen.

Connecting the measured pH values to the results of the hydrogenolysis, it seems that for non-calcined catalysts the addition of acid is obsolete due to the formation of the acidic medium when the catalyst gets in contact with the reaction solution. In the case of the fully reduced catalysts, the addition of more acid would not bring any benefit unless the proton was directly involved in the reaction mechanism.

In case of a bi-functional reaction mechanism based on dehydration on the acidic support like proposed in section 4.4.2, a higher number of acid sites should increase the reaction rate, which obviously is not the case so that no linear correlation can be postulated. However, the acidity or some other property of the catalyst changing with the Si/Al ratio seems to play an important role on the reaction rate.

Besides the zeolites and silica supports, some other support materials such as γ-alumina and several carbon materials have been tested but proved far less adequate for the hydrogenolysis reaction than silicon oxide containing catalyst supports. Figure 26 shows the performance of Ir-Re/Norit SX-1G as a representative for several tested catalysts based on carbon support materials that all led to very similar results. Compared to zeolite or silica based catalysts, the conversion was very low and the selectivity to 1,3-propanediol also did not differ greatly from the other catalysts, in spite of the low conversion which should favour the propanediols, due to their character as intermediate products. One possible cause for this difference in reactivity might be a formation of bigger metal particles that additionally might also be different in structure, resulting in a smaller surface area or other active sites. Another

possibility is the direct participation of the support in the catalytic cycle, for example providing adsorption sites for the reagents.

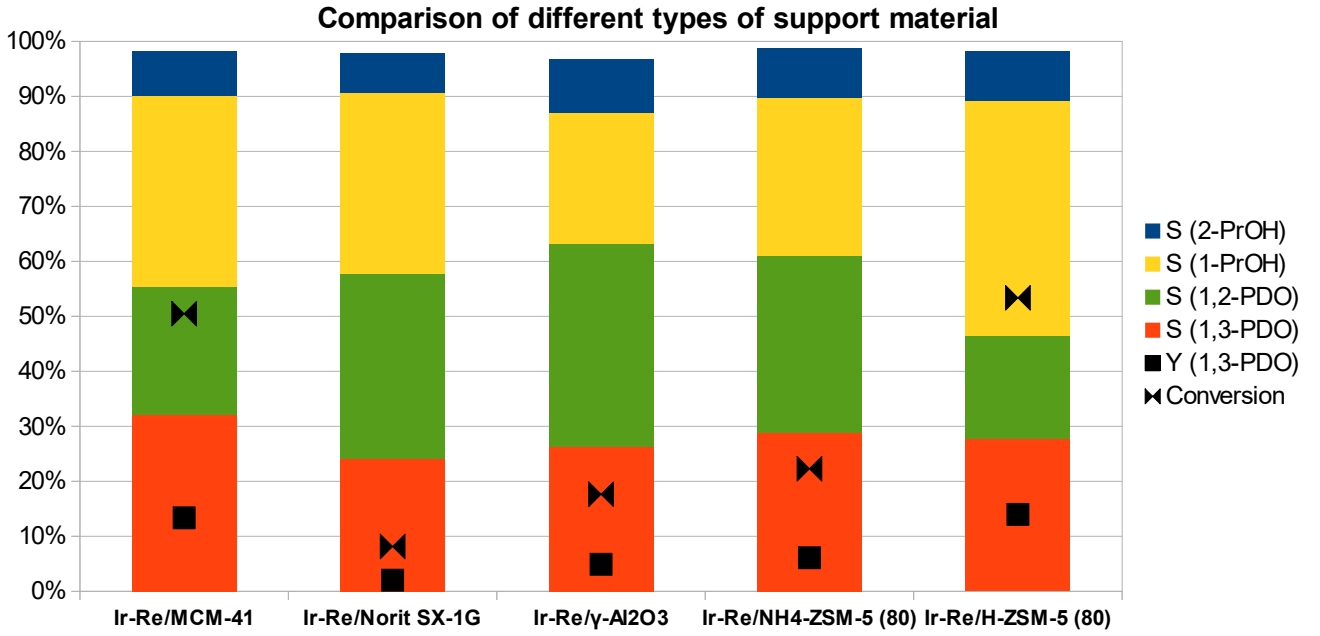

Figure 26 Comparison of the performance of Ir-Re catalysts based on zeolites and non-zeolite support materials with Norit SX-1G being a representative for several tested carbon materials. Reaction conditions: 20%wt. aqueous glycerol solution, 160°C, 5 MPa H_2, 8 h.

γ-alumina as a support material worked out better than the active carbon but clearly not as good as most zeolites and silica supports. The conversion after 8 h reaction time at 433 K stayed below 20%, however, it could be noted that the reaction is more likely to stop after the first step with a propanediol and less likely to produce a propanol, compared to catalysts based on other support materials. Ir-Re/γ-Al_2O_3 also appeared to be able to promote C-C scission under the given reaction conditions as small amounts of ethanol and ethylene glycol could be detected (selectivity of 2% and 1%, respectively, clearly more than with most other catalysts).

On the other hand, using MCM-41 as a support material for iridium and rhenium led to almost the same outcome as the use of H-ZSM-5 (80) or H-BEA (150), except of the different affinity to the formation of 1-propanol.

Within the diverse silica supports, the differences were rather small. As can be seen in Figure 27 and Figure 28, with few exemptions, selectivity as well as glycerol conversion was almost equal for all tested silica supports for iridium-rhenium. The lowest conversion was detected when using an Aerosil 200 silica support, when just 30% of the glycerol was converted, compared to 40 to 50% conversion achieved by catalysts based on most other silica or zeolite supports.

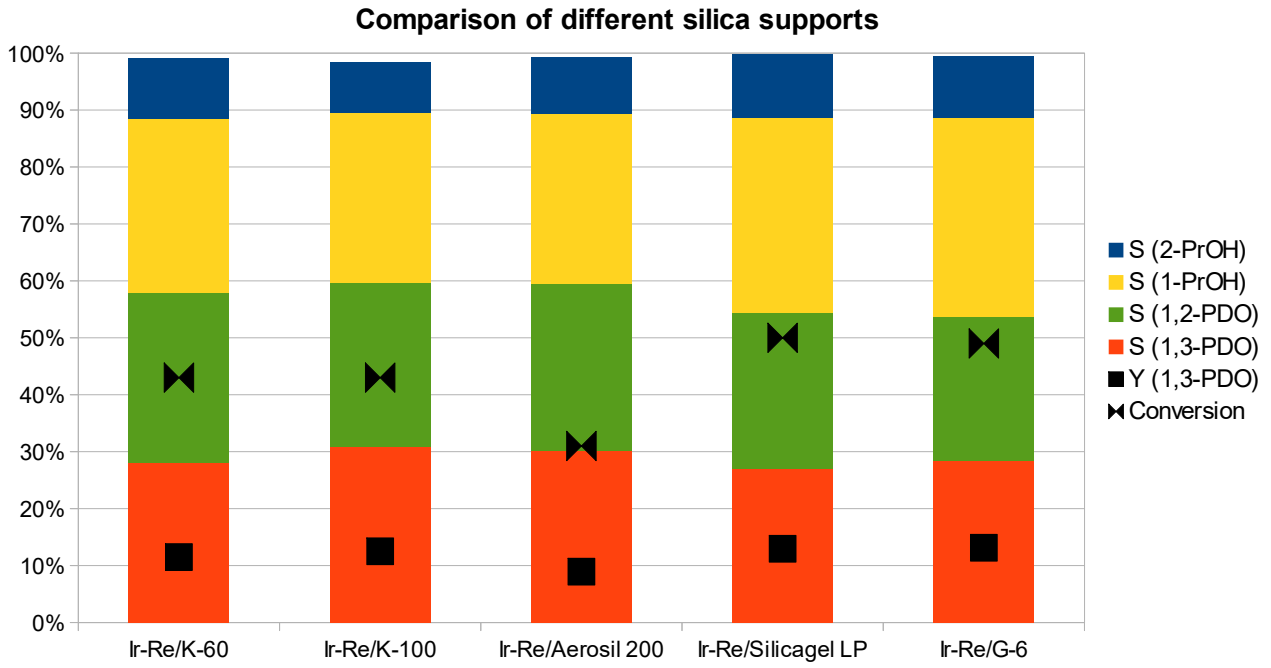

Figure 27 Comparison of different types of silica as support materials for the hydrogenolysis of glycerol. K-60 and K-100: Amorphous silica gel for chromatography (Kieselgel); Aerosil 200: Fumed silica gel; Silicagel LP: Large pore amorphous silica gel; Reaction conditions: 20%wt. aqueous glycerol solution, 160°C, 5 MPa H_2, 8 h.

The main difference between Aerosil and the other tested silica is that Aerosil is a fumed, pyrogenic silica and not derived from precipitation, therefore having no typical pore structure, in spite of the high surface area. After the unsatisfactory results in the preliminary experiments, Aerosil was not used in the further studies and also not thoroughly investigated. Two amorphous silica gels for chromatography (Kieselgel 60 and Kieselgel 100), characterised as spheres with a very narrow particle (40 to 63 µm and 200 to 500 µm, respectively) and pore size (60 Å and 100 Å, respectively) distribution, were also tested as catalyst supports and led to a somewhat lower conversion than catalysts based on G-6 silica, for example.

The G-6 silica has been the standard support material used by the Tomishige group and is one of a series of silica produced by Fuji Silysia Chemical Ltd. For this study, G-6, G-10, Q-6 and Q-10, each with a particle diameter of 75 to 150 µm, have been tested as support materials for the hydrogenolysis of glycerol. These silica show a remarkably narrow pore size distribution with the number after the letter indicating the typical pore size in Å (e.g. more or less 6 Å in the case of G-6 and 10 Å in the case of G-10). Unfortunately, the exact difference between the Q- and G-series remained unclear as both, according to the supplier, consist of 99.5% (G-6 and Q-6) and 99.8% (G-10 and Q-10) silica, respectively, with small impurities of mainly sodium and calcium, amounting to almost 500 ppm each.

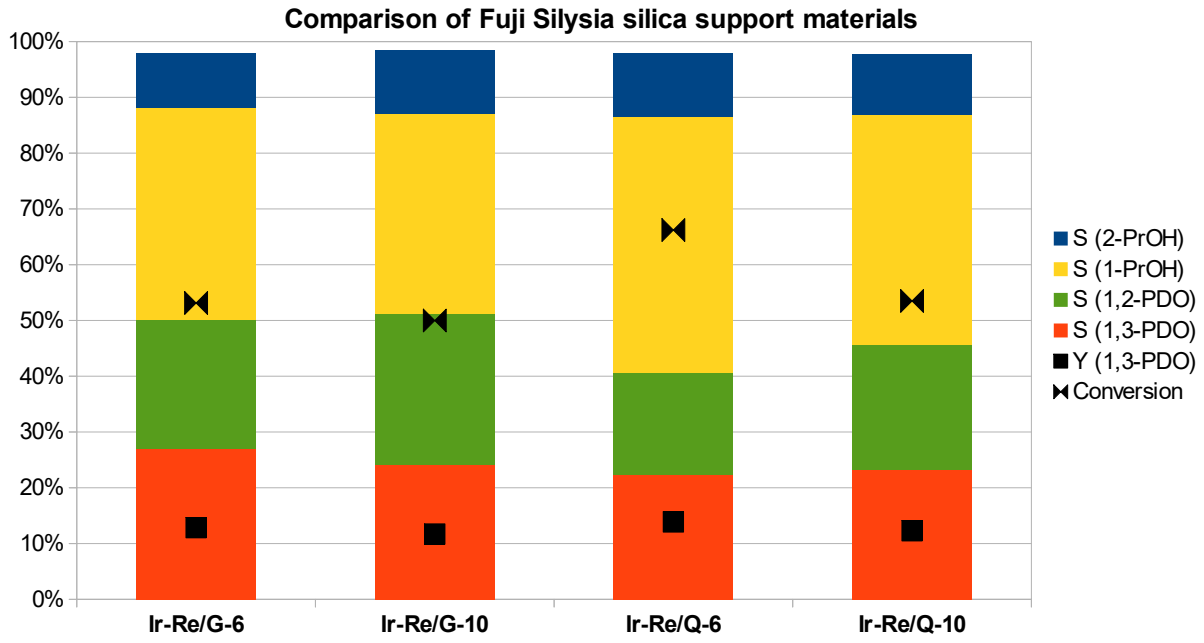

Figure 28 Comparison of several different SiO_2 support materials by Fuji Silysia Chemical Ltd. in the hydrogenolysis of glycerol at 160°C, 5 MPa H_2, 20%wt. glycerol solution and 8 hours reaction time.

This group of silica support material led to relatively high conversions without big effects on the selectivity. The conversion was clearly higher than with almost all other silica supports and on the same level with the "best" zeolites. The most active catalyst found was Ir-Re/SiO_2 (Q-6), however the yield did not increase much due to the progressing consecutive reaction. In order to have a better comparability with the results of the Tomishige group, which worked exclusively with G-6, the G-6 silica was usually used for the series of experiments.

Regarding the BET surface areas, no direct correlation could be found. As shown in Figure 28, Ir-Re/SiO_2 (G-6) and Ir-Re/SiO_2 (G-10) basically led to the same results, even though the G-6 silica has smaller pores and a clearly higher surface area of around 500 m^2/g, almost twice as much as the surface area of G-10 (270 m^2/g). On the other hand, several other silica supports, even with high BET surface areas like Kieselgel 60 (500 m^2/g), were less appropriate as support material for the hydrogenolysis reaction. An important characteristic of the support might be the pore structure: The silica supports provided by Fuji Silysia Chemical Ltd. had a very uniform pore structure in the range of pore diameters of up to 1 nm and led to very high conversions in the hydrogenolysis when compared to other silica supports.

The CO uptake of several catalysts with constant mass ratio of iridium and rhenium on different support materials was examined. As rhenium does not take up any CO, the informative value of these measurements is limited due to the formation of bimetallic particles with rhenium probably covering parts of the iridium particle.

Therefore, no conclusions about the particle size can be drawn from the experiments, but there are some hints about structural similarities. The results show that there is no direct correlation between the catalyst activity and the CO uptake. Ir-Re/SiO_2 (G-6) and Ir-Re/SiO_2 (G-10), for example, adsorbed different amounts of CO (25 and 69 $\mu mol_{CO}/g_{Catalyst}$, respectively), but exhibited very similar performance in the reaction test. On the other hand, carbon supported Ir-Re/Norit SX1 (31 $\mu mol_{CO}/g_{Catalyst}$) and Ir-Re/H-ZSM-5 (90) (37 $\mu mol_{CO}/g_{Catalyst}$) had similar CO uptakes, but very different activities in the hydrogenolysis of glycerol.

Measurements of pyridine adsorption on Ir-Re/H-ZSM-5 (90) as a model catalyst showed that several types of acidic sites are present. Bands at 1447 cm^{-1} and 1600 cm^{-1} that disappear simultaneously (see Figure 29 and Figure 30) when the outgassing temperature passes 370 K belong to the formation of H-bonded pyridine molecules.[137] In this case, the pyridine binds to superficial OH-groups without forming an ionic species. It can also be observed that the peak at 3740 cm^{-1} belonging to terminal Si-OH groups – considered as non-acidic in the literature[138] – almost disappears when the catalyst gets in contact with pyridine and only reappears after outgassing at higher temperatures, pointing out that these groups actually work as an anchor for pyridine-like molecules.

Bands at 1435 cm^{-1}, 1445 cm^{-1} and 1585 cm^{-1} can be attributed to physisorbed pyridine and show that the desorption (negative peaks in Figure 30) of this species happens at relatively low temperatures, just as expected. The typical bands for pyridine adsorption on Brønstedt acid sites at 1640 – 1630 cm^{-1} and 1540 cm^{-1} (expected between 1500 cm^{-1} and 1545 cm^{-1})[137, 139] are visible, but show an unusual behaviour, increasing with outgassing temperature instead of decreasing. Therefore, the existence of higher amounts of Brønstedt acid sites – even though probable – cannot be clearly stated, at least not on the dry catalyst.

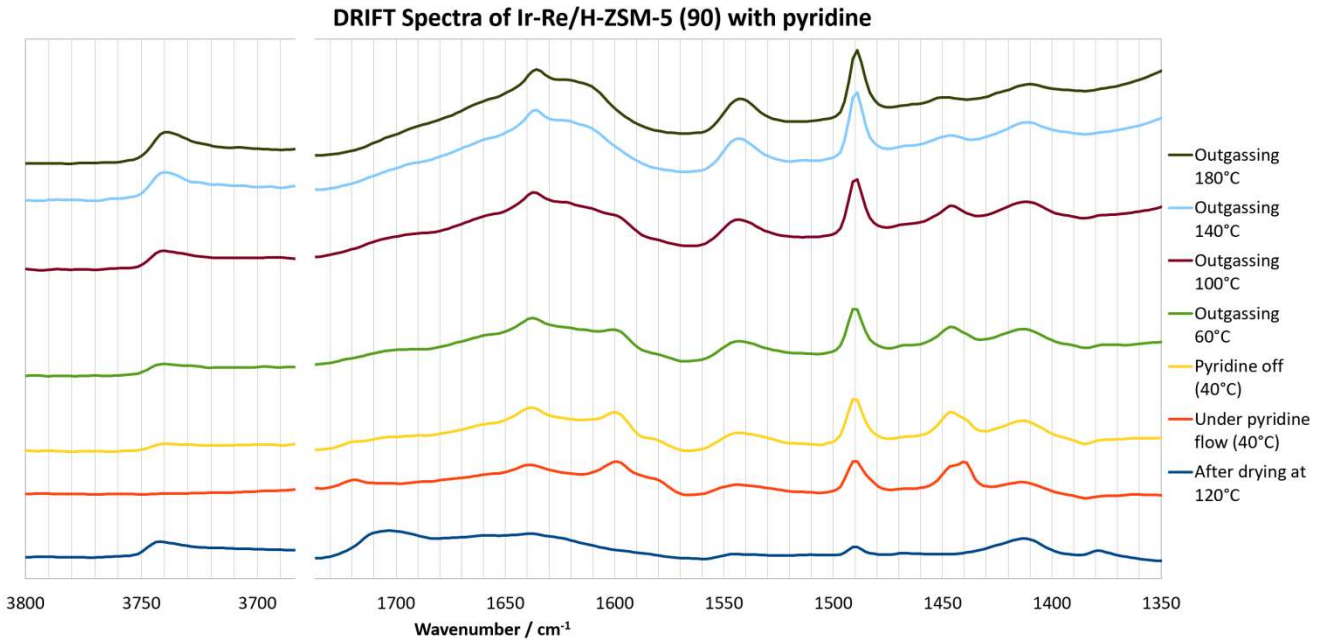

Figure 29 Pyridine adsorption and degassing over Ir-Re/H-ZSM-5 (90). The catalyst was first dried at 120°C for 30 minutes and then a flow of pyridine was passed at 40°C, followed by degasification at increasing temperature up to 180°C.

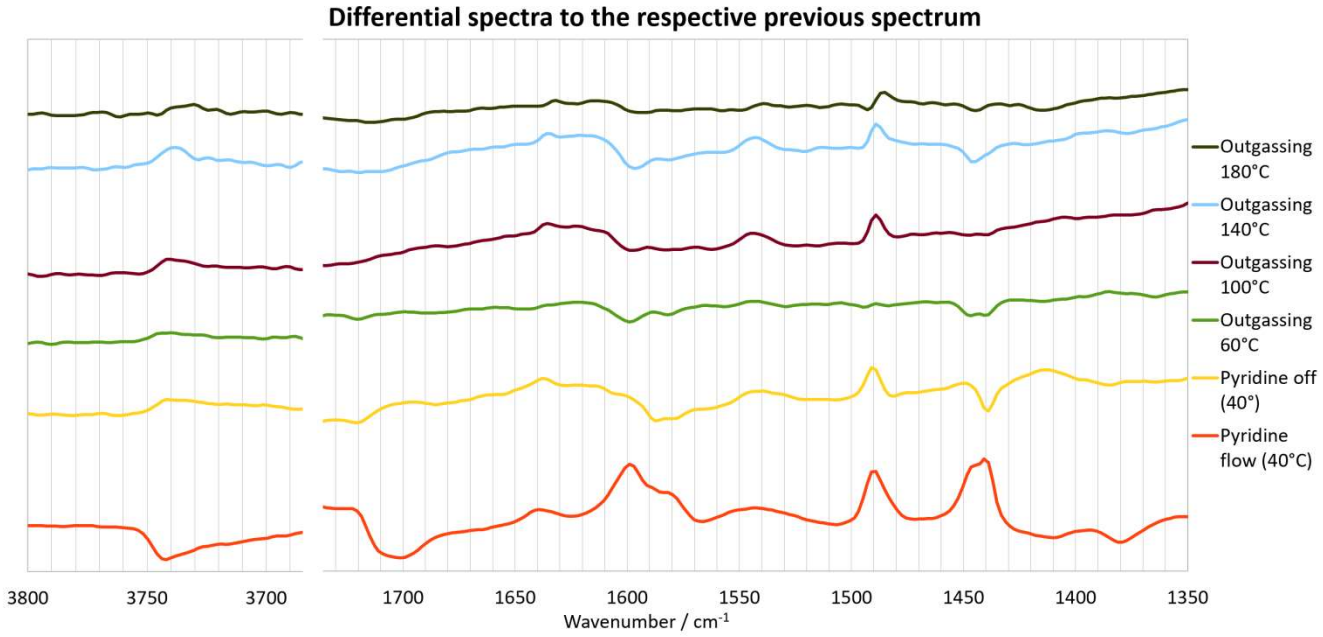

Figure 30 The DRIFT spectra shown in Figure 29 are compared to the respective previous spectrum. The spectrum designated as "pyridine flow (40°C)" is therefore the difference of the spectrum measured under pyridine flow at 40°C and the original spectrum measured after drying while the next one shows the effects of switching off the pyridine flow. This figure allows a better understanding of the connections between the bands. The disappearance of the band at 1600 cm^{-1} (resulting in a "negative" peak) coincide with a band at around 1447 cm^{-1} while a connection of bands at 1435&1445 cm^{-1} and 1585 cm^{-1} (attributed to physisorbed pyridine)[137] can be observed as well.

As the typical band[138] for Brønstedt acidic bridging (Si(OH)Al) hydroxyl groups on the zeolite at 3610 cm^{-1} is not observed, in contrast to the pure support without the metals, shown in Figure 31, the

Brønstedt acid sites could actually originate from the metals.[79] For space reasons, the section around 3610 cm^{-1} was cut out in Figure 29, due to the absence of any peak in this area. Besides, no clear hint of Lewis acid sites (expected at 1633 – 1600 and 1460 – 1445 cm^{-1}, almost the same as the frequency resulting from the coordination of pyridine to non-acidic SiOH-groups) could be found either. The bands observed in this region can be attributed to the silanol groups due to the connection of the re-appearance of the band at 3740 cm^{-1} with the diminishing bands mentioned before. These results actually show that the silanol groups also act as weak Lewis acid sites. However, there is no clear sign of the presence of strong Lewis acid sites that might be caused by metal surfaces, for example.

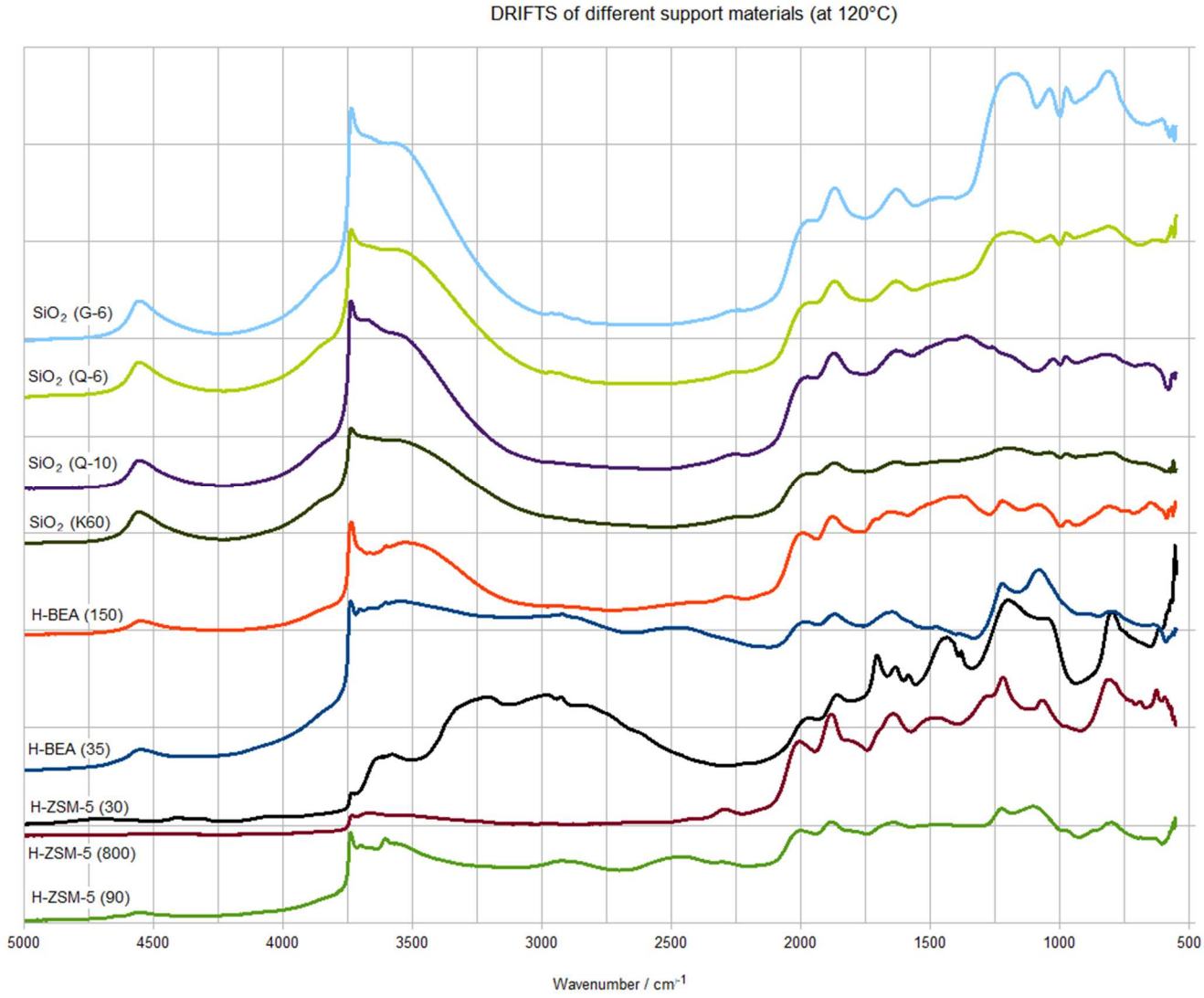

Figure 31 DRIFT spectra of several support materials at 120°C. Two important and characteristic bands are the combined frequency of isolated and vicinal vibrations of Silanol groups at 4550 cm^{-1}[140] and the isolated terminal Si-OH groups at 3740 cm^{-1}.[141]

Combining these results with the measurement of the pH value, it seems that the dry catalyst does not have a big number of acid sites and that those are only formed in the presence of water in the reaction

solution. Comparing the DRIFT spectra of Ir-Re/H-ZSM-5 (90) before the adsorption of pyridine in Figure 29 and of H-ZSM-5 (90) in Figure 31, it appears that the band at 3610 cm^{-1} indicating the presence of Brønstedt acidic hydroxyl groups disappears with the deposition of the metals, similar to what has been reported for iridium[138] and iron[142] on H-ZSM-5.

Looking at the spectra of most of the catalyst support materials used in this study, presented in Figure 31, the absence of the described band at 3610 cm^{-1} in the spectra of several support materials, especially the pure silicas, can be observed. Remembering the fact that these silica supports work as well or even better than most zeolite supports, regarding the activity in the hydrogenolysis of glycerol, it seems that those acidic groups do not play a decisive role in the reaction nor in the formation of the active catalyst (keeping in mind that those hydroxyl groups might be blocked by the impregnated metals as has been mentioned before and can actually be observed in Figure 32).

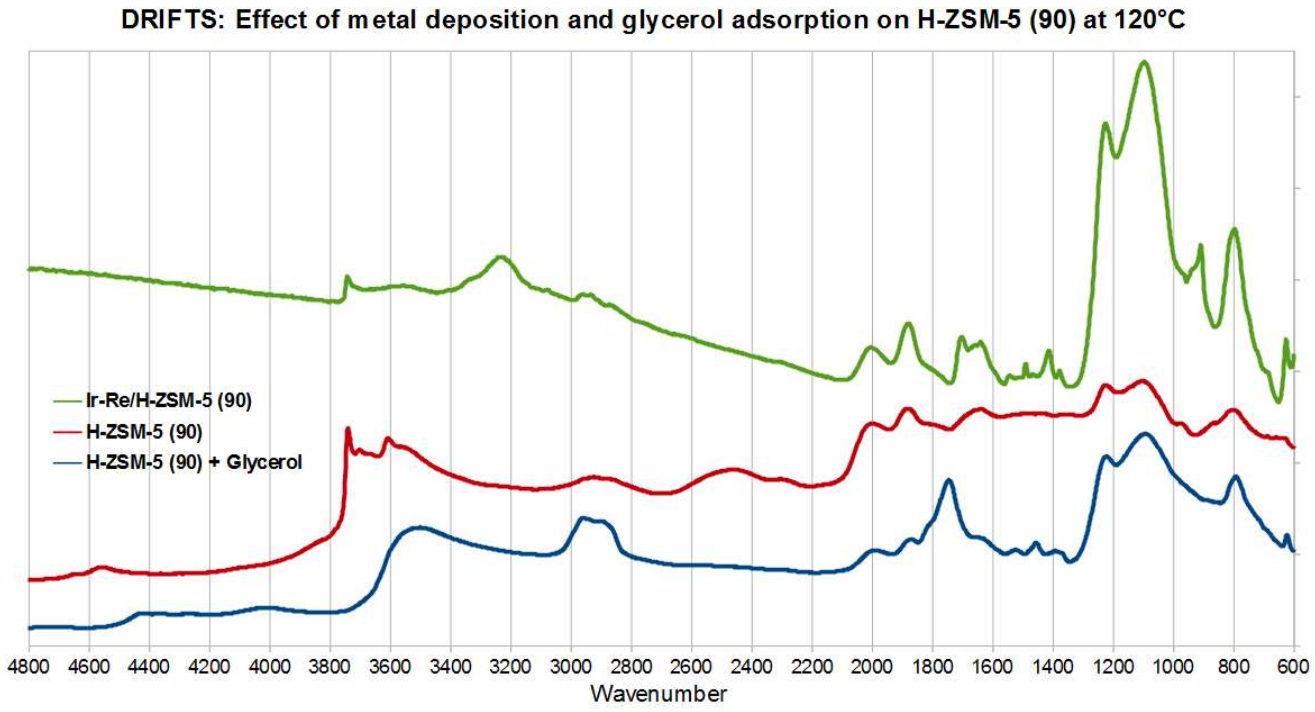

Figure 32 DRIFT spectra of H-ZSM-5 (90) (red), Ir-Re/H-ZSM-5 (90) (green) and glycerol adsorbed on H-ZSM-5 (90). The spectra have been recorded at 120°C under nitrogen, the metal containing catalyst was diluted with KBr in order to increase the reflectance and the signal (compared to the other two measurements) was increased for this graph. For the measurement with glycerol, a 20%wt. glycerol solution was impregnated onto the zeolite, followed by drying at 120°C.

On the other hand, the band for the non-acidic silanol hydroxyl band at 3740 cm^{-1} is very prominent in the spectra of all support materials. Comparing the intensity of this band and how much it stands out (always in relation to other peaks, as DRIFT spectra are not suitable for a quantitative comparison in between different spectra) with the catalytic performance, there seems to be a correlation. The supports

that led to more active catalysts like SiO_2 G-6, Q-6 and also Q-10 as well as H-BEA (150) and H-ZSM-5 (90) appear to have a stronger band at 3740 cm^{-1} than SiO_2 K60 (Kieselgel 60), H-BEA (35), H-ZSM-5 (30) and H-ZSM-5 (800) which led to less active hydrogenolysis catalysts.

Another hint for the importance of this band at 3740 cm^{-1} is that it disappears with the presence of glycerol on the support as can be observed in Figure 32. While the rest of the spectrum – except of the appearance of two new bands between 2800 and 3000 cm^{-1} caused by glycerol and another one around 1750 cm^{-1} (in the typical range of C=O vibrations) – remains the same, the peak attributed to Si-OH silanol groups vanishes, indicating that these surface spots are involved in the adsorption of glycerol, probably by forming a kind of "anchor". Therefore, the availability of these silanol groups on the surface might be the reason for the different activities, concerning the conversion of glycerol in the hydrogenolysis reaction, observed for the catalysts based on different support materials. The supports with a higher concentration of these surface groups (detected by DRIFTS) provide more sites for the adsorption of glycerol and hence a higher reaction rate on the active metal sites. It is important to state that this type of silanol group is not blocked during the deposition of the metals and therefore is likely to be present in the final catalyst under reaction conditions, different from the Brønstedt acidic hydroxyl groups that cause the band at 3610 cm^{-1}.

In the spectrum with glycerol, the band at 1750 cm^{-1}, typical for C=O double bonds, might be due to a partial dehydration of glycerol on the acidic sites during the drying process.

The fact that the adsorption of glycerol is not too strong could be observed at the attempt to measure an infrared spectrum of glycerol adsorbed on Ir-Re/H-ZSM-5. As the catalyst itself is too dark and needs to be diluted with potassium bromide in order to receive a reasonable IR signal, the catalyst was washed with distilled water after the impregnation with glycerol and then dried before being mixed with KBr. The recorded spectrum was identical to the one without glycerol, showing that simple washing in water is sufficient to remove glycerol from the surface. However, the good desorption is an important step in a catalytic cycle, preventing the blocking of active sites.

7.4. Poisoning by steel from the reactor wall

In some publications, glass or Teflon vessels inserted into the stainless steel reactor were used, as a much lower conversion without these inserted vessels was mentioned and a possible poisoning with iron from the reactor wall was assumed.[68] After carrying out a part of the experiments for the present study without an inserted vessel, tests with a Teflon vessel led to a higher conversion and a higher yield, hence this vessel was included in all following reactions.

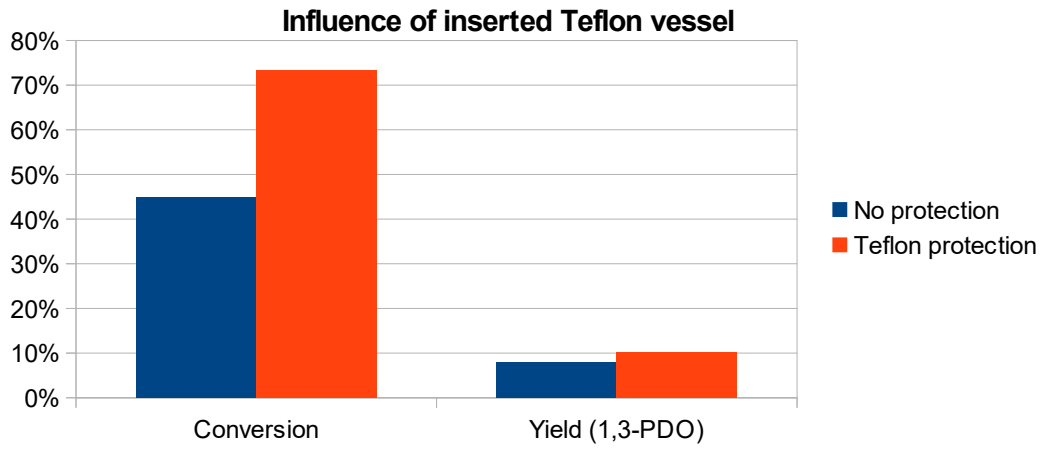

Figure 33 The influence of an inserted Teflon vessel on the hydrogenolysis of glycerol (20%wt. in water) over Ir-Re/SiO_2 (G-6) after 8 hours at 180°C and 5 MPa H_2.

In order to evaluate the cause of this strong influence, 2 mg $Fe(NO_3)_3$ x 9 H_2O was added to the reaction solution of 100 g 20%wt. glycerol solution and 880 mg catalyst (Pt-Re/SiO_2 (G-6)), resulting in a much lower conversion of only half the value that the catalyst obtained without the addition of the iron salt, whereas the selectivity did not change much (see #80 and 81 in Table 8 in the annex). This effect was also observed with iridium containing catalysts, in a small series of experiments in a multi batch reactor (see Figure 34 and Table 9 in the annex).

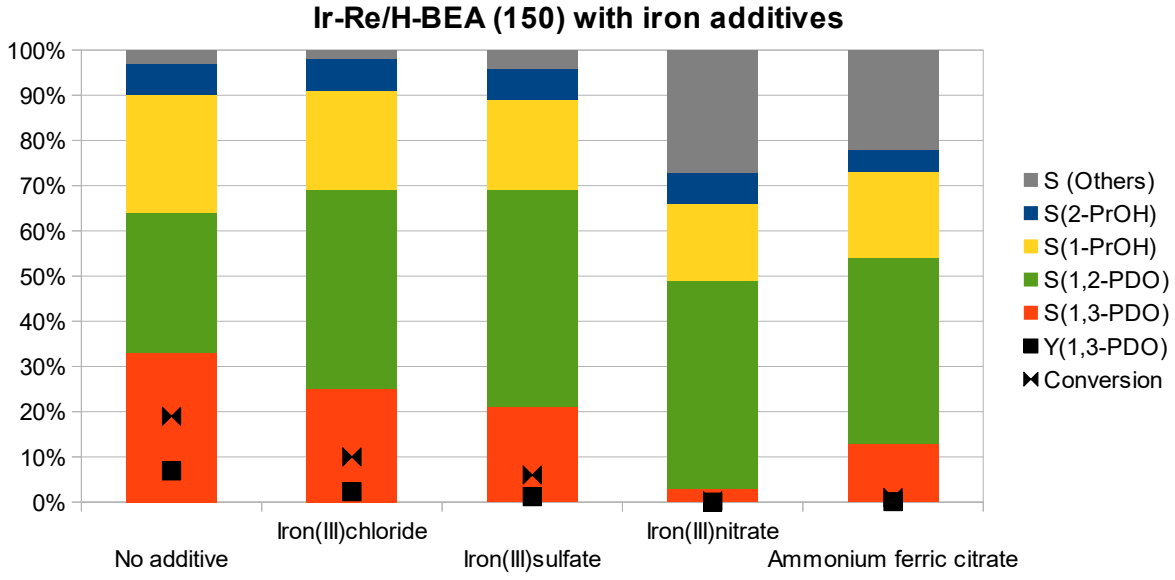

Figure 34 Hydrogenolysis of glycerol over Ir-Re/H-BEA (150) with different iron additives. With the amount of iron not being the same in all experiments, no conclusion can be drawn regarding the different counter ions! Reaction conditions: Multibatch, 160°C, 5.2 MPa H_2 (initial pressure), 8 h, 88 mg catalyst, 10 g glycerol solution (20%wt.). "Others" include ethylene glycol, ethanol, 1-propoxy-2-propanol and unidentified substances.

As platinum and iron are known to form alloys, a strong interaction of iron, coming from the reactor's steel wall, with surface platinum or iridium atoms might cause the inhibition by blocking active sites.

7.5. Influence of active metals

Different active metals were tested in the hydrogenolysis. First of all, the influence of rhenium was examined by preparing mono- and bimetallic catalysts with and without rhenium.

7.5.1. Addition of rhenium

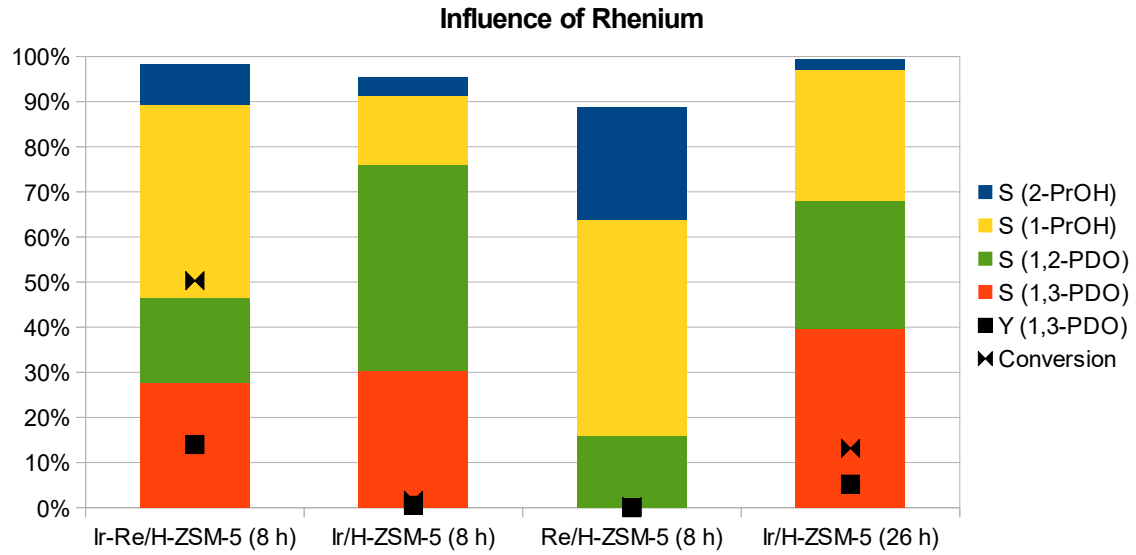

Figure 35 Rhenium proved to have a big influence on the hydrogenolysis of an aqueous 20%wt. glycerol solution at 160°C, 5 MPa H_2 and reaction times of either 8 or 26 hours. H-ZSM-5 on its own was inactive. The missing parts to 100% indicate the presence of other, not specified, side products.

The addition of rhenium caused a tremendous effect on the reaction, especially regarding conversion, but to some extent also selectivity. Rhenium in combination with iridium or platinum strongly enhances the activity in glycerol hydrogenolysis, compared to the almost inactive monometallic catalysts. However, especially in case of iridium, the selectivity does not undergo big changes, only 1-propanol seems to be favoured instead of 1,2-PDO, due to the proceeding consecutive reaction at higher conversions. With the bimetallic catalyst leading to a higher conversion, even when compared to the Ir/H-ZSM-5 at a reaction time of 26 hours, a clear decrease of the selectivity towards 1,2-propanediol and a simultaneous increase in 1-propanol formation can be observed in Figure 35 with the increasing conversion. The formation of 1-propanol has been detected at almost any reaction even at low conversion which indicates either a direct route for the formation from glycerol, without a propanediol as an intermediate, or a relatively strong adsorption after the first reaction, giving time for another hydrogenolysis.

Rhenium on zeolite (reduced at 673 K) without a second noble metal shows a very low activity (less than 1% conversion of glycerol) and does not produce any 1,3-propanediol, forming mainly 1- and 2-propanol, 1,2-propanediol and ethylene glycol. This reduction temperature for the rhenium catalyst

was chosen regarding the measurements of the temperature programmed reduction (TPR) of the precursor, shown in Figure 36.

Table 2 Calculation of the metals final oxidation state from the hydrogen consumption in the TPR measurement shown in Figure 36, assuming that iridium will be reduced first and rhenium second.

Precursor	H_2IrCl_6/H-ZSM-5	H_2IrCl_6-NH_4ReO_4/H-ZSM-5	NH_4ReO_4/H-ZSM-5
Calculated final oxidation state	Ir: 0	Ir: 0 Re: +3	Re: +1

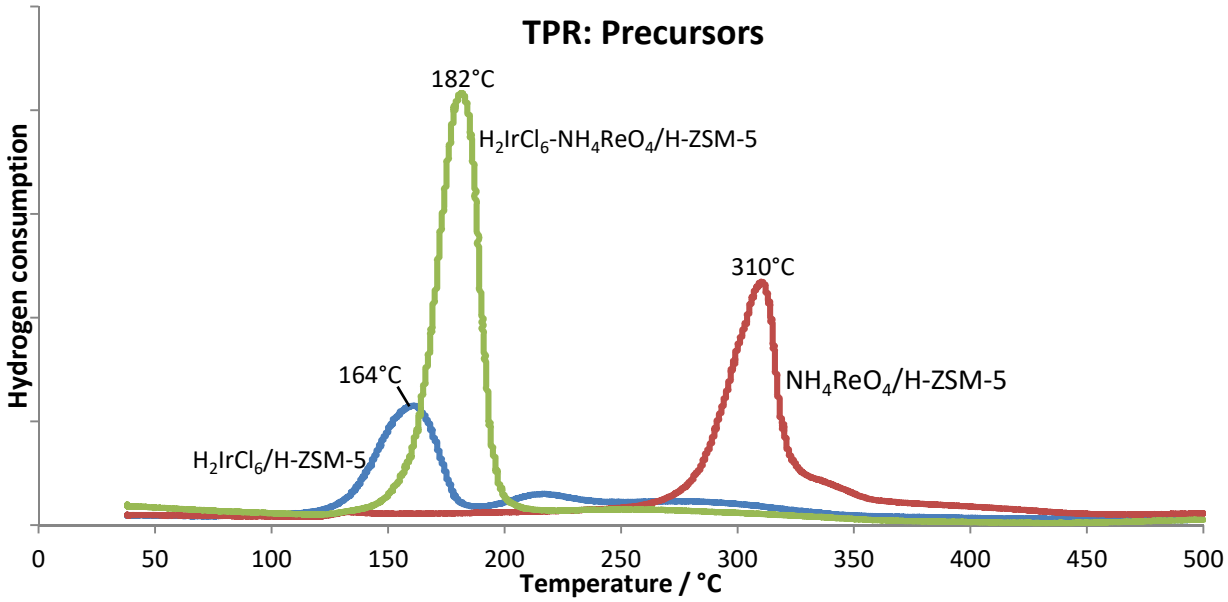

Figure 36 Temperature programmed reduction (TPR) of the precursor on the catalyst support. Conditions: 100 mg sample, 5 K/min, 50 mL/min hydrogen 5.1% in argon; Samples were dried in-situ under argon at 160°C for 30 minutes before the TPR measurement.

The TPR result also clearly shows that a connection between iridium and rhenium must be present and probably some kind of alloy is formed in the catalysts that contain both metals. While NH_4ReO_4 "on its own" (still on the support, but without another metal) is reduced around 550 K to 600 K, the reduction takes place a lot earlier when iridium is present as well, leading to a sharp single peak at 455 K. The bimetallic Ir-Re species hence behave in the reduction like a single metal, being reduced just a little later than the pure iridium species H_2IrCl_6 that leads to a peak of hydrogen consumption around 440 K and much earlier than the monometallic rhenium. Figure 36 also gives an idea why NH_4ReO_4 could still be detected after the standard reduction at 503 K (see Figure 45): These precursor particles will remain in their original state when the distance to the next iridium atom is too big.

These results (hydrogenolysis reaction and TPR) are well aligned with what has been reported in the literature, except of maybe the similar selectivity which did not come out that clearly in previous

works. Obviously, rhenium plays an important role in "preparing" the glycerol molecule for the hydrogenolysis, possibly by facilitating the adsorption and/or changing the electronic or steric configuration of the adsorbate in a way that increases the reaction rate of the hydrogenolysis. The absence of dramatic changes in selectivity gives a hint that rhenium does not participate directly in the hydrogen transfer.

In the case of a ruthenium zeolite catalyst, the addition of rhenium led to a decrease in the reaction rate on a high level and an increase in selectivity towards 1,3-propanediol, however, the selectivity was still very low and not furtherly investigated.

7.5.2. Variation of the noble metal

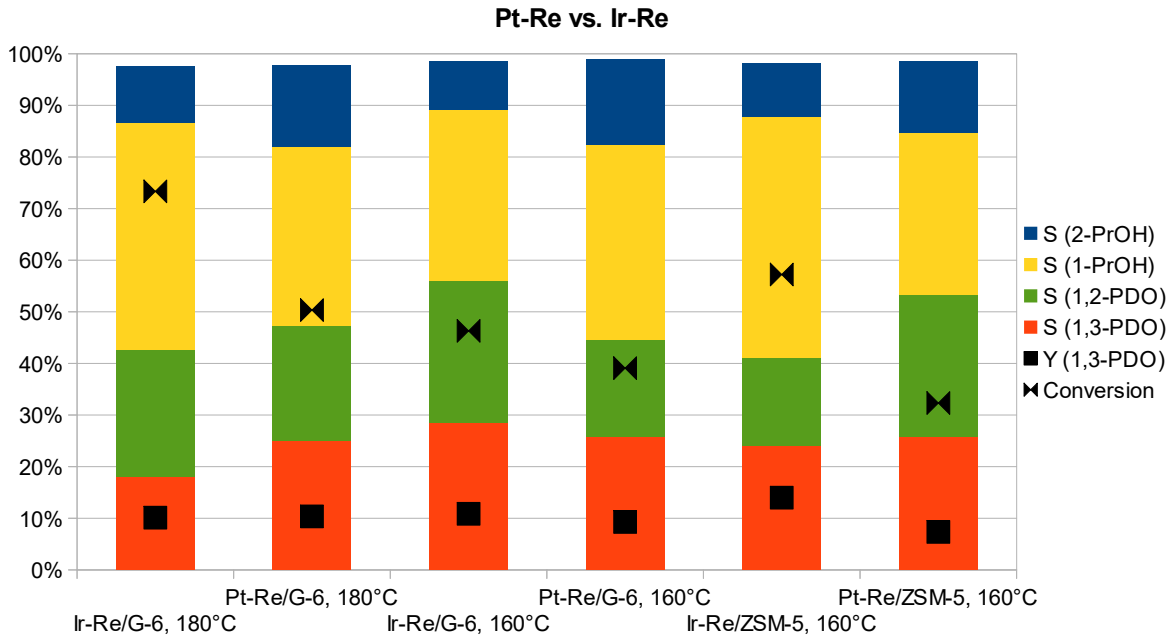

Figure 37 Comparison of Pt-Re/SiO_2 (G-6) and Ir-Re/SiO_2 (G-6) in the hydrogenolysis of glycerol at two different temperatures after 8 hours, Ir-Re/H-ZSM-5 (86) and Pt-Re/H-ZSM-5 (86) are also shown.

When Pt-Re was compared to Ir-Re on different supports, the iridium containing catalyst usually led to a higher conversion and somewhat different selectivity. The higher conversion was detected on different support materials (SiO_2 G-6 and H-ZSM-5 (86)) as well as at different temperatures (160°C and 180°C) with the effect on the zeolite being stronger than on the silica. On G-6, iridium had a beneficial effect on the selectivity towards 1,3-propanediol which could not be clearly detected on the zeolite, either for not being present or for being over-compensated by the consecutive reaction that consumes the propanediols. In all cases, clearly more 2-propanol and relatively less 1-propanol was formed over Pt-Re catalysts when compared to Ir-Re.

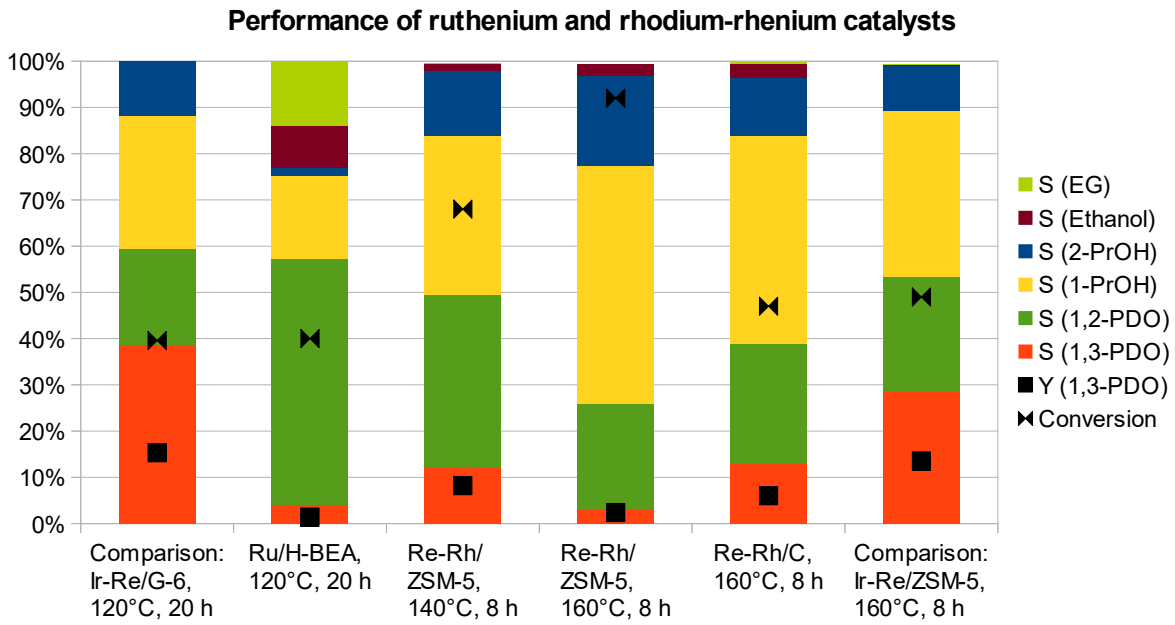

Figure 38 Performance of monometallic ruthenium and bimetallic rhodium-rhenium catalysts, compared to the respective iridium-rhenium systems. Supports used in these experiments: SiO_2 (G-6), H-BEA (150), H-ZSM-5 (90) and Vulcan XC-72 carbon. The Re-Rh/C (Vulcan XC-72) catalyst was supplied by the Dumesic group and equals the one used in their publication.[79] Hydrogenolysis of glycerol (20%wt. in water) performed at 5 MPa H_2. EG: Ethylene glycol.

Monometallic ruthenium catalysts proved to be highly active (more or less equal to comparable bimetallic Ir-Re catalysts), but led mainly to 1,2-propanediol and ethylene glycol with smaller amounts of 1-propanol, ethanol and 1,3-propanediol. The selectivity towards products of C-C scission amounted to more than 20%, even at a low temperature of 393 K; during a test at 473 K the selectivity to ethylene glycol reached even 39%. The recently described[143] addition of small amounts of ruthenium as a tertiary metal to iridium and rhenium on Q-6 silica led – depending on the reaction temperature – to a higher conversion, but lower yield of 1,3-propanediol as mainly 1-propanol was formed (see Figure 39). While the effect at 313 K was rather small, at 333 K the difference between the catalysts with and without ruthenium was clearly visible. However, in this case, it did not really matter whether ruthenium was impregnated together with iridium or in a separate impregnation step with a drying phase in between. Yet, the impregnation order of rhenium and iridium plays an important role as will be discussed later.

Rhodium, when employed together with rhenium, led to a strong acceleration of the hydrogenolysis reaction, compared to the iridium-rhenium catalysts. At 433 K, glycerol was converted almost entirely within the 8 hours reaction time and even at 413 K the conversion reached nearly 70%. The selectivity to 1,3-propanediol was relatively low, though, with 1,2-propanediol, 1- and 2-propanol being formed in larger quantities. Besides, at the higher temperature a reasonable amount of gaseous products was

formed, estimated to be around 15% of the original glycerol amount, calculated from the missing mass balance between the converted glycerol and the products found in the liquid phase.

Another rhodium-rhenium catalyst tested was Rh-Re/C (Vulcan XC-72), which was prepared by the group of Prof. Dumesic according to their publication.[79] The catalyst was tested at the same conditions as a Rh-Re/H-ZSM-5 (90) and an Ir-Re/H-ZSM-5 (90) catalyst (see Figure 38). While the result was in accordance with the literature, where a higher selectivity to 1,3-PDO at a much lower conversion at a lower temperature was reported, this carbon support – like the others mentioned before – also proved to be less appropriate for the hydrogenolysis of glycerol than a H-ZSM-5 zeolite.

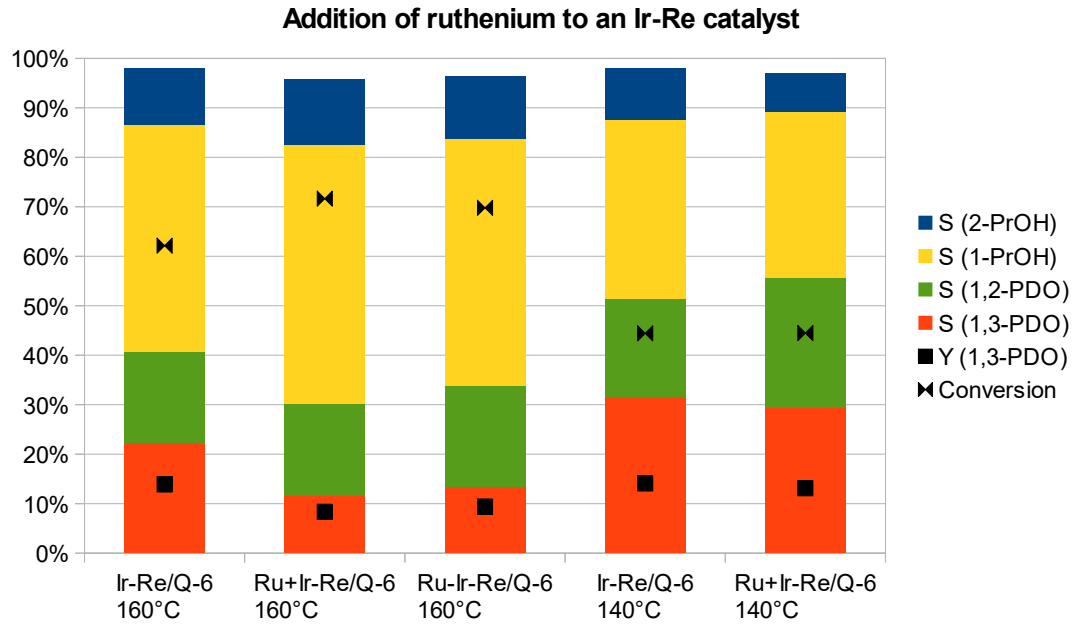

Figure 39 Effect of the addition of ruthenium to an Ir-Re/SiO_2 (Q-6) catalyst at different temperatures. "Ru+Ir-Re" indicates that ruthenium and iridium were impregnated together, followed by drying and an impregnation with rhenium. "Ru-Ir-Re" indicates three distinct impregnation steps. Reaction time: 8 h at 5 MPa H_2. As always, the missing part to 100% represents other liquid products, mainly ethanol.

In contrast to the findings about the impregnation of ruthenium as a tertiary metal, the impregnation order turned out to be very important for the catalytic activity when the order between the noble metal, in this case iridium, and rhenium was changed. As can be seen in Figure 40, the best results in terms of conversion and yield were achieved when iridium was impregnated first, followed by drying at 393 K and the impregnation with the rhenium precursor.

Inverting the impregnation order (see Figure 40) reduced the conversion and the yield almost by half, while a reduction between the two impregnation steps led to an almost inactive catalyst, only a little more active than an iridium catalyst without rhenium. However, the selectivity did not change much, in spite of the very different conversion from one experiment to the other.

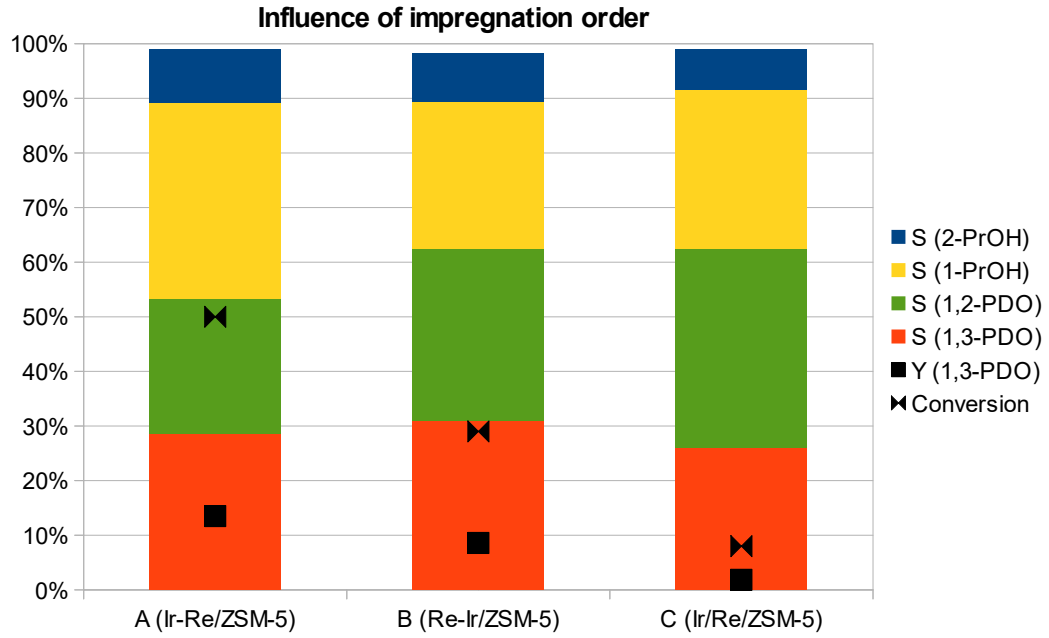

Figure 40 Influence of impregnation order in iridium-rhenium catalysts: A: Iridium impregnated first, followed by drying and rhenium impregnation (standard); B: Rhenium impregnated first, followed by drying and iridium impregnation; C: Iridium impregnated first, followed by reduction under flowing H_2 at 230°C and rhenium impregnation. Support: H-ZSM-5 (90); Reaction conditions: 20%wt. aqueous glycerol solution, 5 MPa H_2, 160°C, 8 h.

These experiments underline the importance of the contact of the two metals and indicate the formation of bimetallic particles on the catalyst support which seem to form especially well when the metals are reduced at the same time. Regarding the influence of rhenium discussed in section 7.5.1 and Figure 35, it seems as if the different preparation methods influence the availability of rhenium on the surface as the effects seen in Figure 40 are similar to the ones observed in case of the addition/subtraction of rhenium. It also gives a hint that a structure with rhenium deposited on iridium is favourable for the conversion of glycerol.

In order to gain a better understanding of the reaction pathways, 1,2- and 1,3-propanediol have been used as a substrate in the hydrogenolysis reaction. The reaction conditions were maintained at 433 K, 5 MPa H_2 pressure and 8 hours reaction time with a 20%wt. solution of the substrate in water. In coherence with the results published by several other groups, 1,2-PDO as well as glycerol turned out to be converted much faster than 1,3-PDO in the hydrogenolysis over Re-Ir/H-ZSM-5 (90), indicating a higher rate for substrates with hydroxyl groups connected to neighbouring carbon atoms. It is also interesting to see that, in case of 1,2-propanediol, there is still a much stronger tendency for an elimination of the secondary hydroxyl group. These results might be interpreted in a way that one of the OH groups – preferentially the terminal one – serves as an “anchor” to the catalyst, while the catalyst geometry favours the attack on the neighbouring hydroxyl group. This image is strengthened by the fact that propanol hardly reacts to consecutive products like propane, which is only found in

very small amounts. Especially at lower reaction temperatures, the difference between the amount of converted glycerol and the amount of reaction products found in the solution stayed clearly below 5%, indicating a limited formation of gaseous products.

Table 3 Different substrates used in aqueous solution (20%wt.) over Ir-Re/H-ZSM-5 (90) at 160°C for 8 hours under 5 MPa H_2. PDO = propanediol, PrOH = propanol.

Substrate	Conversion	S (1,2-PDO)	S (1,3-PDO)	S (1-PrOH)	S (2-PrOH)
Glycerol	50%	25%	28%	36%	10%
1,3-propanediol	22%	-	-	94%	0%
1,2-propanediol	55%	-	-	72%	26%

The abundance of glycerol combined with the relatively high reaction rate explains also why, in spite of the hydrogenolysis involving consecutive reactions, the selectivity did not change much with conversion. When the reaction during heating from room temperature to reaction temperature – right before the moment that is considered the "start" of the reaction – was examined, the product distribution was very similar to the one after the reaction, even though the conversion was very different (1% vs. 50%). The main difference is that the selectivity to 1,2-propanediol is lower and more propanol is formed, as can be expected due to the relatively high reaction rate of 1,2-PDO.

7.6. Influence of pre-treatment

7.6.1. Calcination vs. reduction

The standard preparation procedure for Ir-Re-catalysts in the literature is to calcinate the catalyst in static air at 773 K for 3 h after two impregnation steps. The calcined catalyst is then reduced *in-situ* in water at 473 K before the glycerol is added to the reactor.[67] Also other groups with different catalytic systems usually used calcined catalysts that were reduced just before the reaction,[34, 41-42, 48-49, 60-62, 64, 73-75] whereas examples of works with only-reduced catalysts like Pt-Re/C,[63, 69] Rh-Re/C,[144] Ir-Re/KIT-6 (mesoporous silica)[70] or Rh/CsPW[96] are rare.

In this study, several different approaches for the catalyst pre-treatment were tested. First of all, the catalyst was calcined at 773 K as proposed in the literature and then reduced *ex-situ* before the reaction. In order to avoid re-oxidation during transfer from the tube reactor, in which the reduction took place, to the batch reactor for the hydrogenolysis, this transfer was maintained as short as possible with air contact below one second and also in some experiments the catalyst was transferred inside a glove box. However, the results of these tests did not vary much which indicates that re-oxidation is not an important issue in this case, either due to a very stable catalyst or a quick re-reduction under reaction conditions. TPR analyses (see Figure 41) of the reduced catalysts proved that it is actually a

combination of both reasons. The small peak of the black line (representing the reduction of Ir-Re/H-ZSM-5) below 380 K and the absence of other peaks show that the oxidation in air is small and that it is reversed at temperatures below the reaction temperature used during this work (between 393 K and 473 K). Even the oxidation *in-situ* with a temperature programmed oxidation (heating from 303 K to 473 K with 10 K/min, holding for 10 minutes under 4,91% oxygen in helium) only led to a relatively low level of oxidation (red line), compared to the amount of hydrogen consumed by the calcined catalysts (green line). It can therefore be expected that the transfer to the reactor in air should not have any inhibiting effect onto the hydrogenolysis of glycerol as any oxidation should be reversed quickly under reaction conditions. However, the presence of water should always be considered because it may have an important influence as will be discussed later.

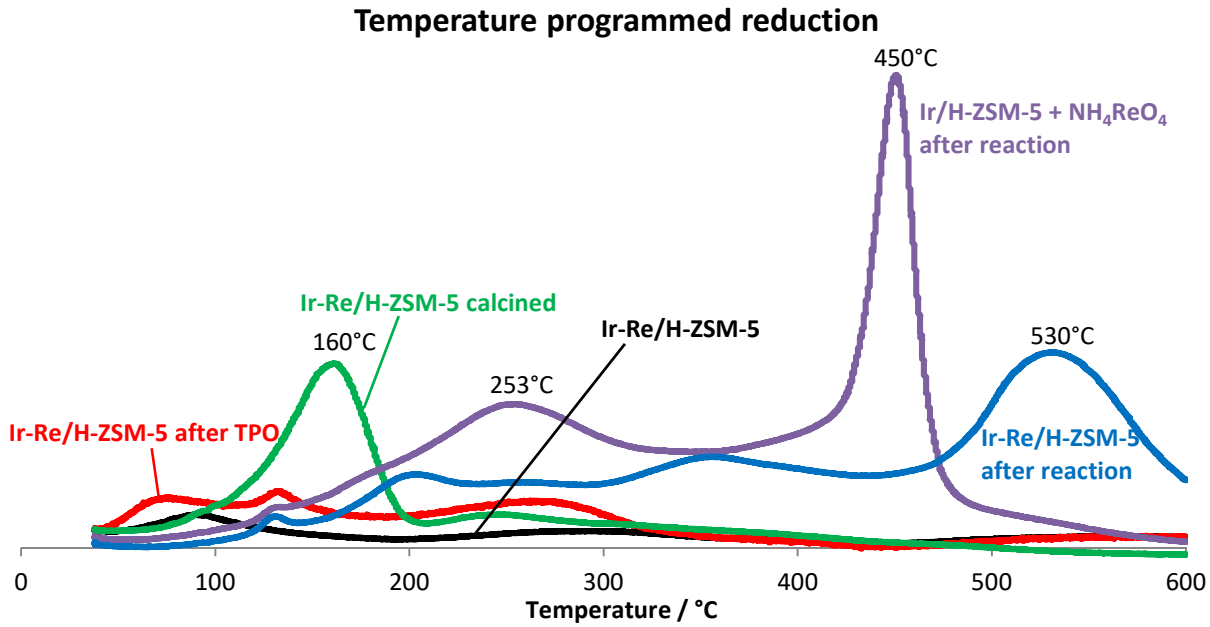

Figure 41 Temperature programmed reduction (TPR) of three fresh and two used catalysts based on H-ZSM-5 (90). **Red:** Ir-Re/H-ZSM-5 (90) after passing a heating ramp to 200°C (10 K/min, 10 min hold) under 4,91% oxygen in helium; **Green:** Ir-Re/H-ZSM-5 (90), calcined in static air at 500°C; **Black:** Ir-Re/H-ZSM-5 (90), reduced at 230°C *ex-situ* and then transferred (after several hours of air contact) to the TPR-oven; **Purple:** Ir/H-ZSM-5 after reaction with NH_4ReO_4 in the reaction solution; **Blue:** Ir-Re/H-ZSM-5 (90) after the reaction; Conditions: 100 mg sample, 5 K/min, 50 mL/min hydrogen 5.1% in argon; Samples were dried in-situ under argon at 160°C for 30 minutes before the TPR measurement. The used catalysts have been washed with distilled water and dried before the measurement.

The TPR analyses of the spent catalyst after washing and drying at 393 K overnight showed broad peaks at relatively high temperatures, probably resulting from the hydrogenation or hydrogenolysis of strongly adsorbed species. Some peaks might also belong to the re-reduction of sintered metal parts of the catalyst that, due to the different steric and electronic environment, reduce at another temperature

than before. The analysis of the purple curve showing Ir/H-ZSM-5 after reaction with NH_4ReO_4 added to the reaction solution will be discussed later together with Table 4 on page 69.

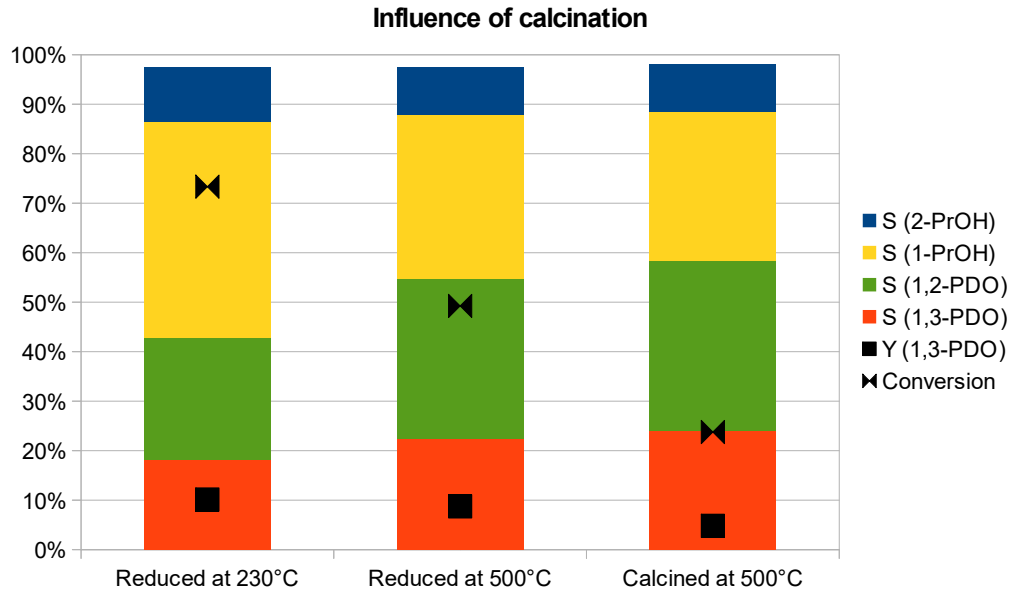

Figure 42 Comparison of the effect of reduction temperatures and calcination on an Ir-Re/SiO_2(G-6) catalyst, tested at 180°C, 8 h reaction time and 5 MPa H_2. The catalysts were (after impregnation and drying) either reduced at 230°C (left), at 500°C (middle) or calcined at 500°C in air followed by a reduction at 230°C (right) before the hydrogenolysis reaction.

With a visible loss of metal during calcination – probably due to volatile rhenium oxide species – and the performance of the catalysts staying below the expected results regarding conversion and yield, the catalyst was also prepared without the calcination step. As can be seen in Figure 42, the results in terms of the aimed product were better in the case of the reduced catalysts with the one reduced at lower temperature outperforming the other ones. The outstanding results of the Tomishige group with calcined catalysts could not be reproduced, even with the *in-situ* reduction mentioned below. On the other hand, the results fitted well to the ones found by Deng et al. with very similar catalysts and reaction conditions.[70]

There are several possible reasons for these differences in reactivity. First of all, the calcined-and-reduced catalyst was found in TEM images (see Figure 43, D) to form agglomerations of metal particles which are likely to decrease metal surface area and inhibit the access of the substrate to the active sites. The size of the small particles does not change with the agglomeration, most particles have a diameter of 2 to 4 nm, in the reduced as well as in the calcined catalysts. Even though no images of the catalyst reduced at 773 K were taken, a similar effect might be responsible for the differences between the catalysts that were reduced at different temperatures. In contrast to that, metal particles on the “only reduced” catalyst (A to C, Figure 43) were found to be highly disperse, even though not very

homogeneously distributed over the support surface. The big (up to 200 nm) particles containing only rhenium and being identified by XRD as NH_4ReO_4 precursor particles (see Figure 43 C andFigure 45) only appeared on “only reduced” catalysts, but are unlikely to be the reason for the higher activity. A stronger incorporation of rhenium into the bimetallic particles at higher reduction temperatures, leading to a lower concentration of active sites on the surface, as has been reported for Rh-Re,[144] might also happen, but could not be confirmed in this case.

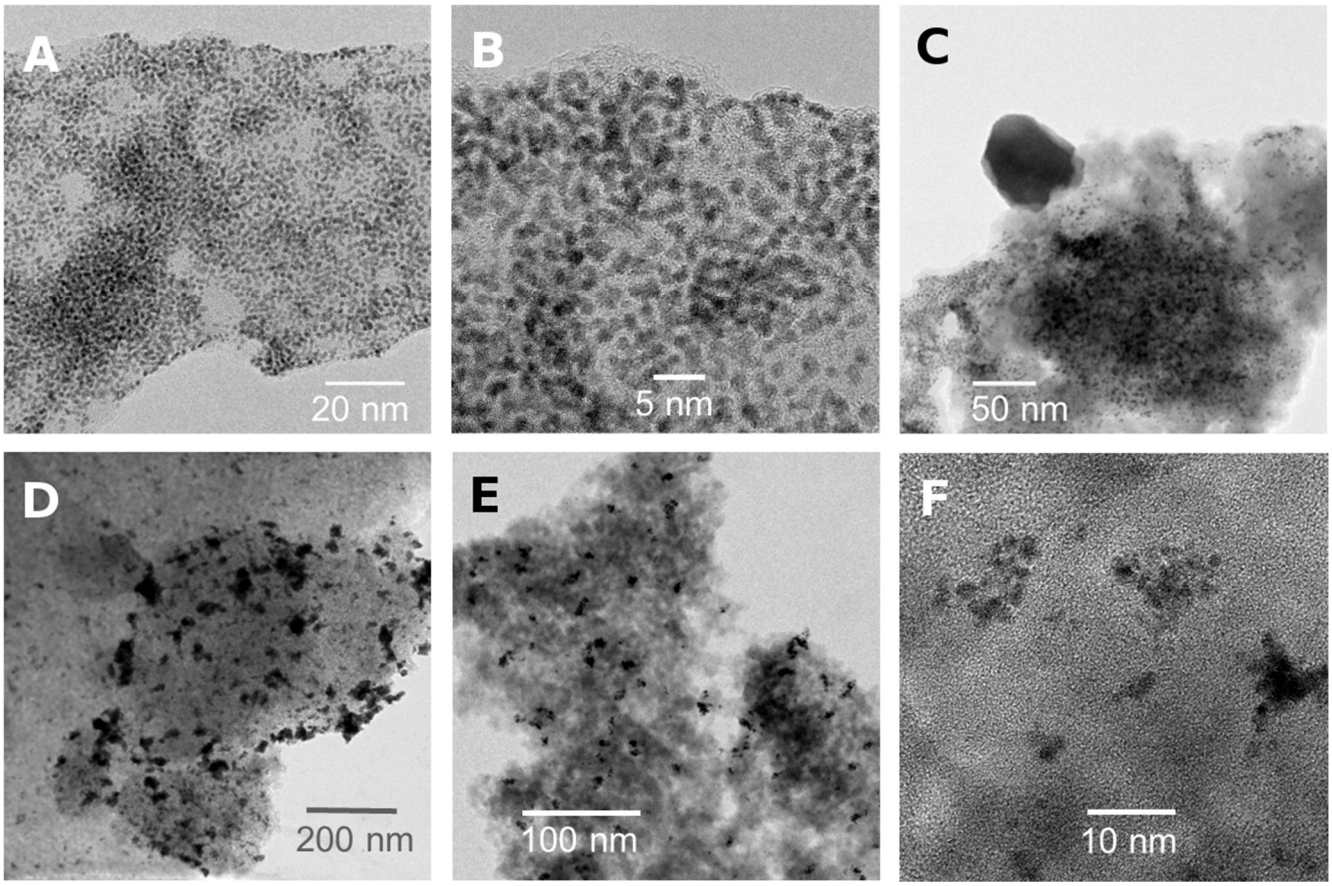

Figure 43 TEM images: A/B: Ir-Re/SiO_2 (G-6), reduced at 230°C in H_2; C: Ir-Re/SiO_2 (Q-6), reduced at 230°C in H_2, the big black spot is a remaining NH_4ReO_4 particle that also appears in the sample of A/B, although not shown here; D: Ir-Re/SiO_2 (G-6), calcined at 500°C in air and reduced at 230°C in H_2; E/F: Ir-Re/SiO2 (G-6), reduced at 230°C in H_2, after hydrogenolysis reaction for 8 hours at 160°C.

Beside this, the pore structure changes with calcination and also during the reaction, just one of the many similarities of calcined and used catalysts. In the literature, a decrease in surface silanol groups with increasing pre-treatment temperature, especially when passing 773 K, has been mentioned and might additionally affect the catalyst performance.[145] On all catalysts, many metal particles were found to be bimetallic, however, the resolution did not allow any statement about the possible formation of rhenium clusters on top of iridium particles as has been discussed in the literature.

Another point causing the difference in reactivity could be the loss of active metal, especially rhenium during the calcination. When the calcination was carried out in flowing air in a glass tube reactor, a mirror-like effect was visible on the glass behind the oven, indicating a metal containing film deposition on the cold parts of the tube. A similar observation was made in the case of calcination in a muffle furnace (static air) where the vessel with the catalyst showed a reflective surface after the calcination process (Figure 44).

The other explanation for the lower reactivity is the one mentioned before that the calcination leads to a structure containing oxygen bridges between iridium and rhenium atoms which cannot be fully reduced any more, affecting the performance. However, the hydrogen consumption during the reduction of the precursors as well as of the calcined catalyst suggested a final oxidation state of rhenium around +3, assuming that iridium was completely reduced, similar to TPR and XANES results in the literature.[66] As there is a difference both between the calcined-and-reduced and the high-temperature-reduced catalyst and the two just-reduced catalysts, it is likely that the agglomeration (sintering) structure plays an important role and maybe also the formation of the oxidised ReO_x, in spite of no direct proof for this in the TPR measurements. The TPR measurements are a hint but do not represent the "real" conditions, especially in case of an *in-situ* reduction which takes place in water and under high hydrogen pressure.

The possible loss of active metal, even though appearing visibly during calcination, could not be confirmed by ICP, at least not in a large scale that might explain the divergence between the results with the differently prepared catalysts.

Figure 44 The formerly white calcination vessel after a small series of calcinations of Ir-Re/SiO_2 catalysts performed in a muffle furnace at 773 K in static air. Both pictures show the same vessel, which was broken for better visualisation of the mirroring effect.

A certain mobility of the metal components during the reduction process could also be proven by employing physical mixtures of Ir/H-ZSM-5 and Re/H-ZSM-5, which were either reduced (*ex-situ*) together or separately at 503 K in flowing hydrogen. The same experiments were also performed with H-BEA instead of H-ZSM-5, but led to the same results and are therefore not mentioned in Table 4. When the two materials were reduced together, the catalyst was more active in the hydrogenolysis reaction than in case of a separate reduction, probably due to a migration of at least one of the metal species under these conditions. However, even the conjoined reduced mixture was still clearly less active than an Ir-Re/H-ZSM-5 catalyst. This proves that a direct contact of iridium and rhenium is crucial for the activity of the catalyst, even though the selectivity is not strongly influenced.

Table 4 Comparison of the effects of the physical distance between iridium and rhenium when prepared together or separately, compared to the case of the addition of the rhenium precursor to the reaction solution and the pure iridium catalyst. The hydrogenolysis was carried out at 160°C for 8 hours, 20%wt. glycerol solution, 5 MPa H_2. The pre-reduction was performed *ex-situ* at 230°C in flowing hydrogen at atmospheric pressure (100 mL/min·g_{Cat}).

Catalyst	Conversion	Selectivity (in liquid phase)				Yield
		1,3-PDO	1,2-PDO	1-PrOH	2-PrOH	(1,3-PDO)
Ir/H-ZSM-5 + Re/H-ZSM-5 *Reduced seperately*	4%	31%	35%	25%	5%	1,2%
Ir/H-ZSM-5 + Re/H-ZSM-5 *Reduced together*	16%	34%	32%	27%	5%	5,3%
Ir/H-ZSM-5 + NH_4ReO_4	11%	27%	35%	29%	8%	2,9%
Ir/H-ZSM-5	2%	30%	46%	15%	4%	0,5%
Ir-Re/H-ZSM-5	50%	28%	19%	43%	9%	14,0%

In one experiment, the rhenium precursor NH_4ReO_4 was – instead of being impregnated onto the support and reduced/calcined – added to the reaction solution, containing an Ir/H-ZSM-5 (80) catalyst. Interestingly, the performance was far better than in case of the Ir/H-ZSM-5 (80) on its own, but still clearly lower than in the case of a pre-reduced Ir-Re catalyst (see Table 4).

Even more surprisingly, the ICP analysis of the used catalyst after washing with water indicated an amount of rhenium equal to the content of freshly prepared bimetallic catalysts. This means that the rhenium salt was in large parts deposited onto the catalyst surface during the hydrogenolysis reaction. It is not clear whether rhenium was reduced and maybe formed an alloy with iridium or whether it is coordinating or somehow else bonding to the surface, either to iridium particles or to the zeolite support. The TPR results neither matched with the reduction of the pure, but supported rhenium precursor nor with any combination of iridium and rhenium measured before:

The TPR analysis (see Figure 41, page 65) of the Ir/H-ZSM-5 catalyst after this experiment with rhenium addition showed a broad peak at 526 K and another large one at 723 K, different from the regular bimetallic Ir-Re/H-ZSM-5 catalyst that exhibited some small peaks of hydrogen consumption at lower temperatures and one big, broad one around 800 K. While the presence of these high-temperature peaks might be due to the reduction of strongly adsorbed species and maybe even coke that were formed during the hydrogenolysis, the difference in the reduction temperatures must be connected to the diverging way of applying rhenium. The height and sharpness of the peak at 723 K indicates a very uniform appearance of the hydrogen consuming species, leaving basically two possible explanations: Either a rhenium species with relatively high resistance against reduction was formed – shifting the peak expected between 450 K (when in direct contact with iridium) and 580 K (reduction of NH_4ReO_4 on H-ZSM-5) to higher temperatures – or rhenium catalysed the decomposition of an agglomerated material at this specific temperature.

As already mentioned when discussing the TEM pictures, some part of the rhenium precursor was not reduced during the standard treatment at 503 K, due to the formation of relatively large particles of NH_4ReO_4 that could be seen via TEM (Figure 43, C) as well as in X-ray diffraction measurements. This observation could only be made on reduced catalysts, the calcined ones did not contain any remaining larger precursor particles.

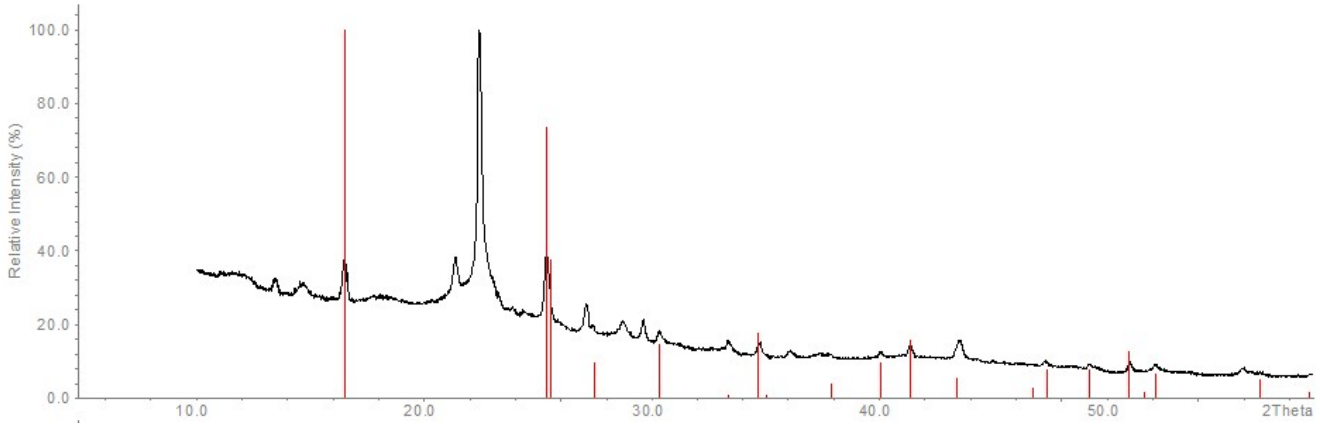

Figure 45 X-ray diffraction measurement of a reduced Ir-Re/SiO_2 catalysts showing that some NH_4ReO_4 particles (marked in red) of the precursor are still present after the reduction and are big enough to give a XRD signal.

However, as could be seen from the experiments with the addition of the precursor to the reaction solution, these particles might be dissolved and reduced during the hydrogenolysis. Also regarding the results of the mentioned experiment, it seems unlikely that a certain concentration of rhenium in the solution is responsible for the higher activity of the just-reduced over the calcined-and-reduced catalysts, because of the far lower conversion and yield when using Ir/H-ZSM-5 + NH_4ReO_4.

7.6.2. Reduction *in-situ*

In a later stage of this work, the catalyst was either reduced or calcined and then pre-reduced in water, already in the hydrogenolysis reactor, for one hour at 473 K. After cooling down, the glycerol and the missing water were added, the reactor was purged with hydrogen and the reaction was started, now at 393 K and for 20 hours. This reduction *in-situ* had a surprisingly strong effect, both on conversion and even selectivity, which was so far relatively unaffected by the other changes in pre-treatment.

A "double-reduced" (*ex-situ* and *in-situ*) Ir-Re/SiO_2 (G-6) catalyst reached 45% conversion and 46% selectivity to 1,3-propanediol, compared with 40% conversion and 39% selectivity under the same reaction conditions (393 K, 20 h) with a catalyst that was not reduced *in-situ*. A calcination in air at 773 K before the reduction *in-situ*, led to results similar to the ones obtained before: The conversion decreased strongly while the selectivity only experienced changes which can be attributed to the consecutive reaction that has a stronger influence in the case of higher conversions, altering mainly the amounts of 1,2-propanediol and 1-propanol found.

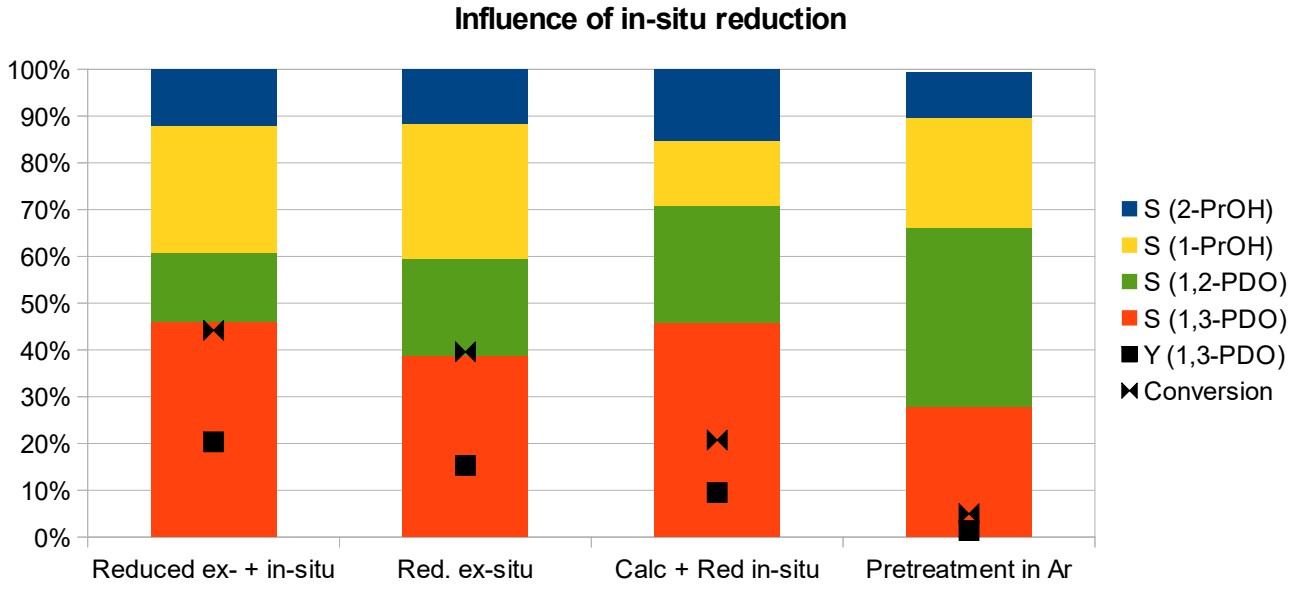

Figure 46 The influence of the pre-treatment of Ir-Re/SiO_2 (G-6) on the hydrogenolysis of 20%wt. glycerol in water (20 h, 120°C, 5 MPa H_2). From left to right: Reduction *ex-situ* at 230°C and *in-situ* in water at 200°C (7 MPa H_2); Reduction *ex-situ* at 230°C; Calcination at 500°C in static air and reduction *in-situ* in water at 200°C; and reduction *ex-situ* at 230°C and pre-treatment *in-situ* under Argon (7 MPa Ar).

The transfer of the catalyst to the reactor in a glove box after reduction *ex-situ* (503 K) and before hydrogenolysis at 393 K did not show any positive effects, interestingly, the conversion was even a bit lower (this result is not shown in the graph) as the air contact in between seemed to have a slightly promoting effect. In summary, these experiments showed that as well the presence of water as the one of hydrogen can be said to be crucial for the enhancement in the hydrogenolysis reaction.

The importance of water during the reduction was shown by the experiments with the glove box, in which the catalyst is assumed to reach the hydrogenolysis reactor in the reduced form, still, the *in-situ* (and hence in water) reduced catalyst outperformed all the others. Yet the importance of hydrogen during the *in-situ* pre-treatment was proven by the utilization of argon instead of hydrogen during this stage. Heating the catalyst, that was reduced *ex-situ* and transferred under air contact to the reactor, to 473 K in water under argon for 1 h led to a strong deactivation of the catalyst with an also strong decrease in the selectivity towards 1,3-propanediol in the following hydrogenolysis of glycerol at 393 K under 5 MPa of hydrogen.

These effects were much stronger than in the case of a calcination of the catalyst which means that a different kind of deactivation must have taken place, with a modification of the active sites that lead to the change in selectivity. One likely explanation is that the modification of the bimetallic particles under these conditions differs from the one taking place in the presence of hydrogen – the one in argon had a strongly inhibiting effect whereas the one in hydrogen promoted the desired reaction both in conversion and selectivity. Another point could be a change in the structure of the support, however, regarding the results of section 7.3 where the influence of the support was investigated, it seems unlikely that this modification could cause such an impact, considering that changes of support material hardly influenced the selectivity in the other experiments.

When the catalyst was calcined *ex-situ* in Argon at 503 K and reduced *in-situ* as described before, the results were very similar to the ones when the catalyst was calcined in air at 773 K, except of a slightly lower conversion. Possibly, the structure that is formed during the pre-treatment in argon is similar to the one formed in air, different from the alloy probably formed under hydrogen, and the catalyst therefore shows a similar, less active, behaviour. The other possibility is that the temperature of 503 K is too low to calcine the catalyst entirely, basically leaving the metal precursor untouched, and the (maybe incomplete) reduction occurs *in-situ* later on.

7.6.3. Pre-treatment and acidic properties

The acidic properties of several catalysts were analysed by the adsorption and temperature programmed desorption (TPD) of ammonia. For this purpose, around 50 mg of catalyst were pre-treated *in-situ* for 1 h at 507 K in 10%vol. H_2/He and then cooled under helium to 323 K, followed by saturation with ammonia at this temperature for 15 minutes. After another 30 minutes of helium flow, desorption started with a heating rate of 10 K/min until 973 K.

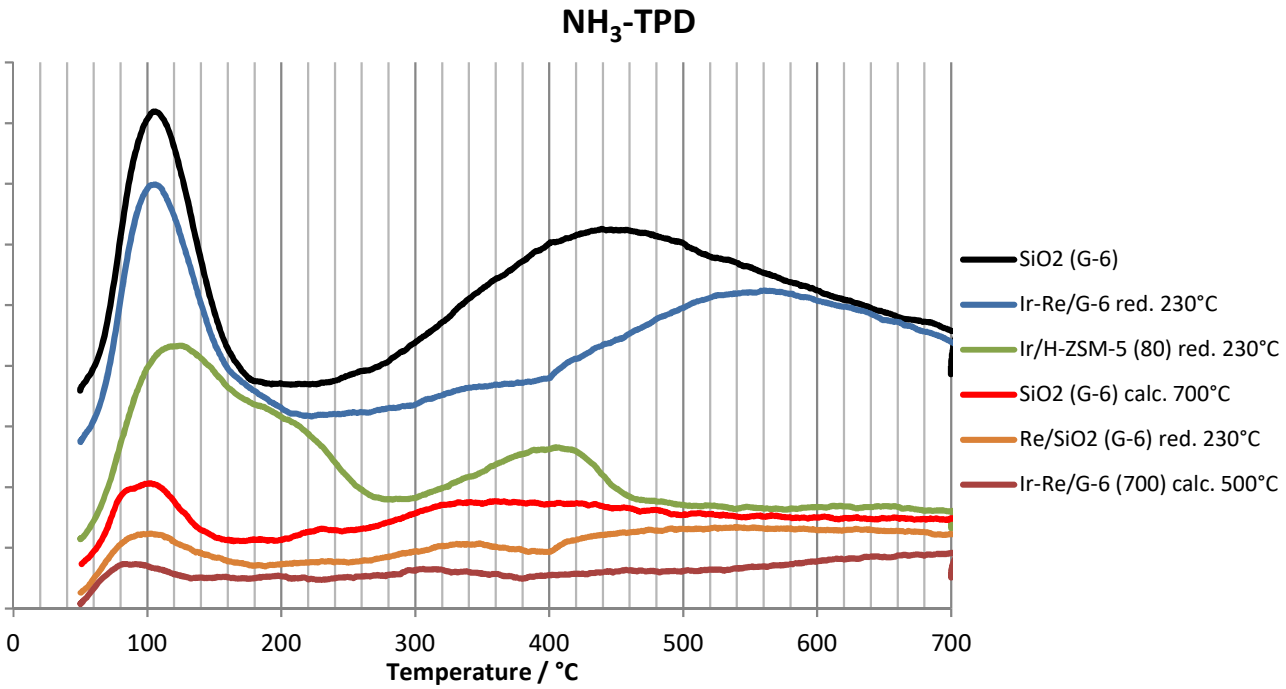

Figure 47 The temperature programmed desorption of ammonia (NH_3-TPD) shows the strength and distribution of acid sites on the dry catalyst. Several catalysts with and without metals were compared after passing different preparation steps. In some cases the G-6 silica support was calcined in a muffle furnace at 700°C (designated as G-6 (700)) while the final catalysts were either reduced in flowing hydrogen at 230°C ("red. 230°C") or calcined at 500°C in a muffle furnace (indicated by "calc 500°C").

The results show that a treatment at high temperatures leads to a significant decrease in the concentration of surface acid sites, resulting in almost no acid sites on Ir-Re/SiO_2 (G-6) (700) which was – following a common, but unpublished procedure of the Tomishige group – calcined at 973 K before and at 773 K after the impregnation with the metal precursors. The catalyst and support materials that were not calcined basically show two desorption peaks, one sharp peak originating from relatively weak acid sites with an ammonia desorption peak around 380 K, and another much broader one at temperatures around 700 K, indicating relatively strong acidic sites. Ir/H-ZSM-5 (80) was included in order to represent a monometallic catalyst, even though the support material is different, because no Ir/SiO_2 catalyst was tested in the hydrogenolysis reaction throughout this work. In the case of this catalyst, another small peak at around 470 K appears which in the literature has been pointed out as typical for H-ZSM-5 zeolites, beside the one at 670 K.[146-147]

Comparing SiO_2 (G-6) and Ir-Re/SiO_2 (G-6), reduced at 503 K, a certain decrease in the number of strong acid sites can be detected, however, the TPD profile does not change dramatically and continues similar to the one of Ir/H-ZSM-5 (80). It can therefore be stated that the application of the metals blocks a part of the acidic sites of the support, but not all of them, remembering that the DRIFT spectra after pyridine adsorption also revealed that a band designated to Brønstedt acidic hydroxyl groups

disappears with the deposition of the metals (see Figure 32). On the other hand, calcinations at high temperature seem to erase almost any acid sites present on the catalyst surface.

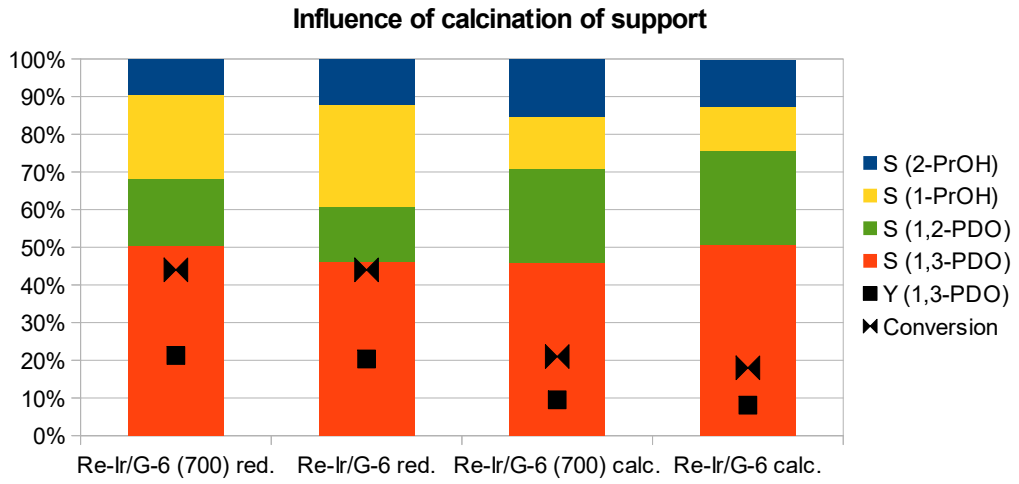

Figure 48 Influence of the calcination of the SiO_2 (G-6) support at 700°C before the impregnation of the metals. All catalysts were reduced in-situ at 200°C and 7 MPa, the reaction conditions were 120°C, 5 MPa H_2, 20%wt. glycerol in water. Catalysts marked with "red." have been reduced *ex-situ* for 1 h at 230°C, those marked with "calc." were calcined for 3 h at 500°C in static air.

Relating these results to the catalyst performance presented in Figure 48, there seems to be no direct correlation between the amount and/or strength of the acid sites and the catalytic performance. The equal performance of the catalysts based on calcined (973 K) and not calcined G-6 silica shows that the absence of acidic sites on the calcined support does not inhibit the hydrogenolysis reaction. To the contrary, the yield of 1,3-propanediol over the catalysts based on the calcined G-6 (700) silica is even a bit higher, though the difference is still within the error margin. Therefore, the almost total absence of acidic sites on the catalyst that is calcined at 773 K after the impregnation seems to be rather a coincidence than the reason for the low performance of these catalysts.

It is important to state that the measurements of the desorption of ammonia are carried out on the dry catalyst and do not exclude the possibility of the formation of acidic sites *in-situ* that might influence the catalytic performance of the catalyst.

7.7. Influence of solvent

In order to investigate the importance of water during the pre-treatment and during the reaction, the hydrogenolysis was performed in a 1:1-mixture of ethanol and water. In one case, the *in-situ* reduction was carried out exclusively in ethanol with the water being added together with the glycerol, and in the other case, no *in-situ* reduction was performed, to be compared to the respective reactions with water as the exclusive solvent. For comparison, the *in-situ* reduction was also performed in the "normal"

reaction solution of 20%wt. glycerol, in other words, the reaction was run at 473 K for one hour and 393 K for 20 hours.

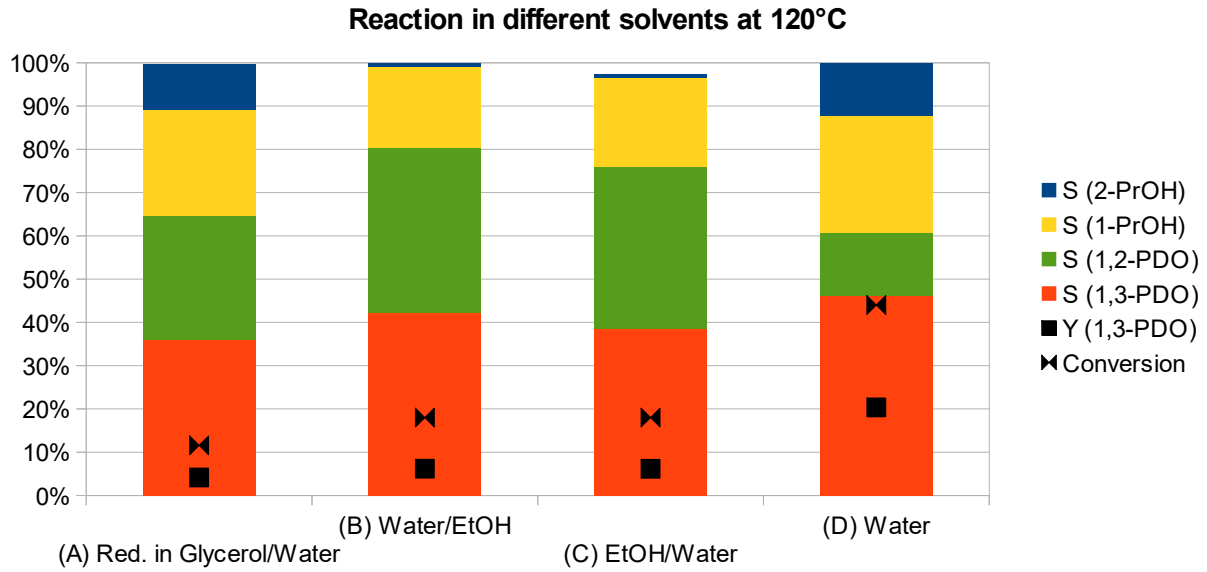

Figure 49 Different solvents were tested for the hydrogenolysis of glycerol at 120°C over Ir-Re/SiO_2 (G-6). In all cases, a 20%wt. solution of glycerol was used, in case A and D in water, in case B and C in a mixture of ethanol and water (20% glycerol, 40% ethanol, 40% water, per weight). (A) Reduction *in-situ* at 200°C in glycerol and water, the conversion during the pre-treatment was not considered for this graph; (B) Reduction in-situ in water, ethanol was added afterwards; (C) Reduction in ethanol, water was added afterwards; (D) Reduction and reaction in water (also shown in Figure 46), for the sake of comparison. No noteworthy conversion of ethanol was detected.

The presence of glycerol during the pre-reduction has an inhibiting effect on the following hydrogenolysis. Not only is the conversion clearly lower than in the case of the catalyst being reduced *in-situ* in water, it is also lower than in the case of no *in-situ* pre-treatment, even if the conversion during the first hour at 473 K is considered. This means that there is at least one mechanism involving glycerol at the reduction temperature that leads to a relatively inactive catalyst. It can neither be just an effect of the temperature stability of the catalyst, due to the good results in pure water, nor can glycerol simply impede the beneficial process that occurs in water – because in this case the results should be equal to the ones without *in-situ* pre-treatment.

One possibility is that the reaction of glycerol on the catalyst at that temperature forms some compounds that lead to a deactivation of the catalyst, for example by forming strong bonds with the active sites on the catalyst. If this was the case, this would be an effect that only starts to be visible at this temperature, because reactions carried out at 453 K (see Figure 37, for example) showed high conversions of up to 70% at 8 hours. As the conversion after one hour at 473 K was already above 20% (at a relatively low selectivity to 1,3-propanediol of 23%), the deactivation seems not to occur at

this temperature, but might also be due to products formed at high temperatures that cause problems (e.g. by strong adsorption) when the temperature is lowered.

The comparison between the experiments using ethanol and water shows that in both cases, with the reduction happening in ethanol as well as in water, the reaction rate is clearly lower than in water. Another difference is that almost no 2-propanol is formed, while more 1,2-propanediol is detected. It seems as if ethanol is obstructing the conversion of glycerol, possibly by adsorbing on the catalyst in a stronger or different way than water and glycerol, as well as the consecutive reaction of 1,2-propanediol, leading to an accumulation of this product. Ethanol itself was not converted in any detectable amount (the threshold for the detection was relatively large, due to the high amount of ethanol present that complicates the detection of small changes). The most likely explanation is that the absence of a second hydroxyl group impedes the reaction of ethanol in the same way as it happens with the propanols, as has been discussed before. Due to the big amount of ethanol present in the reaction solution, it adsorbs frequently on the catalyst and thereby blocks the active sites for the conversion of glycerol. A small difference in selectivity between the tests when the catalyst was pre-reduced either in water or in ethanol was detected (see Table 5). Hence, it seems to actually make a difference whether the reduction occurs in water or in ethanol, but the difference is too small to draw any conclusion.

Table 5 Comparison between the selectivity over Ir-Re/SiO_2 (G-6) reduced *in-situ* in water and in ethanol at 200°C for one hour before the hydrogenolysis reaction performed at 120°C in 20%wt. glycerol, 40%wt. ethanol and 40%wt. water at 5 MPa H_2.

	Reaction Time	Conversion	S (1,3-PDO)	S (1,2-PDO)	S (1-PrOH)	S (2-PrOH)
Reduction	2 h	2%	41%	42%	16%	1%
in Water	20 h	15%	42%	38%	19%	1%
Reduction	2 h	2%	38%	45%	17%	0%
in Ethanol	20 h	16%	38%	38%	21%	1%

Besides, glycerol as well as 1,2-butanediol (1,2-BDO) were used as solvents in reactions at 433 K for 8 hours. In comparison with glycerol/water, glycerol/1,2-BDO led to a clearly lower conversion of glycerol, while the selectivity underwent only small changes, favouring especially 1,2-propanediol. The most likely explanation is that 1,2-butanediol obstructs the hydrogenolysis of glycerol by occupying active sites and reacting itself, even though the conversion was lower than the one of glycerol. Another explanation could be that the presence of water is crucial for the effective functioning of the catalyst, which might actually be the case but probably would not be visible in these experiments, due to the water content as impurity of the reactants.

The conversion of 1,2-butanediol (reaching 6% after 8 hours) resulted in 68% 1-butanol and 32% 2-butanol, which is similar to the selectivity of the conversion of 1,2-propanediol, presented in Table 3 on page 64 where the hydrogenolysis of the secondary hydroxyl group was also favoured. These results are in good agreement with the literature and suggest that the terminal hydroxyl group is more likely to act as an anchor at the catalyst surface while the secondary group is transformed.

Performing the reaction in pure glycerol led to a relatively smaller conversion, this means that a smaller percentage of the present glycerol was converted. This might be due to a higher viscosity and also to a saturation of the catalyst with glycerol, already under "normal" reaction conditions with an only 20%-solution of glycerol in water. The total amount of converted glycerol was slightly higher than in the standard case, the result would be 51% conversion and 16.8% yield if only 20% of the glycerol were considered "available" for the reaction. This indicates that the active sites on the catalyst are occupied almost all of the time and therefore cannot convert more, even with glycerol being available in a higher concentration. The selectivity is similar to the experiment with the diluted solution, with the only difference that the products of the first stage (hydrogenolysis of glycerol) appear a bit more and the products of consecutive reactions a bit less – nothing unexpected regarding the higher concentration of glycerol.

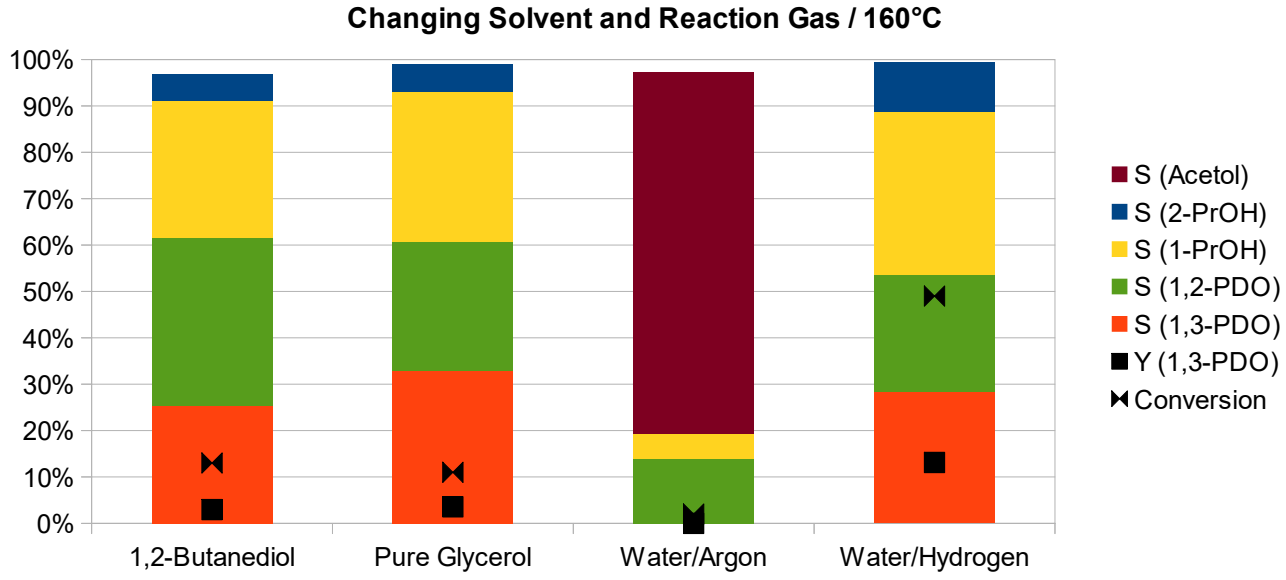

Figure 50 The solvent for the hydrogenolysis of glycerol (20%wt.) over Ir-Re/SiO_2 at 160°C was changed, as well as the reaction gas. The conversion of the solvent 1,2-butanediol amounted to 6%. When the reaction was carried out in pure glycerol, the amount of glycerol transformed was the same as in a 20% solution. When hydrogen was replaced by argon, acetol (hydroxyacetone) was the main product.

The similarity of the results with 20% and 100% glycerol do not imply that water has no important role in the hydrogenolysis because the glycerol used in these experiments always contains small amounts

(up to 0.5%) of water, enough to act catalytically in the reaction mechanism or to modify the structure of the catalyst.

A change of the reaction gas from hydrogen to argon led – not surprisingly – to a much lower conversion of glycerol, reaching 3% after 8 hours at 433 K. The main product was acetol, also known as hydroxyacetone, a dehydration product of glycerol. This shows that the catalyst is indeed capable of conducting an acid-catalysed dehydration as presented in Figure 7 (page 19), even though with a relatively low activity. This low activity makes it difficult to judge whether the reaction pathway via dehydration and hydrogenation plays a significant role under standard conditions as the presence of hydrogen might also have an influence onto the acidic sites of the catalyst and hence the dehydration rate. Interestingly, some hydrogenation products are still formed, namely 1,2-propanediol (around 7 mmol) and 1-propanol (around 2 – 3 mmol), possibly with hydrogen adsorbed on the catalyst surface from the reduction ex-situ that was performed before the reaction or with traces of hydrogen that had remained in the gas pipes, in spite of flushing with argon. The absence of 1,3-propanediol in spite of the small quantities of hydrogen present can also be explained using the mechanism shown in Figure 7 (page 19). Due to the low stability of 3-hydroxypropanal, which is the precursor to 1,3-propanediol in an acid catalysed mechanism, and the low quantity of hydrogen present, the formed 3-hydroxypropanal is more likely to suffer a reverse reaction and rearrangement to the more stable acetol rather than undergo a hydrogenation to 1,3-propanediol.

7.8. Deuterium experiments

Aiming for a deeper understanding of the reaction mechanism, the reaction was carried out using deuterium instead of hydrogen. The resulting solution was then analysed by GCMS and later also by NMR. Surprisingly, the products gave the same mass spectrum signal as the ones of the reaction with hydrogen, indicating that hydrogen from water must have entered the reaction.

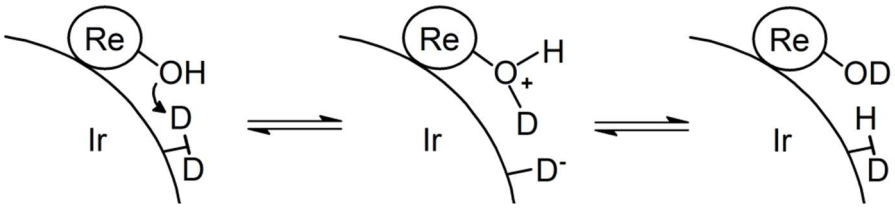

Figure 51 Possible mechanism for the exchange of hydrogen (from water that reacted with rhenium oxide species) and deuterium at the surface of Ir-Re nanoparticles. The molecular adsorption of deuterium on the iridium surface is intended to serve as an example only, as a dissociative adsorption might occur as well.

One way for hydrogen might be through an H-D-exchange shown in Figure 51 where Re-OH origins from the reaction of water with rhenium (oxide) species as discussed before. Due to the abundance of

water, deuterium in Re-OD will be quickly substituted by another hydrogen atom from a water molecule, resulting in Re-OH (ready to react with another adsorbed deuterium) and deuterated water HDO. The same kind of reaction could also happen with a Si-OH group, but the scheme described before seems more likely, due to the acidic properties the catalyst gains with the introduction of the metals, as has been shown by pH measurement.

In the next experiment, the reaction of glycerol and deuterium was carried out in deuterium oxide (D_2O) as solvent. The results were somewhat surprising as the grade of deuteration was much higher than expected and even the starting material glycerol was strongly deuterated. The mass spectrum of 1,3-propanediol (see Figure 52) showed, for example, a shift of up to 6 mass units compared to the not deuterated product. The mass peaks also showed a stronger distribution, indicating that several different deuterated species were present. Analogue results were obtained for 1,2-propanediol, 1-propanol and 2-propanol.

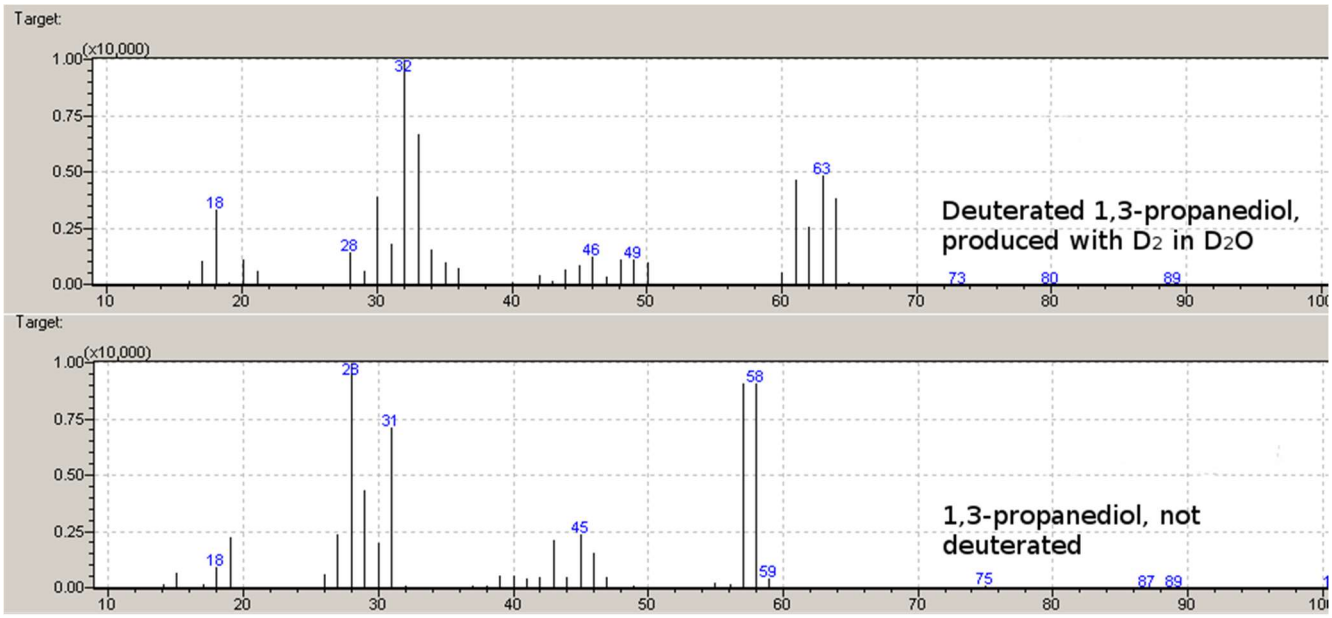

Figure 52 Mass spectrum of 1,3-propanediol resulting from the hydrogenolysis of glycerol on Ir-Re/SiO_2, once with deuterium in D_2O (above) and once with hydrogen in water (below).

NMR examination supported these results, indicating a mixture of highly deuterated species for 1,3-propanediol as well as glycerol with virtually no undeuterated species in spite of glycerol being a starting material. The NMR signal turned out to be very complex due to the high number of different species, so that no information about the exact structure or the ratios in between these species could be gained.

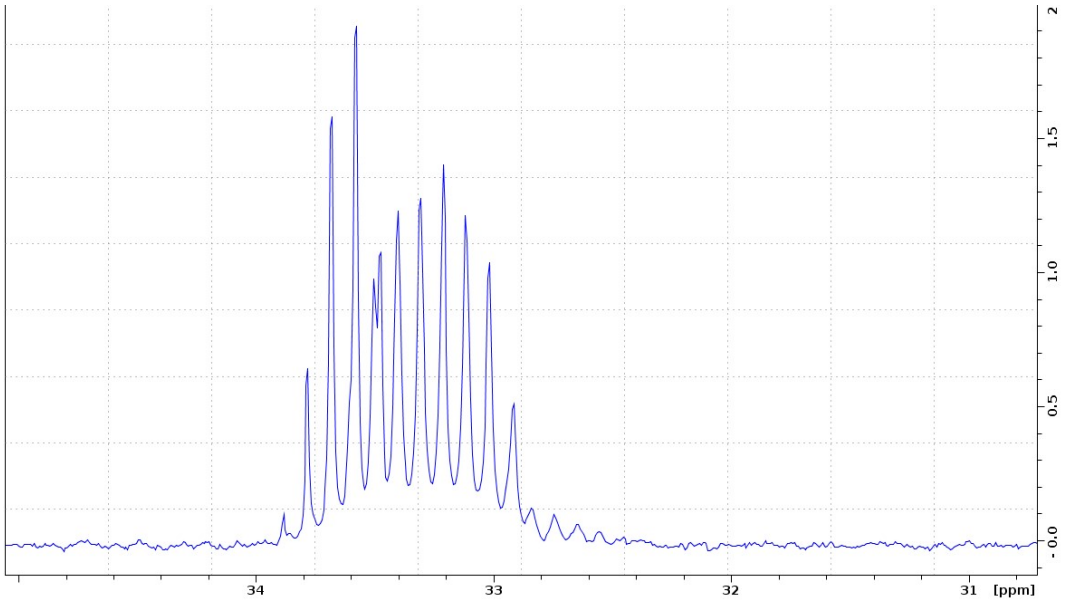

Figure 53 ^{13}C-NMR signal of the middle C in 1,3-propanediol, produced with deuterium in D_2O. Several couplings with neighbouring deuterated carbon atoms cause a complex signal (not deuterated 1,3-PDO would lead to a single peak at around 33.8 ppm).

DEPT-Spectra of the glycerol after the reaction show that not all end-standing carbon have been deuterated (negative peak: not deuterated, positive peak: partly deuterated (1 H, 1 D), completely deuterated species do not appear in the DEPT spectra), however, the split peak indicates the coupling with a neighbouring C-D bond, showing that the middle C underwent a hydrogen-deuterium exchange and species without any deuterium could not be detected.

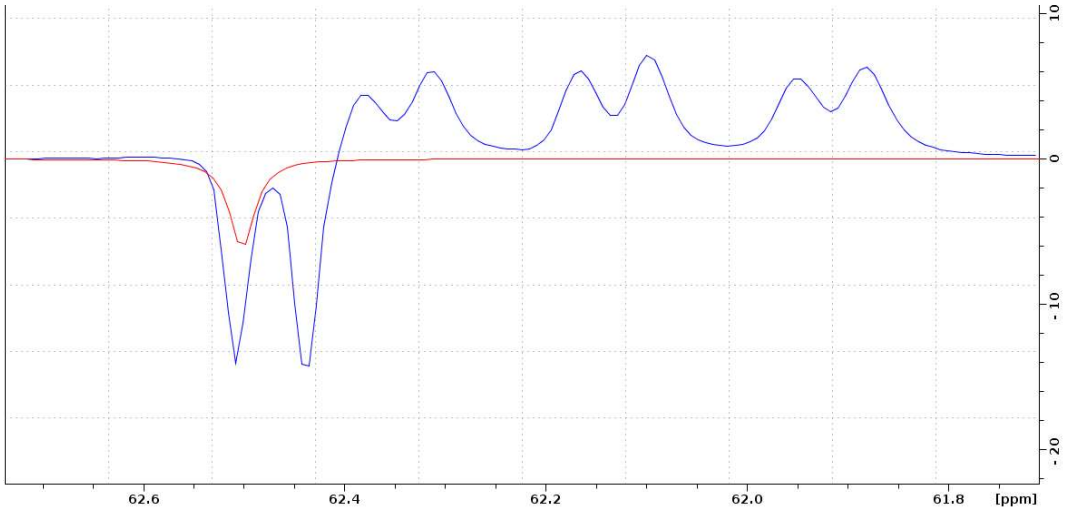

Figure 54 DEPT spectra of the end-standing carbon atom in glycerol before (red line) and after the reaction over Ir-Re/SiO_2 in D_2 and D_2O (blue line).

One possible explanation for these findings could be that the hydrogenolysis reaction is reversible and that the eliminated water (or HDO) is substituted by D_2O in a reverse reaction, in this case probably when the molecule is still adsorbed on the catalyst surface. However, this scenario does not seem very likely, as water (or D_2O) would have to attack an unsubstituted carbon atom instead of a functional

group. More realistic seems a dehydrogenation-deuteration-mechanism as shown in Figure 55, even though this mechanism alone does not explain the incorporation of hydrogen in case of a reaction with deuterium in water and would therefore have to occur together with a reaction like the one described in Figure 51.

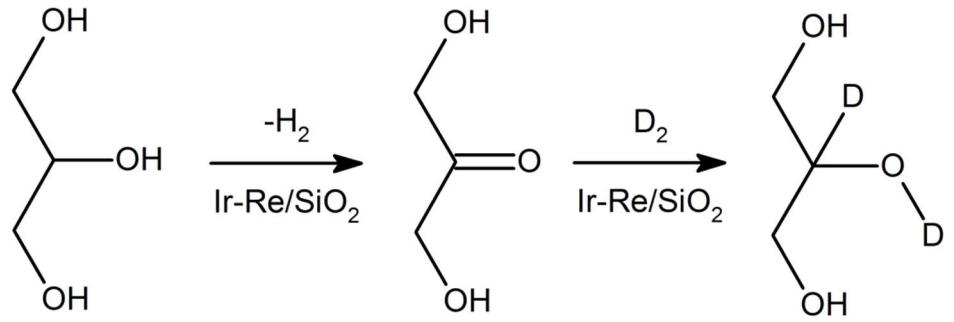

Figure 55 Dehydration-deuteration-mechanism to explain the H-D-substitution on glycerol during the reaction with D_2 in D_2O.

One explanation for all results could be that the hydrogenolysis of glycerol actually occurs via an (acid catalysed) dehydration-hydrogenation mechanism as has been proposed by many authors for any catalyst except of the one used in this study.

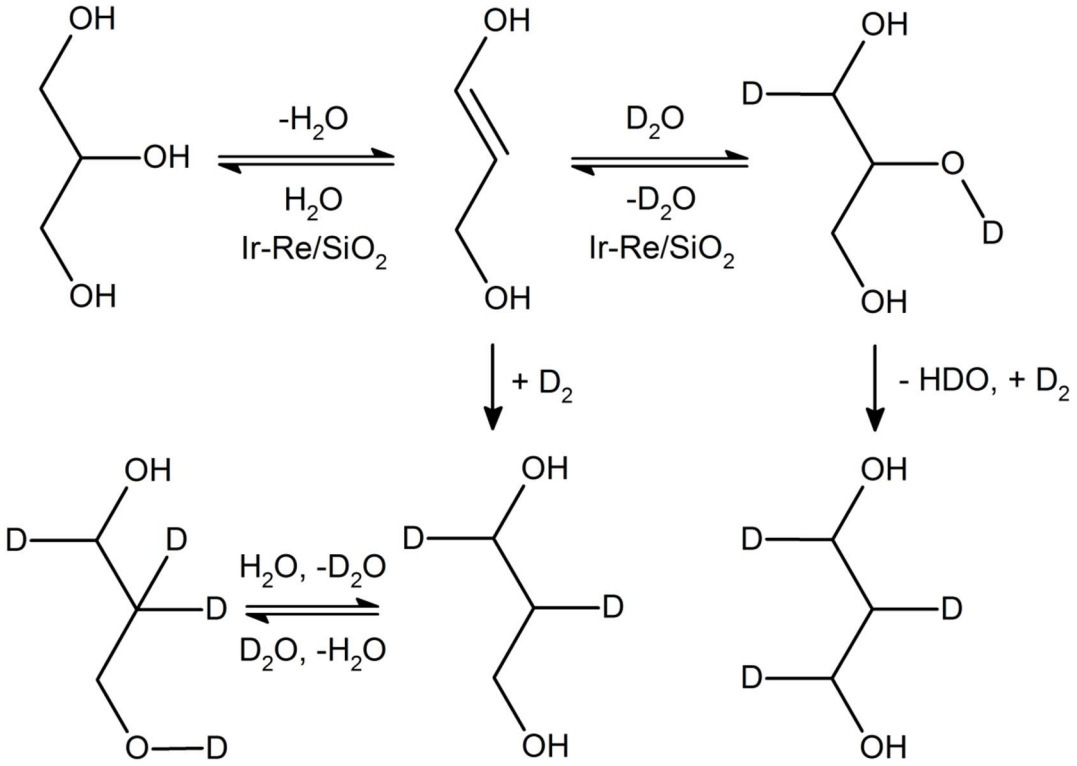

Figure 56 One alternative mechanism to explain the deuteration of glycerol by way of dehydration, followed by the reverse reaction, implementing D_2O instead of water. This might also be the first step of the hydrogenolysis reaction, depicted with some exemplary reactions explaining the formation of highly deuterated species. If one of the terminal hydroxyl groups is eliminated in the dehydration step, a re-hydration with D_2O would lead to the glycerol species detected by NMR, with the middle C of glycerol being deuterated.

Nevertheless, a rapid and reversible dehydration, introducing D_2O in the reverse reaction (see first line of Figure 56), followed by a hydrogenation, likely to occur slower and in competition with desorption, would be a good explanation for the results of the deuterium experiments. In this case, glycerol could adsorb on the catalyst surface, possibly on an acidic rhenium or silica site, and would be dehydrated. The predominant glycerol species found, with the middle carbon atom deuterated, indicates a substitution of a terminal hydroxyl group with an OD group by a dehydration-hydration with H_2O/D_2O. If the intermediate of this reaction was hydrated, 1,2-propanediol would be formed, whereas the mechanism shown in Figure 56 would lead to 1,3-propanediol. The total absence of species with a non-deuterated central carbon, whereas not all end standing carbon atoms were fully deuterated, might be due to the different stability of the intermediates that has been discussed before (see Figure 10). With the higher stability of acetol as intermediate to 1,2-propanediol, this compound is more likely to undergo the reverse reaction with D_2O than the unstable 3-hydroxypropanal which is deuterated faster under those reaction conditions.

Two competing reactions could occur next, either a re-hydration back to Glycerol or a hydrogenation to form a propanediol and, in sequence, a propanol. The experimental results of the deuterium reactions, giving highly deuterated glycerol after reaction in D_2O and "normal" hydrogenated species in water, suggest that the reverse reaction occurs much faster than the hydrogenation step. However, it is not clear whether the non-deuterated products of the reaction in water arise from the reaction of glycerol with hydrogen formed in a mechanism described in Figure 51 or whether glycerol reacts with deuterium first and the products lose their deuterium atoms in a way analogue to the reverse reaction in the first line of Figure 56 – or if maybe both routes apply.

8. Conclusion

After the analysis of the impact of numerous parameters onto the performance of the catalyst, some conclusions can be drawn:

Keeping in mind that the consecutive reaction of the propanediols influences the final detected selectivity, especially in the case of 1,2-propanediol, many parameters did not have a significant impact onto the selectivity of the reaction of glycerol, but a huge impact on the reaction rate. Only a few variables led to a change as well in selectivity as in conversion. In general, factors that change the conversion but not the selectivity are likely to influence the availability of at least one of the reactants, but do not influence the active sites. The strong dependence of the conversion from the support material, for example, is very likely to be caused by the differences in adsorption and hence in the ready availability of glycerol since no hint could be found for a connection with metal particle size.

With FTIR measurements, it could be shown that glycerol adsorbs on terminal Si-OH groups on the pure support and that these groups still exist in the final catalyst. The correlation of the intensity of this band in the IR spectrum with the activity of the catalyst based on this support material adds to the picture that the crucial role of the support for the overall performance of the catalyst comes from the ability of providing the reactant glycerol to the active sites of the hydrogenolysis. The experiment with pure glycerol also indicated that the number of adsorption sites for glycerol might be a limiting factor for the reaction. In addition, the difference in the catalytic activity could not be explained by the differences in BET surface area, metal surface area or number and strength of acidic sites, leaving the adsorption characteristics as the only correlation found.

In contrast to changing the support material, a change in the composition of the metals had a significant influence not only on conversion, but also on selectivity. While the difference between Ir-Re and Pt-Re was relatively small, with Pt-Re being less active and forming more 2-propanol, ruthenium or rhodium brought bigger changes. Unfortunately, in spite of high conversions for Rh-Re and monometallic Ru, the selectivity to 1,3-propanediol turned out to be much lower than in the case of Ir-Re catalysts. Especially ruthenium also catalysed a significant amount of C-C scissions, forming ethanol and ethylene glycol. Surprisingly, the influence of rhenium on the selectivity was rather limited with monometallic iridium leading to a very similar selectivity towards 1,3-propanediol, but at lower conversion. Nevertheless, rhenium had a strong influence on the activity of the catalyst, accelerating the hydrogenolysis. Decisive factors for this acceleration by rhenium are the direct contact between the two metals and also the right order of impregnation, depositing rhenium on top of iridium. These results suggest that the decisive step of the reaction that determines the final product is not very much affected by rhenium, but rather by the noble metal. On the other hand, the acceleration caused by rhenium might be either due to the acidity of Ir-Re particles or to the “anchor effect” of rhenium for glycerol, proposed by the Tomishige group.

With the results of the experiments with deuterium and D_2O, supported by the formation of acetol in the absence of hydrogen and by the detection of C=O double bonds during the adsorption of glycerol in the FTIR, a dehydration and re-hydration of glycerol on the Ir-Re/SiO_2 catalyst can be assumed to happen relatively quickly under reaction conditions. This is a clear hint that the hydrogenolysis reaction actually occurs via an acidic catalysed mechanism and not via a direct hydrogenolysis of the C-O bond. The formation of an acidic solution under the presence of the metals (for an Ir-Re catalyst) also indicates the importance of the acidic properties of the Ir-Re particles. On the other hand, external addition of acid did, depending on the acid used, either show no effect or an inhibiting one, culminating in tungstic acid practically “killing” the catalyst.

Still unclear remains the mechanism of how water and the *in-situ* reduction influence the catalyst. In contrast to the deactivation caused by the calcination of the catalyst, which is probably due to agglomeration of the metal particles, the reduction in water and under higher hydrogen pressure also enhanced the selectivity towards 1,3-propanediol. This means that this kind of pre-treatment changes the active sites since a possible oxidation during the infilling as the reason for the different results could be excluded. Besides, examination of the dry catalyst did not show any correlation between acidic sites and the performance during the hydrogenolysis, which could mean that important changes on the catalyst surface happen in the presence of water.

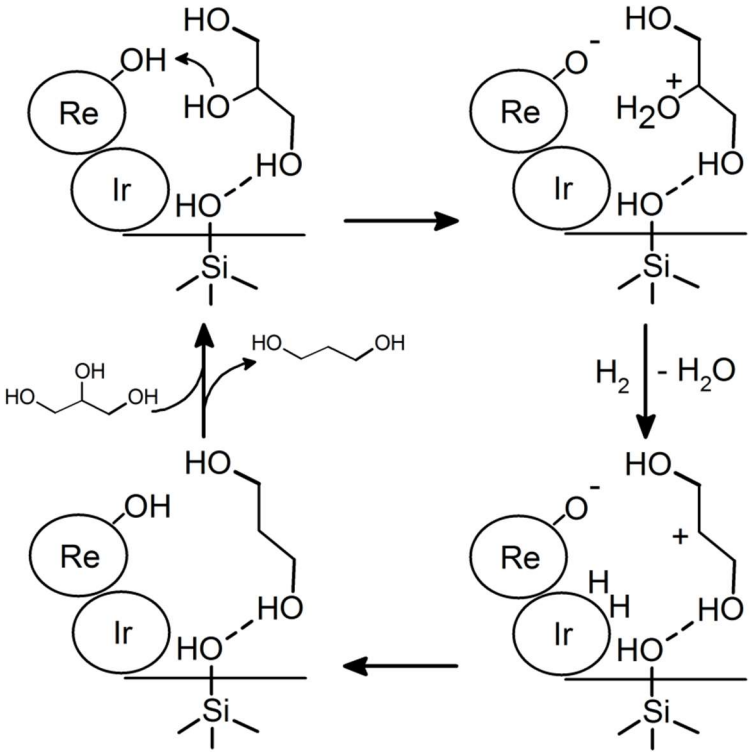

Figure 57 Possible catalytic cycle for the hydrogenolysis of glycerol over Ir-Re/SiO_2, postulated based on the results of this study.

Based on the findings during this work, a possible reaction mechanism can be postulated. In a first step, glycerol adsorbs on the catalyst surface, probably on a Si-OH group, either by substituting a hydroxyl group or via hydrogen bonds. Glycerol might then be transferred to a rhenium adsorption site; however, there is no evidence for that and this possibility is neglected in Figure 57. In the next step, glycerol is dehydrated to form either an adsorbed species of acetol or 3-hydroxypropanal. This species is then hydrogenated by iridium, followed by desorption or a second dehydration, leading to a propanol. One important factor for the selectivity might be which glycerol hydroxyl group adsorbs on the catalyst surface, as this one will not undergo the hydrogenolysis. However, there must be a second important parameter, because some changes, e.g. exchange of the noble metal or the reduction *in-situ*, actually changed the selectivity, pointing to a steric or electronic reason. In case of a mechanism

involving 3-hydroxypropanal and/or acetol (or a respective adsorbed species) as intermediates, the time between the formation of the intermediate and its consecutive hydrogenation will also have a significant influence onto the selectivity, due to the unequal stability of the two intermediates.

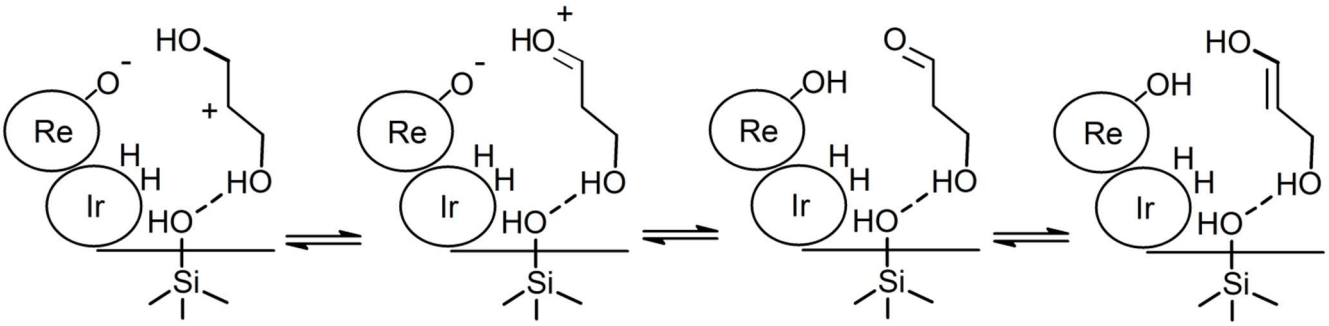

Figure 58 Some of the possible tautomeric structures for the carbocation shown in Figure 57. The negative charge on the oxygen atom attached to rhenium is also likely to be delocalised over the bimetallic particles with oxygen forming a double bond with rhenium.

Another possibility is the two-point-adsorption of glycerol on the catalyst, as well on rhenium as on the silica surface, as depicted in Figure 59. However, this mechanism alone does not explain the formation of propanols and can only be seen as a complementary option to the mechanism presented in Figure 57.

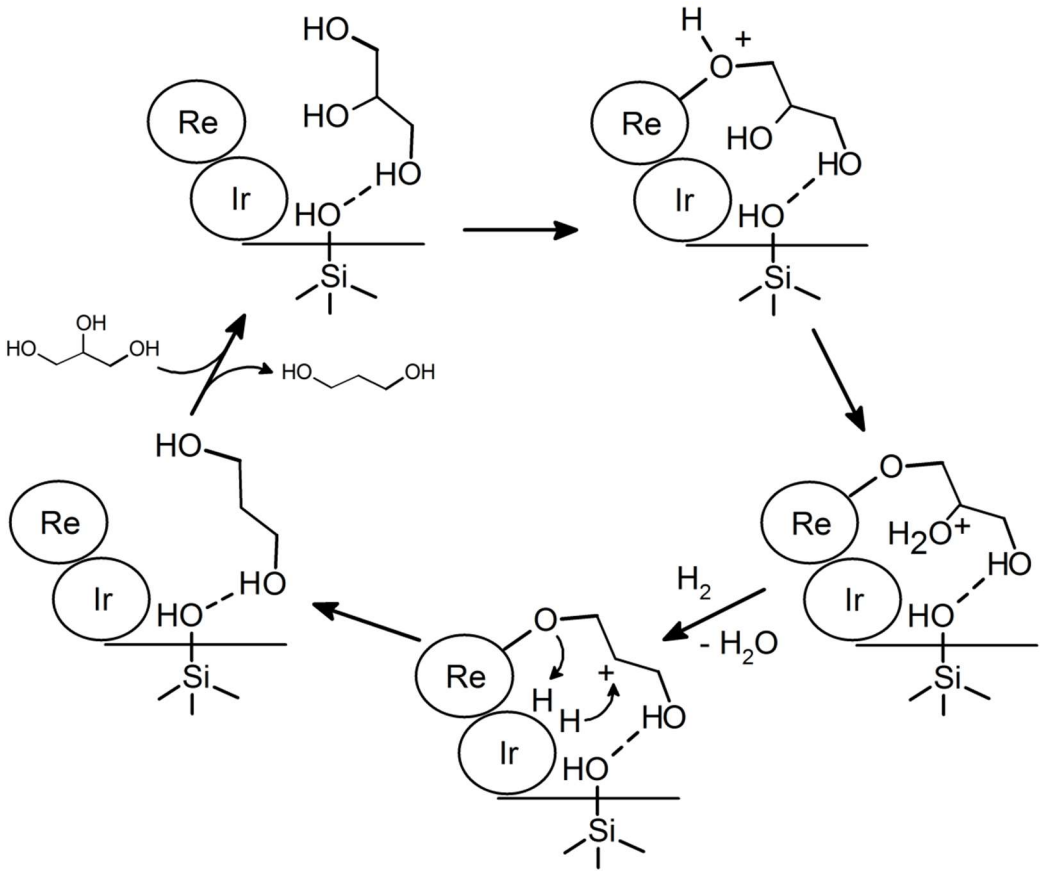

Figure 59 Variation of the mechanism shown in Figure 57 in which the glycerol binds not only to a Si-OH group, but also to rhenium.

9. Summary and Integration of the results in the scope of literature

The strong increase in the biodiesel production in recent years has immensely increased the availability of glycerol as a building block for the chemical industry. However, the selective conversion of glycerol to high-value products like 1,3-propanediol is still difficult and lacks efficiency, resulting in this process being a bottle-neck for the ready availability of valuable high tech products like poly trimethylene terephthalate (PTT), an important polymer for the textile industry. With derivative products like this, the percentage of materials based on renewable resources could be increased significantly, contributing to the diminution of the dependence on fossil resources and to the containment of the climate change.

The conversion of bio-based glycerol is already performed on industrial scale as a biotechnological process, burdened with typical drawbacks of these kinds of processes like low space-time-yields, the need for co-reactants etc. Also, this one as well as actual heterogeneously catalysed industrial processes suffers from yields far below 100%. In principle, heterogeneous catalysts should be able to solve these problems, however, the selective removal of the secondary hydroxyl group has turned out to be far more complex than the formation of 1,2-propanediol and the performance of literature catalysts still leaves a lot to be desired. In order to construct better catalysts, the functionality of the catalyst and the reaction mechanism needs to be understood.

So far, several reaction mechanisms have been proposed for the variety of catalysts tested on this reaction. In most cases, an acid-catalysed mechanism, either with or without hydrogen spillover, has been assumed whereas a direct hydrogenolysis mechanism was proposed for state-of-the-art bimetallic iridium rhenium catalysts. Based on publications right before the beginning of this study, this type of catalyst has been chosen as one of the starting points for the investigation of the mode of operation of the catalyst and the reaction mechanism. Besides, several attempts for innovative catalysts, e.g. using tungsten carbide, other tungsten components or different hydrogenating metals, have been made during the first phase of this work, but, unfortunately, none of them achieved promising results. Therefore, this work focussed then on the investigation of the reaction mechanism.

As the results with Ir-Re catalysts published by the Tomishige group could not be reproduced and the reaction conditions, especially the very low amount of material compared to the size of the reactor (6 g of glycerol solution in a 190 mL reactor), seemed very impractical, new standard conditions were defined in a series of preliminary tests. Most of the reactions of this study have been performed for 8 h at 433 K and 5 MPa of constant hydrogen pressure, enabled by an external hydrogen tank that reduced the necessary gas volume inside the reactor. The most important parameters that were chosen to be

examined were the active metals, the support materials and the pre-treatment conditions. Within the preliminary tests, the importance of an inserted protecting vessel was detected and hence used in all following reactions, probably protecting the catalyst against iron ions from the steel wall of the reactor.

The support material was found to strongly influence the conversion of glycerol whereas the selectivity remained rather unchanged. The best results could be obtained with Ir-Re catalysts based on SiO_2-containing materials like zeolites (H-ZSM-5, H-BEA and MCM-41) or silica (G-6 and Q-6), with the availability of free Si-OH groups on the surface being a very important factor for the catalyst performance, probably due to glycerol adsorption on these sites. Other support materials like alumina or carbon supports proved to be less active in the hydrogenolysis. Besides, no correlation between acidic sites, BET surface area or CO uptake and catalyst performance could be found. Based on these results, SiO_2 (G-6) and H-ZSM-5 (80) were chosen as the main support materials for this study.

Regarding the active metals, the good performance of bimetallic iridium-rhenium catalysts could be confirmed. The presence of rhenium, which had to be in direct contact with the noble metal, led to a massive increase in the reaction rate at which the selectivity did not undergo big changes. The impregnation order was also found to be crucial, iridium had to be impregnated first, followed by rhenium without an intermediate reduction step. However, this was only valid for iridium and rhenium, modifications of the impregnation order of iridium and an eventual tertiary metal did not show this effect. Rhenium on its own turned out to be almost inactive and did not form any 1,3-propanediol whereas Iridium on its own formed a similar product distribution as the bimetallic catalyst, but needed a lot more time for it. Replacing iridium by platinum in bimetallic catalysts with rhenium did not lead to great changes, mainly a slight decrease in glycerol conversion. In contrast to that, ruthenium and rhodium increased the conversion, but formed less 1,3-PDO, resulting in a much lower yield than in case of Ir-Re catalysts.

The pre-treatment was thoroughly investigated, showing that the calcination in air at high temperatures of 773 K or more, which has been used in most works described in the literature, actually inhibited the performance of the catalyst, probably due to an agglomeration of the metal particles and maybe also due to remaining oxygenised species. A simple reduction at 503 K in flowing hydrogen after the impregnation and drying was found to promote the reaction. In addition, in a later stage of the work, an additional reduction *in-situ* in water at 473 K and 7 MPa hydrogen pressure increased the conversion and also the selectivity to 1,3-propanediol, allowing a reduction of the temperature to 393 K at a reaction time of 20 hours, reaching a yield of 21% at 43% conversion, alike literature results of a similar reaction system reported by a group independently from the Tomishige group.[70] It could be

shown that the performance improvement was neither caused by a simple re-reduction after a possible oxidation of the metals during the transfer into the reaction vessel with air contact nor by the presence of dissolved rhenium originating from remaining unreduced precursor. The presence of water as well as the presence of hydrogen was found to be decisive for the success of the *in-situ* reduction pre-treatment. The change in selectivity indicated a change in the catalyst structure which might be caused by the high hydrogen pressure during the reduction, compared to the reduction *ex-situ*.

In a small series of experiments with different solvents, organic solvents with hydroxyl groups like ethanol and 1,2-butanediol reduced the conversion of glycerol, probably due to adsorption of the solvent on active sites. 1,2-butanediol was slowly converted by the catalyst whereas ethanol, with only one hydroxyl group, was hardly converted, similar to 1- and 2-propanol. A reaction in pure glycerol led to amounts of products formed that were comparable to the reaction of a 20%wt. aqueous glycerol solution, indicating that the catalyst is saturated and the availability of glycerol is not a limiting factor. The importance of the presence of water could not be examined due to the water content of the solvents, precluding the possibility of working under water-free conditions even at the very beginning of the reaction.

In accordance with literature results, 1,2-propanediol was converted more or less with the same rate as glycerol whereas 1,3-propanediol reacted much slower. 1,2-propanediol formed about three times more 1-propanol than 2-propanol, indicating that the primary hydroxyl group was more likely to adsorb and the neighbouring hydroxyl group underwent the hydrogenolysis.

Experiments with deuterium instead of hydrogen gave an insight into the mechanism of the hydrogenolysis over an Ir-Re/SiO_2 (G-6) catalyst. It could be shown that the catalyst actually exchanges hydrogen (or deuterium, in this case) atoms between the hydrogen gas phase and water. Another finding was that glycerol and hydrogenolysis products undergo a rapid dehydration and rehydration on the catalyst which led to highly deuterated species of reactant and products. The dehydration activity had been observed in other experiments, once in the absence of hydrogen and once measuring the adsorption of glycerol in DRIFTS, but the deuterium experiments led to a very clear result and also showed the dimension of the dehydration and rehydration reaction, leaving virtually no molecule untouched. It could therefore be concluded that the reaction occurs via an acid-catalysed mechanism. A recent work by Falcone et al., using mainly heavy loaded Pt-Re/SiO_2 catalysts, that has been performed in parallel to this one came to the same conclusion about the mechanism, though based on different tests and arguments, hence complementing the present work.[91] This group was also not able to reproduce the results of the Tomishige group.

Concluding, the main achievement of this work is to show that the Ir-Re catalyst, different from what was proposed so far, actually works as a bifunctional dehydration-hydrogenation catalyst. The results hence combine with the works published for Rh-Re and Pt-Re catalysts by the groups around Prof. Dumesic and Prof. Davis, based on DFT calculations and the aforementioned study, but contradict the proposals of the group around Prof. Tomishige, who has published most articles on Ir-Re catalysts for this reaction so far. A detailed mechanism has been proposed, according to the results of the present study. The influence and importance of several parameters, especially regarding pre-treatment, have been investigated and described in order to simplify the work of following researchers by pointing out several details like the protecting inserted vessel (glass or Teflon), *in-situ* reduction and abstinence of calcination that cause a big effect on the performance of the catalyst.

In terms of reaction outcome, the results are very similar to the ones in a paper published by Deng and Scott,[70] however, conversion and selectivity reported by the Tomishige group could not be reproduced, at least not with calcined catalysts as described in the literature. Not calcined catalysts led to a similar selectivity, but at lower conversion. The best yield of 1,3-propanediol registered was 21% at 43% conversion at 393 K and 5 MPa H_2 after 20 hours reaction time. Typical space-time yields were 2.5 $mmol_{1,3\text{-}PDO}/g_{cat}\cdot h$ at 393 K and 4.5 $mmol_{1,3\text{-}PDO}/g_{cat}\cdot h$ at 433 K, equalling around 31 and 56 mmol, respectively, of 1,3-propanediol formed per hour and per gram of metal (counting iridium and rhenium). These space time yields are in the range of what has been claimed to be the highest one for platinum-tungsten catalysts[78] and also similar to the ones calculated from publications of other works using Ir-Re catalysts.

Comparing these results with the literature of the biotechnological process, in which space-time-yields are calculated in g h^{-1} L^{-1}, the results of this study equal around 2 g h^{-1} L^{-1} at 393 K and 3.5 g h^{-1} L^{-1} at 433 K under the used reaction conditions and are therefore in the typical range of literature results for bio-tech processes (which stayed usually below 5 g h^{-1} L^{-1}). However, in case of the heterogeneously catalysed process, the space-time-yield relating to the volume (g h^{-1} L^{-1}) can be increased by simply adding more catalyst – in contrast to the biological process which is limited by relatively low maximum substrate concentrations resulting in maximum end concentrations of 1,3-PDO of less than 100 g/L. Furthermore, the biological process has several other disadvantages like very long reaction times and the more complex separation of the desired product from the reaction solution.[100] High space-time-yields also usually implicate a low yield of 1,3-PDO like 0.30 mol/mol in the example with the highest reported space-time-yield of 16.4 g h^{-1} L^{-1}.[101]

In comparison to the formation of 1,2-propanediol, the space-time-yield reached for the formation of 1,3-propanediol remain clearly smaller. The highest yield of 1,2-propanediol reached in our group and serving as a benchmark for upcoming studies was 22.1 $g_{1,2\text{-PDO}}$ / (g_{Cu}·h) at 493 K, which equals 290 $mmol_{1,2\text{-PDO}}$ / (g_{Cu}·h) or 70 $mmol_{1,2\text{-PDO}}$ / (g_{Cat}·h). Even though the higher temperature of the process to 1,2-PDO leads to higher values, it seems unlikely that comparable yields could be obtained for 1,3-PDO at higher temperatures with the known catalytic systems. It is also questionable whether catalysts aiming to 1,3-PDO and based on a dehydration-hydrogenation mechanism will ever be able to outperform the catalysts designed for the formation of 1,2-propanediol, due to the unfavourable stability of the intermediate 3-hydroxypropanal, compared to the far more stable acetol.

In summary, with the elucidation of the mechanism and several important parameters, this work is another piece in the puzzle of the "perfect" catalyst for the hydrogenolysis of glycerol as part of the restructuration of the raw material base of modern industrial chemistry, away from fossil resources and to the point of an industry using renewable resources only.

10. References

[1] Intergovernmental Panel on Climate Change,*Climate Change 2014: Synthesis Report. Contribution of Working Groups I, II and III to the Fifth Assessment Report of the Intergovernmental Panel on Climate Change,* (Eds.: R. K. Pachauri, L. A. Meyer), IPCC, Geneva, Switzerland, **2014**.

[2] T. Werpy, G. Petersen,*Top Value Added Chemicals From Biomass* U.S. Department of Energy, **2004**.

[3] J. J. Bozell, G. R. Petersen, *Green Chemistry* **2010**, *12*, 539-554.

[4] N. Rahmat, A. Z. Abdullah, A. R. Mohamed, *Renewable and Sustainable Energy Reviews* **2010**, *14*, 987-1000.

[5] M. McCoy, *Chemical & Engineering News* **2006**, *84*, 7.

[6] D. d. Guzman,*Growing glycerine-to-ECH plants* in *ICIS Green Chemicals*, **2011**.

[7] Allylic products, http://www.solvaychemicals.com/EN/products/chlorinated/Allylicproducts/Allylic_products.aspx.

[8] M. K. Lam, K. T. Lee, A. R. Mohamed, *Biotechnology advances* **2010**, *28*, 500-518.

[9] B. Freedman, E. H. Pryde, T. L. Mounts, *J Am Oil Chem Soc* **1984**, *61*, 1638-1643.

[10] M. Hara *ChemSusChem* **2009**, *2*, 129-135.

[11] L. C. Meher, D. Vidya Sagar, S. N. Naik, *Renewable and Sustainable Energy Reviews* **2006**, *10*, 248-268.

[12] M. E. Borges, L. Díaz, *Renewable and Sustainable Energy Reviews* **2012**, *16*, 2839-2849.

[13] A. Demirbas, *Energy Conversion and Management* **2007**, *48*, 937-941.

[14] N. Viriya-empikul, P. Krasae, B. Puttasawat, B. Yoosuk, N. Chollacoop, K. Faungnawakij, *Bioresource Technology* **2010**, *101*, 3765-3767.

[15] Z. Yang, W. Xie, *Fuel Processing Technology* **2007**, *88*, 631-638.

[16] Y.-M. Park, S.-H. Chung, H. J. Eom, J.-S. Lee, K.-Y. Lee, *Bioresource Technology* **2010**, *101*, 6589-6593.

[17] R. Tesser, M. Di Serio, L. Casale, L. Sannino, M. Ledda, E. Santacesaria, *Chemical Engineering Journal* **2010**, *161*, 212-222.

[18] C. Samart, C. Chaiya, P. Reubroycharoen, *Energy Conversion and Management* **2010**, *51*, 1428-1431.

[19] W. N. N. Wan Omar, N. A. Saidina Amin, *Biomass and Bioenergy* **2011**, *35*, 1329-1338.

[20] N. Kondamudi, S. K. Mohapatra, M. Misra, *Applied Catalysis A: General* **2011**, *393*, 36-43.

[21] C. A. G. Quispe, C. J. R. Coronado, J. A. Carvalho Jr, *Renewable and Sustainable Energy Reviews* **2013**, *27*, 475-493.

[22] M. McCoy, *Chemical & Engineering News* **2009**, *87*, 16-17.

[23] A. Brandner, K. Lehnert, A. Bienholz, M. Lucas, P. Claus, *Topics in Catalysis* **2009**, *52*, 278-287.

[24] X. Lancrenon, J. Fedders, in *Biodiesel Magazine*, **2008**.

[25] F. Yang, M. A. Hanna, R. Sun, *Biotechnology for Biofuels* **2012**, *5*, 13.

[26] R. Asad ur, S. Wijesekara R.G, N. Nomura, S. Sato, M. Matsumura, *Journal of Chemical Technology & Biotechnology* **2008**, *83*, 1072-1080.

[27] C. F. Hansen, A. Hernandez, B. P. Mullan, K. Moore, M. Trezona-Murray, R. H. King, J. R. Pluske, *Animal Production Science* **2009**, *49*, 154-161.

[28] J. Johnson, *Chemical & Engineering News* **2013**, *91*, 40.

[29] *1,3-Propanediol (PDO) Market By Applications (PTT [Polytrimethylene Terephthalate], Polyurethane, Cosmetic, Personal Care & Home Cleaning & other Applications) & Geography - Global Market Trends & Forecasts to 2019*, **2012**.

[30] G. P. da Silva, M. Mack, J. Contiero, *Biotechnology advances* **2009**, *27*, 30-39.

[31] F. R. Lawrence, R. H. Sullivan, *US 3,687,981* **1972**.

[32] H. S. Brown, P. K. Casey, J. M. Donahue, *New Textiles* **2000**.

[33] C. E. Nakamura, G. M. Whited, *Current opinion in biotechnology* **2003**, *14*, 454-459.

[34] L. Huang, Y. Zhu, H. Zheng, G. Ding, Y. Li, *Catalysis Letters* **2009**, *131*, 312-320.

[35] M. Schlaf, *Dalton transactions* **2006**, 4645-4653.

[36] T. M. Che, *US Patent 4,642,394* **1987**.

[37] E. A. Drent, NL), Jager, Willem Wabe (Amsterdam, NL), **2000**.

[38] M. Schlaf, P. Ghosh, P. J. Fagan, E. Hauptman, R. M. Bullock, *Angewandte Chemie International Edition* **2001**, *40*, 3887-3890.
[39] K. Wang, M. C. Hawley, S. J. DeAthos, *Ind. Eng. Chem. Res.* **2003**, *42*, 2913-2923.
[40] S. Zhu, Y. Zhu, S. Hao, L. Chen, B. Zhang, Y. Li, *Catalysis Letters* **2011**, *142*, 267-274.
[41] S. Zhu, Y. Zhu, S. Hao, H. Zheng, T. Mo, Y. Li, *Green Chemistry* **2012**, *14*, 2607-2616.
[42] S. Zhu, X. Gao, Y. Zhu, J. Cui, H. Zheng, Y. Li, *Applied Catalysis B: Environmental* **2014**, *158-159*, 391-399.
[43] S. Zhu, X. Gao, Y. Zhu, Y. Li, *Journal of Molecular Catalysis A: Chemical* **2015**, *398*, 391-398.
[44] S. Zhu, X. Gao, Y. Zhu, Y. Zhu, X. Xiang, C. Hu, Y. Li, *Applied Catalysis B: Environmental* **2013**, *140–141*, 60-67.
[45] S. Zhu, Y. Qiu, Y. Zhu, S. Hao, H. Zheng, Y. Li, *Catalysis Today* **2013**, *212*, 120-126.
[46] E. Tsukuda, S. Sato, R. Takahashi, T. Sodesawa, *Catalysis Communications* **2007**, *8*, 1349-1353.
[47] L.-Z. Qin, M.-J. Song, C.-L. Chen, *Green Chemistry* **2010**, *12*, 1466.
[48] Y. Feng, H. Yin, A. Wang, L. Shen, L. Yu, T. Jiang, *Chemical Engineering Journal* **2011**, *168*, 403-412.
[49] Y. Feng, H. Yin, L. Shen, A. Wang, Y. Shen, T. Jiang, *Chemical Engineering & Technology* **2013**, *36*, 73-82.
[50] S. Priya, V. Kumar, M. Kantam, S. Bhargava, K. R. Chary, *Catalysis Letters* **2014**, *144*, 2129-2143.
[51] S. S. Priya, V. P. Kumar, M. L. Kantam, S. K. Bhargava, K. V. R. Chary, *RSC Advances* **2014**, *4*, 51893-51903.
[52] S. S. Priya, P. Bhanuchander, V. P. Kumar, D. K. Dumbre, S. R. Periasamy, S. K. Bhargava, M. Lakshmi Kantam, K. V. R. Chary, *ACS Sustainable Chemistry & Engineering* **2016**, *4*, 1212-1222.
[53] S. S. Priya, V. P. Kumar, M. L. Kantam, S. K. Bhargava, A. Srikanth, K. V. R. Chary, *Industrial & Engineering Chemistry Research* **2015**, *54*, 9104-9115.
[54] P. K. Vanama, A. Kumar, S. R. Ginjupalli, V. R. C. Komandur, *Catalysis Today* **2015**, *250*, 226-238.
[55] W. Luo, Y. Lyu, L. Gong, H. Du, T. Wang, Y. Ding, *RSC Advances* **2016**, *6*, 13600-13608.
[56] M. Akiyama, S. Sato, R. Takahashi, K. Inui, M. Yokota, *Applied Catalysis A: General* **2009**, *371*, 60-66.
[57] A. Bienholz, H. Hofmann, P. Claus, *Applied Catalysis A: General* **2011**, *391*, 153-157.
[58] J. Chaminand, L. a. Djakovitch, P. Gallezot, P. Marion, C. Pinel, C. c. Rosier, *Green Chemistry* **2004**, *6*, 359.
[59] Y. Gu, A. Azzouzi, Y. Pouilloux, F. Jerome, J. Barrault, *Green Chemistry* **2008**, *10*, 164-167.
[60] L. Gong, Y. Lu, Y. Ding, R. Lin, J. Li, W. Dong, T. Wang, W. Chen, *Applied Catalysis A: General* **2010**, *390*, 119-126.
[61] T. Kurosaka, H. Maruyama, I. Naribayashi, Y. Sasaki, *Catalysis Communications* **2008**, *9*, 1360-1363.
[62] J. Oh, S. Dash, H. Lee, *Green Chemistry* **2011**, *13*, 2004.
[63] O. M. Daniel, A. DeLaRiva, E. L. Kunkes, A. K. Datye, J. A. Dumesic, R. J. Davis, *ChemCatChem* **2010**, *2*, 1107-1114.
[64] A. Shimao, S. Koso, N. Ueda, Y. Shinmi, I. Furikado, K. Tomishige, *Chemistry Letters* **2009**, *38*, 540-541.
[65] Y. Shinmi, S. Koso, T. Kubota, Y. Nakagawa, K. Tomishige, *Applied Catalysis B: Environmental* **2010**, *94*, 318-326.
[66] Y. Amada, Y. Shinmi, S. Koso, T. Kubota, Y. Nakagawa, K. Tomishige, *Applied Catalysis B: Environmental* **2011**, *105*, 117-127.
[67] Y. Nakagawa, Y. Shinmi, S. Koso, K. Tomishige, *Journal of Catalysis* **2010**, *272*, 191-194.
[68] Y. Nakagawa, X. Ning, Y. Amada, K. Tomishige, *Applied Catalysis A: General* **2012**, *433-434*, 128-134.
[69] C. Deng, X. Duan, J. Zhou, D. Chen, X. Zhou, W. Yuan, *Catalysis Today* **2014**, *234*, 208-214.
[70] C. Deng, X. Duan, J. Zhou, X. Zhou, W. Yuan, S. L. Scott, *Catalysis Science & Technology* **2015**.
[71] L. Liu, Y. Zhang, A. Wang, T. Zhang, *Chinese Journal of Catalysis* **2012**, *33*, 1257-1261.
[72] J. ten Dam, K. Djanashvili, F. Kapteijn, U. Hanefeld, *ChemCatChem* **2013**, *5*, 497-505.
[73] T. Mizugaki, T. Yamakawa, R. Arundhathi, T. Mitsudome, K. Jitsukawa, K. Kaneda, *Chemistry Letters* **2012**, *41*, 1720-1722.
[74] R. Arundhathi, T. Mizugaki, T. Mitsudome, K. Jitsukawa, K. Kaneda, *ChemSusChem* **2013**, *6*, 1345-1347.
[75] Y. Zhang, X.-C. Zhao, Y. Wang, L. Zhou, J. Zhang, J. Wang, A. Wang, T. Zhang, *Journal of Materials Chemistry A* **2013**, *1*, 3724.

[76] S. García-Fernández, I. Gandarias, J. Requies, M. B. Güemez, S. Bennici, A. Auroux, P. L. Arias, *Journal of Catalysis* **2015**, *323*, 65-75.
[77] Q. Liu, X. Cao, T. Wang, C. Wang, Q. Zhang, L. Ma, *RSC Advances* **2015**, *5*, 4861-4871.
[78] J. Wang, X. Zhao, N. Lei, L. Li, L. Zhang, S. Xu, S. Miao, X. Pan, A. Wang, T. Zhang, *ChemSusChem* **2016**, n/a-n/a.
[79] M. Chia, Y. J. Pagan-Torres, D. Hibbitts, Q. Tan, H. N. Pham, A. K. Datye, M. Neurock, R. J. Davis, J. A. Dumesic, *Journal of the American Chemical Society* **2011**, *133*, 12675-12689.
[80] I. Furikado, T. Miyazawa, S. Koso, A. Shimao, K. Kunimori, K. Tomishige, *Green Chemistry* **2007**, *9*, 582.
[81] V. Pallassana, M. Neurock, *Journal of Catalysis* **2002**, *209*, 289-305.
[82] Y. Amada, H. Watanabe, M. Tamura, Y. Nakagawa, K. Okumura, K. Tomishige, *The Journal of Physical Chemistry C* **2012**, *116*, 23503-23514.
[83] E. P. Maris, R. J. Davis, *Journal of Catalysis* **2007**, *249*, 328-337.
[84] I. Gandarias, P. L. Arias, J. Requies, M. B. Güemez, J. L. G. Fierro, *Applied Catalysis B: Environmental* **2010**, *97*, 248-256.
[85] M. R. Nimlos, B. S. J., X. Qian, M. E. Himmel, D. K. Johnson, *J. Phys. Chem. A* **2006**, *110*, 6145-6156.
[86] S. Sato, M. Akiyama, R. Takahashi, T. Hara, K. Inui, M. Yokota, *Applied Catalysis A: General* **2008**, *347*, 186-191.
[87] S. N. Delgado, L. Vivier, C. Especel, *Catalysis Communications* **2014**, *43*, 107-111.
[88] E. Gallegos-Suarez, A. Guerrero-Ruiz, I. Rodriguez-Ramos, A. Arcoya, *Chemical Engineering Journal* **2015**, *262*, 326-333.
[89] Y. Li, L. Ma, H. Liu, D. He, *Applied Catalysis A: General* **2014**, *469*, 45-51.
[90] Y. Li, H. Liu, L. Ma, D. He, *RSC Advances* **2014**, *4*, 5503-5512.
[91] D. D. Falcone, J. H. Hack, A. Y. Klyushin, A. Knop-Gericke, R. Schlögl, R. J. Davis, *ACS Catalysis* **2015**, *5*, 5679-5695.
[92] H. Jinbao, L. Chao, W. Shunan, H. Xiaolu, *Acta Chimica Sinica* **2010**, *68*, 1043-1049.
[93] H. Atia, U. Armbruster, A. Martin, *Applied Catalysis A: General* **2011**, *393*, 331-339.
[94] T. Shishido, H. Hattori, *Applied Catalysis A: General* **1996**, *146*, 157-164.
[95] S. Cai, K. Sohlberg, *Journal of Molecular Catalysis A: Chemical* **2003**, *193*, 157-164.
[96] A. Alhanash, E. F. Kozhevnikova, I. V. Kozhevnikov, *Catalysis Letters* **2007**, *120*, 307-311.
[97] A. Freund, *Monatsheft für Chemie* **1881**, *2*, 636-641.
[98] DuPont, **2016**.
[99] A. Hiremath, M. Kannabiran, V. Rangaswamy, *New Biotechnology* **2011**, *28*, 19-23.
[100] F. S. Mendes, M. Gonzalez-Pajuelo, H. Cordier, J. M. Francois, I. Vasconcelos, *Applied microbiology and biotechnology* **2011**, *92*, 519-527.
[101] Y.-N. Zhao, G. Chen, S.-J. Yao, *Biochemical Engineering Journal* **2006**, *32*, 93-99.
[102] A. Kośmider, K. Leja, K. Czaczyk, in *Biodiesel- Quality, Emissions and By-Products* (Ed.: G. Montero), **2011**, pp. 341-364.
[103] B.-R. Oh, J.-W. Seo, M. Choi, C. Kim, *Biotechnol Bioproc E* **2008**, *13*, 666-670.
[104] Y. Mu, H. Teng, D.-J. Zhang, W. Wang, Z.-L. Xiu, *Biotechnol Lett* **2006**, *28*, 1755-1759.
[105] K. V. Yusenko, *Platinum Metals Review* **2013**, *57*, 57-65.
[106] Y. Y. Chong, W. Y. Chow, W. Y. Fan, *Journal of Colloid and Interface Science* **2012**, *369*, 164-169.
[107] J. C. Mol, *Catalysis Today* **1999**, *52*, 377.
[108] J. H. Sinfelt, Google Patents, **1976**.
[109] L. Lloyd, *Handbook of Industrial Catalysts*, 1 ed., Springer US, **2011**.
[110] S. Raseev, in *Thermal and Catalytic Processes in Petroleum Refining*, CRC Press, **2003**.
[111] T. N. Angelidis, D. Rosopoulou, V. Tzitzios, *Industrial & Engineering Chemistry Research* **1999**, *38*, 1830-1836.
[112] G. J. Suppes, in *The Biodiesel Handbook (Second Edition)*, AOCS Press, **2010**, pp. 439-455.
[113] F. Cherubini, A. H. Strømman, in *Biofuels* (Eds.: C. Larroche, S. C. Ricke, C.-G. Dussap, E. Gnansounou), Academic Press, Amsterdam, **2011**, pp. 3-24.
[114] C. J. Sullivan, in *Ullmann's Encyclopedia of Industrial Chemistry*, Wiley-VCH Verlag GmbH & Co. KGaA, **2000**.

[115] L. C. Meher, R. Gopinath, S. N. Naik, A. K. Dalai, *Industrial & Engineering Chemistry Research* **2009**, *48*, 1840-1846.
[116] M. Balaraju, V. Rekha, P. S. S. Prasad, B. L. A. P. Devi, R. B. N. Prasad, N. Lingaiah, *Applied Catalysis A: General* **2009**, *354*, 82-87.
[117] J. Feng, H. Fu, J. Wang, R. Li, H. Chen, X. Li, *Catalysis Communications* **2008**, *9*, 1458-1464.
[118] L. Ma, D. He, *Catalysis Today* **2010**, *149*, 148-156.
[119] Z. Yuan, P. Wu, J. Gao, X. Lu, Z. Hou, X. Zheng, *Catalysis Letters* **2009**, *130*, 261-265.
[120] F. Jian, W. Jinbo, Z. Yafen, F. Haiyan, C. Hua, L. Xianjun, *Chemistry Letters* **2007**, *36*, 1274-1275.
[121] M. A. Dasari, P.-P. Kiatsimkul, W. R. Sutterlin, G. J. Suppes, *Applied Catalysis A: General* **2005**, *281*, 225-231.
[122] S. Wang, H. Liu, *Catalysis Letters* **2007**, *117*, 62-67.
[123] A. Bienholz, F. Schwab, P. Claus, *Green Chemistry* **2010**, *12*, 290.
[124] A. Bienholz, R. Blume, A. Knop-Gericke, F. Girgsdies, M. Behrens, P. Claus, *J. Phys. Chem. C* **2011**, *115*, 999-1005.
[125] T. M. Che, *US4642394* **1987**.
[126] E. Drent, W. W. Jager, *WO1999005085* **1999**.
[127] J. M. Clomburg, R. Gonzalez, *Trends in Biotechnology* **2013**, *31*, 20-28.
[128] A. J. Mattam, J. M. Clomburg, R. Gonzalez, S. S. Yazdani, *Biotechnol Lett* **2013**, *35*, 831-842.
[129] R. J. Argauer, M. Kensington, G. R. Landolt, *US Patent 3702886* **1972**.
[130] Z. Gabelica, N. Blom, E. G. Derouane, *Applied Catalysis* **1983**, *5*, 227-248.
[131] M. Fehlings, A. Drochner, K. Krauss, H. Vogel, R. Suettinger, H. Hibst, *DE 19910291 A1* **2000**.
[132] R. B. LEVY, M. BOUDART, *Science* **1973**, *181*, 547-549.
[133] E. Iglesia, J. E. Baumgartner, F. H. Ribeiro, M. Boudart, *Journal of Catalysis* **1991**, *131*, 523-544.
[134] E. Iglesia, F. H. Ribeiro, M. Boudart, J. E. Baumgartner, *Catalysis Today* **1992**, *15*, 307-337.
[135] E. Iglesia, F. H. Ribeiro, M. Boudart, J. E. Baumgartner, *Catalysis Today* **1992**, *15*, 455-458.
[136] C. B. Rodella, D. H. Barrett, S. F. Moya, S. J. A. Figueroa, M. T. B. Pimenta, A. A. S. Curvelo, V. Teixeira da Silva, *RSC Advances* **2015**, *5*, 23874-23885.
[137] M. I. Zaki, M. A. Hasan, F. A. Al-Sagheer, L. Pasupulety, *Colloids and Surfaces A: Physicochemical and Engineering Aspects* **2001**, *190*, 261-274.
[138] H. D. Setiabudi, S. Triwahyono, A. A. Jalil, N. H. N. Kamarudin, M. A. A. Aziz, *Journal of Natural Gas Chemistry* **2011**, *20*, 477-482.
[139] E. Selli, L. Forni, *Microporous and Mesoporous Materials* **1999**, *31*, 129-140.
[140] A. Davydov, in *Molecular Spectroscopy of Oxide Catalyst Surfaces*, John Wiley & Sons, Ltd, **2003**, pp. 27-179.
[141] H. Zhang, Z. Liu, Z. Feng, C. Li, *Journal of Catalysis* **2008**, *260*, 295-304.
[142] Q. Guo, B. Chen, Y. Li, J. Li, *Catalysis Letters* **2007**, *120*, 65-70.
[143] M. Tamura, Y. Amada, S. Liu, Z. Yuan, Y. Nakagawa, K. Tomishige, *Journal of Molecular Catalysis A: Chemical* **2014**, *388-389*, 177-187.
[144] M. Chia, B. J. O'Neill, R. Alamillo, P. J. Dietrich, F. H. Ribeiro, J. T. Miller, J. A. Dumesic, *Journal of Catalysis* **2013**, *308*, 226-236.
[145] M. Okamoto, K. Nobuhara, K. Jinno, *Journal of Chromatography A* **1991**, *556*, 407-414.
[146] L. Shirazi, E. Jamshidi, M. R. Ghasemi, *Crystal Research and Technology* **2008**, *43*, 1300-1306.
[147] S. Sang, F. Chang, Z. Liu, C. He, Y. He, L. Xu, *Catalysis Today* **2004**, *93–95*, 729-734.

11. Appendix

Table of figures

List of abbreviations

1-PrOH	1-propanol
1,2-PDO	1,2-propanediol
1,3-PDO	1,3-propanediol
1,5-PDO	1,5-pentanediol
2-PrOH	2-propanol
3-HPA	3-hydroxypropanal
a	Factor to determine the response factor of each substance in relation to the 1,5-PDO response factor
A_{Peak}	GC peak area
BET	Method according to Brunauer, Emmett and Teller
cat	Catalyst
c_i	Concentration (mmol/L) of substance i
$c_{i,0}$	Initial concentration (mmol/L) of substance i
$c_{i,end}$	Final concentration (mmol/L) of substance i
DRIFTS	Diffuse reflectance infrared Fourier Transform spectroscopy
EG	Ethylene glycol (1,2-ethanediol)
f	Response factor
FID	Flame ionisation detector
GC	Gas chromatograph or Gas chromatography
GC-MS	Gas chromatography–mass spectrometry
OS	Oxidation state
STA	Silicotungstic acid, $H_4SiW_{12}O_{40}$
STY	Space Time Yield
TEM	Transmission electron microscopy
tmb	Trace metals basis
TPD	Temperature programmed desorption
TPDRO	Temperature programmed desorption, reduction and oxidation
TPO	Temperature programmed oxidation
TPR	Temperature programmed reduction
t_R	Time of reaction
V_R	Volume of the reaction solution

WHSV	Weight hourly space velocity
X	Conversion
XRD	X-Ray Diffraction
Y	Yield

List of chemicals

Chemicals used for catalyst preparation

Name	CAS	Supplier	Purity
Hexachloroplatinic acid	18497-13-7	Umicore/Alfa Aesar	99.95% tmb
Hexachloroiridium acid hydrate	110802-84-1	Aldrich	99.98% tmb
Ammonium perrhenate	13598-65-7	ABCR/Aldrich	99%
Tungstic acid	7783-03-1	ABCR/Aldrich	99%
Ruthenium(III) chloride hydrate	14898-67-0	ABCR	99.9% (36% Ru)
Ammonium metatungstate hydrate	12333-11-8	Fluka	99%
Nickel(II) nitrate hexahydrate	13478-00-7	Merck	ACS
Silicotungstic acid hydrate	12027-43-9	ABCR	Reagent grade
Kieselgel 60 (40 to 63 µm)	7631-86-9	Roth	99.4% (SiO_2)
Kieselgel 100 (200 to 500 µm)	63231-67-4	Roth	99% (SiO_2)
Aerosil 200	112945-52-5	Evonik	99.8% (SiO_2)
Aluminium Oxide (Ba 66/28)	1344-28-1	Heraeus	
H-BEA	1318-02-1	Clariant	-
H-ZSM-5	1318-02-1	Clariant	-
SiO_2 (G-6, G-10, Q-6, Q-10)	7631-86-9	Silysa	99.5% (SiO_2)

Chemicals used for the hydrogenolysis reaction and GC calibration

Name	CAS	Supplier	Purity
Glycerol	56-81-5	Vetec/Roth	99.5%
Water		Merck Simplicity Equipment	18.2 MΩ•cm
Hydrogen	1333-74-0	Air Liquide	99.999%
Argon	7440-37-1	Air Liquide	99.999%
1,3-Propanediol	504-63-2	Fluka	99% (GC)
1,2-Propanediol	57-55-6	Sigma Aldrich	99.5% (GC)
1,5-Pentanediol	111-29-5	Merck	For synthesis
1-Propanol	71-23-8	Aldrich	99.7%
2-Propanol	67-63-0	Aldrich/Fluka	99.5% / 97%
$FeNO_3$ x 9 H_2O	7782-61-8	Fluka	ACS, 98%
$FeSO_4$ x 7 H_2O	7782-63-0	Fluka	ACS, 99%

X-Ray diffraction of catalyst samples

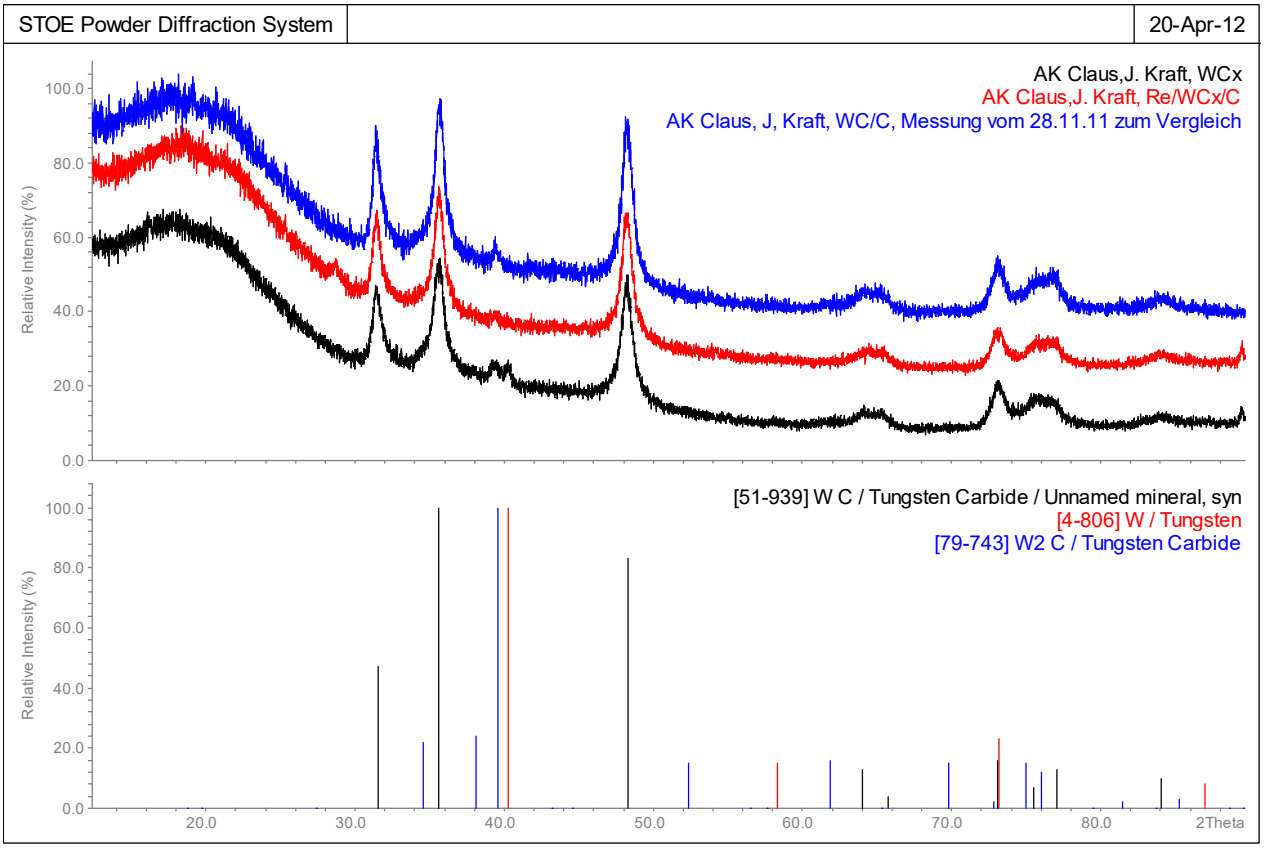

Figure 60 XRD measurement to confirm that the structure of tungsten carbide was maintained during the preparation of the Re/WC_x/C catalyst (red) that has been used in reactions R010 to R012. For the final catalyst, a mixture of WC and W_2C was detected, the support on its own showed small signs of metallic tungsten which disappeared with the deposition of rhenium and further treatment.

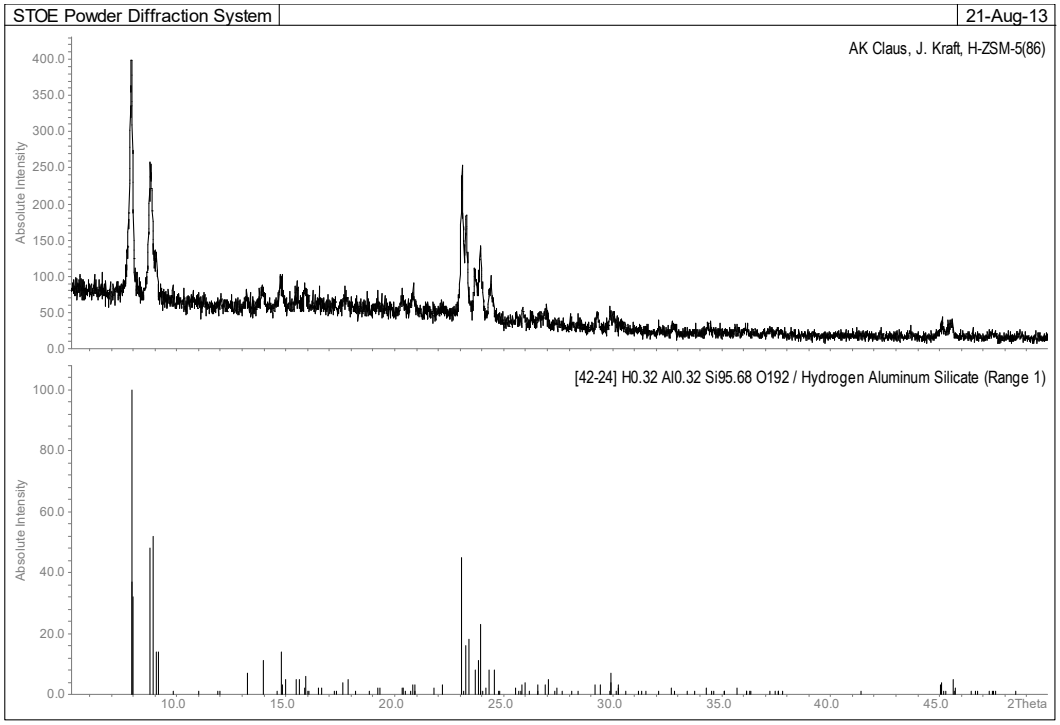

Figure 61 XRD measurement of H-ZSM-5 (86).

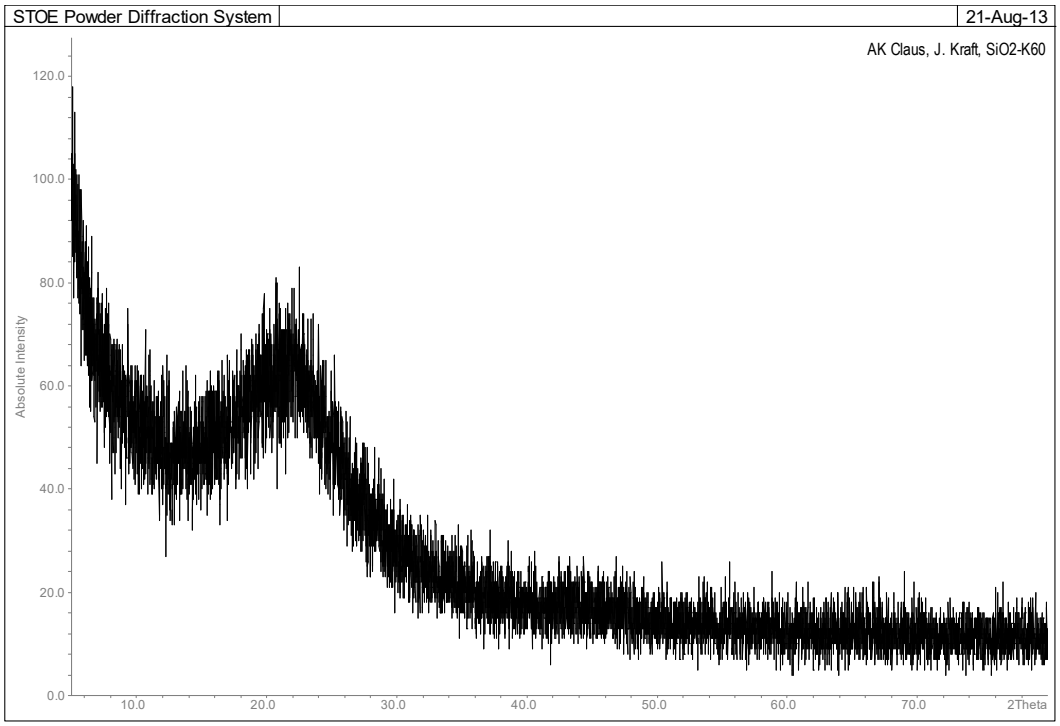

Figure 62 XRD overview measurement of SiO_2 (Kieselgel 60), showing an amorphous structure.

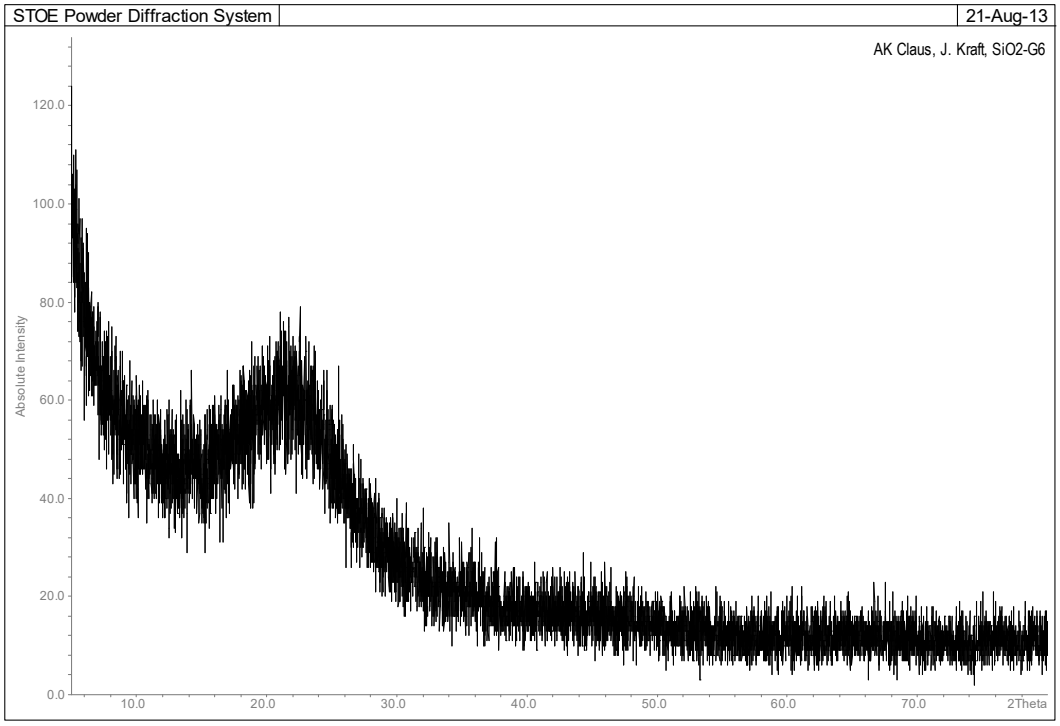

Figure 63 XRD overview measurement of SiO_2 (G-6), showing an amorphous structure.

The XRD measurement of the final catalyst (after reduction at 503 K) with a very long exposure time is shown in Figure 45 on page 70.

GC calibration

Calibration in Campinas using different injection volumes of the same calibration solution (manual injection)

V / µL	$n_{Glycerol}$ / nmol	$A_{Glycerol}$ / pAs	$n_{1,2\text{-PDO}}$ / nmol	$A_{1,2\text{-PDO}}$ / pAs	$n_{1,3\text{-PDO}}$ / nmol	$A_{1,3\text{-PDO}}$ / pAs
0,1	198	59924	78	25219	72	21716
0,1	198	61410	78	31961	72	26932
0,3	595	225447	234	85391	216	72072
0,3	595	202250	234	93878	216	78808
0,4	793	263869	312	91337	288	78530
0,4	793	334172	312	144660	288	130240
0,4	793	273660	312	117134	288	105451
0,5	991	395522	390	124510	360	115143
0,5	991	357531	390	157279	360	141927
0,6	1189	467067	468	156534	432	146538
0,7	1388	516758	546	186085	505	164970
0,8	1586	650945	624	248095	577	224423
0,8	1586	613153	624	234928	577	219830
0,8	1586	645255	624	224150	577	205941
0,9	1784	686331	702	226522	649	205063

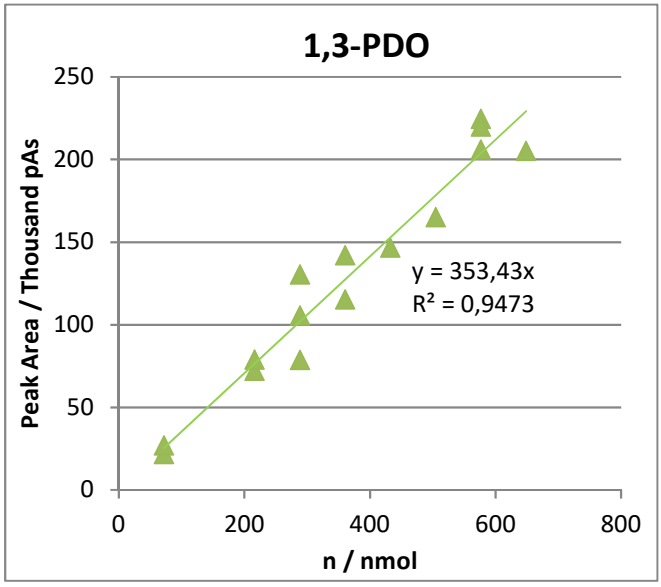

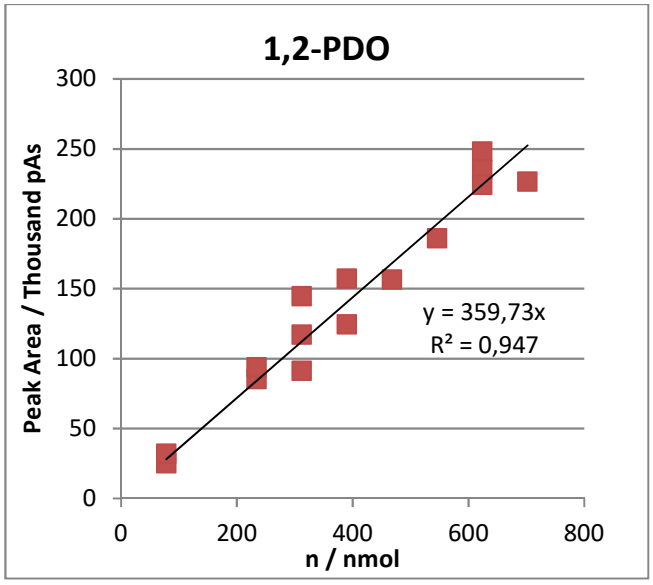

A second calibration solution was prepared for the calibration of 1-propanol in glycerol.

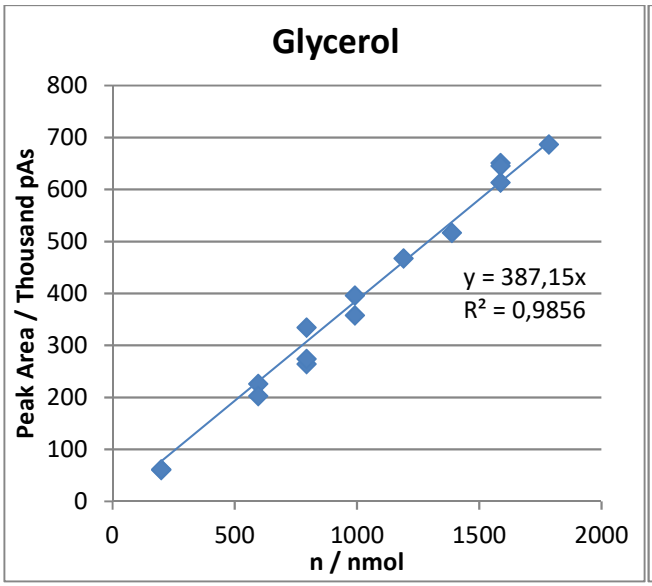

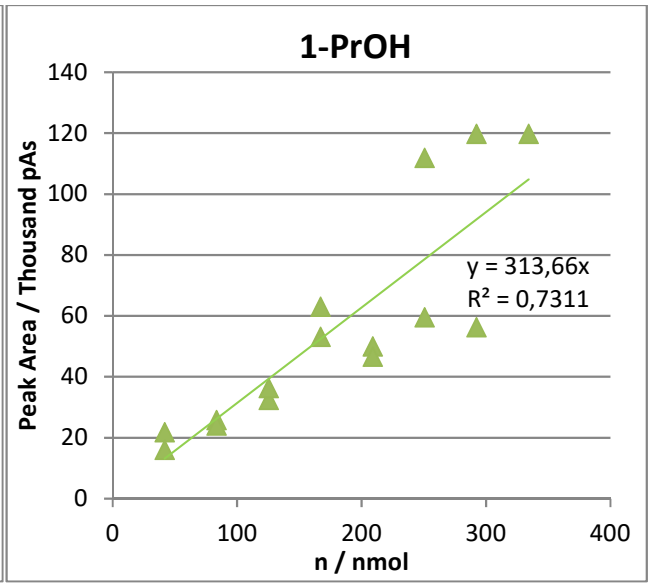

V / µL	$n_{Glycerol}$ / nmol	$A_{Glycerol}$ / pAs	$n_{1\text{-}PrOH}$ / nmol	$A_{1\text{-}PrOH}$ / pAs
0,1	198	72493	42	21804
0,1	198	82111	42	15948
0,2	396	164090	84	25774
0,2	396	167426	84	24015
0,3	595	249354	125	32366
0,3	595	247080	125	36304
0,4	793	321788	167	53071
0,4	793	349795	167	62920
0,5	991	402009	209	49958
0,5	991	420307	209	46592
0,6	1189	493139	251	111850
0,6	1189	474036	251	59462
0,7	1388	571496	292	119756
0,7	1388	542536	292	56208
0,8	1586	697449	334	119756

Factors for a standard injection volume of 0.5 µL:

	Peak area			
	per nmol injected	per mmol/L (Volume of injection: 0,5 µL)	Considered value	Resulting factor f_i
Glycerol	387	194	200	1/200
Glycerol	415	207		
1,2-Propanediol	360	180	180	1/180
1,3-Propanediol	353	177	180	1/180
1-Propanol	314	157	160	1/160

The concentration was then calculated accordingly: $c_i = f_i \times A_{Peak,i}$

First calibration in Darmstadt (used for R048 until R064)

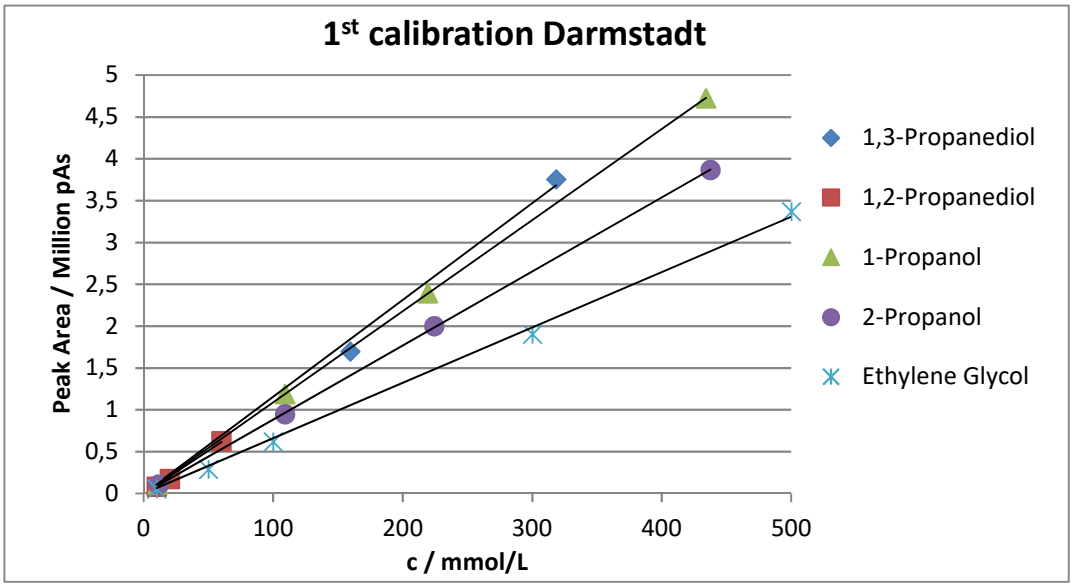

$c_{1,3\text{-PDO}}$ / mmol/L	$A_{1,3\text{-PDO}}$ / pAs	$c_{1,2\text{-PDO}}$ / mmol/L	$A_{1,2\text{-PDO}}$ / pAs	$c_{1\text{-PrOH}}$ / mmol/L	$A_{1\text{-PrOH}}$ / pAs
16	136949	10	84680	11	109857
159	1697786	20	175386	109	1188432
318	3757464	60	627712	219	2393572
1567	17763088			434	4724156
				1086	12006355

$c_{2\text{-PrOH}}$ / mmol/L	$A_{2\text{-PrOH}}$ / pAs	c_{EG} / mmol/L	A_{EG} / pAs
11	107383	10	58313
109	950003	50	290507
224	2001556	100	617639
437	3866756	300	1905977
1086	9907765	500	3369063

Substance	Resulting Factor f_i	
	< 500 mmol	Overall
2-Propanol	$1.13 \cdot 10^{-4}$	$1.13 \cdot 10^{-4}$
1-Propanol	$9.18 \cdot 10^{-5}$	$9.07 \cdot 10^{-5}$
1,2-Propanediol	$9.73 \cdot 10^{-5}$	$9.73 \cdot 10^{-5}$
Ethylene Glycol	$1.51 \cdot 10^{-4}$	$1.51 \cdot 10^{-4}$
1,3-Propanediol	$8.63 \cdot 10^{-5}$	$8.81 \cdot 10^{-5}$
Glycerol	$1.02 \cdot 10^{-4}$	$1.02 \cdot 10^{-4}$

Calibration of the external standard 1,5-pentanediol, used for measurements of R065 and later

$c_{1,5\text{-PDO}}$ / mmol/L	Retention time / min	Peak Area / pAs
10,82	17,59	1349367
10,82	17,59	1364237
10,82	17,59	1397118
20,94	17,60	2621414
20,94	17,60	2637090
20,94	17,60	2647395
52,65	17,63	6570822
52,65	17,63	6834294
52,65	17,63	6951884
103,67	17,66	13241819
103,67	17,66	13495574
103,67	17,66	13818526

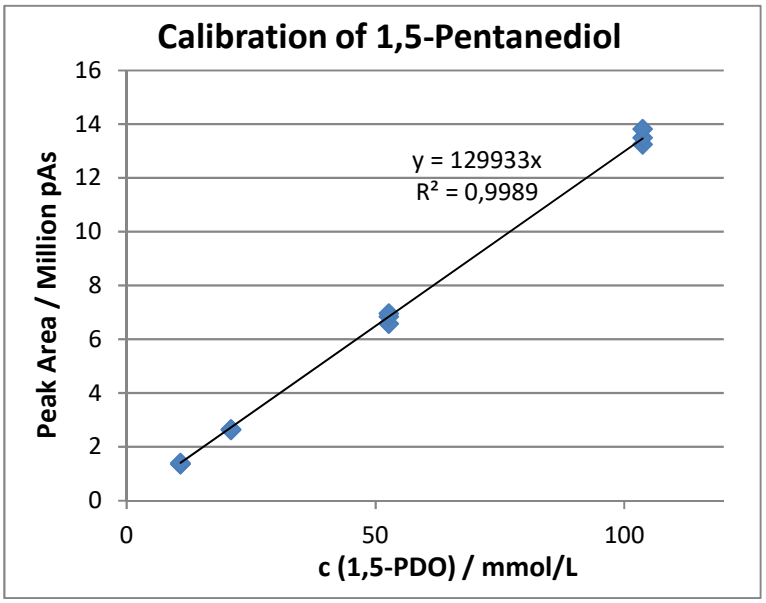

Determination of GC response factors with the external standard

Table 6 Measured values of samples of known composition for the determination of GC response factors.

#	Glycerol		1,3-Propanediol		1,2-Propanediol		1-Propanol		2-Propanol		1,5-Pentanediol	
	c / mmol/L	Peak Area	c / mmol/L	Peak Area	c / mmol/L	Peak Area	c / mmol/L	Peak Area	c / mmol/L	Peak Area	c / mmol/L	Peak Area
1a	572	12928240	568	14892804	536	13367279	724	12538679	250	3484589	18,0	883405
1b	572	13324004	568	15370005	536	13735891	724	12535829	250	3486812	18,0	913307
1c	572	14000472	568	16050073	536	14304769	724	12209984	250	3371114	18,0	955777
2a	1069	21407641	375	9027102	386	9041609	468	8968031	194	3027918	17,8	788643
2b	1069	20995834	375	8888106	386	8904133	468	9091629	194	3068676	17,8	772417
2c	1069	20923542	375	8812623	386	8793222	468	9088891	194	3071106	17,8	768602
3a	1643	32146845	150	3486541	196	4543534	178	3423079	84	1327571	17,4	751480
3b	1643	43607082	150	4406497	196	5453305	178	3174673	84	1233984	17,4	975832
3c	1643	34878596	150	3773769	196	4821364	178	3249238	84	1259724	17,4	822319

Table 7 Factors derived from Table 6 for the determination of the response factors for each compound, depending on the response factor detected for the standard 1,5-pentanediol in each GC measurement: $f_i = a_i \times f_{1,5\text{-}PDO}$. In case of strong variations, the values for the most common conversions were considered for the calculation of the concentration in the reaction samples. The values were confirmed with new calibration solutions from time to time to secure an accurate detection of product concentration.

#	a (Glycerol)	a (1,3-Propanediol)	a (1,2-Propanediol)	a (1-Propanol)	a (2-Propanol)	Simulated Conversion
1a	2,17	1,87	1,97	2,83	2,83	75%
1b	2,17	1,87	1,98	2,93	2,93	75%
1c	2,17	1,88	1,99	3,15	3,06	75%
2a	2,22	1,84	1,89	2,31	2,56	53%
2b	2,21	1,83	1,88	2,23	2,51	53%
2c	2,21	1,84	1,90	2,22	2,50	53%
3a	2,21	1,86	1,87	2,25	2,50	27%
3b	Not considered					27%
3c	2,23	1,88	1,92	2,59	2,74	27%
	2,20	1,86	1,92	2,56	2,70	Average
	2,2	**1,9**	**1,9**	**2,3**	**2,5**	**Considered for calculation**

List of hydrogenolysis reactions

Reactions 1 to 47 have been carried out in Campinas in a 500 mL steel autoclave, the resulting samples were injected four times manually (0.5 µL each) into a gas-phase chromatograph (directly on the column) and analysed according to the response factors mentioned above. In Darmstadt (300 mL steel autoclave with an external gas tank for a constant reaction pressure), reactions 48 to 64 have been analysed by automatic injection using the response factors presented after the ones for Campinas whereas the samples originating from the reactions 65 to 193 were analysed using 1,5-pentanediol as an external standard and three measurements for every sample in order to compensate variations that had occurred during the previous analyses, especially regarding the amount of glycerol detected for the reactions 48 to 64. The conversion X was determined in two ways, once (labelled X_1) by adding up all found products and once (labelled X_2) with the quantity of glycerol left after the reaction. For small conversions below 10%, only X_1 was considered because the absolute error margin of the big glycerol peak was much higher than of the small product peaks, sometimes leading to a negative conversion, indicated as "< 0%". The conversions depicted in chapter 7 usually show a mean conversion, except in special cases, e.g. gas formation over some catalysts at high temperatures.

Table 8 List of all experiments in the single batch reactors.

#	Metal	Support	T / K	p / MPa	m_{cat} / mg	$m_{Glycerol\ solution}$ / g	Pre-treatment	Remarks	t / h	X_1	X_2	$S_{1,3\text{-PDO}}$	$S_{1,2\text{-PDO}}$	$S_{1\text{-PrOH}}$	$S_{2\text{-PrOH}}$	$Y_{1,3\text{-PDO}}$
Campinas																
1	Re	W_xC	423	1.2	150	200	N_2 (773 K, 3 h); Air (573 K, 2 h); H_2 in-situ (493 K, 2.3 - 4.5 MPa H_2)		5	< 0,1%		Conversion too low				
2	Re	W_xC	423	1.4	150	200			6	< 0,1%		Conversion too low				
3	Re	W_xC	443	2	150	200			7	< 0,1%		Conversion too low				
4	Ni-Re	SiO_2	423	1.7	300	200	Air (773 K, 3 h); H_2 in-situ (473 K, 2 MPa H_2)		3	< 0,2%		Conversion too low				
5	Ni-Re	SiO_2	433/473	2.8	300	200	Air (773K, 3 h); H_2 (673 K, 2 h)		4 + 7	4%	2%	0%	94%	2%	1%	0%
6	Ni	W_xC/Norit	448	3.1	185	150	H_2 (673 K, 2 h)	Catalyst by Eyüp Kadioglu	7	< 0,1%		Conversion too low				

#	Metal	Support	T / K	p / MPa	m_{cat} / mg	$m_{Glycerol\ solution}$ / g	Pre-treatment	Remarks	t / h	X_1	X_2	$S_{1,3\text{-PDO}}$	$S_{1,2\text{-PDO}}$	$S_{1\text{-PrOH}}$	$S_{2\text{-PrOH}}$	$Y_{1,3\text{-PDO}}$
7	Ru	WO_3/TiO_2	443	2.4	420	200	H_2 (673 K, 2 h)	Catalyst by Elisabeth Paki	10	0,3%	< 0%	0%	96%	2%	2%	0%
8	Ni	SiO_2	463	3.1	300	200	H_2 (673 K, 1 h)	Catalyst Leuna 6503T	12	1%	< 0%	0%	94%	5%	1%	0%
9	Ni	ZrO_2	463	3.8	330	200	H_2 (673 K, 1 h)	Catalyst Leuna Y43374	22	2%	2%	0%	89%	3%	8%	0%
10	Re	WC/C	453	5.6	250	200	H_2 (653 K, 1.5 h)		9	< 0,1%		Conversion too low				
11	Re	WC/C	453	3.4	250	200	H_2 (653 K, 1.5 h)	40% Glycerol + 10 drops H_2SO_4 conc	8	< 0,1%		Conversion too low				
12	Ir-Re	WC/C (burned)	453	5.1	390	200	N_2 (723 K, 3 h); Air (573 K; 2 h); H_2 (653 K; 1.5 h)	2.5 drops H_2SO_4 conc	20	0,4%	< 0%	0%	39%	3%	58%	0%
13	Ir-Re	SiO_2 (Aerosil 200)	393	5.5	300	30	Air (773 K, 3 h); H_2 (503 K, 1 h)	67% Glycerol + 1 drop H_2SO_4 conc	15	< 0,1%		Conversion too low				
14	Ir-Re	SiO_2 (Aerosil 200)	453	7.2	450	18	Air (773 K, 3 h); H_2 (503 K, 1 h)	67% Glycerol + 4 µL H_2SO_4 conc	12	2%	0,3%	17%	43%	38%	3%	0,4%
15	Pt	STA/SiO_2 (Aerosil 200)	473	5.5	500	60	Air (673 K, 4 h); H_2 (573 K, 2 h)	Catalyst transfer in Glovebox	24	1%	3%	2%	33%	59%	6%	0,1%
16	Ni-Re	STA/SiO_2 (Aerosil 200)	473	5.4	500	60	Air (673 K, 3 h); H_2 (573 K, 1.5 h)	Catalyst transfer in Glovebox	20	6%	8%	0%	62%	14%	1%	0,0%
17	Pt-Re	STA/SiO_2 (Aerosil 200)	473	5.4	430	50	H_2 (653 K, 1 h)	Catalyst transfer in Glovebox	20	8%	10%	8%	34%	38%	7%	0,7%
18	Ir-Re	SiO_2 (Aerosil 200)	393	6.2	500	30	Air (773 K; 3 h); H_2 (503 K, 1 h)	67% Glycerol + 1 drop H_2SO_4 conc, Catalyst transfer in Glovebox	16	0,2%	< 0%	37%	26%	24%	7%	0,1%

#	Metal	Support	T / K	p / MPa	m_{cat} / mg	$m_{Glycerol\ solution}$ / g	Pre-treatment	Remarks	t / h	X_1	X_2	$S_{1,3\text{-PDO}}$	$S_{1,2\text{-PDO}}$	$S_{1\text{-PrOH}}$	$S_{2\text{-PrOH}}$	$Y_{1,3\text{-PDO}}$
19	Ir/Re	SiO_2 (Aerosil 200)	393	6.2	750	90	2 x Static air (773 K; 3 h); H_2 in-situ	66% Glycerol + 13.5 mg H_2SO_4	12	0,2%	< 0%	0%	19%	52%	17%	0,0%
20	Pt-Re	STA/SiO_2 (Aerosil 200)	473	5	415	50	H_2 (503 K, 1 h)	Last 9 h: No stirring	20	8%	6%	5%	39%	42%	3%	0,4%
21	Pt-Re	STA/SiO_2 (Aerosil 200)	473	5	380	54	Static air (773 K; 3 h); H_2 in-situ (503 K, 1 h, 3.2 MPa, no water)		20	3%	< 0%	4%	33%	49%	2%	0,1%
22		W_xC/C	513	7.1	450	150	Used as received	Catalyst by Cristiane Rodella, 1% Glycerol	4	5%	< 0%	0%	32%	34%	0%	0,0%
23	Ir-Re	STA/SiO_2 (Aerosil 200)	473	5	430	50	H_2 (653 K, 1 h)	Catalyst transfer in water	20	19%	17%	9%	5%	32%	45%	1,7%
24	Ir-Re	STA/SiO_2 (Aerosil 200)	473	5	390	50	Static air (773 K; 3 h); H_2 (503 K, 1 h)		20	3%	1%	5%	39%	34%	3%	0,1%
25	Ir-Re	STA/SiO_2 (Aerosil 200)	473	5	445	55	H_2 (503 K, 1 h)		20	15%	11%	7%	51%	28%	4%	1,1%
26	Re	H-ZSM-5 (32)	473	5	900	100	H_2 (573 K, 1 h)		20	5%	8%	4%	4%	84%	3%	0,2%
27	Pt/Re	H-ZSM-5 (32)	473	5	900	100	2 x H_2 (503 K / 573 K, 1 h)		20	44%	46%	16%	7%	67%	1%	7,1%
28	Ir/Re	H-ZSM-5 (32)	473	5	900	100	2 x H_2 (503 K / 573 K, 1 h)		20	27%	23%	15%	8%	70%	1%	4,1%
29		H-ZSM-5 (32)	473	5	900	100	None		20	7%	7%	0%	4%	80%	4%	0,0%
30	Pt/Re	H-ZSM-5 (32)	473	5	900	100	2 x Static air (823 K (Pt) / 773 K (Pt/Re); 3 h); H_2 (573 K, 1 h)		20	36%	33%	15%	4%	70%	1%	5,4%
31	Pt-Re	H-ZSM-5 (32)	473	5	950	100	H_2 (573 K, 1 h)		20	72%	76%	7%	7%	72%	0%	5,1%

#	Metal	Support	T / K	p / MPa	m_{cat} / mg	$m_{Glycerol\ solution}$ / g	Pre-treatment	Remarks	t / h	X_1	X_2	$S_{1,3\text{-PDO}}$	$S_{1,2\text{-PDO}}$	$S_{1\text{-PrOH}}$	$S_{2\text{-PrOH}}$	$Y_{1,3\text{-PDO}}$
32	Pt/Re	STA/SiO_2 (Aerosil 200)	473	5	600	68	2 x H_2 (503 K (Pt) / 653 K (Pt/Re), 1 h)		20	5%	4%	7%	27%	49%	3%	0,3%
33	Ir-Re	SiO_2 (Precipitated, Z 175 AB)	473	5.5	820	91	Static air (773 K; 3 h); H_2 (503 K, 1 h)		20	23%	26%	5%	60%	25%	3%	1,2%
34	6Pt/6Re	H-ZSM-5 (32)	473	5	920	103	2 x H_2 (503 K, 1.5 h (Pt) / 573 K, 1 h (Pt/Re))		4,5	18%	19%	21%	39%	29%	1%	3,5%
									20	46%	62%	10%	14%	64%	1%	4,8%
35	6Pt/6Re	H-ZSM-5 (32)	473	5.3	1000	112	2 x Static air (823 K (Pt), 773 K (Pt/Re); 3 h); H_2 (573 K, 1 h)		2	5%	7%	23%	25%	42%	1%	1,1%
									4	6%	10%	24%	20%	47%	1%	1,4%
									20	34%	35%	16%	5%	68%	2%	5,4%
36	3Pt/3Re	H-ZSM-5 (86)	473	5	1200	125	2 x H_2 (573 K, 1 h)	Catalyst transfer in Glovebox	2	33%	37%	18%	30%	42%	4%	5,9%
									5,5	44%	47%	16%	27%	48%	2%	7,0%
									20	82%	85%	6%	13%	69%	1%	5,1%
37	3Ir-3Re	H-ZSM-5 (86)	473	5	1200	125	Static air (773 K; 3 h); H_2 (503 K, 1 h)	Catalyst transfer in Glovebox	2	14%	17%	31%	25%	37%	1%	4,3%
									4,5	29%	38%	23%	16%	53%	1%	6,7%
									10	40%	49%	19%	12%	59%	0%	7,8%
									20	58%	74%	7%	4%	78%	0%	4,2%
38	3Pt-3Re	H-ZSM-5 (86)	453	5	1200	125	Static air (773 K; 3 h); H_2 (503 K, 1 h)	Catalyst transfer in Glovebox	2	10%	8%	19%	26%	45%	4%	1,8%
									4,5	12%	13%	20%	30%	41%	4%	2,4%
									9	15%	14%	24%	34%	32%	3%	3,6%
									20	33%	41%	17%	20%	55%	2%	5,5%
39	3Pt-3Re	H-ZSM-5 (86)	473	5	1200	125	Static air (773 K; 3 h); H_2 (503 K, 1 h)	Catalyst transfer in Glovebox	2	11%	11%	20%	27%	44%	2%	2,2%
									4,5	16%	16%	19%	20%	52%	1%	3,1%
									8,7	23%	25%	18%	13%	56%	1%	4,3%
									20	47%	52%	11%	7%	73%	0%	5,0%
40	3Pt-3Re	H-ZSM-5 (86)	433	5	1200	130	H_2 (503 K, 1 h)	reaction stopped after 2 h and restarted 2 d after	2	9%	< 0%	23%	35%	31%	8%	2,0%
									5,5	15%	17%	22%	37%	30%	10%	3,3%
									10	21%	22%	25%	41%	25%	8%	5,1%
									20	39%	37%	22%	34%	31%	10%	8,7%

#	Metal	Support	T / K	p / MPa	m_{cat} / mg	$m_{Glycerol\ solution}$ / g	Pre-treatment	Remarks	t / h	X_1	X_2	$S_{1,3\text{-PDO}}$	$S_{1,2\text{-PDO}}$	$S_{1\text{-PrOH}}$	$S_{2\text{-PrOH}}$	$Y_{1,3\text{-PDO}}$
41	3Pt-3Re	H-ZSM-5 (86)	433	5	1200	130	H_2 (503 K, 1 h)	Catalyst transfer in Glovebox (R040 and R041)	5,5	10%	12%	27%	44%	19%	7%	2,8%
									16	20%	22%	24%	38%	28%	9%	4,6%
									20	26%	13%	25%	41%	24%	7%	6,7%
									24	35%	31%	21%	34%	33%	10%	7,5%
42	3Pt/3Re	H-ZSM-5 (86)	413	5	1200	140	2 x Static air (823 K (Pt), 773 K (Pt/Re); 3 h); H_2 (503 K, 1 h)	Catalyst transfer in Glovebox	4,5	2%	3%	22%	41%	21%	9%	0,5%
									10	2%	1%	27%	30%	21%	11%	0,6%
									20	3%	4%	28%	33%	23%	11%	0,9%
									30	5%	< 0%	28%	32%	26%	12%	1,5%
43	3Pt	H-ZSM-5 (86)	473	5	1400	150	H_2 (503 K, 1 h)	Air contact	6,5	6%	< 0%	27%	18%	43%	1%	1,7%
									20	16%	25%	16%	5%	68%	0%	2,6%
44	3Pt	H-ZSM-5 (86)	473	5	1400	150	H_2 (503 K, 1 h)	Transfer in Glovebox	6,4	5%	8%	27%	13%	50%	1%	1,2%
									20	15%	24%	15%	4%	71%	0%	2,2%
45	3Re/2Ni (Ni in support)	W_xC/C	473	5	700	142	H_2 (503 K, 1 h, passivated at RT in Glovebox)	Temperature increased after 20 h of reaction	6,5	1%	1%	2%	8%	64%	1%	0,0%
									20	2%	< 0%	1%	10%	68%	1%	0,0%
			513						+ 5	8%	8%	1%	5%	77%	1%	0,1%
46	3Ru	H-ZSM-5 (86)	473	5	1400	140	H_2 (503 K, 1 h)	39% EG, 12% EtOH	0,75	12%	20%	4%	31%	11%	2%	0,5%
								35% EG, 11% EtOH	5	23%	52%	2%	28%	19%	3%	0,4%
								32% EG, 10% EtOH	9,7	26%	60%	0%	25%	23%	3%	0,0%
								23% EG, 10% EtOH	20	28%	79%	0%	24%	30%	3%	0,1%
47	3Ru/3Re	H-ZSM-5 (86)	473	5	1400	140	2 x H_2 (503 K, 1 h / 573 K, 1 h)	18% EG, 10% EtOH		33%	45%	4%	41%	24%	1%	1,3%
								11% EG, 8% EtOH	20	51%	76%	0%	26%	41%	1%	0,2%
Darmstadt																
48	No catalyst		473	5	0	100		Blind test	5	< 0,1%		Conversion too low				
49	3Pt-3Re	H-ZSM-5 (86)	433	5	635	100	H_2 (503 K, 1 h)	Same catalyst as R040 and R041, H_2 refill through tank	5	1,0%	0%	27%	44%	14%	3%	0,3%
									10	1,3%	4%	25%	47%	15%	4%	0,3%
									20	1,5%	6%	22%	52%	11%	3%	0,3%
									20	1,5%	8%	22%	51%	12%	3%	0,3%

#	Metal	Support	T / K	p / MPa	m_{cat} / mg	$m_{Glycerol\ solution}$ / g	Pre-treatment	Remarks	t / h	X_1	X_2	$S_{1,3\text{-PDO}}$	$S_{1,2\text{-PDO}}$	$S_{1\text{-PrOH}}$	$S_{2\text{-PrOH}}$	$Y_{1,3\text{-PDO}}$
50	Ir-Re (Precursor $IrCl_3$)	SiO_2 (Alfa Aesar)	473	5	850	100	H_2 (503 K, 1 h)	H_2 refill through tank (standard for all following reactions)	2	7%	9%	17%	61%	9%	2%	1,2%
									4	12%	14%	14%	59%	15%	3%	1,6%
									8	18%	22%	12%	61%	13%	3%	2,3%
									8	19%	24%	12%	57%	19%	2%	2,2%
51	Ir-Re (Precursor $IrCl_3$)	SiO_2 (#180)	473	5	850	100	H_2 (503 K, 1 h)		2	3%	5%	17%	62%	17%	1%	0,6%
									4	5%	6%	15%	61%	20%	1%	0,7%
									8	9%	10%	11%	56%	14%	3%	1,0%
52	Ir-Re (Precursor $IrCl_3$)	SiO_2 (K 60)	473	5	850	100	H_2 (503 K, 1 h)		2	12%	13%	21%	48%	17%	3%	2,7%
									4	17%	24%	19%	48%	26%	0%	3,6%
									8	27%	27%	19%	54%	20%	2%	5,5%
									8	29%	32%	17%	48%	28%	2%	5,3%
53	Ir-Re	SiO_2 (Alfa Aesar)	473	5	860	100	H_2 (503 K, 1 h)		2	11%	8%	17%	46%	23%	5%	1,9%
									4	18%	18%	16%	45%	25%	5%	2,9%
									8	32%	37%	13%	42%	32%	6%	4,1%
									8	36%	38%	12%	41%	34%	6%	4,5%
54	Ir	SiO_2 (Alfa Aesar)	473	5	860	100	H_2 (503 K, 1 h)		2	2%	2%	7%	55%	14%	2%	0,1%
									4	1%	4%	5%	51%	18%	2%	0,0%
									8	1%	7%	2%	51%	26%	3%	0,0%
									8	1%	3%	2%	65%	13%	3%	0,0%
55	Pt-Re	SiO_2 (Alfa Aesar)	473	5	850	100	H_2 (503 K, 1 h)		2	8%	8%	21%	40%	25%	8%	1,8%
									4	14%	19%	20%	38%	26%	8%	2,7%
									8	24%	22%	16%	36%	31%	8%	3,7%
									8	27%	27%	17%	38%	29%	8%	4,5%
56	Ir-Re	SiO_2 (Alfa Aesar)	473	5	850	100	Air (773 K; 3 h); H_2 (503 K, 1 h)		2	8%	4%	19%	55%	16%	3%	1,4%
									4	11%	13%	16%	54%	17%	3%	1,7%
									8	17%	17%	16%	55%	16%	4%	2,7%
									8	19%	22%	13%	48%	25%	3%	2,5%

#	Metal	Support	T / K	p / MPa	m_{cat} / mg	$m_{Glycerol\ solution}$ / g	Pre-treatment	Remarks	t / h	X_1	X_2	$S_{1,3\text{-PDO}}$	$S_{1,2\text{-PDO}}$	$S_{1\text{-PrOH}}$	$S_{2\text{-PrOH}}$	$Y_{1,3\text{-PDO}}$
57	Re	SiO_2 (Alfa Aesar)	473	5	915	100	H_2 (503 K, 1 h)		2	1%	1%	1%	15%	4%	0%	0,0%
									8	1%	1%	1%	10%	1%	0%	0,0%
58	Ni-Re	SiO_2 (Alfa Aesar)	473	5	1050	100	H_2 (503 K, 1 h)	34% EG	2	5%	6%	3%	52%	2%	2%	0,2%
								35% EG	4	8%	10%	3%	55%	1%	2%	0,2%
								34% EG	8	16%	18%	3%	56%	2%	2%	0,4%
								33% EG	8	17%	16%	3%	54%	4%	4%	0,5%
59	Pt-Re	SiO_2 (K 60)	473	5	890	100	H_2 (503 K, 1 h)	Addition of 100 mg H-ZSM-5 (86)	2	14%	17%	15%	53%	13%	3%	2,2%
									4	23%	23%	15%	53%	16%	3%	3,3%
									8	33%	36%	14%	54%	22%	2%	4,5%
60	Cu-Re	SiO_2 (Alfa Aesar)	473	5	890	100	H_2 (503 K, 1 h)	Addition of 100 mg H-ZSM-5 (86)	2	2%	3%	10%	68%	9%	0%	0,3%
									4	2%	5%	3%	73%	8%	0%	0,1%
									8	3%	6%	2%	75%	12%	0%	0,1%
61	Ru-Re	H-ZSM-5 (86)	473	5	850	100	Reduced at 573 K (Campinas), Re-reduced at 503 K	27% EG	2	36%	45%	2%	47%	14%	9%	0,9%
								26% EG	4	43%	52%	2%	39%	19%	9%	0,7%
								26% EG	8	37%	65%	1%	35%	22%	8%	0,4%
								23% EG	8	45%	64%	1%	31%	24%	9%	0,4%
62	Pt-Re	SiO_2 (K 60)	473	5	800	100	H_2 (503 K, 1 h)	Inserted glass vessel (broke during reaction)	2	7%	12%	13%	49%	13%	3%	0,9%
									4	10%	12%	13%	53%	15%	2%	1,3%
									8	14%	19%	12%	54%	12%	3%	1,7%
									8	16%	18%	10%	49%	17%	4%	1,6%
63	Pt-Re	Al_2O_3	473	5	900	120	H_2 (503 K, 1 h)	16,7%wt. Glycerol solution	2	2%	< 0%	11%	33%	16%	3%	0,2%
									4	2%	< 0%	15%	45%	19%	1%	0,4%
									8	4%	3%	10%	42%	13%	1%	0,5%
									8	4%	8%	11%	45%	27%	3%	0,5%
64	Ir-Re	Al_2O_3	473	5	870	100	H_2 (503 K, 1 h)		2	8%	5%	17%	54%	15%	1%	1,3%
									4	14%	11%	20%	53%	13%	1%	2,8%
									8	24%	30%	17%	51%	24%	2%	3,9%
									8	25%	33%	15%	48%	28%	3%	3,7%

#	Metal	Support	T / K	p / MPa	m_{cat} / mg	$m_{Glycerol\ solution}$ / g	Pre-treatment	Remarks	t / h	X_1	X_2	$S_{1,3\text{-PDO}}$	$S_{1,2\text{-PDO}}$	$S_{1\text{-PrOH}}$	$S_{2\text{-PrOH}}$	$Y_{1,3\text{-PDO}}$
65	Ir-Re	SiO_2 (K 60)	453	5	965	100	H_2 (503 K, 1 h)	Inserted Teflon vessel (standard for all following reactions)	8	30%	30%	19%	43%	26%	8%	6,6%
66	Ir-Re	SiO_2 (K 60)	473	1.7	900	106	H_2 (503 K, 1 h)	0.7 MPa D_2 + 1 MPa Ar	12	7%	9%	9%	53%	25%	4%	0,7%
67	(Ir+Re)	SiO_2 (K 60)	453	5	915	100	H_2 (503 K, 1 h)		8	39%	43%	19%	35%	34%	10%	7,6%
68	(Ir+Re)	SiO_2 (K 60)	453	5	920	100	H_2 (503 K, 1 h)	No Teflon, Catalyst stored under air for 3 d	8	25%	29%	19%	42%	29%	8%	4,9%
69	(Ir+Re)	SiO_2 (K 60)	453	5	930	100	H_2 (503 K, 1 h)	No Teflon	8	28%	36%	19%	40%	30%	8%	5,4%
70	Ir-Re	SiO_2 (G-6)	453	5	870	100	H_2 (503 K, 1 h)		8	56%	73%	18%	25%	44%	11%	10,1%
71	Ir-Re	SiO_2 (G-6)	453	5	880	100	H_2 (773 K, 1 h)	HT Reduction	8	39%	49%	22%	32%	33%	10%	8,7%
72	Ir-Re	SiO_2 (G-6)	453	5	865	100	Air (773 K; 3 h); H_2 (503 K, 1 h)		8	20%	24%	24%	34%	30%	10%	4,8%
73	Pt-Re	SiO_2 (G-6)	453	5	880	100	H_2 (773 K, 1 h)		8	41%	50%	25%	22%	35%	16%	10,4%
74	Pt-Re	SiO_2 (G-6)	453	5	880	100	Air (773 K; 3 h); H_2 (503 K, 1 h)		8	1%	6%	0%	40%	39%	14%	0,0%
75	Pt	SiO_2 (G-6)	453	5	880	100	H_2 (773 K, 1 h)		8	0%	1%	11%	11%	24%	10%	0,0%
76	Pt	SiO_2 (G-6)	453	5	880	100	Air (773 K; 3 h); H_2 (503 K, 1 h)		8	0%	4%	16%	24%	16%	5%	0,0%
77	Ir-Re	SiO_2 (G-6)	453	5	880	100	H_2 (503 K, 1 h)	Like R070	8	52%	73%	19%	26%	42%	11%	10,0%
78	Ir-Re	SiO_2 (G-6)	433	5	880	100	H_2 (503 K, 1 h)	Lower T	8	38%	46%	28%	28%	33%	9%	10,9%
79	Ir-Re	SiO_2 (G-6)	453	5	880	100	H_2 (503 K, 1 h)	No Teflon	8	36%	45%	22%	37%	31%	9%	7,9%

#	Metal	Support	T / K	p / MPa	m_{cat} / mg	$m_{Glycerol\ solution}$ / g	Pre-treatment	Remarks	t / h	X_1	X_2	$S_{1,3\text{-PDO}}$	$S_{1,2\text{-PDO}}$	$S_{1\text{-PrOH}}$	$S_{2\text{-PrOH}}$	$Y_{1,3\text{-PDO}}$
80	Pt-Re	SiO_2 (G-6)	433	5	880	100	H_2 (503 K, 1 h)		8	36%	39%	26%	19%	38%	16%	9,3%
81	Pt-Re	SiO_2 (G-6)	433	5	880	100	H_2 (503 K, 1 h)	2 mg $FeNO_3$	8	14%	17%	25%	28%	30%	16%	3,4%
82		SiO_2 (G-6)	453	5	855	100		Support only	8	0%	< 0%	9%	3%	47%	20%	0,0%
83	(Pt+Re)	SiO_2 (G-6)	433	5	880	100	H_2 (503 K, 1 h), Impregnated together	500 rpm	8	24%	27%	28%	21%	35%	15%	6,7%
84	(Pt+Re)	SiO_2 (G-6)	433	5	880	100		750 rpm	8	33%	31%	24%	20%	38%	17%	7,8%
85	Ir-Re	H-ZSM-5 (86)	433	5	835	95	H_2 (503 K, 1 h)	750 rpm (new standard)	8	58%	57%	24%	17%	47%	10%	14,0%
86	Pt-Re	H-ZSM-5 (86)	433	5	850	97,5	H_2 (503 K, 1 h)		8	29%	32%	26%	28%	32%	14%	7,4%
87	Ir-Re	H-ZSM-5 (86)	413	5	845	96,5	H_2 (503 K, 1 h)	Lower T	8	23%	23%	36%	25%	29%	10%	8,3%
88	Ir/Re	H-ZSM-5 (86)	433	5	825	94	2 x H_2 (503 K, 1 h)		8	7%	8%	26%	36%	29%	7%	1,8%
89		H-ZSM-5 (86)	433	5	860	100		Support only	8	0%	< 0%	Conversion too low				
90		H-ZSM-5 (86)	453	5	860	100		Support only	8	0%	0%	Conversion too low				
91	Ir-Re	H-ZSM-5 (86)	433	5	880	100	H_2 (503 K, 1 h)	Ir Precursor: $IrCl_3$	8	32%	34%	31%	28%	32%	8%	10,0%
92	Ir-Re	NH_4-ZSM-5 (80)	433	5	880	100	H_2 (503 K, 1 h)	Zeolite support not calcined, Ir Precursor: $IrCl_3$	8	21%	22%	29%	32%	29%	9%	6,1%
93	Ir-Re	SiO_2 (G-10)	433	5	880	100	H_2 (503 K, 1 h)		8	49%	50%	24%	27%	36%	11%	11,7%
94	Ir-Re	H-ZSM-5 (80)	433	5	880	100	H_2 (503 K, 1 h)	Ir Precursor: $IrCl_3$	8	51%	51%	28%	18%	43%	9%	14,0%

#	Metal	Support	T / K	p / MPa	m_{cat} / mg	$m_{Glycerol\ solution}$ / g	Pre-treatment	Remarks	t / h	X_1	X_2	$S_{1,3\text{-PDO}}$	$S_{1,2\text{-PDO}}$	$S_{1\text{-PrOH}}$	$S_{2\text{-PrOH}}$	$Y_{1,3\text{-PDO}}$
95	Ir-Re	H-ZSM-5 (80)	433	5	880	100	H_2 (503 K, 1 h)		8	50%	53%	28%	19%	43%	9%	14,0%
96	Ir-Re	H-ZSM-5 (80)	433	7.2	880	100	H_2 (503 K, 1 h)		8	57%	62%	25%	22%	41%	10%	14,1%
97	Ir-Re	H-BEA (150)	433	5	880	100	H_2 (503 K, 1 h)		8	52%	56%	28%	17%	44%	9%	14,7%
98	Ir-Re	H-ZSM-5 (80)	413	5	880	100	H_2 (503 K, 1 h)		8	26%	27%	37%	24%	29%	9%	9,6%
99	Ir-Re	H-ZSM-5 (86)	433	5	880	100	H_2 (503 K, 1 h)	Ir Precursor: $IrCl_3$	8	44%	47%	28%	22%	39%	9%	12,3%
100	Ir-Re	SiO_2 (G-6)	433	5	880	100	H_2 (503 K, 1 h)		8	51%	62%	27%	21%	39%	10%	14,1%
101	Ir-Re	H-ZSM-5 (32)	433	5	880	100	H_2 (503 K, 1 h)		8	25%	29%	29%	33%	29%	7%	7,3%
102	Ir-Re	Al_2O_3	433	5	880	100	H_2 (503 K, 1 h)		8	19%	18%	26%	37%	24%	10%	4,9%
103	Ir-Re	SiO_2 (G-6)	433	5	880	100	H_2 (503 K, 1 h)	Like R100	8	47%	51%	26%	24%	38%	11%	12,2%
104	Ir-Re	H-BEA (35)	433	5	880	100	H_2 (503 K, 1 h)		8	46%	49%	25%	25%	40%	9%	11,4%
105	Ir-Re	SiO_2 (G-6)	433	5	880	100	H_2 (503 K, 1 h)	Stored 5 d in air, 500 rpm	8	45%	48%	27%	24%	37%	11%	12,2%
106	4Ir-2Re	H-ZSM-5 (80)	433	5	880	100	H_2 (503 K, 1 h)		8	38%	42%	31%	21%	38%	8%	11,8%
107	4Ir-2Re	H-ZSM-5 (80)	433	5	880	100	H_2 (503 K, 1 h)		8	49%	55%	26%	19%	44%	9%	12,8%
108	4Ir-2Re	H-BEA (150)	433	5	880	100	H_2 (503 K, 1 h)		8	47%	49%	30%	15%	44%	9%	13,9%
109	Ir-Re	H-BEA (150)	433	5	880	100	H_2 (503 K, 1 h)	1 drop H_2SO_4	8	44%	43%	30%	18%	41%	9%	13,4%
110	NH_4ReO_4+Ir	H-ZSM-5 (80)	433	5	861	100	H_2 (503 K, 1 h)	Addition of NH_4ReO_4 (54 mg)	8	11%	11%	27%	35%	29%	8%	2,9%

#	Metal	Support	T / K	p / MPa	m_{cat} / mg	$m_{Glycerol\ solution}$ / g	Pre-treatment	Remarks	t / h	X_1	X_2	$S_{1,3\text{-PDO}}$	$S_{1,2\text{-PDO}}$	$S_{1\text{-PrOH}}$	$S_{2\text{-PrOH}}$	$Y_{1,3\text{-PDO}}$
111	Ir-Re	H-ZSM-5 (80)	433	5	880	100	H_2 (503 K, 1 h)	25 mg H_2SO_4	8	26%	53%	32%	28%	31%	7%	8,5%
112	Ir-Re	H-ZSM-5 (80)	433	5	880	100	H_2 (503 K, 1 h)		8	41%	56%	30%	24%	36%	8%	12,6%
113	Ir-Re	SiO_2 (G-6)	433	5	880	100	H_2 (503 K, 1 h)	H_2SO_4 addition (10 mg)	8	48%	49%	26%	24%	38%	11%	12,5%
114	Ir-Re	H-ZSM-5 (80)	433	5	880	100	H_2 (503 K, 1 h)	HNO_3 addition (20 mg)	8	28%	31%	27%	32%	28%	10%	7,7%
115	Ir	H-ZSM-5 (80)	433	5	880	100	H_2 (503 K, 1 h)		8	2%	< 0%	30%	46%	15%	4%	0,5%
116	Ir-Re	H-ZSM-5 (80)	433	5	880	100	H_2 (503 K, 1 h)	2.4 mg $FeSO_4$	8	33%	30%	30%	26%	34%	8%	9,9%
117	Ir-Re	MCM-41	433	5	880	100	H_2 (503 K, 1 h)		8	42%	50%	32%	23%	35%	8%	13,4%
118	Ir-Re	SiO_2 (G-6)	433	5	880	100	H_2 (503 K, 1 h)		8	47%	53%	27%	23%	38%	10%	12,8%
119	Ir-Re	Norit SX-1	433	5	880	100	H_2 (503 K, 1 h)		8	10%	8%	24%	33%	33%	8%	2,5%
120	Ir-Re	Norit SX Plus	433	5	880	100	H_2 (503 K, 1 h)		8	9%	7%	24%	34%	33%	7%	2,3%
121	Ir-Re	Norit SX-1	433	5	880	100	H_2 (503 K, 1 h)	Precipitation catalyst, acc. to Gallezot	8	0%	< 0%	9%	11%	53%	4%	0,0%
122	Ir-Re	Norit SX-1G	433	5	880	100	H_2 (503 K, 1 h)		8	8%	8%	24%	34%	33%	7%	2,0%
123	Ir-Re	H-BEA (150)	433	5	880	100	H_2 (503 K, 1 h)		8	58%	60%	25%	18%	45%	10%	14,3%
124	Ir-Re	H-BEA (150)	433	5	880	100	H_2 (503 K, 1 h)	9.5 mg HCl 2N	8	50%	54%	30%	18%	42%	8%	14,8%
125	Ir/Re	H-BEA (150)	433	5	880	100	2 x H_2 (503 K, 1 h)	Addition of 1 drop HCl 2N on Re impregnation	8	10%	7%	28%	33%	27%	8%	2,7%

#	Metal	Support	T / K	p / MPa	m_{cat} / mg	$m_{Glycerol\ solution}$ / g	Pre-treatment	Remarks	t / h	X_1	X_2	$S_{1,3\text{-PDO}}$	$S_{1,2\text{-PDO}}$	$S_{1\text{-PrOH}}$	$S_{2\text{-PrOH}}$	$Y_{1,3\text{-PDO}}$
126	Ir-Re	H-BEA (150)	433	5	880	100	H_2 (503 K, 1 h)	Addition of 1 drop HCl 2N on Re impregnation	8	58%	59%	25%	19%	44%	10%	14,2%
127	5Pt-5Re	Norit SX-1G	433	5	880	100	H_2 (723 K, 3 h)	According to Daniel et al.	8	14%	12%	28%	27%	31%	11%	3,8%
128	Ir-Re	SiO_2 (Q-6)	433	5	880	100	H_2 (503 K, 1 h)		8	67%	68%	21%	15%	50%	11%	14,2%
129	Ir-Re	SiO_2 (Q-10)	433	5	880	100	H_2 (503 K, 1 h)		8	53%	53%	23%	22%	41%	11%	12,3%
130	Pt-Re	SiO_2 (Q-6)	433	5	880	100	H_2 (503 K, 1 h)		8	57%	60%	22%	18%	41%	16%	12,7%
131	Pt-Re	SiO_2 (Q-10)	433	5	880	100	H_2 (503 K, 1 h)		8	50%	47%	23%	19%	40%	16%	11,2%
132	Re + Ir	H-BEA (150)	433	5	2 x 440	100	H_2 (503 K, 1 h)	Re/H-BEA + Ir/H-BEA, reduced together	8	16%	15%	34%	28%	30%	6%	5,4%
133	Re + Ir	H-BEA (150)	433	5	2 x 440	100	H_2 (503 K, 1 h)	Re/H-BEA + Ir/H-BEA	8	4%	0%	34%	33%	23%	5%	1,2%
134	Ir-Re	SiO_2 (Q-6)	433	5	880	100	H_2 (503 K, 1 h)		8	62%	66%	22%	18%	46%	11%	13,9%
135	Ir-Re	SiO_2 (Q-6)	413	5	880	100	H_2 (503 K, 1 h)		8	44%	42%	32%	20%	36%	10%	14,1%
136	(Ir+Ru)-Re	SiO_2 (Q-6)	433	5	880	100	H_2 (503 K, 1 h)	Ru and Ir impregnated together	8	72%	83%	12%	19%	52%	13%	8,4%
137	Ru-Ir-Re	SiO_2 (Q-6)	433	5	880	100	H_2 (503 K, 1 h)	3 impregnation steps	8	70%	79%	13%	20%	50%	13%	9,4%
138	Re + Ir	H-ZSM-5 (80)	433	5	2 x 440	100	H_2 (503 K, 1 h)	Re/H-ZSM-5 (80) + Ir/H-ZSM-5 (80), reduced together	8	16%	20%	34%	32%	27%	5%	5,3%
139	Re + Ir	H-ZSM-5 (80)	433	5	2 x 440	100	H_2 (503 K, 1 h)	Re/H-ZSM-5 (80) + Ir/H-ZSM-5 (80)	8	4%	3%	31%	35%	25%	5%	1,2%
140	Ir-Re	SiO_2 (Q-6)	433	5	880	100	H_2 (503 K, 1 h)	Like R134	8	66%	69%	21%	17%	48%	12%	13,8%

#	Metal	Support	T / K	p / MPa	m_{cat} / mg	$m_{Glycerol\ solution}$ / g	Pre-treatment	Remarks	t / h	X_1	X_2	$S_{1,3\text{-PDO}}$	$S_{1,2\text{-PDO}}$	$S_{1\text{-PrOH}}$	$S_{2\text{-PrOH}}$	$Y_{1,3\text{-PDO}}$
141	Ir-Re	H-ZSM-5 (30)	433	5	880	100	H_2 (503 K, 1 h)		8	43%	46%	28%	25%	38%	7%	11,9%
142	Ir-Re	H-ZSM-5 (90)	433	5	880	100	H_2 (503 K, 1 h)		8	55%	59%	24%	20%	43%	10%	13,4%
143	Ir-Re	H-ZSM-5 (200)	433	5	880	100	H_2 (503 K, 1 h)	Pressure issues	8	23%	22%	31%	28%	30%	9%	7,1%
144	Ir-Re	H-ZSM-5 (800)	433	5	880	100	H_2 (503 K, 1 h)		8	31%	28%	29%	28%	30%	10%	9,1%
145	Ir-Re	H-ZSM-5 (200)	433	5	880	100	H_2 (503 K, 1 h)	Like R143	8	18%	14%	31%	32%	27%	9%	5,7%
146	Ir-Re	H-ZSM-5 (27)	433	5	880	100	H_2 (503 K, 1 h)		8	27%	29%	32%	28%	31%	6%	8,5%
147	Rh-Re	Vulcan XC-72	433	5	880	100	Used as received	Catalyst made by Dumesic group	8	46%	48%	13%	26%	45%	13%	6,0%
148	Ir-Re	H-ZSM-5 (90)	298 - 433	2.5	880	100	H_2 (503 K, 1 h)	Heating up, cooling down, storing closed system for 18 hours	0,5	1%	< 0%	35%	32%	16%	10%	0,3%
			303	3.5					18	1%	< 0%	35%	36%	15%	10%	0,3%
149	(Ir+Ru)-Re	SiO_2 (Q-6)	413	5	880	100	H_2 (503 K, 1 h)	Same catalyst as R136	8	44%	44%	29%	26%	33%	8%	13,1%
150	Rh-Re	H-ZSM-5 (90)	433	5	880	100	H_2 (503 K, 1 h)		8	79%	97%	3%	23%	51%	20%	2,4%
151	Re	H-ZSM-5 (90)	433	5	880	100	Reduced 673 K	Catalyst transfer in Glovebox	8	0%	0%	0%	16%	48%	25%	0,0%
152	4Ir-2Re	H-ZSM-5 (90)	433	5	880	100	H_2 (503 K, 1 h)		8	36%	41%	31%	21%	37%	8%	11,4%
153	Ir-Re	H-ZSM-5 (90)	433	5	880	100	H_2 (503 K, 1 h)		8	32%	33%	29%	29%	31%	8%	9,5%
154	Ir-Re	H-ZSM-5 (90)	433	5	880	100	H_2 (673 K, 1 h)		8	26%	29%	34%	28%	30%	6%	8,9%

#	Metal	Support	T / K	p / MPa	m_{cat} / mg	$m_{Glycerol\ solution}$ / g	Pre-treatment	Remarks	t / h	X_1	X_2	$S_{1,3\text{-PDO}}$	$S_{1,2\text{-PDO}}$	$S_{1\text{-PrOH}}$	$S_{2\text{-PrOH}}$	$Y_{1,3\text{-PDO}}$
155	Rh-Re	H-ZSM-5 (90)	413	5	880	100	H_2 (503 K, 1 h)		8	67%	70%	12%	37%	34%	14%	8,2%
156	Ir-Re	H-ZSM-5 (90)	413	5	880	100	H_2 (503 K, 1 h)		8	30%	32%	37%	25%	28%	9%	11,2%
157	Ir-Re	H-ZSM-5 (90)	433	5	880	100	H_2 (503 K, 1 h)	1,3-PDO instead of glycerol	8	23%	20%		0%	94%	0%	
158	Ir-Re	H-ZSM-5 (90)	433	5	880	100	H_2 (503 K, 1 h)	1,2-PDO instead of glycerol	8	46%	61%	0%		72%	26%	
159	Ir-Re	H-ZSM-5 (90)	433	5	880	100	H_2 (503 K, 1 h)		8	41%	47%	29%	28%	33%	9%	11,7%
160	Re-Ir	H-ZSM-5 (90)	433	5	880	100	H_2 (503 K, 1 h)	Inverse impregnation order	8	28%	30%	31%	32%	27%	9%	8,6%
161	Ir-Re	SiO_2 (K 60)	433	5	880	100	H_2 (503 K, 1 h)		8	41%	46%	28%	30%	31%	11%	11,5%
162	Ir-Re	H-ZSM-5 (90)	433	5	880	100	H_2 (503 K, 1 h)	Excess water impregnation	8	38%	46%	28%	27%	34%	10%	10,8%
163	Re-Ir	H-ZSM-5 (90)	433	5	880	100	H_2 (503 K, 1 h)	Excess water + inverse impr. order	8	29%	39%	31%	30%	29%	9%	8,9%
164	Ir-Re	H-ZSM-5 (90)	433	5	750	85	Dried (393 K, overnight)	Used and washed catalyst from R159	8	19%	27%	33%	32%	25%	8%	6,3%
165	Ir-Re	H-ZSM-5 (90)	433	5	880	100	H_2 (503 K, 1 h)	Like R142	8	47%	52%	28%	25%	36%	10%	13,5%
166	Ir-Re	H-ZSM-5 (90)	433	5	880	100	H_2 (503 K, 1 h)	Stirrer protected with Teflon tape	8	39%	43%	30%	28%	32%	9%	11,8%
167	Ir-Re	H-ZSM-5 (90)	393	5	880	100	H_2 (503 K, 1 h)	Lower T	20	32%	31%	38%	24%	25%	11%	12,5%
168	Ir-Re	SiO_2 (G-6)	433	5	880	100	H_2 (503 K, 1 h)	R118 reloaded	8	46%	55%	28%	25%	35%	11%	13,1%
169	Ir-Re	SiO_2 (K 100)	433	5	880	100	H_2 (503 K, 1 h)		8	40%	52%	31%	29%	30%	9%	12,5%
170	Ir-Re	Aerosil 200	433	5	880	100	H_2 (503 K, 1 h)		8	30%	31%	30%	29%	30%	10%	8,9%

#	Metal	Support	T / K	p / MPa	m_{cat} / mg	$m_{Glycerol\ solution}$ / g	Pre-treatment	Remarks	t / h	X_1	X_2	$S_{1,3\text{-PDO}}$	$S_{1,2\text{-PDO}}$	$S_{1\text{-PrOH}}$	$S_{2\text{-PrOH}}$	$Y_{1,3\text{-PDO}}$
171	Ir-Re	Silicagel LP	433	5	880	100	H_2 (503 K, 1 h)		8	48%	52%	27%	28%	34%	11%	12,9%
172	Ir-Re	G-6 (700°C)	393	5	880	100	Static air (773 K/ 3 h), Reduced in-situ		20	21%	16%	46%	25%	14%	15%	9,5%
173	Ir-Re	G-6 (700°C)	393	5	880	100	H_2 (503 K, 1 h), Reduced in-situ		20	42%	48%	50%	18%	22%	9%	21,3%
174	Ir-Re	SiO_2 (G-6)	393	5	880	100	H_2 (503 K, 1 h), Reduced in-situ		20	44%	43%	46%	15%	27%	12%	20,3%
175	Ir-Re	SiO_2 (G-6)	393	5	880	100	Static air (773 K/ 3 h), Reduced in-situ		20	16%	18%	51%	25%	12%	12%	8,1%
176	Ir-Re	G-6 (700°C)	393	5	830	94	Reduced in-situ	Used catalyst from R173	20	36%	37%	51%	19%	18%	12%	18,2%
177	Ir	H-ZSM-5 (80)	433	5	880	100	H_2 (503 K, 1 h)	Long term of R115	26	13%	18%	40%	29%	29%	2%	5,2%
178	Ir-Re	SiO_2 (G-6)	473	5	880	100	H_2 (503 K, 1 h), Reduced in-situ in the glycerol solution	Conversion during pre-treatment	1	20%	28%	23%	37%	30%	8%	4,5%
			393					Conversion after pre-treatment	1 + 17	9%	3%	49%	39%	7%	4%	4,6%
									1 + 20	12%	8%	36%	29%	25%	10%	4,6%
179	Ir-Re	SiO_2 (G-6)	433	5	880	100	H_2 (503 K, 1 h)	Solvent: 1,2-Butanediol	2	6%	7%	24%	34%	31%	6%	1,3%
									4	8%	7%	22%	34%	35%	7%	1,7%
									8	12%	21%	25%	36%	29%	6%	3,0%
180	Ir-Re	SiO_2 (G-6)	433	5	880	100	H_2 (503 K, 1 h)	Solvent: Glycerol	4	6%	11%	34%	29%	30%	6%	2,1%
									8	11%	12%	33%	28%	32%	6%	3,6%
181	Ir-Re	SiO_2 (G-6)	433	5	880	100	H_2 (503 K, 1 h)	Reaction under Argon instead of H_2; S_{Acetol}: 78%	4	2%	3%	2%	10%	4%	0%	0,0%
									8	2%	4%	0%	14%	5%	0%	0,0%
182	Ir-Re	SiO_2 (G-6)	393	5	880	100	H_2 (503 K, 1 h), in-situ: Ar (473 K, 1 h)	In-situ "reduction" under Ar, reaction in H_2	20	5%	2%	28%	38%	24%	10%	1,4%
183	Ir-Re	SiO_2 (G-6)	393	5	880	100	H_2 (503 K, 1 h)		4	12%	12%	44%	24%	21%	11%	5,4%
									20	40%	38%	39%	21%	29%	12%	15,3%

#	Metal	Support	T / K	p / MPa	m_{cat} / mg	$m_{Glycerol\ solution}$ / g	Pre-treatment	Remarks	t / h	X_1	X_2	$S_{1,3\text{-PDO}}$	$S_{1,2\text{-PDO}}$	$S_{1\text{-PrOH}}$	$S_{2\text{-PrOH}}$	$Y_{1,3\text{-PDO}}$
184	Ir-Re	SiO_2 (G-6)	393	5	880	100	H_2 (503 K, 1 h), in-situ: Ar (473 K, 1 h)	In-situ "reduction" under Argon, reaction in H_2	20	0%	6%	7%	28%	32%	9%	0,0%
185	Ir-Re	SiO_2 (G-6)	393	5	880	100	Ar (503 K, 1 h), Reduced in-situ	Calcination in Argon	20	12%	15%	51%	22%	17%	11%	6,2%
186	Ir-Re	SiO_2 (G-6)	393	5	690	81	H_2 (503 K, 1 h), Reduced in-situ	Catalyst transfer in Glovebox	4	6%	14%	44%	30%	17%	9%	2,5%
									20	22%	30%	41%	28%	21%	10%	8,8%
187	Ir-Re	SiO_2 (G-6)	393	5	880	100	H_2 (503 K, 1 h), Reduced in-situ	Red. in Water, Rct. with 40%wt. EtOH	2	2%	13%	41%	42%	16%	1%	1,0%
									20	15%	25%	42%	38%	19%	1%	6,2%
188	Ir-Re	SiO_2 (G-6)	393	5	880	100	H_2 (503 K, 1 h), Reduced in-situ	Red. in EtOH	2	2%	9%	38%	45%	17%	0%	0,6%
									20	16%	23%	38%	38%	21%	1%	6,2%
189	Ir-Re	SiO_2 (G-6)	393	5	900	103	H_2 (503 K, 1 h)	Catalyst transfer in Glovebox	4	7%	9%	47%	24%	17%	8%	3,2%
									20	31%	31%	43%	20%	23%	9%	12,1%
190	Ir-Re	SiO_2 (G-6)	393	5	880	100	H_2 (503 K, 1 h), Reduced in-situ	In-situ-Red	20	33%	38%	51%	20%	19%	10%	15,6%
									48	59%	60%	43%	17%	28%	12%	23,2%
191	Ir-Re	SiO_2 (G-6)	393	5	1400	98	H_2 (503 K, 1 h)	Deuterium! 40%wt. Glycerol	24	53%	56%	38%	19%	33%	11%	20,1%
192	Ru	H-BEA (150)	393	5	880	100	H_2 (623 K, 3 h)	14% EG, 9% EtOH	20	33%	46%	4%	53%	18%	2%	1,40%
193	Ir-Re	SiO_2 (G-6)	393	5	880	100	H_2 (503 K, 1 h), Reduced in-situ	Addition of H_2WO_4 (51 mg)	20	1%	3%	46%	21%	19%	15%	0,60%

The amount of metal is 4%wt. each, if not stated differently. “Reduced in-situ” refers to the standard *in-situ* reduction of the catalyst in water (usually 50 g) at around 7 MPa for one hour at 473 K. In case of two samples for the same reaction time, the latter one describes the one taken from the reactor after opening it, whereas former samples were taken through a sample pipe.

Table 9 List of reactions in the multibatch reactor.

#	Metal	Support	T / K	p / MPa	m_{cat} / mg	$m_{Glycerol\ solution}$ / g	Remarks	t / h	X_1	X_2	$S_{1,3\text{-PDO}}$	$S_{1,2\text{-PDO}}$	$S_{1\text{-PrOH}}$	$S_{2\text{-PrOH}}$	$Y_{1,3\text{-PDO}}$
MB01-1	4Ir-2Re	H-BEA (150)	433	5.5	88	10.6	Impregnation with excess water	6	10%	8%	28%	38%	22%	8%	2,7%
MB01-2					88	10.1		6	9%	5%	29%	37%	23%	8%	2,6%
MB01-4					88	10.1		6	7%	11%	26%	41%	20%	8%	1,8%
MB01-5					89	10.0		6	9%	10%	28%	36%	23%	8%	2,4%
MB02-1	Ir-Re	Norit SX-1	433	5.5	87	10.0	Precipitation catalyst, acc. to Gallezot	8	0,4%	< 0%	18%	23%	35%	9%	0,1%
MB02-2					88	11.4		8	0,2%	< 0%	10%	19%	41%	6%	0,0%
MB02-4					88	10.5		8	0,3%	< 0%	8%	16%	42%	5%	0,0%
MB02-5					88	10.4		8	0,3%	3%	10%	21%	44%	5%	0,0%
MB03-1	Ir-Re	Norit SX-1G	433	5.5	87	9.9		8	5%	2%	21%	37%	33%	6%	1,0%
MB03-2					87	11.6	8 mg H_2SO_4	8	3%	5%	20%	40%	32%	5%	0,6%
MB03-4					87	9.9	5 mg HCl	8	4%	3%	21%	36%	33%	6%	0,8%
MB03-5					87	10.0	3 mg HNO_3	8	1%	< 0%	18%	31%	38%	5%	0,2%
MB04-1	Ir-Re	H-BEA (150)	433	5.2	87	10.6		8	19%	18%	29%	38%	24%	6%	5,5%
MB04-2					87	11.5		8	17%	18%	28%	37%	26%	7%	4,8%
MB04-4					87	11.5		8	15%	16%	26%	39%	25%	7%	4,0%
MB04-5					88	11.7		8	18%	18%	30%	27%	33%	7%	5,5%
MB05-1	Ir-Re	H-BEA (150)	433	5.2	88	11.0		8	21%	17%	33%	31%	26%	7%	6,9%
MB05-2					87	10.6	10 mg H_2SO_4	8	2%	< 0%	27%	39%	20%	6%	0,6%
MB05-4					87	10.4	8 mg HCl	8	6%	5%	26%	41%	20%	6%	1,6%
MB05-5					87	10.7	13 mg HNO_3	8	3%	0%	17%	51%	17%	7%	0,5%
MB06-1	Ir/Re	H-BEA (150)	433	5.2	87	11.3	Addition of 1 drop HCl 2N on Re impregnation	8	6%	7%	27%	41%	21%	7%	1,5%
MB06-2					87	10.5		8	5%	7%	28%	45%	18%	6%	1,3%

#	Metal	Support	T / K	p / MPa	m_{cat} / mg	$m_{Glycerol\ solution}$ / g	Remarks	t / h	X_1	X_2	$S_{1,3\text{-PDO}}$	$S_{1,2\text{-PDO}}$	$S_{1\text{-PrOH}}$	$S_{2\text{-PrOH}}$	$Y_{1,3\text{-PDO}}$
MB07-1	Ir-Re	SiO_2 (Q-6)	433	5.2	87	13.0	5%wt. Glycerol	8	46%	56%	27%	41%	23%	8%	12,4%
MB07-2					88	11.5		8	57%	61%	20%	33%	34%	11%	11,5%
MB07-4					87	11.7	10%wt. Glycerol	8	13%	14%	24%	43%	22%	8%	3,2%
MB07-5					88	12.3		8	42%	45%	25%	27%	36%	10%	10,6%
MB08-2	Ir-Re	SiO_2 (Q-6)	433	5	87	13.0	Deuterium! 5%wt. Glycerol	8	87%	99%	5%	5%	69%	19%	4,1%
MB09-2	Ir-Re	H-BEA (150)	433	5	87	13.0	Deuterium! 5%wt. Glycerol	8	73%	74%	27%	34%	31%	7%	19,9%
MB10-1	Ir-Re	H-BEA (150)	433	5.2	88	9.9	2 mg $FeCl_3$	8	9%	11%	25%	44%	22%	7%	2,3%
MB10-2					87	10.3	6 mg $Fe_2(SO_4)_3$	8	6%	6%	21%	48%	20%	7%	1,2%
MB10-4					87	10.0	16 mg $Fe(NO_3)_3$	8	0,3%	0,3%	3%	46%	17%	7%	0,0%
MB10-5					88	10.0	Ammonium ferric citrate	8	1%	< 0%	13%	41%	19%	5%	0,1%

The experiments in the multibatch reactor have been carried out in four of the five mini-batches, due to a leakage in mini-batch number three. The number in the very left column of the table indicates MB for multibatch, then the number of the experiment and finally the number of the mini-batch used. In all cases, the pre-treatment of the catalyst was a reduction *ex-situ* at 503 K in flowing hydrogen for one hour. All mini-batches had an inserted Teflon vessel, but no external tank, meaning that the pressure dropped with time when hydrogen was consumed by the reaction.

Curriculum vitae

Personal information

Name	Johannes Kraft
Date/Place of birth	31.10.1984, Frankfurt/Main
Nationality	German

Education

Since 2011 Darmstadt, Germany, and Campinas, Brazil	PhD in Chemistry at TU Darmstadt "Heterogeneously catalysed hydrogenolysis of glycerol to 1,3-propanediol" Supervisor: Prof. Dr. rer. nat. habil. Peter Claus Part of the experimental work at Campinas State University (UNICAMP), Stay in Campinas: Feb. 2011 – Sept. 2012. Scholarship by German Academic Exchange Service (DAAD) and Darmstadt Graduate School of Excellence Energy Science and Engineering.
Out. 2004 – Set. 2010 Darmstadt, Germany, and Campinas, Brazil	Chemistry at TU Darmstadt Degree: Diplom-Ingenieur Title of diploma thesis: "Hydrodeoxygenation of ethyl acetate on Ni and Mo catalysts" Experimental work for final diploma thesis at UNICAMP from March to July 2010 with scholarship by DAAD;
Set. 2006 – Jul. 2007 Bristol, England	Student Exchange at University of Bristol (England) Project equivalent to Final Year Masters undergraduate project, topic: "Producing birefringent particles in non-polar solvents"
Abitur	Philipp-Reis-Schule, Friedrichsdorf

Professional experience

May 2015 – July 2016 Cerquilho, Brazil	ELANTAS Isolantes Elétricos do Brasil Position: Research and Development Coordinator
Since October 2016 Friedrichsdorf and Berlin, Germany	Friedrichsdorfer Institut zur Nachhaltigkeit (IzN) and Technical Support Unit (TSU) of the NAMA Facility, Berlin Position: Advisor to IzN and TSU during the assessment of the 4th Call for NAMA Support Projects.

Johannes Kraft

In der Lach 9

61381 Friedrichsdorf

Deutschland

Darmstadt, den 19. Juni 2017

Erklärung

Ich erkläre hiermit, dass ich meine Dissertation selbstständig und nur mit den angegebenen Hilfsmitteln angefertigt habe.

_____

Johannes Kraft

Johannes Kraft

In der Lach 9

61381 Friedrichsdorf

Deutschland

Darmstadt, den 19. Juni 2017

Erklärung

Ich erkläre hiermit, noch keinen Promotionsversuch unternommen zu haben.

_____

Johannes Kraft